

The role of basal ganglia circuitry in motivation

Fernanda Carvalho Poyraz

Submitted in partial fulfillment of the
requirements for the degree of
Doctor of Philosophy
under the Executive Committee
of the Graduate School of Arts and Sciences

COLUMBIA UNIVERSITY

2016

© 2016

Fernanda Carvalho Poyraz

All rights reserved

ABSTRACT

The role of basal ganglia circuitry in motivation

Fernanda Carvalho Poyraz

The basal ganglia are a set of subcortical nuclei in the forebrain of vertebrates that are highly conserved among mammals. Classically, dysfunction in the basal ganglia has been linked to motor abnormalities. However, it is now widely recognized that in addition to their role in motor behavior, these set of nuclei play a role in reinforcement learning and motivated behavior as well as in many diseases that present with abnormal motivation. In this dissertation, I first provide a review of the literature that describes the current state of research on the basal ganglia and the background for the original studies I later present. I describe the anatomy and physiology of the basal ganglia, including how structures are interconnected to form two parallel pathways, the direct and the indirect pathways. I further review published studies that have investigated how the basal ganglia regulate motor behavior and motivation. And finally, I also summarize findings on how disruption in basal ganglia circuitry function has been linked to a number of neuropsychiatric diseases, with special focus on the symptoms of schizophrenia. I then present original data and discuss the results of three studies investigating basal ganglia function and behavior.

In the first study, I investigated the bridging collaterals, axon collaterals of direct-pathway medium spiny neurons (dMSNs) in the striatum that target the external segment of the globus (GPe), the canonical target of indirect-pathway medium spiny neurons (iMSNs). Previous work in the Kellendonk laboratory has linked these collaterals to increased dopamine D2 receptor (D2R) function and increased striatal excitability, as well as to abnormal locomotor

response to stimulation of the direct pathway. I expanded on these findings by first demonstrating that bridging collaterals form synaptic contacts with GPe cells. I was also able to generate a viral vector to selectively increase excitability in specific populations of MSNs. I used this virus to show that chronically increasing excitability of the indirect pathway, but not the direct pathway, leads to a circuit-level change in connectivity by inducing the growth of bridging collaterals from dMSNs in the GPe. I also confirmed that increased density of bridging collaterals are associated with an abnormal locomotor response to stimulation of striatal dMSNs and further demonstrated that chronic pharmacologic blockade of D2Rs can rescue this abnormal locomotor phenotype. Furthermore, I found that motor training reverses the enhanced density of bridging collaterals and partially rescue the abnormal locomotor phenotype associated with increased collaterals, thereby establishing a new link between connectivity in the basal ganglia and motor learning.

In the second study, I conducted a series of experiments in which I selectively increased excitability of the direct or indirect pathway in specific striatal sub-regions that have been implicated in goal-directed behavior, namely the DMS and NA core. I found that this manipulation was not sufficient to induce significant effects in different behavioral assays of locomotion and motivation, including the progressive ratio and concurrent choice tasks. These findings also suggest that increased bridging collateral density does not have a one-to-one relationship with the motivational deficit of D2R-OE_{dev} mice, as previously hypothesized.

In the third and final study, my original aim was to determine whether the motivational deficit of D2R-OE_{dev} mice, induced by upregulation of D2Rs in the striatum, could be reversed by acutely activating G_{ai}-coupled signaling in the indirect pathway in these animals. I found that this manipulation increased motivation in D2R-OE_{dev} mice but also in control littermates. This

effect was due to energized behavioral performance, which, however, came at the cost of goal-directed efficiency. Moreover, selective manipulation of MSNs in either the DMS or NA core showed that both striatal regions contribute to this effect on motivation. Further investigation aimed at understanding how $G_{\alpha i}$ -coupled signaling affects striatal circuit function revealed that activating a $G_{\alpha i}$ -coupled receptor did not lead to a significant change in somatic MSN activity *in vivo* or to a change in neuronal excitability *in vitro*. In contrast, the GPe, which receives monosynaptic inhibition from the indirect pathway, showed disinhibited activity when $G_{\alpha i}$ signaling was activated in striatal iMSNs. In addition, as drug therapies for psychiatric diseases are not usually given acutely but involve long-term, continuous administrations, I also studied how chronically decreasing function of iMSNs would affect behavior. I showed that chronically activating a $G_{\alpha i}$ -coupled receptor in iMSNs does not lead to a measurable effect on locomotion or motivation, a behavioral desensitization response that can be recovered within 48 h and may be due to receptor desensitization to the drug or circuit-level compensation to a chronic decrease in iMSN function.

Finally, I conclude this dissertation with a general discussion addressing how the findings from each study can be related to each other to provide a more complete understanding of how basal ganglia function regulate behavior, how disruption in the basal ganglia can underlie neuropsychiatric disease, and how strategies to target basal ganglia function should be employed to treat disorders of motivation. I conclude this dissertation by proposing new avenues of research for further exploring my findings.

TABLE OF CONTENTS

LIST OF FIGURES	iii
CHAPTER 1: GENERAL INTRODUCTION	
<hr/>	
OVERVIEW	1
BASAL GANGLIA ANATOMY AND PHYSIOLOGY	
CONNECTIVITY AND PATHWAYS	2
NEUROPHYSIOLOGY OF MEDIUM SPINY NEURONS	12
STRIATAL PATHWAYS AND BEHAVIOR	
MOTOR BEHAVIOR	19
MOTIVATION	22
STRIATAL PATHWAYS AND DISEASE	31
CHAPTER 2: BRIDGING COLLATERALS	
<hr/>	
INTRODUCTION	39
MATERIALS AND METHODS	46
RESULTS	
SYNAPTIC CONTACTS	52
REGULATION BY INDIRECT PATHWAY	53
ASSOCIATION WITH BEHAVIORAL ACTIVATION OF DIRECT PATHWAY	56
REGULATION BY MOTOR TRAINING	59
DISCUSSION	64

CHAPTER 3: INCREASING EXCITABILITY OF STRIATAL PATHWAYS

INTRODUCTION	71
MATERIALS AND METHODS	73
RESULTS	
INCREASING EXCITABILITY OF DIRECT PATHWAY	80
INCREASING EXCITABILITY OF INDIRECT PATHWAY	87
DISCUSSION	93

CHAPTER 4: INDIRECT PATHWAY FUNCTION AND MOTIVATION

INTRODUCTION	99
MATERIALS AND METHODS	102
RESULTS	
ACUTE BEHAVIORAL EFFECTS OF DECREASING INDIRECT-PATHWAY FUNCTION	113
ELECTROPHYSIOLOGICAL EFFECTS ON EXCITABILITY	127
SOMATIC EFFECTS ON NEURONAL ACTIVITY IN THE INTACT ORGANISM	128
EFFECTS ON NEURONAL ACTIVITY OF PALLIDAL NEURONS	138
CHRONIC EFFECTS OF DECREASING INDIRECT-PATHWAY FUNCTION	141
DISCUSSION	151

CHAPTER 5: GENERAL DISCUSSION

SUMMARY AND IMPLICATIONS OF MAIN FINDINGS	160
FUTURE DIRECTIONS	165
REFERENCES	170

LIST OF FIGURES

CHAPTER 1: GENERAL INTRODUCTION

FIGURE 1: Connectivity and pathways in the basal ganglia **6**

FIGURE 2: Striatal sub-regions and motivation **27**

CHAPTER 2: BRIDGING COLLATERALS

FIGURE 3: Physiological and anatomical changes can be induced by dopamine D2R upregulation in the striatum **40**

FIGURE 4: Increased bridging collaterals are associated with enhanced GPe inhibition **41**

FIGURE 5: D2R overexpression decreases striatal inward rectifying currents through downregulation of K_{ir2} channels **43**

FIGURE 6: Increased bridging collaterals are associated with disrupted behavioral activation of direct pathway **45**

FIGURE 7: dMSNs form synaptic contacts in the GPe **52**

FIGURE 8: $Kir2.1^{AAA}$ can be expressed selectively in dMSNs or iMSNs **54**

FIGURE 9: Bridging collaterals are regulated by excitability of the indirect pathway **55**

FIGURE 10: Retraction of bridging collaterals can rescue behavioral activation of direct pathway	58
FIGURE 11: D2R-OE _{dev} mice have a motor impairment that improves with training	60
FIGURE 12: Rotarod training induces retraction of bridging collaterals in D2R-OE _{dev} mice	61
FIGURE 13: Rotarod training partially rescues abnormal behavioral activation of direct pathway	63
 <u>CHAPTER 3: EXCITABILITY OF STRIATAL PATHWAYS AND MOTIVATION</u> <hr/>	
FIGURE 14: Effects of chronically increasing excitability of direct pathway in the DMS	83
FIGURE 15: Chronically increasing excitability of dMSNs in the DMS potentiates locomotor response to acute amphetamine	84
FIGURE 16: Effects of chronically increasing excitability of direct pathway in the NA core	86
FIGURE 17: Effects of chronically increasing excitability of indirect pathway in the DMS	89
FIGURE 18: Effects of chronically increasing excitability of iMSNs in the NA core	91

FIGURE 19: Kir2.1^{AAA} was selectively expressed in targeted regions **92**

CHAPTER 4: INDIRECT-PATHWAY FUNCTION AND MOTIVATION

FIGURE 20: The G_{ai}-coupled designer receptor hM4D can be expressed selectively in specific striatal regions **114**

FIGURE 21: The G_{ai}-coupled designer receptor hM4D can be expressed selectively in iMSNs **115**

FIGURE 22: Motivational deficit of D2R-OE_{dev} mice can be reproduced in animals expressing hM4D in iMSNs **116**

FIGURE 23: Decreasing function of indirect pathway increases motivation in D2R-OE_{dev} and control littermates **117**

FIGURE 24: Decreasing function of indirect pathway increases locomotion in D2R-OE_{dev} and control littermates **119**

FIGURE 25: Both D2R-OE_{dev} mice and control littermates can learn to hold down a lever to obtain a food reward **120**

FIGURE 26: Decreasing function of indirect pathway energizes behavioral performance at the expense of goal-directed efficiency **122**

FIGURE 27: Inhibiting the indirect pathway in either DMS or NA core leads to enhanced motivation **123**

FIGURE 28: Inhibiting the indirect pathway in both DMS and NA core has larger effect on motivation than separate inhibition to either DMS or NA core	124
FIGURE 29: Mice expressing hM4D receptors in iMSNs in either DMS or NA core respond to acute CNO treatment with increased locomotion	125
FIGURE 30: Activating hM4D receptors in iMSNs in the DMS or NA core does not affect sensitivity to reward value	126
FIGURE 31: Membrane excitability properties at the soma of iMSNs expressing hM4D are not changed in vitro by treatment with CNO (part 1)	128
FIGURE 32: Membrane excitability properties at the soma of iMSNs expressing hM4D are not changed in vitro by treatment with CNO (part 2)	129
FIGURE 33: The $G\alpha_i$ -coupled designer receptor hM4D and the calcium sensor GCaMP can be co-expressed in iMSNs in the DMS	130
FIGURE 34: Somatic calcium activity of iMSNs in the DMS is correlated with motor activity in freely-behaving mice	131
FIGURE 35: Heat maps and traces of motor activity and calcium activity for all SAL/CNO experiments imaging iMSNs in DMS	132

FIGURE 36: Correlation between iMSN calcium activity and motor activity was observed in all mice tested	133
FIGURE 37: Activating hM4D receptors in iMSNs does not decrease MSN calcium activity at the somatic level	134
FIGURE 38: Locomotor activity and variability of calcium transients were not affected by CNO in mice co-expressing hM4D and GCaMP6f in iMSNs unilaterally in small region of DMS	135
FIGURE 39: Analysis of event calcium imaging data yields similar findings as analysis of raw calcium transients	137
FIGURE 40: Activating hM4D receptors in striatal iMSNs leads to increased neuronal activity in GPe	139
FIGURE 41: Increased GPe activity after treatment with CNO was observed in all mice imaged	140
FIGURE 42: Chronically activating G_{ai} signaling in iMSNs in both the DMS and NA core does not affect motivation in D2R-OE _{dev} or control littermates	142
FIGURE 43: Oral consumption of CNO induces a behavior response in mice	143
FIGURE 44: Chronically activating G_{ai} signaling in iMSNs in either the DMS or NA core does not affect motivation in mice	145

FIGURE 45: Mice expressing hM4D in iMSNs in either DMS or NA core being chronically treated with CNO no longer respond to acute CNO treatment, but response is recovered 48 h after ending chronic treatment	147
FIGURE 46: Mice expressing hM4D in iMSNs in either DMS or NA core being chronically treated with CNO do not display locomotor response to acute CNO treatment	149
FIGURE 47: Mice expressing hM4D in iMSNs in either DMS or NA core recover locomotor response to acute CNO treatment after being taken off chronic CNO treatment for 48 h	150

ACKNOWLEDGEMENTS

A number of individuals have provided help and support as I completed my dissertation work. I would like to express my appreciation and deepest gratitude to the following people who, in one way or another, contributed to making this work possible.

I am deeply indebted to my thesis advisor, **Dr. Christoph Kellendonk**, who has been an exceptional mentor. His commitment to science and curiosity about how the brain controls behavior has been inspirational. I have no doubt that I made the right decision in joining his research group. Throughout the time I worked in his laboratory, he was available when I had any questions or concerns and always provided high-quality feedback for every development of my research in a timely manner. I also appreciate how he has been sensitive to my career goals and sensible in prioritizing my interests as a student. Dr. Kellendonk is largely responsible for my formation as a competent scientist by giving me diverse opportunities to develop a variety of skills that I will need throughout my career. I will always look up to him and will try to emulate his scientific objectivity, integrity, and tenacity as I pursue my own academic endeavors.

I would also like to thank the faculty members of my thesis committee, **Dr. Peter Balsam**, **Dr. Mark Ansorge**, and **Dr. David Sulzer**, who have guided my thesis research by providing important feedback as I advanced through each stage of different projects. During thesis committee meetings, they have shared their own expertise and experiences to help steer my research to interesting and fruitful directions. They have also collaborated by offering their own laboratory resources for my work. And in this aspect, I am particularly grateful to Dr. Balsam, who allowed me to conduct operant experiments in his laboratory.

My sincere gratitude also goes to **Dr. John Salamone**, who agreed to be the external examiner for my thesis defense. As will be made clear in this dissertation, his work on motivation has inspired my scientific curiosity on how the basal ganglia control behavior and was fundamental for the conception of the questions that led to my thesis research.

I am especially grateful to **Dr. Maxime Cazorla**, former post-doctoral fellow in the Kellendonk laboratory, who directly worked with me as I started the research studies presented in this dissertation. In those early stages, he was an outstanding teacher, both in sharing his knowledge about the complexities of basal ganglia circuitry and in teaching me skills for designing experiments and performing different laboratory techniques. His optimism and excitement about new findings were highly motivating.

Other past and current members of the Kellendonk laboratory also deserve to be acknowledged for experiencing first-hand the different turns of my research projects, for sharing practical advice, and for making the Kellendonk laboratory a collaborative environment for discussing science. Specifically, I would like to thank the postdoctoral fellows, **Dr. Sebastien Parnaudeau**, **Dr. Eduardo Gallo**, and **Dr. Sarah Canetta**, who, as my seniors, expressed interest in my research and were always ready to give me advice on how to interpret complicated results and move further as I collected new data. Each of them also contributed to teaching me how to do patch-clamp electrophysiology, a difficult technique that I would never have learned without their patient guidance. The graduate students, **Scott Bolkan**, **Abigail Clark**, and **Jozsef Meszaros** have shared with me the ups-and-downs of being a graduate student. In particular, Scott is someone I admire for his hard work and scientific achievements. Abigail has lightened up my days by being a wonderful friend and companion inside and outside the laboratory. And Jozsef has stirred my enthusiasm about data analysis with a computational perspective. The

laboratory technicians, **Bhavani Rhamesh**, **Mariya Shegda**, and **Lindsay Kenney** have provided crucial support, without which many of the experiments I conducted would not have been possible. All members of the Division of Molecular Therapeutics have also been very supportive and helpful in the laboratory. Specifically, with her resourcefulness, **Val Morose**, the Division's laboratory manager, has facilitated day-to-day work by making the processes of ordering supplies and maintaining laboratory equipment as smooth as they can possibly be. And **Dr. Jonathan Javitch**, the Division's chair, has also been an excellent mentor who encouraged me to join Dr. Kellendonk's laboratory and provided valuable feedback for my work during laboratory meetings.

I would like to thank two collaborators who were key for the successful completion of my thesis research. First, **Matthew Bailey**, doctoral student in the Balsam laboratory, developed the progressive hold-down task that I used in the study presented in Chapter 4. He also provided me with many resources for analysis of operant data, which turned out to be vital for my studies. And second, **Dr. Mazen Kheirbek**, assistant professor in the laboratory of Dr. Rene Hen, introduced me to *in vivo* calcium imaging and guided me through every practical step of this new technique, which was instrumental for the successful completion of my dissertation work, as will be evident in the results presented in Chapter 4.

In addition, I would like to especially thank **Eva Holzner**, an undergraduate student from Barnard College, whose involvement and hard work contributed greatly to many experiments presented in this dissertation, including key aspects of the study presented in Chapter 4. But most important than her hard work, I thank Eva for giving me the opportunity to be a mentor and to feel responsible for inspiring scientific curiosity in a young person.

Finally, I thank the directors and coordinators of Columbia University's MD/PhD Program and Neurobiology & Behavior Doctoral Program for their administrative support, especially the MD/PhD Program directors for their advice as I had to make important decisions at transition points between medical school and graduate school.

DEDICATION

First and foremost, I dedicate my dissertation work to the three most important people in my life, my mother **Edna Maria Delmondes Carvalho**, my sister, **Marina Delmondes de Carvalho Rossi**, and my husband, **Salih Poyraz**. My mother has always been supportive of my decision to pursue a career in science, and she always had loving words of comfort during my most stressful times as a doctoral student. Having also been a doctoral student herself, my sister always valued my academic endeavors and encouraged me to move forward as I encountered obstacles in my career path. And finally, I cannot overemphasize the love and support of my husband every day when I returned home from the laboratory, and his understanding when I had to change weekend plans to do experiments. These three individuals make me feel special and loved, and they have provided the emotional foundation I needed to carry on and successfully complete my dissertation work.

I would also like to dedicate this dissertation to the memory of my father, **Jose Fernando Moreira de Carvalho**, who unfortunately died prematurely and could not witness my formation as a scientist. As a child, I remember how he encouraged my achievements in school, and my memory of him has always been inspiring and motivating, even so now, many years later, as I get ready to complete this important phase of my scientific training.

CHAPTER 1

GENERAL INTRODUCTION

OVERVIEW

The basal ganglia are a set of subcortical nuclei in the forebrain of vertebrates that are highly conserved among mammals. These nuclei are interconnected with various brain regions, including cortex, thalamus, and brain stem, forming complex circuits that have been implicated in a number of behavioral processes. The gross connectivity between the basal ganglia and other regions of the brain have been described since the seventeenth century (Willis, 1664), with early anatomical studies characterizing the gross interconnectivity among these nuclei (Percheron et al., 1994). As new research tools became available, neuroscientists have been able to more carefully dissect circuits, and the anatomy of the basal ganglia has been further linked to physiology and behavior. Historically, the basal ganglia were first implicated in motor behavior through early observations in patients with Parkinson's disease, Huntington's disease, and brain lesions (Albin et al., 1989). However, basal ganglia dysfunction has also been observed in patients with neuropsychiatric disease, such as drug addiction and schizophrenia. This set of nuclei is now widely recognized for their involvement in reinforcement learning and motivated behavior, as well as in a number of diseases that present with abnormal motivation.

Involvement of the basal ganglia in disorders of motivation provided the impetus for the work presented here. In the following sections, I will first review the literature relevant to the original studies I conducted, including the anatomy and physiology of the basal ganglia and what is known about their function in normal behavior and diseased states. For consistency, as the original research findings I present in this dissertation were conducted in mice, most of my

review of the literature will include studies done in rodents. But at appropriate points, I will also discuss how these findings relate to work done in primates and humans. After reviewing the literature, I will describe in detail the three studies I conducted. In the first study, I contributed to the anatomical and functional characterization of the “bridging collaterals”, axon collaterals that interconnect the direct and indirect pathways of the basal ganglia and may be important in schizophrenia. In the second study, I tested whether chronic manipulations increasing excitability of specific pathways in the basal ganglia could affect motivation. And finally, in the last study I investigated how decreasing function of the indirect pathway of the basal ganglia, both acutely and chronically, affects motivation and neuronal activity, providing mechanistic and behavioral insight for development for new therapies for disorders of abnormal motivation. I conclude this dissertation with a general discussion that brings together findings from all three studies and proposes future directions for my work.

BASAL GANGLIA ANATOMY AND PHYSIOLOGY

CONNECTIVITY AND PATHWAYS

The basal ganglia are composed of a bilateral set of evolutionarily conserved nuclei in the vertebrate forebrain. Anatomically, the striatum, comprising the dorsal striatum and nucleus accumbens (NA) – also referred to as the ventral striatum – is the largest of these nuclei and is considered the main input nucleus of the basal ganglia. In primates, the striatum is composed of the caudate nucleus and putamen, which are separated by the internal capsule. In rodents, however, there are no physical barriers separating striatal sub-regions. The striatum receives glutamatergic inputs from both cortex and thalamus. Cortical inputs to the striatum comes from a

broad range of cortical regions, including sensory, motor, and associational cortex, in a highly topographical manner (Alexander et al., 1986). The thalamic inputs to the striatum come predominantly from midline and intralaminar nuclei (Berendse and Groenewegen, 1990, Erro et al., 2001, Van der Werf et al., 2002, Vercelli et al., 2003, Yasukawa et al., 2004, Doig et al., 2010). Most of these synaptic inputs are axo-dendritic, targeting the dendritic spines of medium spiny neurons (MSNs) – also known as spiny projection neurons – which express both NMDA and AMPA glutamate receptors (Carter et al., 2007). MSNs make up 95% of all neurons in the striatum and connect the striatum to other nuclei of the basal ganglia through GABAergic projections (Kemp and Powell, 1971). The other 5% of neurons in the striatum are interneurons that release acetylcholine or GABA. These interneurons are known to also receive cortico-thalamic excitatory inputs, and they can synapse on other interneurons or on MSNs (Calabresi et al., 2000, Tepper et al., 2010).

The other structures in the basal ganglia include the pallidum, substantia nigra, and subthalamic nucleus. The pallidum consists of the globus pallidus and its ventral extension, the ventral pallidum (VP). The globus pallidus consists of two functionally distinct parts, the internal segment of the globus pallidus (GPi) and the external segment of the globus pallidus (GPe). Pallidal neurons are GABAergic and tonically active, providing inhibitory tone to neurons in the nuclei to which they project (Surmeier et al., 2005). The substantia nigra is another structure of the basal ganglia, and it is located in the midbrain. Functionally, it can be divided into the substantia nigra pars compacta (SNc) and the substantia nigra pars reticulata (SNr). The SNc contains dopaminergic neurons, while neurons in the SNr are more similar to pallidal neurons in that they are GABAergic and tonically inhibit the nuclei to which they project (Surmeier et al., 2005). Together, the GPi and SNr are considered output nuclei because, unlike other nuclei of

the basal ganglia, they project to structures outside the basal ganglia, predominantly the thalamus. Finally, the subthalamic nucleus (STN) is also part of the basal ganglia and is composed of tonically-active glutamatergic projection neurons (Surmeier et al., 2005). Interconnectivity among all these nuclei can be complex, and it is useful to describe it by considering the basal ganglia as an integral component of the cortico-basal ganglia-thalamo-cortical loop.

Information received by the striatum, the main input nucleus of the basal ganglia, flows to other nuclei through two parallel pathways, the direct and indirect pathways, arising from distinct populations of MSNs distributed uniformly throughout the striatum and approximately equal in number (Valjent et al., 2009). The direct pathway is formed by MSNs that express the dopamine D1 receptor (D1R), as well as the peptide neurotransmitters substance P and dynorphin. The indirect pathway, in turn, arises from MSNs that express the dopamine D2 receptor (D2R) in addition to the adenosine A2A receptor and the neuropeptide enkephalin. The gene and protein expression profiles of these two neuronal populations have been characterized by immunohistochemistry, *in situ* hybridization, as well as single-cell RT-PCR studies (Gerfen and Young, 1988, Surmeier et al., 1996, Matamales et al., 2009). The segregation of these two populations of striatal MSNs has been further confirmed in transgenic mice using bacterial artificial chromosomes (BAC) expressing fluorescent proteins under the control of the promoters for the D1R and D2R genes, *Drd1* and *Drd2*, respectively (Gong et al., 2003, Ade et al., 2011). Using these BAC transgenic mice, researchers have demonstrated that D1Rs and D2Rs are co-expressed in fewer than 5% of MSNs in the adult striatum (Bertran-Gonzalez et al., 2008, Shuen et al., 2008). Thus, at the somatic level, two populations of MSNs can be readily distinguished based on their gene expression profiles.

As suggested by their name, MSNs of the direct pathway (dMSNs) project directly to the output nuclei of the basal ganglia, the GPi and SNr. The latter two nuclei project mainly to the thalamus, including the ventral anterior, ventral lateral, and mediodorsal nuclei, as well as to the superior colliculus and pedunculopontine nucleus in both rodents and primates (Moriizumi and Hattori, 1992, Shink et al., 1997, McFarland and Haber, 2002, Bodor et al., 2008, Kaneda et al., 2008). Some researchers have proposed that GPi and SNr function as basal ganglia output nuclei in segregated loops, with the GPi predominantly targeting the motor cortex via the ventrolateral thalamus, while the SNr preferentially targets association cortical areas via the ventroanterior and mediodorsal thalamus (Romanelli et al., 2005). Regardless of the specific thalamic nuclei to which they project, the majority of neurons in the SNr and GPi inhibit the thalamus by providing GABAergic tone to its targets. As a result, increased dMSN activity, or activation of the direct pathway of the basal ganglia, inhibits the basal ganglia output nuclei, thereby providing a net disinhibition of the thalamus.

MSNs of the indirect pathway (iMSNs), in turn, can have the opposite effect on the output of the basal ganglia. These striatal neurons only project to the GPe or to the VP. Neurons in the GPe are known to provide inhibitory tone to the output nuclei of the basal ganglia by synapsing on neurons in the STN, which in turn send excitatory projections to the GPi and SNr (Kita and Kitai, 1987). Since pallidal neurons are GABAergic and neurons in the STN are glutamatergic, through a polysynaptic circuit, the net effect of iMSNs on basal ganglia output is to decrease disinhibition to the thalamus. Figure 1 outlines the connectivity of the direct and indirect pathways described above, illustrating how the distinct neuroanatomical organization of these pathways can lead to opposing effects on basal ganglia output.

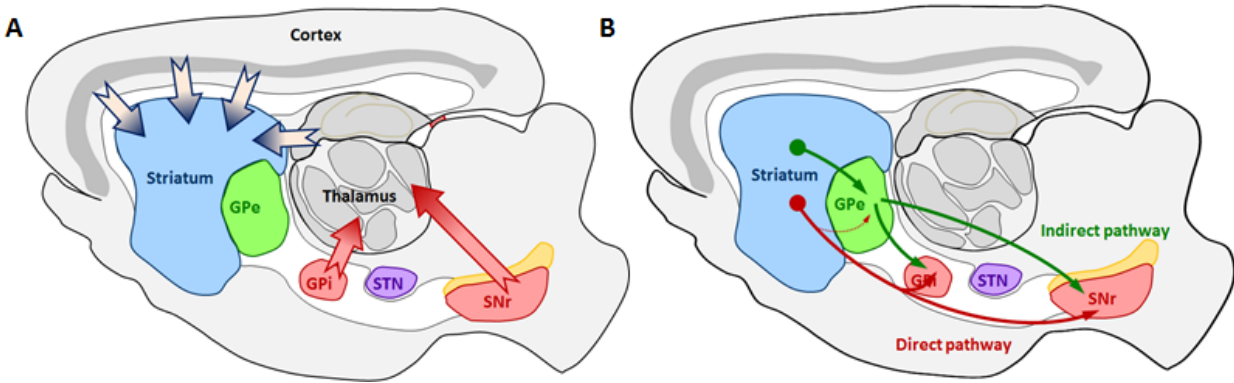


Figure 1: Connectivity and pathways in the basal ganglia. **A.** The striatum is the main input nucleus of the basal ganglia and receives excitatory inputs from the cortex and thalamus (blue arrows). The internal segment of the globus pallidus (GPI) and the substantia nigra pars reticulata (SNr) are the main output nuclei of the basal ganglia; they project to regions outside the basal ganglia, predominantly the thalamus (red arrows). **B.** Within the basal ganglia two parallel pathways interconnect input and output nuclei. The direct pathway is formed by striatal medium spiny neurons (MSNs) that project monosynaptically to the GPI or SNr, output nuclei of the basal ganglia (solid red arrows). Many of the direct-pathway MSNs (dMSNs) also have axon collaterals that project to the external segment of the globus pallidus (GPe) (dotted red arrow). In contrast, the indirect pathway arising from striatal MSNs (iMSNs) interconnect with the output nuclei of the basal ganglia, the GPI and SNr, through a polysynaptic circuit via the GPe or ventral pallidum (VP, not shown) and subthalamic nucleus (STN, connection not shown) (solid green arrows).

Despite the conceptual appeal of having two dichotomous circuits that provide opposing influences on basal ganglia output, a number of functionally-relevant anatomical complexities exist within this circuitry. For instance, while iMSNs project exclusively to the GPe or VP, not all dMSNs project only to the SNr or GPI. In the dorsal striatum, dMSNs that project to the output nuclei of the basal ganglia are known to also extend axonal collaterals to the GPe, classically known to be the targets of iMSNs (Wu et al., 2000, Fujiyama et al., 2011), and axon terminals of dMSNs arising from the NA can also be found in the pallidum (Lu et al., 1998). Moreover, the GPe has been shown to project back to the striatum (Staines and Fibiger, 1984). Another exception to the direct/indirect pathway dichotomy is the fact that, in contrast to the GPe, the VP can function as an output nucleus of the basal ganglia, much like the GPI and SNr, as some cells in the VP have been shown to project to the mediodorsal thalamus (Tripathi et al., 2013). Finally, the STN is also part of a third pathway that can influence basal ganglia output,

the so-called hyperdirect pathway. Excitatory projections, predominantly from motor cortex but also prefrontal regions, have been shown to directly target the STN, allowing cortical information to enter the basal ganglia bypassing the striatum (Haynes and Haber, 2013).

Despite these exceptions, the circuit connectivity described above and illustrated in Figure 1 explains how the basal ganglia are integrated in a loop with the cortex and thalamus. The striatum receives corticothalamic inputs and relays neural information to the output nuclei of the basal ganglia either directly via the dMSNs or indirectly via iMSNs. Influence from both the direct and indirect pathways determines whether neurons in the SNr and GPe will inhibit or disinhibit their thalamic targets. Thalamic nuclei, in turn, send excitatory projections to the cortex and can project directly back to the striatum, thereby closing the cortico-basal ganglia-thalamo-cortical loop. Anatomical tracing studies in both rodents and primates have demonstrated that functional regions in the cortex that send inputs to the basal ganglia are connected with specific areas of each nucleus of the basal ganglia and the thalamus, revealing a topographical pattern of connectivity through cortex, basal ganglia, and thalamus composed of a series of parallel, segregated loops (Haber and Calzavara, 2009). Data in primates have also demonstrated that terminals from different functional regions converge at nodes within the corticostriatal pathway (Haber et al., 2006, Calzavara et al., 2007). From a circuitry point of view, this organization allows for specific loops to be activated or inhibited independently. Therefore, it is conceptually feasible that opposing influence of the direct and indirect pathways on basal ganglia output can occur simultaneously on different loops when animals engage in complex behaviors: while the direct pathway promotes thalamic disinhibition to drive specific behaviors via a particular loop, the indirect pathway maintains thalamic inhibition via competing loops to suppress unwanted actions.

In addition to being integrated in a series of loops with the cortex and thalamus, the basal ganglia are modulated by dopaminergic neurons in the midbrain located both in the SNc and ventral tegmental area (VTA). Dopaminergic terminals densely innervate dMSNs and iMSNs throughout the entire striatum (Moss and Bolam, 2008). One functionally-relevant feature of dopaminergic terminals in the striatum is that they exhibit presynaptic D2R expression thought to function as autoreceptors in a negative feedback mechanism, whereby their activation leads to decreased release of dopamine (Sesack et al., 1994, Ford, 2014). Moreover, presynaptic D2R expression in the striatum does not only occur in the terminals of dopaminergic neurons, as cortical afferent presynaptic terminals to the striatum have also been shown to express D2Rs (Wang and Pickel, 2002). The presynaptic expression of D2Rs in the striatum has posed a challenge to the study of D2R function in iMSNs since pharmacological agents targeting this receptor in the striatum can bind to both presynaptic and postsynaptic receptors, and it can be difficult to experimentally isolate the effects elicited by targeting D2Rs in each of these neuronal compartments.

Histologically, the striatum displays another level of heterogeneity in its organization into patch (striosome) and matrix compartments that have specialized gene expression as well as different inputs and outputs. The patch compartment has enriched immunoreactivity for enkephalin, substance P, as well as cholinergic muscarinic receptors and mu opioid receptors (Graybiel et al., 1981, Moriwaki et al., 1996, Bernard et al., 1999). In contrast, the matrix compartment has high acetylcholinesterase activity, somatostatin-immunoreactive fibers, and GABAergic neurons that co-express calbindin (Graybiel and Ragsdale, 1978, Herkenham and Pert, 1981, Gerfen, 1984, Gerfen et al., 1985). Patches receive inputs from the prelimbic cortex and project to the SNc, while the matrix receives inputs from sensory and motor cortical regions

and projects to the SNr (Gerfen, 1984). The connectivity of striatal patch and matrix compartments has been proposed to represent a second level of functional organization in the basal ganglia in addition to the parallel circuits formed by the direct and indirect pathways (Gerfen, 1992).

Moreover, different types of striatal neurons form synaptic contacts locally within the striatum. MSN-to-MSN lateral inhibition represents one type of such synaptic contact. In addition to projecting outside of the striatum, both dMSNs and iMSNs are known to extend richly-branching axon collateral arbors around their cell bodies (Kawaguchi et al., 1989). GABAergic synapses between these collaterals and GABA_A receptors on neighboring MSNs represent a lateral inhibition mechanism via which striatal output may be further regulated (Czubayko and Plenz, 2002). Using BAC transgenic mice, researchers have characterized MSN-to-MSN lateral connectivity by demonstrating that, while iMSNs project both to other iMSNs and to dMSNs, dMSNs locally synapse only onto other dMSNs (Taverna et al., 2008).

Synapses involving striatal interneurons represent a second type of local connectivity within the striatum. Among striatal interneurons, it is known that the GABAergic interneurons form feed-forward inhibitory synaptic connections with both MSNs and neighboring interneurons (Koos and Tepper, 1999). In addition, cholinergic interneurons release acetylcholine in the striatum, and changes in their activity have been linked to motor and reinforcement learning in primates (Kimura et al., 1984, Aosaki et al., 1994). However, the mechanisms by which acetylcholine affects basal ganglia output are not well characterized. Although MSNs lack nicotinic receptors (Luo et al., 2013), they express muscarinic receptors that are thought to mediate increased MSN excitation when acetylcholine is released from cholinergic interneurons, even in the absence of synaptic input (Hsu et al., 1996, Hsu et al., 1997,

Galarraga et al., 1999). Studies using optogenetics have also demonstrated that activation of cholinergic interneurons triggers dopamine release from presynaptic terminals in the striatum (Cachope et al., 2012, Threlfell et al., 2012). In addition, cholinergic interneurons express D2Rs and their activity can be modulated by dopamine (Yan et al., 1997). Thus, even though they represent a small minority of neurons in the basal ganglia, striatal interneurons can influence basal ganglia output by modulating dopamine release and activity of MSNs.

With an understanding of the parallel circuits that integrate basal ganglia input and output, it is important to also acknowledge specific differences in the anatomical connectivity involving the dorsal striatum and the NA. These differences exist at the level of afferents and efferents and further reinforce the concept that the basal ganglia are integrated in parallel loops with the cortex and thalamus. Afferent dopaminergic modulation from the midbrain to the striatum target striatal sub-regions selectively. The vast majority of dopaminergic neurons projecting to the dorsal striatum come from the SNc, while those projecting to the NA come from the VTA (Ungerstedt, 1971, Fallon and Moore, 1978, Gerfen et al., 1987). In respect to cortical inputs, the dorsal striatum receives inputs from associative and sensorimotor cortical areas, while the NA receives inputs from the orbitofrontal cortex and other limbic cortical areas (Gerfen, 1984, Nakano et al., 2000). There are also differences in the efferent targets of striatal MSNs arising from the dorsal striatum and NA. Consistent with their dorsal-ventral orientation, iMSNs in the dorsal striatum project to the GPe, while iMSNs in the NA project to the VP. Similarly, among the dMSNs that project to the pallidum, those arising from the dorsal striatum target the GPe, while those arising from the NA target the VP. Moreover, it is known that in the dorsal striatum, projections from dMSNs to the GPe are predominantly axon collaterals from neurons that also project to output nuclei of the basal ganglia (Kawaguchi et al., 1990, Wu et al.,

2000, Fujiyama et al., 2011). Although axon terminals of dMSNs arising from the NA can also be found in the VP (Lu et al., 1998), it is not known if these terminals represent axon collaterals. Moreover, functional differences related to anatomical connectivity have been reported between dMSN “non-canonical” projections from the dorsal striatum to the GPe and those from the NA to the VP. One recent study estimated that 18% of the neurons in the GPe receive input from dMSNs in the dorsal striatum, while as many as 50% of the neurons in the VP receive inputs from dMSNs in the NA (Kupchik et al., 2015).

The dorsal striatum and NA can be further divided into sub-compartments. The medial and lateral regions of the dorsal striatum receive inputs from distinct cortical regions. While sensorimotor cortex projects to the dorsolateral striatum (DLS), associative cortical structures, including medial prefrontal cortex and anterior cingulate, project to the dorsomedial striatum (DMS) (Pan et al., 2010). The NA, in turn, can be anatomically subdivided into core and shell. The core of the NA receives inputs from associative and limbic cortex (Brog et al., 1993), much like the DMS. In contrast, the shell of the NA has very distinct morphological and anatomical properties when compared to the rest of the striatum and is considered by some to be part of the extended amygdala (Alheid and Heimer, 1988, Heimer et al., 1991, Heimer et al., 1997). Compared to the NA core, neurons in the NA shell have lower density of dendritic spines and less branching (Meredith et al., 1992). The NA shell also receives afferent innervation from different cortical and subcortical structures compared to those of the core, including lateral hypothalamus and brainstem (Brog et al., 1993). In addition to innervating the VP and GPi, the NA shell also project to the VTA, as well as to the lateral hypothalamus and other structures in the extended amygdala (Heimer et al., 1991). Despite this traditional sub-compartmentalization, it has also been proposed that functional sub-regions within the striatum follow a gradient along

the dorsolateral-to-ventromedial axis, especially when considering the source of corticostriatal inputs (Moriwaki et al., 1996).

In summary, although a number of exceptions have been described, the basal ganglia can be conceptually framed as integrated in serial loops with the cortex and thalamus, with the direct and indirect parallel pathways providing opposing influence on basal ganglia output. Activity in this circuit is modulated internally by striatal interneurons and externally by dopaminergic neurons that project to the striatum.

NEUROPHYSIOLOGY OF MEDIUM SPINY NEURONS

Much of the intrinsic neurophysiological properties of dMSNs and iMSNs, as well as their influence on basal ganglia output, have been characterized both *in vitro* and *in vivo*. Both dMSNs and iMSNs have a low resting membrane potential in the absence of corticothalamic input. At rest, inward rectifying K_{ir2} potassium channels, expressed in abundance by all striatal MSNs, hold the membrane potential near the equilibrium potential of potassium (Wilson, 1993). In response to glutamatergic synaptic inputs from the cortex and thalamus, MSNs can depolarize if inputs have enough temporal and spatial convergence to overwhelm K_{ir2} channels and cause them to close, allowing the membrane potential to reach spike threshold (Wilson and Kawaguchi, 1996). Slice electrophysiological recordings from genetically-identified iMSNs and dMSNs have demonstrated that both types of MSNs share similar passive membrane properties, including resting membrane potential, action potential properties, input resistance, and afterhyperpolarization amplitude (Cepeda et al., 2008). Using optogenetic tools to identify dMSNs and iMSNs, findings from *in vivo* electrophysiology experiments are in line with *in vitro* data and provide further insight on how MSN activity is related to behavior. Both types of MSNs

show similarly low baseline activity when animals are not engaging in motor actions and are concomitantly active during initiation of action sequences (Jin et al., 2014b), presumably driven by strong corticothalamic inputs that reverse hyperpolarization in MSNs to allow initiation of behavioral programs.

Even though dMSNs and iMSNs exhibit similar passive membrane properties and general levels of activity *in vivo*, there are many known functional differences between these two neuronal populations that can lead to different responses to synaptic input. Some of these functional differences arise from differences in the morphology of dMSNs and iMSNs. In rodents, the total dendritic length of iMSNs is smaller than that of dMSNs (Gertler et al., 2008). From this difference in dendritic surface area, with no evident dissimilarity in the density of synaptic inputs to dMSNs and iMSNs, some have inferred that dMSNs receive more glutamatergic inputs than iMSNs (Gerfen and Surmeier, 2011). In addition, smaller dendritic length leads to lower membrane capacitance, which can account for the higher intrinsic excitability of iMSNs compared to dMSNs that has been demonstrated in a number of studies using slice physiology (Kreitzer and Malenka, 2007, Cepeda et al., 2008, Gertler et al., 2008, Lobo et al., 2010).

However, most of the physiological differences between dMSNs and iMSNs can be attributed to the different dopamine receptors they express that are thought to mediate diverging modulatory effects of dopamine on these two populations of striatal neurons. It is thought that activation of D1Rs leads to somatic depolarization and facilitates spiking in dMSNs, while activation of D2Rs on iMSNs has the opposing effect, causing cells to become less likely to depolarize and fire action potentials. However, although researchers have some insight on how

membrane conductances can be changed upon activation of D1Rs and D2Rs on the cell surface of MSNs, much of the intracellular mechanisms underlying these effects remain unknown.

The D1R is a $G_{\alpha s/olf}$ -protein-coupled receptor that activates adenylate cyclase and consequently increases production of cyclic AMP (cAMP). High levels of cAMP in MSNs lead to the activation of protein kinase A (PKA), which induces phosphorylation of various substrates, as well as activation of immediate early gene expression and modulation of ion channels. Some specific physiological effects of D1R activation on MSNs have been described. For instance, intracellular signaling activated by D1Rs has been shown to increase Ca_v1 L-type channel currents (Surmeier et al., 1995, Galarraga et al., 1997) and to decrease somatic A-type potassium currents (Kitai and Surmeier, 1993). D1R activation in MSNs can also reduce N- and P-type calcium currents (Surmeier et al., 1995) that control activation of calcium-dependent potassium currents (Vilchis et al., 2000). In addition, bypassing G protein signaling, the second intracellular loop of the D1R has been shown to interact directly with the C-terminal region of N-type $Ca_v2.2$ channels and mediate inhibition or internalization of these channels both in transfected cells and in native tissue (Kisilevsky et al., 2008, Kisilevsky and Zamponi, 2008). Moreover, in both transfected cells and cultured neurons, the D1R has been shown to interact with the NR1 and NR2A subunits of the glutamatergic NMDA receptor (Lee et al., 2002, Fiorentini et al., 2003).

In contrast, D2Rs are $G_{\alpha i/o}$ -protein-coupled receptors that when activated leads to inhibition of adenylate cyclase and decreased cAMP production. Decreased production of cAMP decreases PKA activity, which can have a modulatory effect on ions channel conductances. Assuming that dMSNs and iMSNs express similar intracellular signaling proteins, it is expected that activation of D2Rs in iMSNs would have opposite physiological effects compared to

activation of D1Rs in dMSNs. Studies using slice electrophysiology have indeed shown this dichotomy for some conductances regulated by G protein signaling. For instance, in contrast to the effect of activating D1Rs, activation of D2Rs reduces Ca_v1 L-type channel currents (Hernandez-Lopez et al., 1997, Hernandez-Lopez et al., 2000). In heterologous cell culture systems, it has been demonstrated that D2Rs can also activate G-protein coupled inwardly rectifying potassium (GIRK) channels via the $G_{\beta\gamma}$ subunit (Kuzhikandathil et al., 1998, Lavine et al., 2002). The activation of GIRKs induced by activation of D2Rs and other G-protein coupled receptors (GPCRs) has an inhibitory effect on neurons and could potentially mediate several functions of dopamine *in vivo* (Luscher and Slesinger, 2010). However, the striatum expresses low levels of GIRK channels (Karschin et al., 1996), and D2R-dependent outward currents that are characteristic of GIRKs cannot be readily measured in MSNs unless GIRK channels are artificially overexpressed (Marcott et al., 2014). Thus, the well-characterized GIRK-mediated decrease in excitability promoted by $G_{\alpha i}$ signaling is likely not relevant for D2Rs expressed in MSNs. Moreover, the D2R can also interact directly with the NR2B subunit of the NMDA receptor in response to high extracellular dopamine in the postsynaptic density microdomain of excitatory synapses in striatal neurons (Liu et al., 2006). Thus, most studies investigating the physiological effects of dopamine on D1Rs and D2Rs suggest that activation of each receptor leads to opposing downstream effects, reinforcing a dichotomy between these two neuronal populations.

It is also important to note that two splice variants of the D2R exist, the D2R long and short isoforms (D2L and D2S, respectively), which are identical except for an insert of 29 amino acids in the third extracellular loop of the D2L isoform (Dal Toso et al., 1989). Some differences in subcellular distributions and coupling to G proteins have been reported for these two D2R

isoforms (Montmayeur et al., 1991, Uziel et al., 2000, Morris et al., 2007, De Mei et al., 2009). However, D2Rs expressed postsynaptically by iMSNs are predominantly of the D2L type (Uziel et al., 2000), and therefore it can be inferred that the physiological effects described above measured in striatal MSNs are likely mediated by the D2L isoform.

The 32-kDa dopamine- and cAMP-regulated phosphoprotein (DARPP-32) is a substrate of PKA that plays a role in dopamine signaling in striatal MSNs, mediating some of the opposite physiological effects of D1R and D2R activation. Phosphorylation of DARPP-32 at threonine 34 by PKA activates the protein phosphatase 1 (PP1) inhibitory function of DARPP-32 (Hemmings et al., 1984). Studies in BAC transgenic mice overexpressing DARPP-32 tagged for immunoprecipitation have shown that enhanced D1R stimulation results in increased phosphorylation of DARPP-32 in response to PKA activation in dMSNs, whereas stimulation of D2Rs in iMSNs reduces phosphorylation of DARPP-32 at threonine 34, presumably as a consequence of reduced PKA activation (Bateup et al., 2008) and/or the dephosphorylation of threonine 34 by the calmodulin-dependent protein calcineurin that is also activated by increased intracellular Ca^{2+} after activation of D2Rs (Nishi et al., 1997). In MSNs, the phosphorylation state of multiple PKA targets, such as ionotropic glutamate and GABA receptors, is the result of an equilibrium between PKA and PP1 activity (Greengard et al., 1999, Greengard, 2001). Therefore, DARPP-32 is a regulator protein that acts to amplify PKA signaling and can mediate the opposing functions of D1Rs and D2Rs in the striatum.

In addition, several MAP kinases have been shown to mediate signaling involved in the physiological effects of dopamine. Observations in heterologous cell culture systems suggest that both D1Rs and D2Rs can regulate the MAP kinases extracellular signal regulated kinases 1 and 2 (ERK1 and ERK2) (Chen et al., 2004, Wang et al., 2005). Pharmacological studies *in vivo* have

shown that psychostimulants that lead to high extracellular dopamine, such as amphetamine or cocaine (Valjent et al., 2006), and the D2R antagonist haloperidol (Pozzi et al., 2003) enhances phosphorylation of ERK1 and ERK2 in the striatum. These findings were confirmed with BAC transgenic mice, further revealing that psychostimulants activate ERK selectively in dMSNs, while haloperidol activates ERK selectively in iMSNs (Bertran-Gonzalez et al., 2008). Furthermore, it has also been shown that ERK phosphorylation mediated by D1Rs in the striatum involves an interaction with the NMDA glutamate receptor and requires the presence of endogenous glutamate (Valjent et al., 2000, Valjent et al., 2005, Pascoli et al., 2011). In cell culture, D2R-mediated ERK signaling has been shown to be dependent on $G_{\alpha i}$ protein coupling (Ghahremani et al., 2000, Beom et al., 2004). Thus, evidence suggests that some of the dichotomous physiological effects of activating D1Rs and D2Rs in striatal MSNs may be mediated by ERK signaling.

Another important distinction between dMSNs and iMSNs and how they can be modulated by dopamine via D1Rs and D2Rs, respectively, relates to the different affinities of dopamine for each type of receptor. The affinity of D2Rs for dopamine is reported to be 10- to 100-fold greater than that of D1Rs (Missale et al., 1998). However, most measures of affinity for dopamine have been made using displacement of radiolabeled antagonists from receptors expressed in heterologous systems, and these methods do not take into account the coupling efficacy to downstream signaling cascades. Even though it is problematic to infer that these measurements reflect what happens *in vivo*, many researchers have proposed that D2Rs are preferentially activated by basal (tonic) extracellular levels of dopamine, while burst (phasic) firing of dopaminergic neurons mainly activates the low-affinity D1Rs (Grace et al., 2007, Surmeier et al., 2011). Researchers have also proposed that both D1Rs and D2Rs can exist in

both high- and low- affinity states with similar affinities to dopamine in their high-affinity states (Cumming, 2011). These observations have led to different conceptual models of how dopamine may affect activity in the basal ganglia during reinforcement learning (Goto and Grace, 2005, Grace et al., 2007), but the actual relevance of tonic and phasic dopamine and dopamine receptor affinity states to basal ganglia output and behavior still needs to be fully tested with selective manipulations *in vivo*.

Table 1 summarizes the main biochemical and physiological effects that have been shown to result from activation of D1Rs or D2Rs on striatal MSNs. It is important to note, however, that most studies reporting electrophysiological changes induced by activation of D1Rs and D2Rs in striatal MSNs were done with whole-cell patch clamp in acute slices, a technique that allows researchers to measure changes in conductances in the soma but not in other cellular compartments, including dendrites and axon terminals. A few studies have used two-photon microscopy and calcium sensors to determine how excitability of MSNs are specifically affected at proximal and distal dendrites, confirming that dendrites of iMSNs are more excitable than those of dMSNs and demonstrating that activation of D2Rs can suppress dendritic excitability of iMSNs (Carter and Sabatini, 2004, Carter et al., 2007, Day et al., 2008). Moreover, it is known that D2Rs are also expressed in the presynaptic terminals of iMSNs targeting the GPe (Levey et al., 1993, Yung et al., 1995), and some findings have shown that dopamine can modulate GABA release from iMSN terminals targeting pallidal neurons via presynaptic D2Rs (Floran et al., 1997, Wei et al., 2013, Mamad et al., 2015). A role for D2Rs acting on presynaptic terminals of iMSNs to suppress GABA release has also been demonstrated for axon collaterals that target neighboring MSNs (Tecuapetla et al., 2009, Kohnomi et al., 2012).

Table 1: Biochemical and physiological effects of activating D1Rs and D2Rs in MSNs

	Target	Effect	References
Activation of D1Rs	$G_{as}, G\alpha_{olf}$	Stimulates cAMP production	
	Ca _v 1 L-type channel	Increases currents	(Surmeier et al., 1995, Galarraga et al., 1997)
	A-type K ⁺ channels	Decreases currents	(Kitai and Surmeier, 1993).
	N- and P -type Ca ²⁺ channels	Decreases currents	(Surmeier et al., 1995)
	Ca ²⁺ - dependent K ⁺ channels	Activates currents	(Vilchis et al., 2000)
	N-type I Ca _v 2.2 channel	Inhibition and internalization	(Kisilevsky et al., 2008, Kisilevsky and Zamponi, 2008)
	NR1 and NR2A NMDA subunits	Interacts	(Lee et al., 2002, Fiorentini et al., 2003)
	DARPP-32	Increases phosphorylation	(Bateup et al., 2008)
	ERK1 and ERK2	Increases phosphorylation	(Valjent et al., 2006)
Activation of D2Rs	$G_{ai}, G\alpha_0$	Inhibits cAMP production	
	Ca _v 1 L-type channel	Decreases currents	(Hernandez-Lopez et al., 2000)
	NRB NMDA subunit	Interacts	(Liu et al., 2006)
	DARPP-32	Decreases phosphorylation	(Bateup et al., 2008)
	ERK1 and ERK2	Decreases phosphorylation	(Pozzi et al., 2003)

STRIATAL PATHWAY AND BEHAVIOR

MOTOR BEHAVIOR

Despite the complexities in anatomy and function, a number of studies suggest that the opposing influence on output to the thalamus exerted by the two main pathways of the basal ganglia mediate opposing influences on behavior, with the direct pathway being permissive for behavior initiation and the indirect pathway being inhibitory. This opposition has been most clearly demonstrated in the domain of motor behavior, and as a result, the two pathways have been classically referred to as the “go” (direct) and “no-go” (indirect) pathways.

Combining knowledge of basal ganglia connectivity and dopamine receptor function, dopamine depletion studies and observed effects of psychostimulants provided some initial evidence in support of this classical model. The neurotoxin 6-hydroxydopamine (6-OHDA) can selectively destroy dopaminergic neurons and has been used to model parkinsonism in different species (Ungerstedt, 1968). When locally delivered into the striatum, 6-OHDA is taken up by dopaminergic terminals and induces cell death (Blum et al., 2001). The loss of dopaminergic modulation to the striatum that ensues leads to robust motor impairments in both rodents and primates (Blesa and Przedborski, 2014). In contrast, psychostimulants such as cocaine and amphetamine, which increase extracellular dopamine by blocking dopamine reuptake through the dopamine transporter (DAT), induces hyperactive motor behavior in rodents (Jaber et al., 1997).

Pharmacological studies measuring the effect of selective dopamine receptor agonists and antagonists on motor behavior have further elucidated the role of dMSNs and iMSNs on motor control. D1R agonists have a stimulatory effect on locomotor activity in rodents, while treatment with D2R agonists leads to a biphasic locomotor response, characterized by decreased activity at low doses and behavioral activation at high doses (Eilam et al., 1992). This biphasic effect can be explained by the fact that D1Rs are only expressed postsynaptically, while D2Rs are expressed both presynaptically and postsynaptically (Sesack et al., 1994). While selective D1R stimulation in striatal dMSNs increases locomotor activity by activating the direct pathway, D2R agonists in the striatum can lead to activation of postsynaptic receptors on iMSNs and presynaptic autoreceptors in dopaminergic terminals. Presynaptic D2Rs have been shown to provide negative feedback to dopamine neurons, decreasing dopamine release into the striatum (Starke et al., 1989) and likely mediating the initial decreased activity of the biphasic motor

response to D2R agonists. In addition, presynaptic D2Rs are predominantly of the D2S isoform, while postsynaptic D2Rs are predominantly of the D2L isoform (Usiello et al., 2000, De Mei et al., 2009). As a result, different contributions of D2S and D2L isoforms are thought to also mediate the biphasic response of D2R agonists on motor behavior.

The most direct evidence for a dichotomy between direct and indirect pathways on motor output comes from optogenetics studies. Using Cre-dependent expression of the excitatory opsin channelrhodopsin-2 (ChR2) in the dorsal striatum of *Drd1*-Cre and *Drd2*-Cre mice, researchers have shown that activating dMSNs leads to increased movement initiation in freely-behaving animals, while activating iMSNs increases freezing and bradykinesia, and decreases initiation of movements (Kravitz et al., 2010). Similar optogenetic manipulations in the NA, however, do not elicit similar changes in locomotor activity (Lobo et al., 2010). In agreement with this negative finding, studies using optogenetics to activate dopaminergic terminals projecting from the VTA to the NA also did not show difference in locomotor activity induced by either phasic or tonic stimulation (Chaudhury et al., 2013). These studies suggest that the control of locomotor activity by the direct and indirect pathways and their modulation by dopamine may be mediated primarily by the dorsal striatum.

Other strategies have also been used to demonstrate the opposing effects on motor output by the direct and indirect pathways. For instance, in one study, researchers selectively ablated iMSNs in the entire striatum by locally delivering diphtheria toxin to animals that selectively expressed the diphtheria toxin receptor in iMSNs (Durieux et al., 2009). Consistent with a role of the indirect pathway in inhibiting locomotion, they found that ablating iMSNs induced hyperlocomotion in mice (Durieux et al., 2009). In another study, selective deletion of DARPP-32 in iMSNs or dMSNs was performed to probe the roles of direct and indirect pathways in

controlling motor behavior (Bateup et al., 2010). This study showed that DARPP-32 deletion in dMSNs decreased basal and psychostimulant-induced locomotion, while DARPP-32 deletion in iMSNs led to increased locomotor activity in mice (Bateup et al., 2010), thereby directly implicating DARPP-32 in supporting the opposing functions of direct and indirect pathways on motor behavior.

Despite evidence emphasizing the opposing functions of direct and indirect pathways, it is known that complex, coordinated activity of both pathways are necessary for the precise regulation of motor output. *In vivo* calcium imaging has shown that both dMSNs and iMSNs show increased activity when animals engage in motor actions, yet are inactive when animals are not moving (Cui et al., 2013). To expand on these observations, another study used *in vivo* electrophysiology to investigate how activity of dMSNs and iMSNs change while animals engage in action sequences. They confirmed that these two types of neurons are concomitantly active during initiation of action sequences, but their activities can differ while the action sequence is ongoing (Jin et al., 2014a). As previously suggested, based on the anatomical organization of the basal ganglia in segregated, parallel loops, these findings are consistent with a model in which both pathways are active in different loops when animals initiate movements: while the direct pathway functions to activate wanted motor programs, the indirect pathway may be activated to suppress unwanted motor programs. These studies further suggest the importance of balanced direct- and indirect-pathway output for appropriate control of motor behaviors.

MOTIVATION

The basal ganglia are also thought to regulate motivated behaviors, and this regulation has been largely studied in the context of dopaminergic modulation of striatal function. Motivation can be defined as the activation of goal-directed behavior. Animals have the adaptive

ability to approach life-sustaining aspects of their environment, which can be considered rewards, and to withdraw from what may be life-threatening. Motivation pertains to animals' goal-directed approach behavior to learned rewards, and potential rewards, including exploration of their environment and engagement in actions that have been previously reinforced by rewards. Furthermore, in addition to what is *external* and can produce and reinforce motivated behavior, the induced *internal* state that produces and reinforces such behaviors can also be considered rewarding (Ikemoto, 2010). This conceptual framework will be helpful in interpreting the body of data concerning how dopamine and the basal ganglia regulate motivation.

It is important to explicitly describe specific aspects of motivation and explain how researchers can probe different phases of reinforcement learning and the different components of motivation that are at play when subjects engage in reward-seeking behavior. In order to effectively engage in motivated behavior, subjects must first learn that certain actions lead to rewarding outcomes. In this initial phase, subjects can learn several features of an action-outcome association, which include the value of the reward, the amount of expended effort required to obtain the reward, and the specific action contingencies for achieving that outcome. Once subjects learn an action-outcome association, several components of motivation are simultaneously at play during reward-seeking behavior. For instance, animals must determine how to direct their behavior to specific actions based on how much they bias their decision on associations related to reward value, required effort, and contingency. These biases characterize motivational states that can be assessed experimentally with instrumental tasks by measuring both action selection and action vigor, which represent the “directional”, goal-directed component and the “activational”, arousal component of motivation, respectively (Salamone and Correa, 2012). Most of the behavioral studies described in this section attempt to understand how

the basal ganglia mediate motivated behavior by manipulating a specific aspect of basal ganglia function and assaying behavior. In reviewing these studies, I use the framework described above to identify reproducible findings that can guide understanding of how different striatal sub-region may selectively regulate motivated behavior through dopaminergic modulation of the direct and indirect pathways.

In the 1980s, Wolfram Schultz and colleagues conducted single-cell recordings of dopaminergic neurons in the midbrain in primates performing an instrumental task involving reaching movements for a food reward in response to auditory and visual cues (Aebischer and Schultz, 1984, Schultz, 1986). These researchers found that phasic activity of midbrain dopamine neurons that project to the striatum was associated with the presentation of the visual or auditory stimuli that would be followed by the food reward. Despite an established link between dopamine and motor function, execution of reaching movements was less significantly associated with dopaminergic activity, indicating that activity of midbrain dopaminergic neurons does not encode specific movement parameters. These observations gave rise to a model of reinforcement learning now known as the reward prediction error hypothesis that predicts that phasic dopamine release from midbrain neurons to the striatum signals a discrepancy between the predicted and expected rewarding properties of an outcome (Schultz, 1998).

The role of dopaminergic modulation of basal ganglia function on motivated behavior has been further supported by research with psychostimulant drugs, including cocaine and amphetamine, both of which strongly increases extracellular dopamine concentrations in the striatum (Di Chiara and Imperato, 1988). Researchers have applied the reward prediction error hypothesis to psychostimulant drug addiction, proposing that recurring drug-induced positive prediction errors produce a potentiated increase in the rewarding value of states or actions

associated with drug use, prompting compulsive drug-seeking behavior (Redish, 2004). However, the predictive value of this model of drug addiction has been challenged (Panlilio et al., 2007). Nevertheless, regardless of how drug-seeking behavior can be modeled using the reward prediction error hypothesis, studies investigating the reinforcing properties of psychostimulants have provided insight on how dopamine regulates goal-directed behavior by affecting basal ganglia function. Several lesion studies and intracranial self-administration studies have specifically implicated NA dopamine in the effects of psychostimulants on behavior. It has been demonstrated that psychostimulants preferentially increase dopamine concentrations in the NA compared to the dorsal striatum (Di Chiara and Imperato, 1988). In agreement with this observation, local depletion of dopamine with 6-OHDA or local infusion of dopamine receptor antagonists in self-administration studies suggest that psychostimulants act preferentially in the NA (Lyness et al., 1979, Roberts et al., 1980, Maldonado et al., 1993, McGregor and Roberts, 1993).

Although both psychostimulants and natural rewards lead to increased extracellular dopamine in the striatum, it has been estimated that drugs like cocaine and amphetamine increase concentrations of dopamine by an additional order of magnitude when compared to natural rewards, such as food and sexual stimuli (Damsma et al., 1992, McCullough and Salamone, 1992, Wise et al., 1995, Fiorino et al., 1997, Bassareo and Di Chiara, 1999, Ranaldi et al., 1999, Ikemoto et al., 2015). Despite inducing lower extracellular dopamine in the striatum and relatively smaller effects on motivated behavior compared to psychostimulants, a significant body of research has investigated the role of striatal dopamine in regulating motivation for natural rewards. And, as discussed below, similar to studies on the rewarding effects of

psychostimulant drugs, many studies of motivation for natural reward have also focused on the effects of dopamine in the NA.

A large body of literature has characterized how NA dopamine regulates motivation for food. In this field, researchers have been able to dissociate motivation from feeding behavior, as dopamine depletion or local infusions of D1R and D2R antagonists in the NA does not substantially impair food intake (Ungerstedt, 1971, Koob et al., 1978, Salamone et al., 1993, Baldo et al., 2002). Evidence also suggest that NA dopamine is not involved in the hedonic reactivity to food, as dopamine depletion in the NA does not decrease appetitive taste reactivity for food (Berridge and Robinson, 1998). Instead, researchers have demonstrated specific roles for NA dopamine on the goal-directed aspects of motivated behavior. For instance, in instrumental tasks in which animals are given the choice to either expend little or no effort to obtain a small reward or expend a greater effort to obtain a larger reward, dopamine depletion or pharmacological blockade of dopamine receptors in the NA reduce selection of the more effortful behaviors associated with higher reinforcement (Salamone et al., 1994). In line with a role of NA dopamine on reward-related action selection, one study using local infusions of dopamine antagonists into the NA showed that both D1R and D2R blockers impair operant responding specifically in situations in which animals had to select a new set of approach actions for reward-seeking, a behavior they call “flexible approach” (Nicola, 2010). Moreover, Pavlovian-to-instrumental transfer (PIT), defined as the ability of a reward-paired cue to initiate or invigorate reward-seeking actions, has also been shown to depend on NA dopamine (Parkinson et al., 2002). With the advent of optogenetics and cell-specific mouse lines, researchers have confirmed that dopamine release from the VTA to the NA is in itself rewarding, as measured by conditioned place preference and self-administration of light stimulation (Tsai et

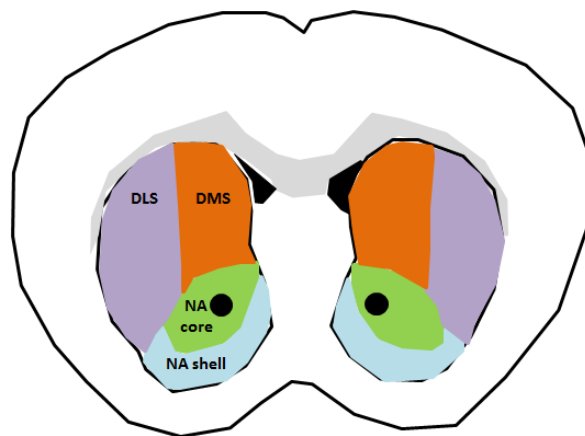
al., 2009, Ilango et al., 2014a, Steinberg et al., 2014). In addition, an optogenetics study using a food-seeking operant task showed that activation of dopaminergic neurons in the VTA facilitates the development of reinforcement during reward seeking (Adamantidis et al., 2011). Overall, therefore, studies using experimental methods as diverse as dopamine depletion, pharmacology, and optogenetic have established that dopamine modulation in the NA regulates many aspects of goal-directed behavior for natural rewards.

Despite a large body of evidence implicating dopaminergic projections from the VTA to the NA in motivation, even before the era of optogenetics, electrical stimulation studies had suggested that dopaminergic neurons in the SNc that project to the dorsal striatum are also involved in motivation (Routtenberg and Malsbury, 1969, Ritter and Stein, 1974, Corbett and Wise, 1980). And more recently,

optogenetics studies have further confirmed that stimulation of dopaminergic neurons in the SNc can be as rewarding as stimulation of dopaminergic neurons in the VTA

(Rossi et al., 2013, Ilango et al., 2014b).

Given that dopamine modulation of both dorsal and ventral regions of the striatum have been linked to motivation, many lesion and pharmacological studies have also



- Dorsomedial striatum** → goal-directed behavior, performance vigor
- Dorsolateral striatum** → habit formation
- Nucleus accumbens core** → goal-directed behavior, effort-based choices
- Nucleus accumbens shell** → sensory specificity of outcomes, hedonic reactivity

Figure 2: Striatal sub-regions and motivation. The striatum can be divided into dorsal and ventral regions. The dorsal striatum can be further subdivided into dorsomedial striatum (DMS) and dorsolateral striatum (DLS). The ventral part of the striatum is the nucleus accumbens (NA), which is composed of both core and shell compartments. Lesion and pharmacological studies have implicated each of these striatal sub-regions in specific aspects of motivated behavior.

sought to identify how sub-regions of the striatum may be selectively important for different aspects of motivation. In the remainder of this section, I describe in detail a number of findings pertaining to the involvement of different striatal sub-regions on specific aspects of motivation. The general conclusions that can be drawn from these studies are summarized in Figure 2.

Similar and distinct roles for the NA core and shell in different aspects of motivated behavior have been demonstrated. In a pharmacological study, infusion of D1R or D2R antagonists selectively into the NA core or shell showed that dopamine antagonism into either region could reduce instrumental responding for high-effort rewards (Nowend et al., 2001). A role for effort-based decision making was further confirmed for the NA core, as dopamine depletion of this region similarly impaired behavioral response to high-effort rewards in a cost-benefit T-maze task (Mai et al., 2012). Using a different approach to decrease NA function, a study using infusions of muscimol and baclofen into the shell or core compartments of the NA demonstrated that the NA core, but not the shell, appears to be part of the neural circuit that biases choices towards larger rewards associated with a greater effort cost (Ghods-Sharifi and Floresco, 2010). Other specific dissociations between NA sub-compartments have been identified. For instance, post-training excitotoxic lesions of the NA core, but not the shell, selectively affected outcome devaluation (Corbit et al., 2001), implicating the NA core in encoding the value of rewards. In the same study, animals with lesions in the NA shell had intact sensitivity to reward value, but instead failed to show positive transfer in a PIT test (Corbit et al., 2001). Researchers have attempted to distinguish how NA core and shell regulate two different types of PIT, general PIT (G-PIT) and outcome-specific PIT (S-PIT). While G-PIT is usually demonstrated using a single response procedure, which is typically interpreted in terms of the general arousing properties of the conditioned stimulus, in S-PIT animals are usually given

Pavlovian conditioning with two conditioned stimuli each paired with different outcomes and tested on how each stimulus can influence specific instrumental responding. A dissociation between NA sub-regions was found in a study showing that muscimol inactivation of the NA core abolished G-PIT and spared S-PIT, while inactivation of the NA shell abolished S-PIT and spared G-PIT (Corbit and Balleine, 2011). This finding is in line with previous studies showing that excitotoxic lesion or infusion of dopamine antagonists selectively into the NA core also abolished G-PIT (Hall et al., 2001, Lex and Hauber, 2008). These studies, therefore, point to a role of the NA shell in processing the sensory specificity of outcomes. Consistent with this idea, researchers have shown that the NA shell, but not other striatal sub-regions, can mediate animals' hedonic experience of rewards via the opioid system in the striatum (Pecina and Berridge, 2005, Castro and Berridge, 2014). Thus, while the NA core have been implicated in goal-directed behavior by modulating reward-seeking behavior based on reward value and effort, the NA shell seems to be more involved in processing the sensory specificity of outcomes, including hedonic reactivity to rewards through processes that appear to be independent of dopamine.

Functional and anatomical studies of the dorsal striatum predict a stronger link between the DMS and motivation than between the DLS and motivation because the DMS receives inputs from prefrontal cortex and anterior cingulate, regions that have been implicated in affective functions, while the DLS receives inputs predominantly from sensorimotor cortex (Pan et al., 2010). Behavioral experiments have indeed confirmed this dissociation. For instance, excitotoxic lesions to the DLS, but not the DMS, disrupt habit formation of operant responding and does not affect sensitivity to the reward value (Yin et al., 2004, Hilario et al., 2012). In contrast, lesions to the DMS done either before or after instrumental training revealed that the DMS plays a role in

the acquisition of action-outcome associations as well as in the expression of these associations by encoding outcome value and contingency (Yin et al., 2005). The DMS has also been linked to action vigor, as one study showed that excitotoxic lesion to this striatal sub-region impaired state-dependent modulation of vigor in an instrumental task in rodents (Wang et al., 2013). Thus, while the DLS has been more clearly linked to motor function and appears to mediate habit formation in instrumental tasks of incentive motivation, the DMS has been consistently implicated in goal-directed behavior and in modulating performance vigor.

Although a number of studies have identified or proposed specific mechanisms by which dopamine may modulate motivated behavior and have provided insight on which striatal sub-regions may be important for specific aspects of motivation, few studies have rigorously probed how the direct and indirect pathways of the basal ganglia control specific aspects of motivation. And most studies that have manipulated these two pathways selectively have studied motivation for drugs of abuse (Durieux et al., 2009, Lobo et al., 2010, Bock et al., 2013, Hikida et al., 2013). The few studies investigating pathway-specific functions in motivation for natural rewards support an opposing influence of direct and indirect pathways on reward-seeking behavior, similar to that proposed for motor behavior. For instance, one study using optogenetics to bypass dopamine signaling and selectively activate dMSNs and iMSNs in the DMS in mice showed that activation of the direct pathway appeared to be rewarding and led to persistent self-stimulation, while indirect pathway stimulation appeared to be aversive on a more transient timescale (Kravitz et al., 2012). Another study using optogenetics to selectively stimulate dMSNs or iMSNs in the DMS demonstrated that selective activation of each pathway can introduce opposite biases in the distribution of choices in an operant task of goal-directed action selection (Tai et al., 2012). Although these studies help understand how the parallel pathways of the basal

ganglia arising from different striatal sub-regions regulate motivated behavior for natural rewards, more research is needed in this field.

In conclusion, incentive motivation, defined as the activation of goal-directed behavior, requires learning of action-outcome associations and can be dissected into separate components, such as action selection and action vigor, that can often be studied experimentally. Dopaminergic modulation of specific striatal sub-regions has been selectively implicated in different aspects of motivated behavior for natural rewards. And basal ganglia output regulated by activity of the direct and indirect pathways has also been linked to motivation. However, although genetic tools have become available for selectively targeting neuronal populations in the rodent striatum, comprehensive studies using these tools to probe how dMSNs and iMSNs in different striatal sub-regions regulate motivation for natural rewards are still lacking.

STRIATAL PATHWAYS AND DISEASE

Dysfunction of the basal ganglia has been implicated in many neuropsychiatric diseases, many of which involve abnormalities in motor functions or motivation. These diseases include Parkinson's disease, Huntington's disease, drug addiction, obsessive-compulsive disorder (OCD), Tourette's syndrome, attention deficit hyperactivity disorder (ADHD), and schizophrenia. In this section, I will first provide an overview of how basal ganglia dysfunction has been shown to underlie symptoms in each of these disorders, with particular emphasis on dopaminergic modulation of the direct and indirect pathways. Then I will describe in more detail research on schizophrenia that implicates D2R hyperfunction in certain symptoms of this disease. Large emphasis will be placed on one particular mouse model of schizophrenia

endophenotypes, as insight obtained from this model provided the groundwork for most of the studies I present in this dissertation.

Dysfunction of the basal ganglia underlies many motor neurological disorders, including Parkinson's disease and Huntington's disease. In Parkinson's disease, muscular rigidity, bradykinesia postural instability, and tremor are thought to be caused by depletion of dopamine in the midbrain (Albin et al., 1989). Lack of dopaminergic modulation of both direct and indirect pathways can explain impaired motor output when considering that dopamine normally acts to disinhibit basal ganglia output to the thalamus via these two parallel pathways. Interestingly, even though Parkinson's disease is more notably characterized by motor abnormalities, lack of motivation is also highly prevalent in patients with this disease (Pedersen et al., 2009). And although largely correlational, imaging studies have demonstrated differences in dopamine binding to D2Rs between patients with Parkinson's diseases with lack of motivation and those without this symptom (Thobois et al., 2010). The motor symptoms observed in Huntington's disease can also be explained using the classic model of basal ganglia circuitry. This disease is characterized by abnormal involuntary writhing movements, known as chorea, that result from a polyglutamine expansion in the ubiquitously-expressed huntingtin protein, which for unknown reasons leads to the degeneration of certain types of neurons, including striatal MSNs. The classical model of basal ganglia circuitry has been employed to explain symptoms in Huntington's disease, with researchers proposing that hyperkinetic, choreic movements in the early stages of disease result from initial dysfunction of iMSNs, which are preferentially lost in this disorder, while hypokinesia during the late disease stages is a consequence of further injury to dMSNs (Reiner et al., 1988, Spektor et al., 2002).

The basal ganglia have been also implicated in symptoms in a number of psychiatric disorders, including drug addiction, OCD, Tourette's syndrome, and ADHD. Drug addiction can be classified as a disorder of abnormally high motivation that leads patients to lose control over drug intake. Given that drugs of abuse increase extracellular dopamine in the striatum and can theoretically promote reward-seeking behavior via effects on both direct and indirect pathways, the basal ganglia have been hypothesized to be a site where the neuroplastic events that underlie addictive behaviors take place (Lobo and Nestler, 2011, Luscher and Malenka, 2011, Nestler, 2013, van Huijstee and Mansvelder, 2014). Among patients with OCD, structural abnormalities in cortico-basal ganglia-thalamo-cortical loops have been demonstrated (Rodman et al., 2012, de Wit et al., 2014). And one of the current hypotheses for the etiology of OCD is that abnormal activity in the orbitofrontal cortex and NA underlie symptoms. This hypothesis is supported by findings in rodent models that stimulation of this specific cortico-striatal loop can both produce and ameliorate compulsive-like behaviors (Ahmari et al., 2013, Burguiere et al., 2013, Ahmari, 2015). Among neurodevelopmental disorders, Tourette's syndrome is characterized by simple and complex motor tics, and local pharmacological inactivation of dorsal striatal neurons has been able to reproduce some of these repetitive behaviors in primates (Worbe et al., 2009). Finally, ADHD is a neurodevelopmental disorder that leads to hyperactivity, impulsiveness, and cognitive impairments. Psychostimulants that increase extracellular levels of dopamine are paradoxically efficacious in treating this disorder, and the theories that have been proposed to explain this phenomenon have posited that patients with ADHD have either abnormal cortico-basal ganglia-thalamo-cortical activity (Vaidya et al., 1998, Max et al., 2002, Sullivan and Brake, 2003, Shafritz et al., 2004) or abnormal dopaminergic modulation in the basal ganglia (Gainetdinov and Caron, 2001, Heiser et al., 2004, Larisch et al., 2006).

Schizophrenia is a highly heterogeneous disorder that is characterized by so-called positive, negative and cognitive symptoms. The positive symptoms – also known as psychotic symptoms – include hallucinations, delusions and disordered thought processes. However, most patients also exhibit impairments in a number of social, emotional and cognitive behaviors. Such deficits are categorized as either negative symptoms (e.g. social withdrawal, anhedonia and deficits in incentive motivation) or cognitive symptoms (e.g. impairments in working memory, behavioral flexibility, verbal memory, reference memory and cognitive processing speed). Although negative and cognitive symptoms are not required for diagnosis, they are present in a high proportion of patients and can be particularly insidious for patient outcomes (Fenton and McGlashan, 1991, Green et al., 2000). At the global functional level, the basal ganglia have been implicated in both positive and negative symptoms of schizophrenia. Neuroimaging studies have demonstrated abnormal basal ganglia activity while patients engage in tasks of reinforcement learning that characterize the negative symptoms (Esslinger et al., 2012, Nielsen et al., 2012). In addition, it has been shown that intrinsic activity in the striatum is increased in patients during psychosis and correlates with severity of positive symptoms (Ettinger et al., 2013). Therefore, it has been proposed that altered basal ganglia function is part of the etiology of the disorder (Simpson et al., 2010).

The dopaminergic system is the neurotransmitter system most robustly implicated in schizophrenia pathology, with disruptions in subcortical dopamine systems linked to the positive symptoms and disruptions in cortical dopamine transmission linked to cognitive impairment. The former idea refers to the long-standing dopamine hypothesis originally formulated by van Rossum in the 1960s, which posits that dopamine hyperactivity is central to psychosis in schizophrenia (Baumeister and Francis, 2002). In the 1950s, the dopamine

antagonist chlorpromazine was accidentally discovered as an antipsychotic medication. Later in the 1970s Philipp Seeman, Solomon Snyder and colleagues found that the therapeutic dose of antipsychotic medication is inversely proportional to their binding affinity for dopamine receptors (Creese et al., 1976, Seeman et al., 1976). Despite many efforts by the pharmaceutical industry, all antipsychotic medications used to treat patients with schizophrenia still target D2Rs – the main site of action of chlorpromazine.

Using post-mortem analyses, direct evidence for alterations in the dopamine system were uncovered in the 1980s. These studies consistently showed increased levels of D2Rs in the brains of patients with schizophrenia (Mita et al., 1986, Hess et al., 1987), particularly in the striatum (Joyce et al., 1988, Marzella and Copolov, 1997). Numerous imaging studies have also pointed to increased density of D2Rs in the striatum of patients with schizophrenia, with Laruelle calculating a 12% increase in striatal D2R density in drug-naïve or drug-free patients after comparing 13 imaging studies (Laruelle, 1998). However, a more recent meta-analysis suggests it is still unclear whether the increase in D2R density is truly present early in the disorder or if it is due to subsequent antipsychotic treatment (Howes et al., 2012). Dopamine depletion experiments have additionally reported increased basal occupancy of striatal D2Rs in drug-free patients that not only correlates with positive symptoms but predicts their response to antipsychotics, thus suggesting a tight relationship between D2R hyperfunction in the striatum and psychosis (Abi-Dargham et al., 2000).

Impairments in the striatal dopamine system have also been observed at the presynaptic level. Increased striatal uptake of ^{18}F -fluorodopa (or L- β - ^{11}C -DOPA) and increased amphetamine-induced dopamine release have been repeatedly measured in patients as an indication of presynaptic dopamine hyperfunction (Howes et al., 2012). These alterations appear

to occur early on in the disease process as they are observed in prodromal subjects that are at high risk for conversion to schizophrenia (Howes et al., 2009), and newer imaging tools with higher spatial resolution have revealed that the largest effect size of these abnormalities is not in the limbic striatum, as has been postulated for many years, but rather in the associative striatum – a striatal area that receives dense input from several prefrontal cortical areas, including the dorsolateral prefrontal cortex (Kegeles et al., 2010, Howes et al., 2012).

Based on the above-described observations of increased D2R occupancy and density in the striatum of patients, a mouse model that overexpresses D2Rs throughout development selectively in the striatum was developed to reproduce this pathophysiological aspect of schizophrenia. This approach allows for an assessment of the causal consequences on brain function and on behaviors relevant to the cognitive or negative symptoms that are downstream of striatal D2R hyperfunction. Specifically, the bi-transgenic tetracycline-sensitive expression system was used to selectively overexpress D2Rs in the striatum in a temporally controlled, reversible manner to generate the D2R-OE_{dev} mice (Kellendonk et al., 2006). D2R-OE_{dev} mice have 15% higher D2R binding capacity than wild-type mice, which is in the range of what has been calculated by a meta-analysis of imaging studies in patients with schizophrenia (Kellendonk et al., 2006). D2R-OE_{dev} mice display cognitive deficits in working memory, a well-established cognitive deficit of the disorder (Bach et al., 2008), as well as deficits in incentive motivation, with rigorous behavioral testing of D2R-OE_{dev} mice revealing that this motivational deficit cannot be explained by anhedonia, motor dysfunction or decreased appetite (Drew et al., 2007, Ward et al., 2009, Simpson et al., 2011, Simpson et al., 2012). Instead, this deficit is associated with an inability to adapt behavior to reward and reflects a deficit in incentive motivation similar to what has been observed in patients with schizophrenia (Fervaha et al., 2013, Gold et al., 2013,

Wolf et al., 2014). The deficit in motivation observed in D2R-OE_{dev} mice can be rescued when the overexpression of D2Rs is reversed to normal levels by switching off transgene expression, suggesting that concurrent up-regulation of D2Rs in the striatum is contributing to this deficit (Drew et al., 2007).

In an attempt to more precisely and mechanistically understand how this pathophysiology may contribute to the motivational deficit, the Kellendonk laboratory examined how upregulation of D2Rs in striatal MSNs affects the physiological function and anatomical connectivity of these neurons. Published work from the Kellendonk laboratory showed that D2R-OE_{dev} mice have increased neuronal excitability and decreased dendritic arborization of MSNs in both the direct and indirect pathways that result from decreased function and expression of the inward rectifier potassium channel 2 family (K_{ir}2.1/2.3) (Cazorla et al., 2012). These physiological and morphological changes are reversed by switching off transgene expression in adult animals and restoring D2R expression to normal levels (Cazorla et al., 2012). Moreover, evidence from this mouse model suggests that D2R overexpression not only increases MSN excitability but also alters the anatomical and functional balance of the dorsal striatal output pathways (Cazorla et al., 2014). Axon collaterals of dMSNs that target the GPe have the potential to bridge direct and indirect pathways and alter the balance of basal ganglia output; therefore, they have been referred to as “bridging collaterals”. Studies in the Kellendonk laboratory has shown that the bridging collaterals are extremely plastic in the adult animal and their density appears to be regulated by D2R expression (Cazorla et al., 2014). Genetic up-regulation of striatal D2Rs enhances the density of bridging collaterals, whereas genetic down-regulation leads to a gene dosage-dependent decrease (Cazorla et al., 2014). Moreover, increased bridging collaterals of D2R-OE_{dev} mice can be reversed by reinstating lower excitability by re-

expressing wild-type K_{ir2} channels in the striatum (Cazorla et al., 2014). The functional importance of these bridging collaterals has been confirmed with *in vivo* direct pathway stimulation during anesthetized recordings of GPe activity and also using *in vivo* direct pathway stimulation in behaving animals. *In vivo* recordings during direct pathway stimulation in D2R-OE_{dev} mice revealed enhanced inhibition of GPe activity, and *in vivo* direct pathway stimulation in D2R-OE_{dev} mice impaired the behavioral activation that is normally observed after stimulation of the direct pathway (Kravitz et al., 2010, Cazorla et al., 2014). Together, these results strongly suggest that the reversible anatomical changes observed in the bridging collaterals of the dorsal striatum in D2R-OE_{dev} mice are a consequence of the alteration in neuronal excitability that result from decreased K_{ir2} expression in MSNs. The reversibility of motivational deficits, MSN excitability, and bridging collateral density when switching off D2R up-regulation offers an enticing link between pathophysiology and behavior.

CHAPTER 2

BRIDGING COLLATERALS

INTRODUCTION

In the classical model of basal ganglia circuitry, the direct and indirect pathways arising from striatal MSNs are often described as segregated both functionally and anatomically. However, a number of studies have challenged this view. Tracing studies in rodents have demonstrated that MSNs that project to the GPi and SNr have axon collaterals that target the GPe (Kawaguchi et al., 1990, Wu et al., 2000, Fujiyama et al., 2011). Similar findings were also confirmed in primates (Levesque and Parent, 2005). In fact, these studies suggest that only a small minority of striatal MSNs (3% of all labeled neurons in the rat) project only to the output structures of the basal ganglia, while closer to half (60% of all labeled neurons) project to the GPi and SNr and possess axon collateral terminal fields in the GPe (Kawaguchi et al., 1990, Wu et al., 2000, Fujiyama et al., 2011). Anatomically, these collaterals have the potential to bridge the direct and indirect pathways, and they are referred to here as “bridging collaterals”. The functional relevance of the bridging collaterals in regulating the output of the basal ganglia and behaviors that depend on the balance of direct and indirect pathways is still largely unknown.

A mouse model of chronic upregulation of D2Rs in the striatum provides some insight on the potential regulatory mechanisms and functional relevance of the bridging collaterals. Transgenic D2Rs are overexpressed throughout development in striatal MSNs of D2R-OE_{dev} mice, and this mouse has been shown to model endophenotypes of schizophrenia (Kellendonk et al., 2006, Drew et al., 2007). D2R-OE_{dev} mice display more excitable MSNs, a phenotype that can be reversed by turning off transgenic overexpression of D2Rs in adulthood (Cazorla et al.,

2012) (Figure 3A). Similarly, these animals display increased density of bridging collaterals when D2Rs are overexpressed (Figure 3B). In addition, the density of collaterals can be reduced to control levels when D2R overexpression is genetically turned off in the adult and reversed back to high levels when the striatal D2R transgene is subsequently allowed to be expressed (Figure 3C). These findings suggest that bridging collaterals are highly plastic in adult animals. The observations that MSN excitability and density of bridging collaterals can be modulated by

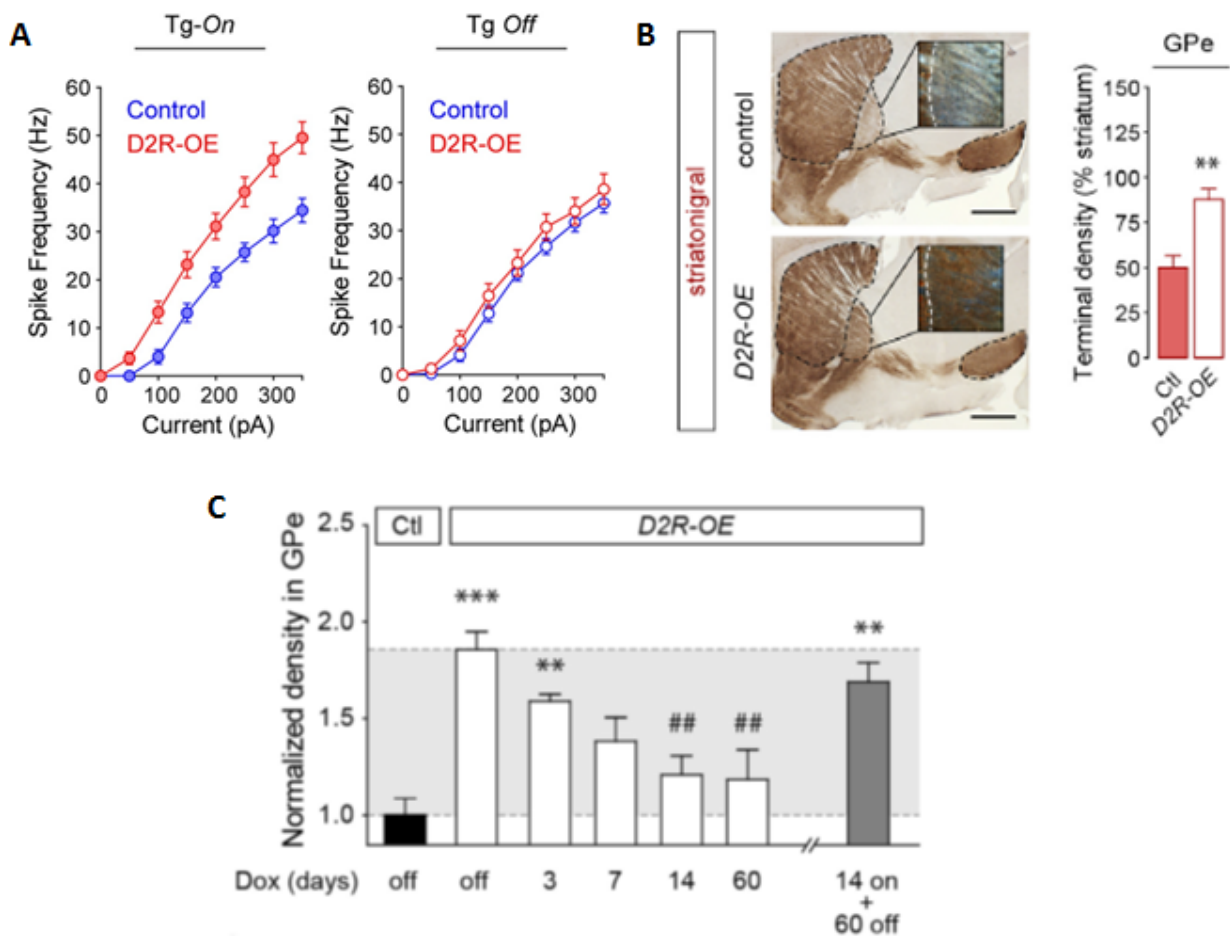


Figure 3: Physiological and anatomical changes can be induced by dopamine D2 receptor (D2R) upregulation in the striatum. **A.** Input-output curves for MSNs recorded from 3-month-old D2R-OE_{dev} mice are significantly right-shifted compared to those for MSNs of control mice; this difference is reversed when transgenic D2R overexpression is turned off (Cazorla et al., 2012). **B.** Bridging terminals of dMSNs in the GPe are increased in D2R-OE_{dev} mice (Cazorla et al., 2014). **C.** Kinetics of bridging collateral retraction in the GPe of D2R-OE_{dev} mice treated with doxycycline for increasing time periods and regrowth after re-expressing the transgene for 60 days (14 on + 60 off) (Cazorla et al., 2014).

D2R expression in the striatum raise the question of whether some of the behavioral phenotypes of D2R-OE_{dev} mice may be mediated by the bridging collaterals.

Moreover, direct evidence that terminal fields of dMSN in the GPe form functional synapses with pallidal neurons is lacking. In an attempt to address this question, previous work in the Kellendonk laboratory used *in vivo* electrophysiology to show that optogenetic stimulation of dMSNs leads to greater inhibition of GPe activity in D2R-OE_{dev} mice compared to control littermates, presumably because of increased bridging collaterals (Cazorla et al., 2014) (Figure 4). Inhibition of the pallidum after activation of the dMSNs was compared to inhibition induced by activation of iMSNs, an established monosynaptic pathway. Since the time course of inhibition following stimulation of dMSNs or iMSNs were comparable, these electrophysiology data are consistent with a functional monosynaptic pathway emerging also from dMSNs via the bridging collaterals. To further confirm this interpretation, I attempted to use a different

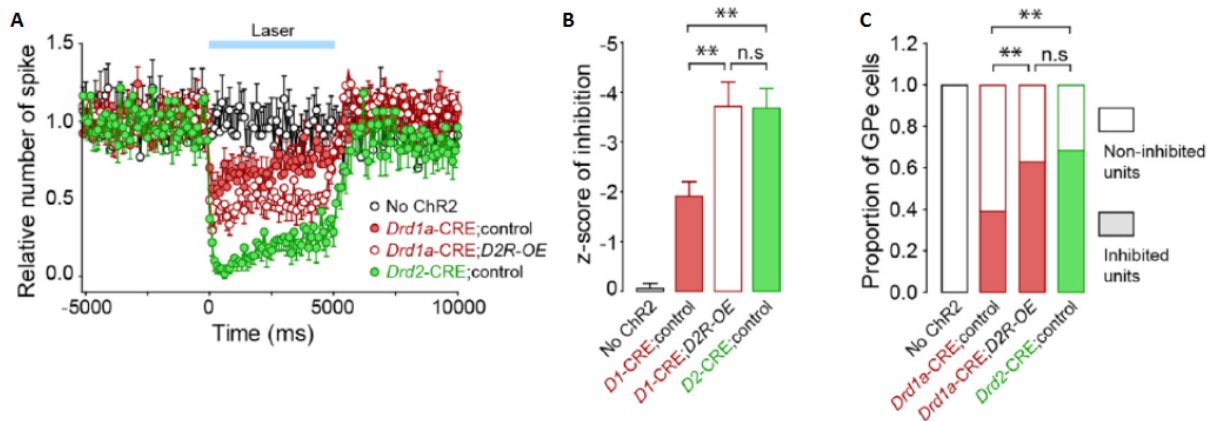


Figure 4: Increased bridging collaterals are associated with enhanced GPe inhibition. Optogenetic activation of the direct pathway reveals inhibition in the GPe that is enhanced in D2R-OE_{dev} mice. **A.** Graphs of relative firing frequency in GPe neurons for direct comparison of four groups before, during, and after 5-s laser illumination. **B.** Change in firing rate during laser-induced stimulation of direct or indirect pathway expressed as a z score of the pre-stimulation firing rate distribution. **C.** Proportion of GPe cell units for which basal firing rate is significantly decreased after laser stimulation. (Cazorla et al., 2014).

approach to positively establish that dMSNs form synaptic contacts in the GPe. I selectively transfected dMSNs with a virus vector designed to label synaptic sites in order to determine whether dMSNs form synapses in the GPe that would correspond to the terminal fields of the bridging collaterals.

In many circuits in the brain, neuronal activity has been shown to regulate axonal projections and shape connectivity between brain structures (Catalano and Shatz, 1998, Hua et al., 2005, De Marco Garcia et al., 2011). Given that D2R-OE_{dev} mice exhibit more excitable striatal MSNs, the Kellendonk laboratory has investigated whether increased activity in these neurons can mediate plasticity involving the growth of bridging collaterals. Previous work has demonstrated that decreased function of K_{ir}2 channels could account for increased MSN excitability in D2R-OE_{dev} mice (Cazorla et al., 2012) (Figure 5A-B). Moreover, rescuing excitability of MSNs in D2R-OE_{dev} mice by overexpressing the wild-type K_{ir}2.1 channel in the striatum or by treating animals chronically with the D2R antagonist haloperidol was sufficient to retract bridging collaterals in the adult animal (Cazorla et al., 2014) (Figures 5C-D). These findings led to the question of whether activity-dependent plasticity involving bridging collaterals was only relevant in the D2R-OE_{dev} mouse model or whether excitability could also be involved in regulating bridging collaterals in developmentally normal animals.

The endogenous K_{ir}2.1 channel is a tetrameric ion channel that is abundantly expressed in striatal MSNs and is responsible for rapid inward rectification of potassium from the extracellular space, preventing high extracellular potassium from depolarizing neurons. The K_{ir}2.1^{AAA} gene codes for a mutant monomer – the GYG motif of the pore region is replaced by three alanine residues (AAA) – that renders the channel inactive when incorporated into its tetrameric structure, resulting in a dominant-negative effect that effectively increases excitability

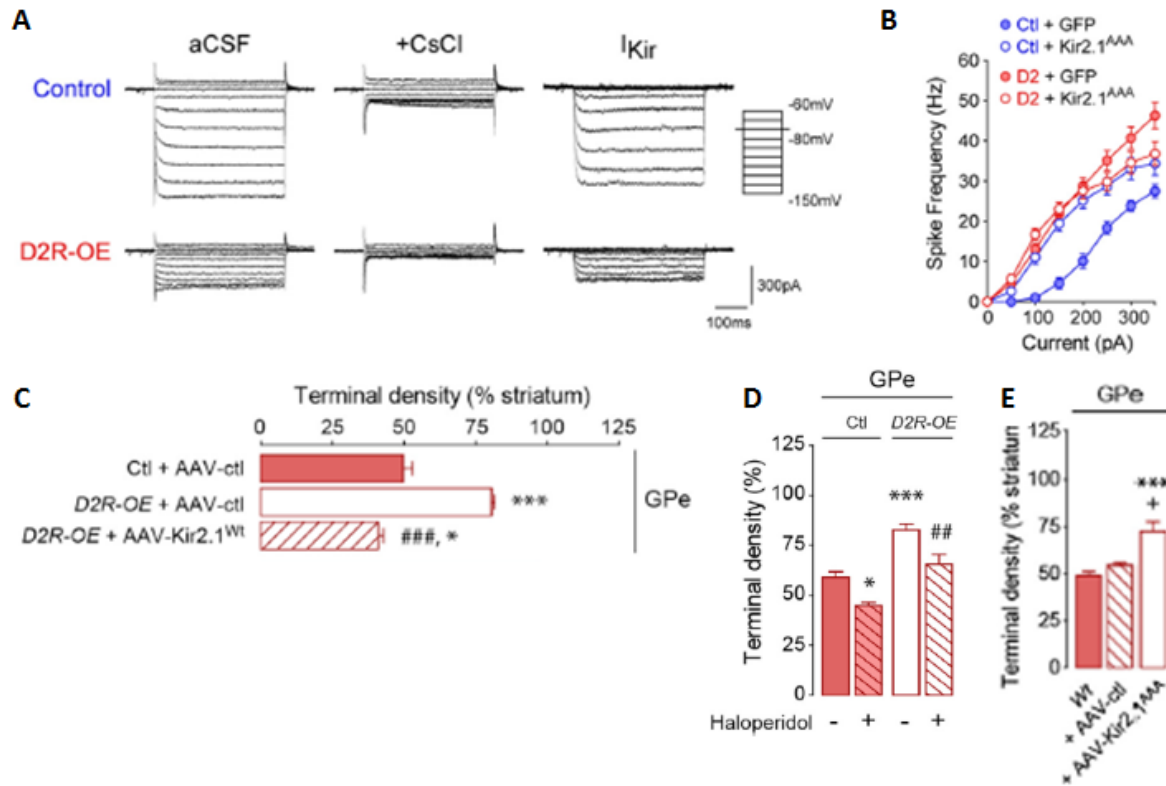


Figure 5: D2R overexpression decreases striatal inward rectifying currents through downregulation of K_{ir2} channels. **A.** Representative inward rectifying currents obtained for negative membrane potentials (-60 to -150 mV in 10-mV steps) in control and D2R-OE_{dev} mice (Cazorla et al., 2012). K_{ir} channel currents (I_{Kir}) are isolated by subtracting remaining currents in presence of cesium (CsCl) to total currents (ACSF). **B.** Striatal expression of the dominant-negative $K_{ir2.1}^{AAA}$ channel is sufficient to induce MSN hyperexcitability measured by comparing input-output curves (Cazorla et al., 2012). **C.** Increased bridging terminal density is restored in D2R-OE_{dev} mice after striatal transfection with AAV-Kir2.1WT-IRES-hrGFP (Cazorla et al., 2014). **D.** Bridging collaterals show reduced density in D2R-OE_{dev} mice and control littermates after treatment with haloperidol for 14 days (Cazorla et al., 2014). **E.** Increasing MSN excitability promotes the growth of bridging collaterals terminal fields in the GPe of adult mice (Cazorla et al., 2014).

of neurons expressing this transgene (Preisig-Muller et al., 2002, Cazorla et al., 2012). The Kellendonk laboratory has expressed $K_{ir2.1}^{AAA}$ in the striatum to show that increasing MSN excitability by decreasing function of this channel in the striatum can induce growth of bridging collaterals in wild-type animals (Cazorla et al., 2014) (Figure 5E). Based on these observations, I further studied regulation of bridging collaterals by selectively increasing excitability in iMSNs and dMSNs to determine whether activity-dependent plasticity mediating growth of the bridging

collaterals may be specifically controlled by the direct or indirect pathways of the basal ganglia. I therefore generated an adeno-associated virus (AAV) to manipulate excitability of specific neuronal populations in the striatum via Cre-dependent expression of the trans-dominant negative mutant $K_{ir}2.1^{AAA}$ channel.

In addition, I also investigated how bridging collaterals may be relevant for behavior. Optogenetic stimulation of the direct pathway has been shown to induce increased locomotor activity in mice (Kravitz et al., 2010). Using a similar paradigm, the Kellendonk laboratory expressed ChR2 in the direct pathway of D2R-OE_{dev} mice and control littermates to test for a behavioral phenotype that could be linked to the bridging collaterals. This experiment confirmed that stimulation of dMSNs increases locomotion in control mice, while in D2R-OE_{dev} mice, stimulation of dMSNs led to a paradoxical decrease in locomotion. In addition, when $K_{ir}2.1^{AAA}$ was expressed in the indirect pathway in the dorsal striatum of developmentally normal animals, a manipulation that leads to increased density of bridging collaterals, stimulation of dMSNs also led to decreased locomotor activity (Cazorla et al., 2014) (Figure 6). Based on these findings, I attempted to further confirm the link between the bridging collaterals and this behavioral phenotype by investigating whether treating D2R-OE_{dev} mice chronically with haloperidol, a manipulation previously shown to retract bridging collaterals, could rescue the abnormal locomotor response to activation of dMSNs in D2R-OE_{dev} mice.

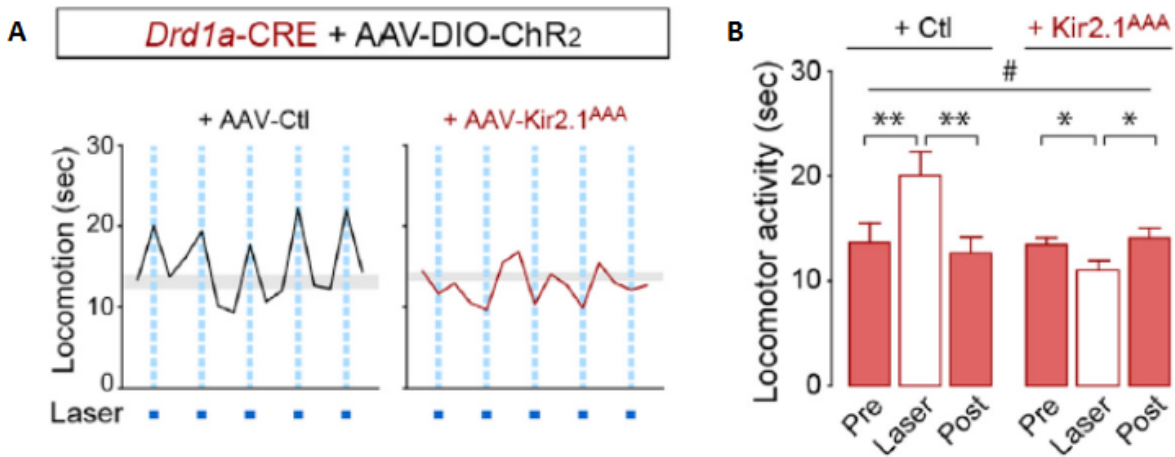


Figure 6: Increased bridging collaterals are associated with disrupted behavioral activation of direct pathway. Behavioral activation after direct-pathway stimulation is disrupted in mice expressing Kir2.1^{AAA} in the striatum. **A.** Traces showing mean locomotor activity of mice co-expressing Cre-dependent ChR2 and non-conditional Kir2.1^{AAA} or a control gene in the striatum during open field performance. **B.** Mean locomotor activity of 5 30-s sessions before laser stimulation (pre), during laser stimulation (laser), and after laser stimulation (post) for mice in both groups (Cazorla et al., 2014).

Furthermore, evidence that growth and retraction of the bridging collaterals can be affected by D2Rs via their effects on neuronal excitability suggested that regulating the density of bridging collaterals could be a mechanism by which chronic changes in the dopamine system modulate basal ganglia output. Due to the importance of the basal ganglia in motor coordination, I tested D2R-OE_{dev} mice in the rotarod test of motor performance and found that D2R-OE_{dev} mice show a deficit in motor coordination. However, D2R-OE_{dev} mice improve their performance in the rotarod test with ongoing training and, after three weeks, reach the level of performance of control littermates. Given the evidence for exercise-dependent functional plasticity in cortico-striatal input (Costa et al., 2004), I asked whether retraction of collaterals was associated with improved motor performance in D2R-OE_{dev} mice. In addition, I also investigated whether rotarod training could reverse the functional imbalance of the direct and indirect pathways in D2R-OE_{dev} mice.

Thus, based on previous work done in the Kellendonk laboratory establishing a link between D2R function in the striatum and the bridging collaterals, I conducted a series of experiments to expand on these findings. First, I confirm that dMSNs form synaptic contacts in the GPe. Second, I provide anatomical and behavioral evidence that further supports a link between indirect-pathway function and plasticity involving the bridging collaterals. And finally, I describe a novel phenomenon whereby behavioral intervention can modify anatomical connectivity in the brain and affect the balance of direct and indirect pathways.

MATERIALS AND METHODS

Viral construct

The AAV1/2-Syn-DIO-Synaptophysin-GFP virus was obtained from Dr. Thomas Jessell, and the AAV5-EF1 α -DIO-ChR2(H134R)-eYFP and AAV2-EF1 α -DIO-mCherry viruses were purchased from the University of North Carolina Vector Core. The AAV2/1-Syn-DIO-Kir2.1AAA-IRES-mCherry virus was made from a DNA construct generated by molecular cloning. To generate the Syn-DIO-Kir2.1AAA-IRES-mCherry viral construct, the IRES-mCherry sequence, excised using the restriction enzyme *NotI* from IRES-mCherry3Myc-pCAGEN (obtained from Dr. Jonathan Javitch), was ligated into pcDNA3.1-IRKAAA-HA (obtained from Dr. Paul Slesinger) immediately following the IRKAAA-HA sequence after linearizing the latter plasmid with *BamHI*. The IRKAAA-HA-IRES-mCherry sequence from the resulting plasmid was amplified by PCR with designer primers to introduce *NheI* and *AscI* restriction sites flanking the amplified sequence. The PCR product was then digested with *NheI* and *AscI*, and the digested fragment was ligated to the backbone fragment of pAAV-Syn-DIO-SF-D2RL-Venus (obtained from Dr. Jonathan Javitch), also digested with *NheI* and *AscI*. This

procedure led to replacement of the SF-D2RL-Venus sequence with the IRKAAA-HA-IRES-mCherry sequence. The DIO-Kir2.1AAA-IRES-mCherry DNA construct was submitted to Vector Biolabs for packaging into AAV2/1.

Animals

All animal protocols used in the present study were approved by the Institutional Animal Care and Use Committees of Columbia University and New York State Psychiatric Institute. *Drd1*-GFP (X60Gsat/Mmmh), *Drd1*-Cre (FK150Gsat/Mmcd), and *Drd2*-Cre (ER44Gsat/Mmcd) mice on a C57BL/6J background were purchased from the Mutant Mouse Resource & Research Centers (National Institutes of Health). *Drd1*-GFP mice were crossed to either *Drd1*-Cre or *Drd2*-Cre mice to obtain *Drd1*-GFP/*Drd1*-Cre or *Drd1*-GFP/*Drd2*-Cre double transgenic mice, respectively. The generation of D2R-OE_{dev} mice has been described previously (Kellendonk et al., 2006). TetO-D2R mice have been backcrossed onto the C57BL/6J background and CaMKII α -tTA mice backcrossed onto the 129SveVTac background. To generate D2R-OE_{dev} mice, tetO-D2R/C57BL6 mice were crossed with CaMKII α -tTA/129SveVTac mice. Double transgenic mice express the transgenic D2R, and these animals were crossed to *Drd1*-GFP or *Drd1*-Cre mice to obtain the triple transgenic D2R-OE_{dev}/*Drd1*-GFP or D2R-OE/*Drd1*-Cre mice, respectively. For all experiments that included D2R-OE_{dev} animals, controls were littermates that were positive for the Cre or GFP transgenes but negative for the TetO or tTa transgenes. Both male and female adult mice at least 8-weeks old were used in this study. Mice were housed under a 12:12-hour light:dark cycle in a temperature-controlled environment, and all behavioral testing was done during the light cycle. Food and water were available *ad libitum*.

Construction of fiberoptics

Fiberoptics implanted into the brain for optical stimulation experiments were constructed in house by interfacing a 200-mm, 0.37-numerical-aperture optical fiber (Fiber Instrument Sales) with a 1.25-mm stick zirconium ferrule. The fiber extended 4 mm beyond the end of the ferrule. Fibers were attached with epoxy resin into the ferrules, and subsequently cut with a diamond pen and polished. All fibers were calibrated to have a least 80% efficiency of light transmission. Fiberoptic patch cords with a 200-mm core diameter were also constructed in house using an FC/PC connectorization kit (Thor Labs).

Stereotaxic injections and fiberoptic implantations

For all viral injection surgeries mice were anesthetized with a mixture of ketamine and xylazine (100 mg/kg and 10 mg/kg) injected by intraperitoneal injection. Animals were then placed in a stereotaxic apparatus and body temperature was maintained at 37 °C with a heating pad. Small cranial windows (< 0.5 mm) were drilled at the appropriate sites and viruses were delivered at an average rate of 100 nL/min using glass pipettes (tip opening 10-15 μm). All stereotactic coordinates were measured relative to bregma. A total of 0.4-0.5 μL volume was delivered into each site for all injections. The DMS was targeted bilaterally with viral injections (anterior-posterior (AP) +1.0 mm, medial-lateral (ML) ±1.8 mm, dorsal-ventral (DV) -3.4 mm). For surgeries that also involved fiberoptic implantation, implants were done immediately following glass pipette used for viral injection were removed. Fiberoptic implants were placed bilaterally into the DMS, above the site targeted with the AAV5-ef1a-DIO-ChR2(H134R)-eYFP virus (AP: +1.0 mm, ML: ±1.8 mm, DV: -3.3 mm). The implant was secured to the skull using dental cement (Dentsply). All behavioral experiments or histological analysis were done at least four weeks after surgery to allow for stable viral transfection.

Drug treatment

Chronic treatment with haloperidol (1 mg/kg/day) was performed using osmotic minipumps (Alzet) designed to deliver the drug at a steady rate of 0.5 μ L/h over 14 days. Haloperidol was dissolved in 8.5% lactic acid (6 parts by volume) and neutralized with 1 N NaOH (4 parts by volume). Vehicle solution consisted of a mixture of 8.5% lactic acid and 1 N NaOH at a 6:4 ratio by volume. Drug and vehicle solutions were prepared on the same day of implantation. Minipumps were filled with either drug or vehicle and implanted into mice subcutaneously in the interscapular region under isoflurane anesthesia.

Behavioral assays

Rotarod training

A rotarod apparatus (Ugo Basile) was used to measure motor coordination and motor learning. On each day of training, each mouse was placed on the rotating rotarod system in three individual trials. In each trial mice were allowed to stay on the rotarod for up to 10 min, and the latency to fall was recorded if animals fell before the 10 min elapsed. Mice were immediately placed back in their homecage after falling from the rotarod or after the 10 min elapsed for each trial. The rotarod was set to accelerating mode (0 rpm to full speed in 5 min) on the first three days of training, and acceleration was started after mice were placed on the rotarod. On each of the first three days, mice were subjected to three identical trials, with acceleration from 0 to 20 rpm on the first day, 0 to 30 rpm on the second day, and 0 to 40 rpm on the third day. On all subsequent days of training mice were subjected to three trials per day with the rotarod set to constant mode with different speeds: 20 rpm in the first trial, 30 rpm in the second trial, and 40 rpm in the third trial on each day of training. In all trials with constant speed, animals were individually placed on the rotarod while the rotarod was already rotating at the specified speed.

In vivo optical stimulation

Assessment of locomotor activity with stimulation of dMSNs was done in acrylic activity chambers (42 cm long × 42 cm wide × 38 cm high) equipped with infrared photobeams for motion detection (Kinder Scientific). Mice with fiberoptic implants were first briefly immobilized for attachment of fiberoptic patch cords connected to a laser (473 nm) adjusted to give an output of 2 mW light intensity. The laser was controlled by a stimulator through which the laser could be manually switched to on and off modes. Turning the laser on led to constant light output. Once the patchcords were connected, mice were placed in the activity chamber where they were allowed to move freely and habituate for 5 min. After the first 5 min, the laser was switched on and off in a series of 5 stimulation trials. Each stimulation trial lasted 90 s; the laser was off during the first 30 s, it was then switched on for the duration of the subsequent 30 s, and it was finally turned off during the last 30 s. Animals were video recorded during the entire session to allow for *post-hoc* hand scoring of motor activity.

Histology and immunohistochemistry

For all histological analysis of brain tissue following behavioral experiments, mice were anesthetized with a mixture of ketamine and xylazine (100 mg/kg and 10mg/kg, respectively), delivered by intraperitoneal injection, and transcardially perfused, first with phosphate buffered saline (PBS) and then with 4% paraformaldehyde. Following perfusion, brains were post-fixed in 4% paraformaldehyde for 24 hours and then transferred to PBS. Brains were sliced into 50- μ m sagittal sections using a vibratome and every section was collected.

For co-localization analysis and confirmation of virally targeted region and fiberoptic placement, immunohistochemistry using fluorescence was performed on free-floating sections by treating sections first with blocking buffer (0.5% bovine serum albumin, 5% horse serum, 0.2%

Triton X-100), followed by the primary rabbit dsRed polyclonal antibody (1:250, Clontech, cat. 632496) and chicken anti-GFP polyclonal antibody (1:1000, Abcam, cat. ab13970) and the appropriate fluorescent-labeled secondary antibodies. Sections were washed with 0.2% Triton X-100 after incubation with antibodies and with 50 mM Tris-Cl pH 7.4 before mounting. Sections were mounted on glass slides and subsequently coverslipped for imaging with VectaShield containing DAPI (Vector Labs). For confirmation of spread of viral infection in targeted structures, images were acquired at 2.5x magnification using a Hamamatsu camera attached to a Carl Zeiss epifluorescence microscope. For analysis of co-expression of immune-labelled proteins, images were acquired at 40x using a Nikon Ti Eclipse inverted microscope for scanning confocal microscopy. Micrographs were processed using ImageJ software (National Institutes of Health).

For quantification of bridging collaterals, immunohistochemistry using 3,3'-diaminobenzidine (DAB) was performed on free-floating sections by treating sections first with blocking buffer (0.5% bovine serum albumin, 5% horse serum, 0.2% Triton X-100). Every fourth section covering the GPe and SNr from one hemisphere in their entirety (6 sections per mouse) was stained using a rabbit polyclonal antibody against aequorea GFP (1:2000; Molecular Probes). The signal was revealed using a biotinylated anti-rabbit antibody (1:1000; Jackson ImmunoResearch), together with the Vectastain ABC and DAB peroxidase substrate kits (Vector Labs, cat. PK-4000 and SK-4100, respectively). Contrast was intensified using 0.025% nickel cobalt and 0.02% nickel ammonium sulfate. Sections were dehydrated, cleared, and mounted on slides with Permount (Fisher Scientific). Brightfield and darkfield photomicrographs were taken using an AxioImager 2 microscope (Zeiss) connected to an AxioCam video camera. Terminal density was evaluated using GFP staining. Quantification was performed using ImageJ using two

random counting frames per structure and per slice with background subtraction. Optical density was measured for striatum, GPe, and SNr, and all values reported are in percentage of striatal optical density.

Data analysis and statistics

All data collected in the current study were processed with Excel (Microsoft). Statistical analyses were done with either Excel or Prism 5 (GraphPad). For normally-distributed data sets, including optical density of terminal fields, locomotor activity, and ambulatory distance, two-way analyses of variance (ANOVAs) were conducted. Bonferroni *post hoc* tests were conducted when appropriate. Because of the nature of the rotarod task, data was not normally distributed and therefore the Log-rank non-parametric test was used for statistical analysis.

RESULTS

SYNAPTIC CONTACTS

To confirm that the bridging collaterals form synaptic contacts in the GPe, I obtained a virus vector that allowed Cre-dependent selective labeling of synaptic vesicles. This virus vector (AAV1/2-Syn-DIO-Synaptophysin-GFP) was designed to express the synaptic vesicle protein synaptophysin fused to GFP in transfected cells, thereby labeling all synaptic contacts of transfected neurons. I injected this virus into the

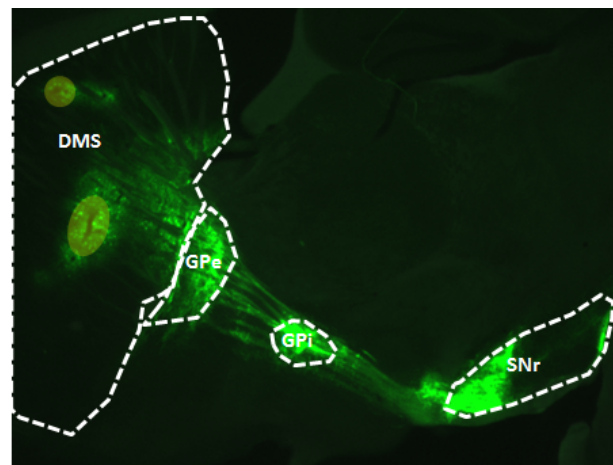


Figure 7: dMSNs form synaptic contacts in the GPe. A Cre-dependent virus for expression of synaptophysin fused to GFP was injected into the DMS of *Drd1*-Cre mice (tract marks of injection pipette highlighted in yellow) for restricted expression in dMSNs. GFP signal, indicating regions where dMSNs form synaptic contacts was observed in the striatum around the injection site, in the output nuclei of the basal ganglia (GPi and SNr), as well as in the GPe.

DMS of *Drd1-Cre* mice and subsequently located regions in the basal ganglia that showed GFP fluorescence. As showed in Figure 7, transfection of striatal dMSNs with this virus led to labeling of both GPi and SNr, the output nuclei of the basal ganglia. In addition, labeling was also observed within the striatum itself around the injected site, confirming that MSNs form local synaptic contacts, presumably with neighboring MSNs. Most importantly, however, robust labeling was observed in the GPe, confirming that dMSNs projecting from the DMS form synaptic contacts with cells in the GPe. These synaptic contacts likely correspond to axon terminal fields of the bridging collaterals.

REGULATION BY INDIRECT PATHWAY

In order to study how the bridging collaterals may be selectively regulated by activity of the direct or indirect pathways, I constructed a Cre-dependent viral vector to restrict expression of the trans-dominant negative $K_{ir}2.1^{AAA}$ channel to either the direct or indirect pathway to determine which population of MSNs mediates the growth of collaterals. The DNA construct for the AAV2/1-Syn-DIO-Kir2.1AAA-IRES-mCherry was generated by sub-cloning the sequences for $K_{ir}2.1^{AAA}$ and IRES-mCherry from pcDNA3.1-IRKAAA-HA and IRES-mCherry3Myc-pCAGEN, respectively, into the backbone of pAAV-SyI-DIO-SF-D2RL-Venus. Figure 4 shows scheme of the viral vector construct as well as micrographs from sections immune-stained for mCherry, confirming expression restricted to dMSNs or iMSNs. To confirm specificity, the virus was injected into the DMS of *Drd1-GFP*⁺ mice that were also *Drd1-Cre*⁺, *Drd1-Cre*⁻, *Drd2-Cre*⁺, or *Drd2-Cre*⁺. Since GFP is expressed in dMSNs in *Drd1-GFP*⁺ mice (Figure 8B), injection of AAV2/1-Syn-DIO-Kir2.1AAA-IRES-mCherry into *Drd1-GFP*⁺/*Drd1-Cre*⁺ led to co-expression of GFP and mCherry in dMSNs in the striatum (Figure 8C), and no mCherry expression was

detected when the virus was injected into *Drd1-GFP⁺/Drd1-Cre⁻* animals (Figure 8D). In contrast, when *Drd1-GFP⁺/Drd2-Cre⁺* animals were injected with the viral vector, expression of both GFP and mCherry were detected in the striatum, but no cells co-expressed both fluorescent markers (Figure 8E). The specificity of viral expression to Cre-positive cells was further confirmed by the lack of mCherry expression in the striatum of *Drd1-GFP⁺/Drd2-Cre⁻* mice also injected with the virus (Figure 8F).

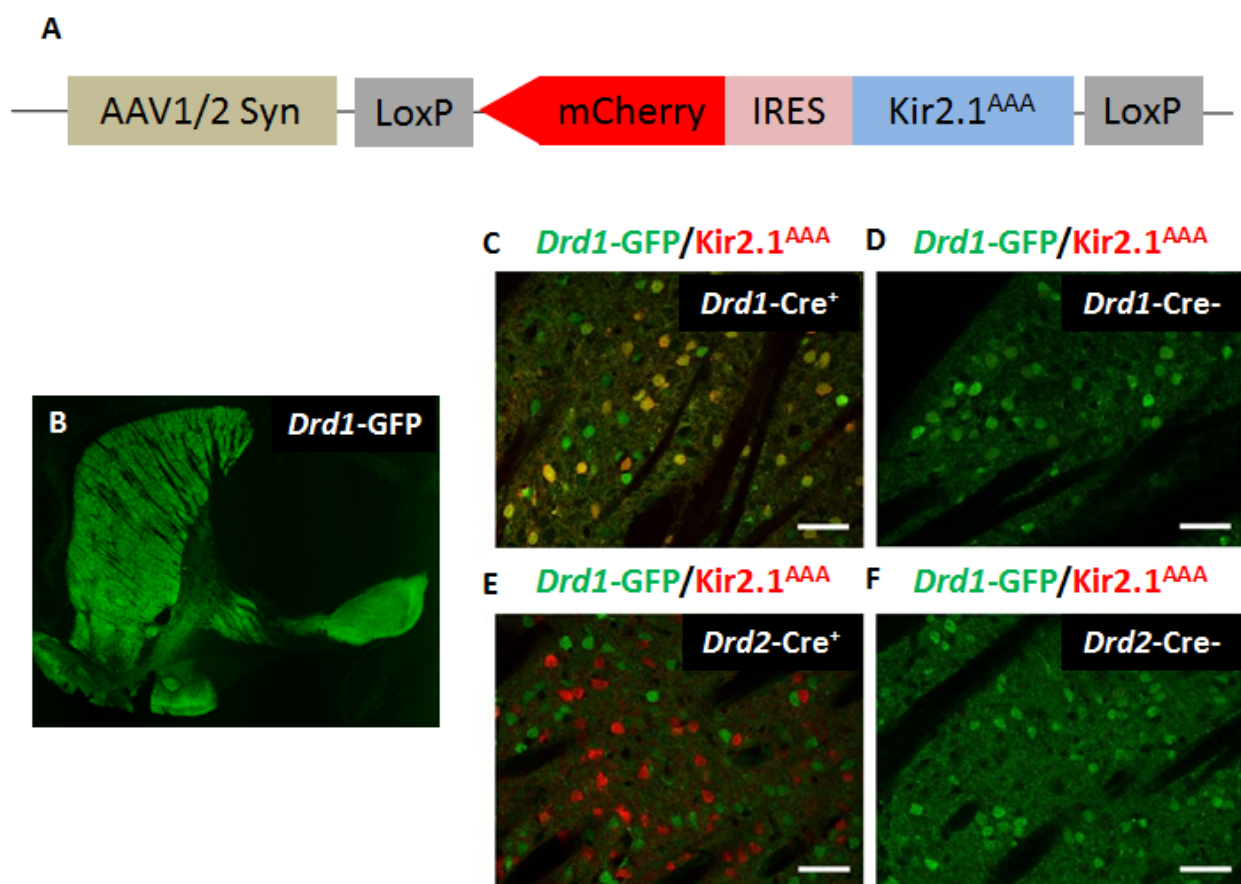


Figure 8: Kir2.1^{AAA} can be expressed selectively in dMSNs or iMSNs. A. Schematic of viral DNA construct used to generate the AAV2/1-Syn-DIO-Kir2.1AAA-IRES-mCherry virus that was used to selectively express Kir2.1^{AAA} in Cre-positive neurons. B. GFP signal in sagittal section of *Drd1-GFP* BAC transgenic mouse used in C-F. Striatal expression of Kir2.1^{AAA}/mCherry (red) and GFP (green) in *Drd1-GFP⁺/Drd1-Cre⁺* (C), *Drd1-GFP⁺/Drd1-Cre⁻* (D), *Drd1-GFP⁺/Drd2-Cre⁺* (E), *Drd1-GFP⁺/Drd2-Cre⁻* (F) Scale bar, 1 mm.

Previous work from the Kellendonk laboratory has demonstrated that nonselective expression of $K_{ir}2.1^{AAA}$ in the dorsomedial striatum leads to increased neuronal excitability and can induce growth of bridging collaterals in mice (Cazorla et al., 2012, Cazorla et al., 2014). Having confirmed the generation of a new virus to selectively express $K_{ir}2.1^{AAA}$ in Cre-positive cells, the virus was injected into the DMS of $Drd1-GFP^+/Drd1-Cre^+$ and $Drd1-GFP^+/Drd2-Cre^+$ adult mice to determine how increased excitability in specific populations of striatal MSNs, dMSNs or iMSNs, contributes to the growth of bridging collaterals. As a control, the AAV2-EF1 α -DIO-mCherry virus was also injected in littermates of the same genotype. After waiting four weeks following viral injection to allow stable expression of transfected $K_{ir}2.1^{AAA}$ in dMSNs or iMSNs, mice were sacrificed and the density of GFP-positive terminal fields in the GPe, representing bridging collaterals from striatal dMSNs, were quantified. Compared to

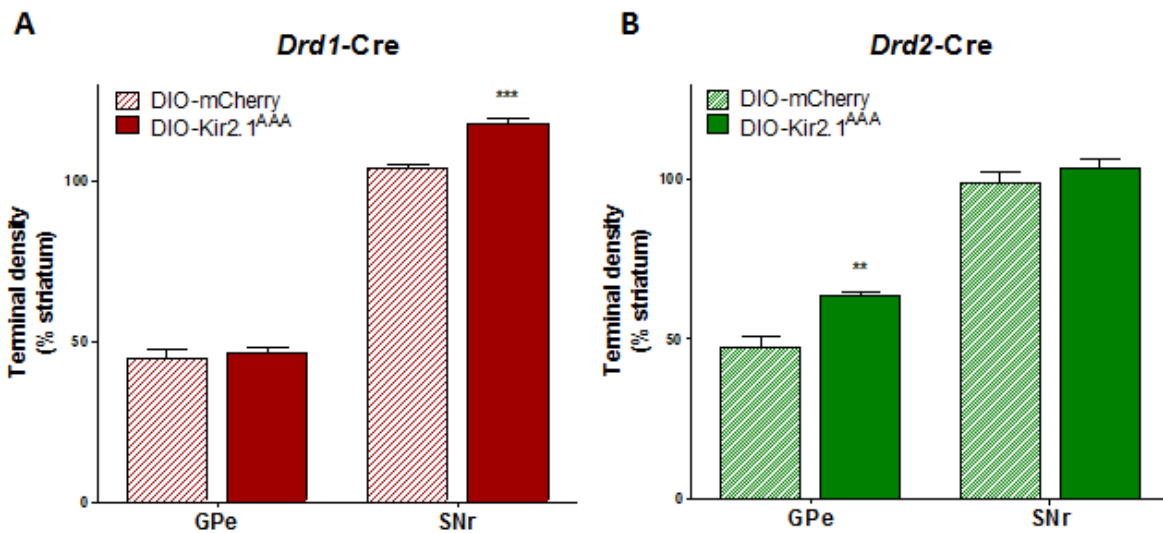


Figure 9: Bridging collaterals are regulated by excitability of the indirect pathway. A. Expression of $K_{ir}2.1^{AAA}$ in dMSNs did not significantly change the density of dMSN terminal fields in the GPe but led to a significant increase in the density of terminal fields in the SNr ($p = 0.0012$; Bonferroni post hoc test: GPe: $p > 0.05$; SNr: $p < 0.001$). **B.** Expression of $K_{ir}2.1^{AAA}$ in iMSNs significantly increased the density of GFP-positive terminal fields of dMSNs in the GPe, but did not significantly change the density of terminal fields in the SNr ($p = 0.0049$; Bonferroni post hoc test: GPe: $p < 0.01$; SNr: $p > 0.05$). A total of 4 *Drd2-Cre* and 3 *Drd2-Cre* mice injected with each virus were used for this analysis.

expression of a control gene, expression of $K_{ir}2.1^{AAA}$ in dMSNs did not lead to a significant change in the density of bridging collaterals, while a significant increase in the density of terminal fields in the SNr, the main projection target of dMSNs, was observed ($F_{(1,12)} = 17.76$; $p = 0.0012$ Bonferroni *post hoc* test: GPe: $p > 0.05$; SNr: $p < 0.001$; $n = 4$ mice per group) (Figure 9A). In contrast, expression of $K_{ir}2.1^{AAA}$ in the indirect pathway led to a significant increase in the density of bridging collaterals, and no change was observed in the density of terminal fields in the SNr ($F_{(1,12)} = 14.81$; $p = 0.0049$ Bonferroni *post hoc* test: GPe: $p < 0.01$; SNr: $p > 0.05$; $n = 3$ mice per group) (Figure 9B). These findings show that chronically increasing excitability of iMSNs in adult mice is sufficient to promote the growth of bridging collaterals (axon collaterals originating from striatal dMSNs), whereas chronically increasing excitability of dMSNs did not promote the growth of these collaterals. Chronically increasing excitability of dMSNs, however, was sufficient to increase the density of terminal fields to the SNr, one of the main target nuclei of the direct pathway.

ASSOCIATION WITH BEHAVIORAL ACTIVATION OF DIRECT PATHWAY

Having shown that activity in the indirect pathway can induce a circuit-level connectivity change in the basal ganglia, I proceeded to investigate whether this change in connectivity could be relevant for behavior. Two previous findings from the Kellendonk laboratory led to the question of whether the D2R antagonist haloperidol could affect basal ganglia output at the behavioral level by changing the density of bridging collaterals. First, it was previously shown that increased bridging collateral density in D2R-OE_{dev} mice, induced by D2R upregulation, could be reversed in adult animals by chronic treatment with the D2R antagonist haloperidol (Cazorla et al., 2014). And second, increased density of bridging collaterals was shown to be

associated with abnormal locomotor activation upon optogenetic stimulation of the direct pathway (Cazorla et al., 2014). Thus, to further investigate whether pharmacologically targeting the indirect pathway could have behavioral effects associated with the bridging collaterals, Cre-dependent ChR2 was expressed in dMSNs in the DMS of D2R-OE_{dev}/*Drd1*-Cre mice and control *Drd1*-Cre littermates. Fiberoptic implants were also placed in the DMS of these mice to allow for temporally-controlled light-stimulation of dMSNs while animals were allowed to move freely. Before behavioral testing, animals were treated for 14 days with the D2R antagonist haloperidol or vehicle.

Figure 10 shows how stimulation of dMSNs affected movement initiation in D2R-OE_{dev} and control littermates after chronic treatment with haloperidol or vehicle. As previously reported (Kravitz et al., 2010), control animals treated with vehicle moved more when the laser was turned on compared to when the laser was turned off ($F_{(2,14)} = 21.11$, $p = 0.0006$; Bonferroni's multiple comparisons: PRE vs. LASER: $p < 0.001$; LASER vs. POST: $p < 0.01$, PRE vs. POST: $p > 0.05$; $n = 5$ mice) (Figure 10). Moreover, as had been previously demonstrated in the Kellendonk laboratory, D2R-OE_{dev} mice paradoxically moved less when the laser was turned on compared to when the laser was turned off ($F_{(2,14)} = 58.71$, $p < 0.0001$; Bonferroni's multiple comparisons: PRE vs. LASER: $p < 0.001$; LASER vs. POST: $p < 0.001$, PRE vs. POST: $p > 0.05$; $n = 5$ mice) (Figure 10). Compared to animals treated with vehicle, animals treated with haloperidol, including both D2R-OE_{dev} mice and control littermates, showed decreased movements at baseline when the laser was turned off ($F_{(1,20)} = 31.40$, $p < 0.0001$; Bonferroni *post hoc* tests, D2R-OE_{dev}: $p < 0.001$, 5-6 mice per treatment, Control: $p < 0.05$, $n = 5-8$ mice per treatment) (Figure 10). Nevertheless, after chronic treatment with haloperidol, control mice still responded with increased locomotion to laser stimulation ($F_{(2,17)} = 39.44$, $p <$

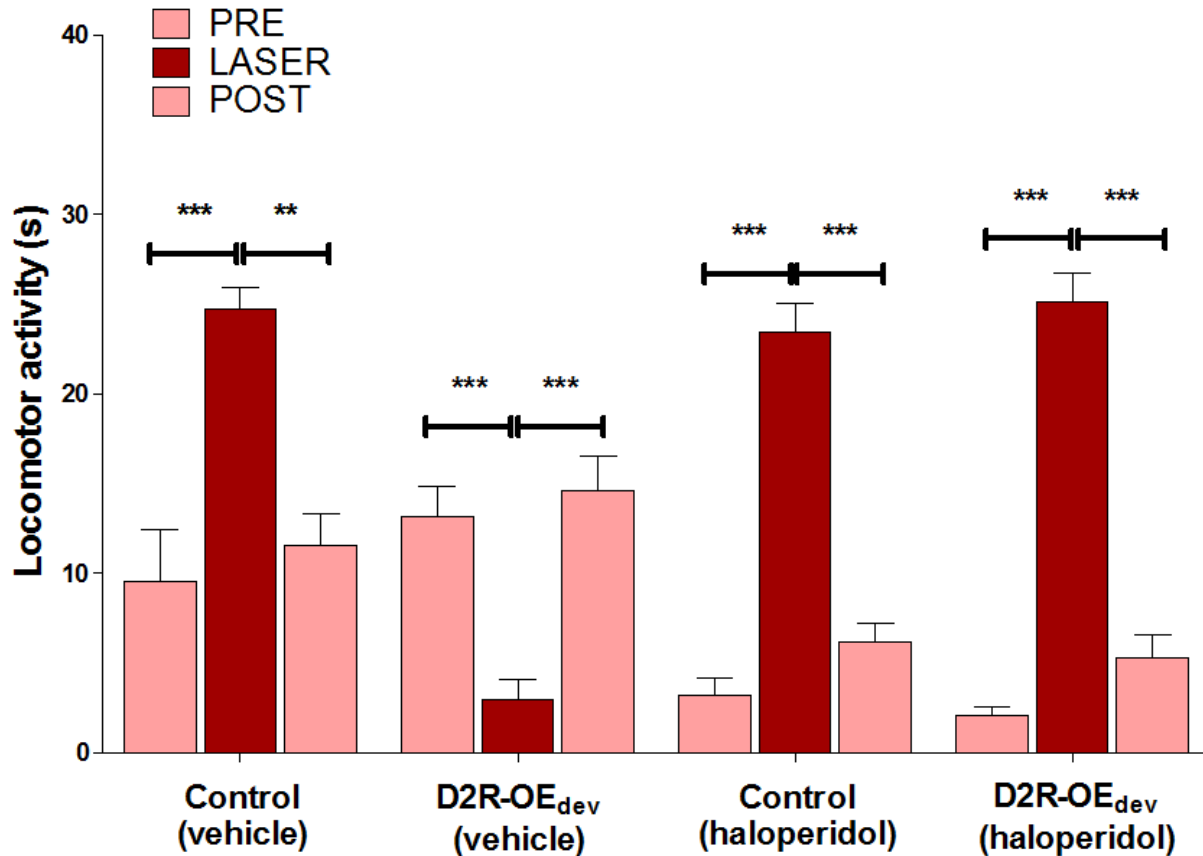


Figure 10: Retraction of bridging collaterals can rescue behavioral activation of direct pathway. Mean locomotor activity of 5 30-s sessions before laser stimulation (PRE), during laser stimulation (LASER), and after laser stimulation (POST) for D2R-OE_{dev} mice and control littermates treated with haloperidol or vehicle for 14 days. Control animals treated with vehicle moved more when the laser was turned on compared to when the laser was turned off ($p = 0.0006$; Bonferroni's multiple comparisons: PRE vs. LASER: $p < 0.001$; LASER vs. POST: $p < 0.01$, PRE vs. POST: $p > 0.05$). D2R-OE_{dev} mice moved less when the laser was turned on compared to when the laser was turned off ($p < 0.0001$; Bonferroni's multiple comparisons: PRE vs. LASER: $p < 0.001$; LASER vs. POST: $p < 0.001$, PRE vs. POST: $p > 0.05$). Control mice still responded with increased locomotion to laser stimulation after treatment with haloperidol ($p < 0.0001$; Bonferroni's multiple comparisons: PRE vs. LASER: $p < 0.001$; LASER vs. POST: $p < 0.001$, PRE vs. POST: $p > 0.05$). After chronic treatment with haloperidol, D2R-OE_{dev} mice responded to laser stimulation of dMSNs with increased movement ($p < 0.0001$; Bonferroni's multiple comparisons: PRE vs. LASER: $p < 0.001$; LASER vs. POST: $p < 0.001$, PRE vs. POST: $p > 0.05$). A total of 5 control mice treated with vehicle, 5 D2R-OE_{dev} mice animals treated with haloperidol, 8 control mice treated with haloperidol, and 6 D2R-OE_{dev} mice treated with haloperidol were assayed for this analysis.

0.0001; Bonferroni's multiple comparisons: PRE vs. LASER: $p < 0.001$; LASER vs. POST: $p < 0.001$, PRE vs. POST: $p > 0.05$; $n = 8$ mice) (Figure 10). Most remarkably, however, after chronic treatment with haloperidol, D2R-OE_{dev} mice no longer exhibited decreased movements

when the laser was turned on but instead responded to laser stimulation of dMSNs with increased movement similarly to control animals ($F_{(2,17)} = 114.3$, $p < 0.0001$; Bonferroni's multiple comparisons: PRE vs. LASER: $p < 0.001$; LASER vs. POST: $p < 0.001$, PRE vs. POST: $p > 0.05$; $n = 6$) (Figure 10). Therefore, chronic haloperidol treatment was sufficient to fully rescue a behavioral phenotype associated with increased bridging collaterals.

REGULATION BY MOTOR TRAINING

Thus far, I have provided evidence demonstrating that the bridging collaterals (axon collaterals of dMSNs that target the GPe) can increase in density when chronic excitability of iMSNs is increased and are associated with disrupted behavioral activation upon stimulation of dMSNs. Since D2R-OE_{dev} mice show increased density of bridging collaterals and their growth and retraction are plastic even in the adult animal, I hypothesized that other behavioral phenotypes of D2R-OE_{dev} mice may also be associated with these collaterals. In addition to the anatomical and physiological phenotypes of D2R-OE_{dev} described so far, these animals also display a deficit in motor coordination compared to control littermates, as measured by impaired performance on the rotarod task. As shown in Figure 11, while control mice are able to remain on a horizontal rod rotating at constant 20 rpm or 30 rpm speeds for 10 min without extensive training, D2R-OE_{dev} mice exhibit impaired performance in comparison during the first week of training (Log-rank tests: 20 rpm: $\chi^2 = 7.429$, $p = 0.0064$; 30 rpm: $\chi^2 = 4.531$, $p = 0.0333$; $n = 5$ mice per genotype). However, while this impairment is most pronounced in the first week, the difference decreased with ongoing motor training, and at the end of three weeks, D2R-OE_{dev} mice can perform at a similar level to their control littermates (Log-rank tests: 20 rpm: $\chi^2 = 1.000$, $p = 0.3173$; 30 rpm: $\chi^2 = 2.242$, $p = 0.1343$; $n = 5$ mice per genotype) (Figure 11).

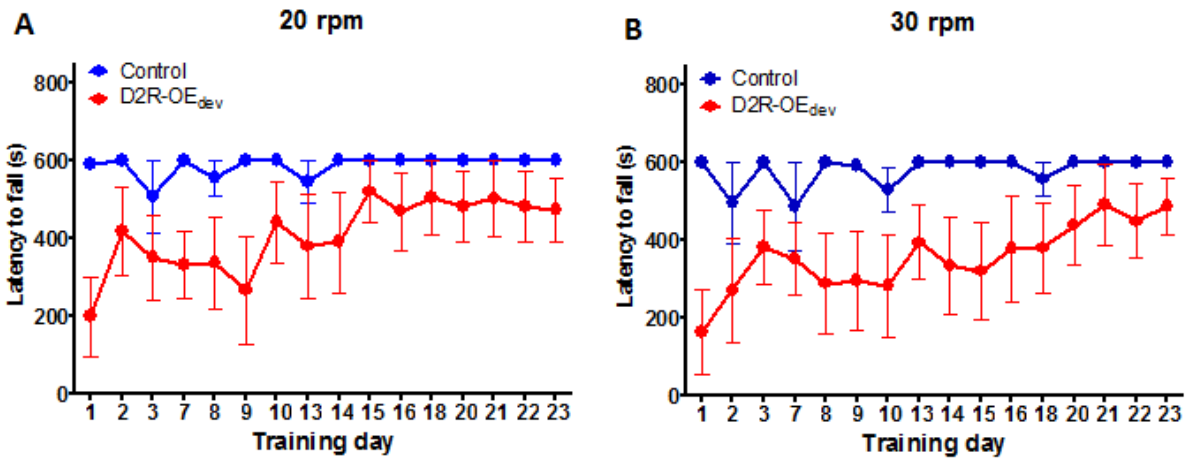


Figure 11: D2R-OE_{dev} mice have a motor impairment that improves with training. Performance in the rotarod, measured as latency to fall from a rod rotating at (A) 20 rpm and (B) 30 rpm is shown for D2R-OE_{dev} mice and control littermates. During the first week of training in the rotarod task, D2R-OE_{dev} mice exhibit impaired performance in comparison to control littermates (20 rpm: $p = 0.0064$, 30 rpm: $p = 0.0333$). At the end of three weeks of training, D2R-OE_{dev} mice can perform at a similar level to their control littermates (20 rpm: $p = 0$; 30 rpm: $p = 0.1343$). A total of 5 mice per genotype were assayed for this analysis.

Given that the time course of this effect was comparable to the time course of growth and retraction of bridging collaterals, together with evidence for exercise-dependent functional plasticity in cortico-striatal input (Costa et al., 2004), I questioned whether plasticity involving the bridging collaterals could be associated with improved performance of D2R-OE_{dev} in the rotarod task after repeated motor training. To this end, I trained D2R-OE_{dev}/*Drd1*-GFP and *Drd1*-GFP control mice daily on the rotarod task for three weeks and measured density of bridging collaterals after training. Statistical analysis revealed a significant effect of rotarod training ($F_{(1,15)} = 13.96$, $p = 0.0467$, $n = 3-6$ mice per group) (Figure 12) Specifically, after daily motor training in the rotarod task, D2R-OE_{dev} mice had decreased density of bridging collaterals compared to D2R-OE_{dev} mice that were never trained in this motor task (Bonferroni *post hoc* test: $p < 0.01$, $n = 3-6$ mice per training condition) (Figure 12). Among control littermates not expressing the D2R transgene, rotarod training did not appear to affect the density of bridging collaterals (Bonferroni *post hoc* test: $p > 0.05$, $n = 4-6$ mice per training condition) (Figure 12).

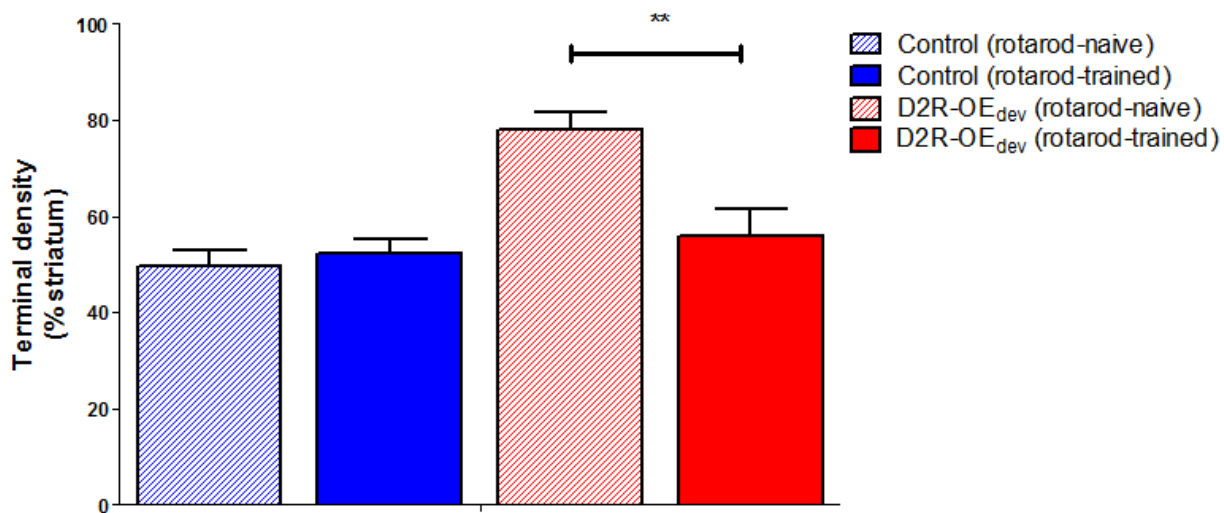


Figure 12: Rotarod training induces retraction of bridging collaterals in D2R-OE_{dev} mice. Quantification of bridging collaterals in D2R-OE_{dev} and control littermates that were rotarod-naïve or trained in the rotarod for three weeks showed a significant effect of rotarod training ($p = 0.0467$). Among control mice, rotarod training did not affect density of bridging collaterals (Bonferroni post hoc test: $p > 0.05$). Rotarod-trained D2R-OE_{dev} mice had decreased density of bridging collaterals compared to rotarod-naïve D2R-OE_{dev} (Bonferroni post hoc test: $p < 0.01$). A total of 3 rotarod-naïve control mice, 6 rotarod-trained control mice, 4 rotarod-naïve D2R-OE_{dev} mice, and 6 rotarod-trained D2R-OE_{dev} mice were used for this analysis.

Given the potential implications of this experience-induced plasticity for disease-modifying therapies in schizophrenia, I decided to further explore this phenomenon. I hypothesized that rotarod training might be sufficient to reverse the functional imbalance of the direct and indirect pathways in D2R-OE_{dev} mice, as measured by motor output following stimulation of dMSNs. Therefore, I expressed ChR2 selectively in dMSNs in the DMS of D2R-OE_{dev}/*Drd1*-Cre mice and control *Drd1*-Cre littermates. Fiberoptic implants were also placed into the DMS of these mice to allow for temporally-controlled light-stimulation of dMSNs while animals moved freely. After undergoing surgery, D2R-OE_{dev} mice and control littermates were divided into subgroups; a subset of animals of each genotype underwent daily rotarod training for at least three weeks while the other half remained rotarod-naïve. Following training, I used the same behavioral paradigm used to demonstrate the behavioral effect of chronic haloperidol in D2R-OE_{dev} mice to measure motor activity induced by light-stimulation of dMSNs in D2R-OE_{dev}

and control mice that were rotarod-trained or rotarod-naive. Figure 13 shows motor performance for animals trained in the rotarod, as well as measures of locomotor response to stimulation of the direct pathway after rotarod training. Similar to performance of the previous cohort (see Figure 13), among animals that received rotarod training, D2R-OE_{dev} showed an initial impairment in motor performance compared to control mice (Log-rank tests: 20 rpm: $\chi^2 = 4.521$, $p = 0.0335$; 30 rpm: $\chi^2 = 10.43$, $p = 0.0012$) that was no longer present after three weeks of rotarod training (Log-rank tests: 20 rpm: $\chi^2 = 2.560$, $p = 0.1096$; 30 rpm: $\chi^2 = 1.421$, $p = 0.2333$) (Figure 13A-B). Since I have previously demonstrated that three weeks of rotarod training is sufficient to induce retraction of bridging collaterals in D2R-OE_{dev} mice, I tested whether motor training could also rescue the disrupted behavioral phenotype of D2R-OE_{dev} upon optogenetic stimulation of dMSNs. Figure 13C shows measures of locomotor activity when rotarod-trained and rotarod-naïve D2R-OE_{dev} and control mice were tested in the optogenetic open field paradigm. I was able to reproduce the impaired behavioral activation of D2R-OE_{dev} mice with stimulation of striatal dMSNs, as rotarod-naïve D2R-OE_{dev} mice showed reduced locomotor activity when the laser was turned on compared to when the laser was turned off ($F_{(2,11)} = 8.721$, $p = 0.0168$; Bonferroni's multiple comparisons: PRE vs. LASER: $p < 0.05$; LASER vs. POST: $p < 0.05$, PRE vs. POST: $p > 0.05$; $n = 4$) (Figure 13C). Among control animals, rotarod training did not affect increased locomotion induced by stimulation of dMSNs, and both rotarod-naïve ($F_{(2,20)} = 6.607$, $p = 0.0116$; Bonferroni's multiple comparisons: PRE vs. LASER: $p < 0.05$; LASER vs. POST: $p < 0.05$, PRE vs. POST: $p > 0.05$; $n = 7$) and rotarod-trained ($F_{(2,32)} = 6.986$, $p = 0.0050$; Bonferroni's multiple comparisons: PRE vs. LASER: $p < 0.001$; LASER vs. POST: $p < 0.05$, PRE vs. POST: $p > 0.05$; $n = 11$) mice responded to laser stimulation with increased locomotor activity (Figure 13C). Remarkably, however, D2R-OE_{dev} mice trained in the rotarod

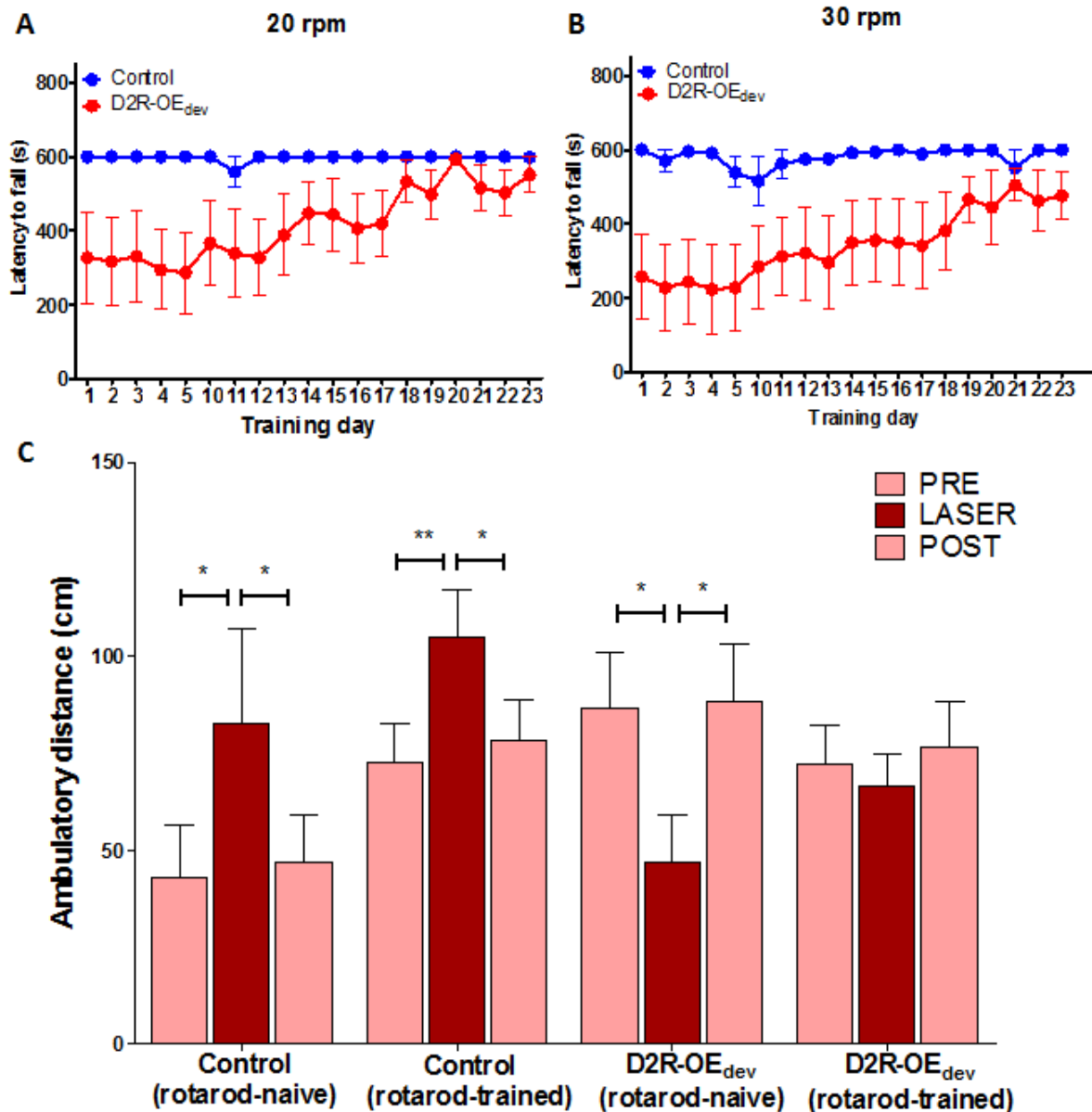


Figure 13: Rotarod training partially rescues abnormal behavioral activation of direct pathway. A-B. Performance in the rotarod, measured as latency to fall from a rod rotating at (A) 20 rpm and (B) 30 rpm is shown for D2R-OE_{dev} mice and control littermates that underwent rotarod training. During the first week of training, D2R-OE_{dev} mice exhibited impaired performance in comparison to control littermates (20 rpm: $p = 0.0064$; 30 rpm: $p = 0.0333$). At the end of three weeks of training, D2R-OE_{dev} mice performed at a similar level to their control littermates (20 rpm: $p = 0.1096$; 30 rpm: $p = 0.2333$). C. Mean locomotor activity of 5 30-s sessions before laser stimulation (PRE), during laser stimulation (LASER), and after laser stimulation (POST) for D2R-OE_{dev} mice and control littermates that were either rotarod-naïve or trained in the rotarod for at least three weeks. Rotarod-naïve control animals moved more when the laser was turned on compared to when the laser was turned off ($p = 0.0116$; Bonferroni's multiple comparisons: PRE vs. LASER: $p < 0.05$; LASER vs. POST: $p < 0.05$, PRE vs. POST: $p > 0.05$); rotarod-naïve D2R-OE_{dev} mice moved less when the laser was turned on compared to when the laser was turned off ($p = 0.0168$; Bonferroni's multiple comparisons: PRE vs. LASER: $p < 0.05$; LASER vs. POST: $p < 0.05$, PRE vs. POST: $p > 0.05$). Control mice still responded with increased locomotion to laser stimulation after rotarod training ($p = 0.0050$; Bonferroni's multiple comparisons: PRE vs. LASER: $p < 0.001$; LASER vs. POST: $p < 0.05$, PRE vs. POST: $p > 0.05$). But rotarod-trained D2R-OE_{dev} mice no longer responded to laser stimulation of dMSNs with decreased movement ($F_{(2,38)} = 0.4662$, $p = 0.6335$). A total of 7 rotarod-naïve control mice, 4 rotarod-trained control mice, 11 rotarod-naïve D2R-OE_{dev} mice, and 12 rotarod-trained D2R-OE_{dev} mice were used for this analysis.

no longer responded to stimulation of dMSNs with decreased locomotion during laser stimulation ($F_{(2,38)} = 0.4662$, $p = 0.6335$; $n = 12$) (Figure 13C). Therefore, behavioral intervention through motor training was sufficient to partially rescue an abnormal behavioral phenotype of D2R-OE_{dev} associated with the balance of direct and indirect pathways.

DISCUSSION

In summary, in the current study I provide mechanistic insight on plasticity involving the bridging collaterals, as well as evidence related to how the bridging collaterals may regulate behavior and how behavior may regulate the bridging collaterals. First, I demonstrated that bridging collaterals form synaptic contacts with GPe cells. I was also able to generate a viral vector to selectively increase excitability in specific populations of MSNs. I used this virus to demonstrate that chronically increasing excitability of the indirect pathway, but not the direct pathway, leads to a circuit-level change in connectivity by inducing the growth of bridging collaterals from dMSNs in the GPe. I also confirmed that increased density of bridging collaterals are associated with an abnormal locomotor response to stimulation of striatal dMSNs and demonstrated that chronic pharmacologic blockade of D2Rs can rescue this abnormal locomotor phenotype. Furthermore, I demonstrated that motor training can lead to changes in the density of bridging collaterals and partially rescue the abnormal locomotor phenotype associated with increased collaterals, thereby establishing a new link between connectivity in the basal ganglia and motor learning.

Many studies have established a role for neuronal activity in the regulation of axonal growth and in shaping proper connectivity within neural circuits (Catalano and Shatz, 1998, Hua et al., 2005, De Marco Garcia et al., 2011). Neuronal excitability via changes in the function of

K_{ir} channels have been shown to regulate plasticity in a variety of neurons and brain circuits (Burrone et al., 2002, Hartman et al., 2006). In the current study, I contributed to the characterization of a new form of plasticity in the basal ganglia using a genetic tool that knocks down K_{ir}2 channel function. By generating and characterizing the AAV2/1-Syn-DIO-Kir2.1AAAIRES-mCherry virus, I provide a useful tool for research on the effects of neuronal excitability on brain circuit plasticity and behavior. Numerous mouse lines are available in which Cre recombinase is expressed in selective neuronal populations. I expect, therefore, that this viral construct will be used to study how chronically increasing excitability in restricted neuronal populations can affect neuronal circuits and behavior in a variety of brain regions and animal models.

However, one limitation to the use of the AAV2/1-Syn-DIO-Kir2.1AAA-IRES-mCherry virus is that I did not perform an extensive characterization of how transfecting K_{ir}2.1^{AAA} into MSNs affects neuronal excitability. The original experiments done in the Kellendonk laboratory that showed that non-conditional expression of K_{ir}2.1^{AAA} in the DMS leads to increased MSN excitability were done using a virus (AAV2-CMV-Kir2.1AAA-IRES-hrGFP) that had the cytomegalovirus (CMV) promoter instead of the synapsin (Syn) promoter to drive K_{ir}2.1^{AAA} expression. The CMV promoter is known to lead to higher but more transient expression of virally-transfected genes in neurons compared to the Syn promoter using AAV vectors in rodents (McCown et al., 1996, Paterna et al., 2000, Kugler et al., 2003). In addition, these two promoters have been shown to preferentially drive transgene expression in different cells types (Gholizadeh et al., 2013). Thus, although robust viral transfection was observed for both viruses, as measured by fluorophore signal in striatal MSNs, it cannot be immediately assumed that transfection with both viruses resulted in equal expression of K_{ir}2.1^{AAA} in MSNs. The internal ribosomal entry site

(IRES) in both constructs allowed expression of fluorophores (hrGFP or mCherry) as separate proteins, and their pattern of expression do not represent the pattern of expression of Kir2.1^{AAA} in the cell. Since an HA tag is included in the Kir2.1^{AAA} sequence in both constructs, immunohistochemically probing for the HA tag would be a reasonable strategy to directly compared Kir2.1^{AAA} expression using each virus. Or, alternatively, slice physiology characterization of intrinsic excitability in genetically-identified dMSNs and iMSNs after transfection with the AAV2/1-Syn-DIO-Kir2.1AAA-IRES-mCherry construct could be directly compared to previously collected slice physiology data using the AAV2-CMV-Kir2.1AAA-IRES-hrGFP construct (Cazorla et al., 2012).

Another limitation of the study is the fact that all manipulations of excitability targeted the DMS even though increased excitability in MSNs throughout the striatum has been measured in D2R-OE_{dev} mice (Cazorla et al., 2012). It would be informative, for example, to characterize how increasing excitability of MSNs in the DLS may affect density of bridging collaterals. Given that the DLS is known to be part of the motor cortico-basal ganglia-thalamic loop and in this study I also implicate the bridging collaterals in motor learning, it is plausible the collaterals are regulated by MSN excitability in this striatal sub-region. Moreover, it is not known if structures analogous to the bridging collaterals are also formed by dMSNs in the NA projecting to the VP. The tools used in this study to measure density of collaterals in *Drd1*-GFP mice could also be employed to measure terminal field density in the VP. Given recent evidence that as much as 50% of GPe neurons receive inputs from dMSNs (Kupchik et al., 2015), it is plausible that plasticity involving the density dMSN terminal fields in the VP may also be mediated by MSN excitability.

The fact that the D2R-OE_{dev} mouse recapitulates increased striatal D2R function, as seen in patients with schizophrenia, and also exhibits phenotypes reminiscent of this disease (Kellendonk et al., 2006, Drew et al., 2007) raises the question of whether density and function of bridging collaterals may also be increased in schizophrenia. Furthermore, the robust effect of the D2R antagonist and antipsychotic haloperidol on retracting the bridging collaterals and rescuing an abnormal behavioral phenotype of D2R-OE_{dev} mice suggests that a similar phenomenon may underlie the mechanism via which haloperidol alleviates symptoms in patients. In fact, all antipsychotics currently used to treat schizophrenia are either antagonists or weak partial agonists for D2Rs. These medications take weeks to reach their full efficacy in patients, suggesting that neural plasticity results from chronic downregulation of D2R function. This evidence supports a possible link between the collaterals and schizophrenia. Testing these hypotheses in patients could lead to important insight on the pathophysiology of schizophrenia and potentially new tools for therapies that target specific circuit elements in the basal ganglia. One first step to determine the strength of the association between the bridging collaterals and pharmacological treatment would be to test whether other antipsychotic medications, including atypical antipsychotics that also antagonize D2Rs, can retract bridging collaterals in D2R-OE_{dev} mice.

Furthermore, the findings presented here demonstrating that bridging collaterals are also associated with motor learning may have implications for schizophrenia beyond motor control. Patients with schizophrenia have increased striatal D2R availability, which predicts treatment response to antipsychotic medication (Abi-Dargham et al., 2000). I propose that not only antipsychotics but also behavioral intervention may be efficacious in patients by retracting bridging collaterals, possibly correcting an anatomical imbalance in the cortico-basal ganglia-

thalamo-cortical loops involved in psychosis. In line with this idea, a recent study has demonstrated that behavioral therapy can be effective in treating psychosis (Leff et al., 2013). Since bridging collaterals are regulated by neuronal activity and given previous evidence for behavioral-induced functional plasticity in cortico-striatal inputs (Costa et al., 2004), my demonstration that behavioral training can lead to changes in connectivity in the basal ganglia is consistent with the idea that, by engaging activity in cortico-striatal circuits, behavioral intervention may alter the anatomy of the same striatal output pathways that are sensitive to antipsychotic medication. This idea is attractive, as cognitive behavioral therapy is widely discussed as adjunct therapy for schizophrenia. Elucidating the circuits and mechanisms by which these therapies exert their effects may be important for developing safer, effective therapies for patients with schizophrenia.

One way to strengthen the link between behavioral intervention through motor training and retraction of bridging collaterals would be to obtain parallel measures of collateral density, rotarod performance, and locomotor response to stimulation of the direct pathway. In order to obtain such data set, mice expressing four different transgenes would be required, D2R-OE_{dev} mice (CaMKIIa-tTa⁺/TetO-D2R⁺) that are also positive for *Drd1*-GFP, and *Drd1*-Cre. Thus, a large breeding colony would be necessary, and the data collected would be merely correlational. In addition, large cohorts may be necessary to establish strong associations between behavioral measures and density of bridging collaterals. In the current study, regression analyses were underpowered for establishing correlations between measures of rotarod performance and density of collaterals, or measures of behavioral response to direct-pathway stimulation and density of collaterals.

Given the well-accepted theory that the basal ganglia are integrated with the thalamus and cortex in parallel loops that regulate different types of behaviors, it may be possible that plasticity involving the bridging collaterals is topographically-specified by the loops that are preferentially activated. The finding from the Kellendonk laboratory that D2R-OE_{dev} mice have a larger increase in the density of bridging collaterals in the more medial aspect of the GPe compared to controls supports this hypothesis (Cazorla et al., 2014). It is plausible that motor training in the rotarod task leads to selective retraction of collaterals in specific medial-lateral or dorsal-ventral aspects of the GPe. If such selective retraction occurs, it is also possible that expression of ChR2 in the DMS may not have been optimal to activate basal ganglia loops that undergo bridging collateral plasticity with rotarod training. In fact, the DLS, rather than the DMS, is a striatal sub-region that has been more strongly established as be part of sensorimotor cortico-basal ganglia-thalamo-cortical loop (Pan et al., 2010). Thus, it may be possible that the rescue of locomotor response to stimulation of the direct pathway after rotarod training would have been more robust if ChR2 was expressed in the DLS.

Finally, in order to move from correlational analyses and establish a causal link between behavioral intervention and altered connectivity in the basal ganglia, it would be necessary to directly and specifically target the bridging collaterals. Optogenetics would be one strategy to establish causality, as ChR2 or the inhibitory opsin Archaeorhodopsin-3 (Arch3.0) could be Cre-dependently expressed in dMSNs and the bridging collaterals selectively targeted with fiber optics placed in the GPe. This approach would answer whether stimulating or inhibiting the bridging collaterals during motor learning tasks can affect performance, causally linking the collaterals to behavior. However, opsins such as ChR2 and Arch3.0 are expressed throughout axonal projections, and laser illumination of the GPe would also stimulate dMSN projections to

the SNr and GPI, potentially confounding the results. Therefore, some technical limitations still need to be overcome to establish a causal relationship between the bridging collaterals and behavior.

CHAPTER 3

EXCITABILITY OF STRIATAL PATHWAYS AND MOTIVATION

INTRODUCTION

By studying the phenotypes induced by altered MSN excitability and connectivity in D2R-OE_{dev} mice, I showed in Chapter 2 how the balance of the direct and indirect pathways can be important for regulating behaviors mediated by the basal ganglia. Using optogenetics, I contributed to establishing that increased bridging collaterals are associated with enhanced pallidal inhibition and disrupted locomotor response to stimulation of the direct pathway. Moreover, the D2R antagonist and antipsychotic haloperidol reverses both the morphological changes and the disruption in locomotor activation of D2R-OE_{dev} mice. These findings suggest that an increase in bridging collaterals, as observed in D2R-OE_{dev} mice, may also be involved in the generation of symptoms of schizophrenia. Positive symptoms, such as hallucinations and delusions, cannot currently be modeled in the mouse. As a model of schizophrenia endophenotypes, D2R-OE_{dev} mice exhibit phenotypes that resemble both the cognitive deficits and the impaired motivation seen in patients with this disorder (Kellendonk et al., 2006, Drew et al., 2007). Similar to what is observed in patients with schizophrenia, the motivational deficit of D2R-OE_{dev} mice is consistent with an impairment in assessing effort in anticipation of a reward as these mice will expend less effort to obtain a reward despite having intact hedonic reactivity to rewards (Drew et al., 2007, Gard et al., 2009). However, while the deficits in working memory observed in D2R-OE_{dev} mice appear to result from developmental processes and are not reversed when D2R overexpression is turned off in adulthood, the motivational deficit of D2R-OE_{dev} mice appears to be more directly linked to striatal overexpression of D2Rs because this deficit is

rescued when levels of striatal D2R expression is reverted to baseline in the adult animal (Kellendonk et al., 2006, Drew et al., 2007). Since the bridging collaterals are regulated by chronic changes in excitability of MSNs via changes in K_{ir2} channel function, as demonstrated and discussed in Chapter 2, I hypothesized that increased density of bridging collaterals and/or increased excitability might underlie impaired incentive motivation in D2R-OE_{dev} mice.

To test this hypothesis, I attempted to phenocopy the motivation deficit of D2R-OE_{dev} mice by downregulating $K_{ir2.1}$ channel function in selective populations of striatal MSNs. For this purpose, I used cell-type restricted expression of the trans-dominant negative mutant $K_{ir2.1}^{AAA}$ channel in the mouse striatum, in either dMSNs or iMSNs and in specific striatal sub-regions, to chronically increase excitability of these neurons. Increased excitability in D2R-OE_{dev} mice is observed in both dMSNs and iMSNs and in both dorsal and ventral regions of the striatum (Cazorla et al., 2012). However, the DMS and NA core have been more consistently implicated in the activation of goal-directed behavior (Corbit et al., 2001, Yin et al., 2005). Therefore, I chose to target the DMS or the NA core to manipulate excitability in a pathway-specific manner. I assessed motivation using instrumental tasks, including a progressive ratio schedule of reinforcement and a concurrent choice task. Both of these tasks have been validated in rodents and can provide reliable measures of how much effort an animal is willing to expend to obtain a food reward (Salamone et al., 2003, Bradshaw and Killeen, 2012). In addition, I also tested whether chronically increasing excitability of dMSNs or iMSNs in specific striatal sub-regions alters locomotor activity in mice. Thus, in addition to investigating how excitability in different circuits and brain regions may contribute to the motivation phenotype of D2R-OE_{dev} mice, I also aimed to understand how the basal ganglia regulate motivated behavior for natural rewards through specific striatal sub-circuits.

MATERIALS AND METHODS

Animals

All animal protocols used in the present study were approved by the Institutional Animal Care and Use Committees of Columbia University and New York State Psychiatric Institute. *Drd1*-Cre (FK150Gsat/Mmcd) and *Drd2*-Cre (ER44Gsat/Mmcd) on a C57BL/6J background were purchased from the Mutant Mouse Resource & Research Centers (National Institutes of Health). Both male and female adult mice at least eight weeks old were used in this study. Mice were housed under a 12:12-hour light:dark cycle in a temperature-controlled environment, and all behavioral testing was done during the light cycle. Food and water were available *ad libitum*, except when they were being trained or tested in operant behavioral tasks, during which time mice were only given 2 h per day of unrestricted feeding time, which occurred immediately after testing session. Mice were also food deprived on days when they underwent testing for food preference, during which time they were given an additional hour of unrestricted feeding with laboratory chow immediately after each test session.

Stereotaxic injections

For all viral injection surgeries mice were anesthetized with a mixture of ketamine and xylazine (100 mg/kg and 10 mg/kg) administered by intraperitoneal injection. Animals were then placed in a stereotaxic apparatus and body temperature was maintained at 37 °C with a heating pad. Small cranial windows (< 0.5 mm) were drilled at the appropriate sites and viruses were delivered at an average rate of 100 nL/min using glass pipettes (tip opening 10-15 μm). All stereotactic coordinates were measured relative to bregma. A total of 0.4-0.5 μL volume was delivered into each site for all injections. Two bilateral sites of injection were used for targeting

the DMS to allow diffusion of the virus to the entire region (site A: AP: +1.3 mm, ML: \pm 1.4 mm, DV: -3.3; site B: AP +0.9 mm, ML \pm 2.0 mm, DV -3.4 mm). The NA core was targeted bilaterally with one set of coordinates (AP: +1.7 mm, ML: \pm 1.2 mm, DV: 4.0 mm). All behavioral experiments were started least four weeks after surgery to allow for stable viral transfection.

Drug treatments

D-Amphetamine (Sigma A5880) was dissolved in sterile saline (0.9% NaCl) at 0.2 mg/mL and administered via intraperitoneal injection at a dose of 2 mg/kg. Amphetamine solution was prepared on the same day of experiment.

Behavioral assays

Open field locomotion

Locomotor activity in an open field was assessed in acrylic activity chambers (42 cm long \times 42 cm wide \times 38 cm high) equipped with infrared photobeams for motion detection (Kinder Scientific). To measure baseline locomotion, mice were placed in the open field, and activity was automatically recorded for 60 min. To measure amphetamine-induced locomotion, mice were similarly placed in the open field after the system had been programmed to interrupt recording 90 min after starting a session, at which point mice were administered amphetamine and placed back in the open field. Recording of locomotor activity resumed for another 90 min immediately after injections.

Operant training and progressive ratio

Operant training and testing were done in experimental chambers equipped with liquid dippers, retractable levers, head entry detector in the feeder trough, a house light, and an exhaust fan. Unless otherwise indicated, for every session the dipper was submerged into a tray containing evaporated milk, so that raising the dipper provided a reward of one drop of evaporated milk into the feeder trough. Throughout the study, each animal was subjected to only one operant session per day.

Mice were first trained to consume the liquid reward from the dipper located inside the feeder trough. In the first session, they were placed inside the chambers with the dipper in the raised position, providing access to a drop of evaporated milk. The dipper was retracted 10 seconds after the first head entry into the feeder trough. A variable inter-trial interval (ITI) ensued, followed by a new trial identical to the first. The session ended after 30 minutes or 20 dipper presentations. On the following day, mice underwent another session similar to the first, except that the dipper retraction was response-independent. During each trial, the dipper was raised for 8 seconds and then lowered independently of whether mice had made a head entry. The session ended after 30 minutes or 30 dipper presentations. All mice underwent dipper training for 2 days before moving on to Pavlovian training. All mice underwent one hour-long Pavlovian training session, in which the mechanical dipper was raised approximately once per minute for 5 seconds. Immediately before the dipper was raised, the lever was extended into the chamber for 6 seconds to allow mice to associate the lever extension to the milk reward. Whether the mouse pressed the lever or not, the dipper was raised when the lever was retracted, providing access to the reward. In the subsequent phase of training, mice were required to press a lever to earn the milk reward. At the beginning of a session, the lever was extended into the chamber, and lever presses were reinforced on a continuous reinforcement (CRF) schedule. In CRF and in all

subsequent sessions, the reward consisted of raising the dipper with a drop of evaporated milk in it for 5 seconds. The lever was retracted after every two times the mouse earned a reward, and then was re-extended after a variable ITI (averaging 30 seconds). The session ended when the mouse earned 60 reinforcements, or one hour elapsed. Mice continued undergoing daily CRF sessions until they earned 60 rewards in two consecutive sessions. When all mice reached criterion, they were moved to training fixed interval (FI) schedules.

In FI schedule training, lever presses were not reinforced until after a fixed interval (timed relative to the lever extension) had elapsed. Mice began on FI 4 s schedule, meaning that the first lever press occurring 4 s after lever extension was reinforced. Each reinforcement was followed by a variable ITI (mean of 30 seconds; range of 110 seconds), during which the lever remained retracted. The start of a new trial was signaled by the extension of the lever. Each session consisted of a maximum of 36 trials or 1 hour. Mice were subjected to sessions with increasing intervals on each day; the FI durations were 4, 8, 16, and 24 s. All animals were required to complete all 36 trials in the FI 24 s schedule before being tested in the progressive ratio schedule.

The progressive ratio task directly assesses operant motivation by quantifying the amount of effort a subject is willing to expend to earn a reward. The progressive ratio schedule used was one in which the amount of presses required to obtain each successive reward increased exponentially by a power of two. Motivation was measured by recording the total number of lever presses made and number of rewards earned during a session, as well as how long a subject continued to respond before giving up. Each session could last up to 2 hours but ended early if the mouse did not press the lever for 3 minutes. Mice underwent 5-7 consecutive days of testing in the progressive ratio schedule.

Concurrent choice

All mice were first tested in the progressive ratio schedule before being trained for the concurrent choice task. A random ratio (RR) schedule, consisting of a constant probability of reinforcement for each lever press, was used to train animals for this task. All mice were first trained for at least 2 days in an hour-long RR 5 sessions, in which on average every fifth lever press was rewarded. Following this training, animals were subjected to the concurrent choice task, consisting of RR sessions, in which animals could press a lever to obtain a milk reward, in operant boxes that also contained 8-12 g freely accessible laboratory chow in a dish. Increasing ratios were used (RR5, RR10, RR20) with concurrent choice (i.e. freely available chow), and all mice underwent at least two sessions with each ratio. For the experiments in which mice were virally injected in the DMS, an RR 30 schedule of reinforcement was also used, and mice were also tested at least twice in RR 30 session without concurrent free chow available. The amount of food consumed by each mouse in each session was calculated by subtracting the weight of the food remaining after a session from the weight of the food pellet measured before the session.

Outcome devaluation

In this task, mice are tested to determine whether or not they are pressing the lever because they have formed a habit, or if they are still sensitive to the outcome. The reward is therefore devalued by allowing mice to have unlimited access to the reward for a specified time period prior to the trial. If mice are truly pressing the lever in order to obtain the reward, they should press the lever fewer times throughout the session if they have been exposed to the reward beforehand. Here, the valued reward was sweetened evaporated milk, and standard mouse chow served as the control. Mice were therefore pre-fed with the valued reward or a non-valued reward before testing. The mice were then placed in an operant chamber with a lever

extended, but lever presses were not reinforced throughout the session. Because this non-reinforced task should extinguish pressing behavior, mice were trained in RR 30 sessions for 1-2 days in between devaluation testing days in order to maintain high press rates.

On outcome devaluation testing days, mice were first pre-fed with either the valued reward (sweetened evaporated milk) for 30 min or laboratory chow – a control food which they had never been trained to associate as a reward for lever pressing – for 1 h. Mice were only given 30 min of access to the valued reward in order to prevent complete satiation with milk, which might have resulted in complete loss of motivation to obtain the reward during the session. All mice were single-housed during pre-feeding. Immediately after pre-feeding mice were placed in an operant chamber with an extended lever for 15 minutes without ever receiving a reward. Testing occurred on two different days in a randomized design so that each mouse received pre-feeding with milk or chow once. The number of lever presses made in each session was measured for assessment of outcome devaluation.

Food preference

Assessment of food preference was always done at the end of all operant training and testing. On separate days, mice were subjected to two food preference sessions, in which they were individually placed in standard holding cages with access to different foods or water. In one session, mice had access to freely available evaporated milk and laboratory chow, and in the other session mice had access to freely available water and laboratory chow. The order of sessions was counterbalanced for each experimental group. Total consumption of milk, chow, and water was calculated for each mouse by measuring the weight of the food or the volume of milk or water before and after each session.

Histology and immunohistochemistry

For all histological analysis of brain tissue following behavioral experiments, mice were anesthetized with a mixture of ketamine and xylazine (100 mg/kg and 10mg/kg, respectively), administered by intraperitoneal injection, and were transcardially perfused, first with PBS and then with 4% paraformaldehyde. Following perfusion, brains were post-fixed in 4% paraformaldehyde for 24 hours, and then transferred to PBS. Brains were then sliced into 50- μ m coronal sections using a vibratome and every section was collected.

For confirmation of virally targeted regions, immunohistochemistry using fluorescence was performed on these free-floating sections by treating sections first with blocking buffer (0.5% bovine serum albumin, 5% horse serum, 0.2% Triton X-100), followed by the primary rabbit dsRed polyclonal antibody (1:250, Clontech, cat. 632496) and subsequently with goat anti-rabbit IgG (H+L) secondary antibody Alexa Fluor 568 conjugate (1:1000, Thermo Fisher Scientific, cat. A-11011). Sections were washed with 0.2% Triton X-100 in between incubation with antibodies and with 50 mM Tris-Cl pH 7.4 before mounting. Sections were mounted on glass slides and subsequently coverslipped for imaging with VectaShield containing DAPI (Vector Labs). Images were acquired at 2.5x magnification using a Hamamatsu camera attached to a Carl Zeiss epifluorescence microscope. Micrographs were processed using ImageJ software (National Institutes of Health).

Data analysis and statistics

All data collected in the current study were processed with Excel (Microsoft). Statistical analyses were done with either Excel or with Prism 5 (GraphPad). Most data sets were normally distributed and Student's t test, repeated-measures ANOVAs, or two-way ANOVAs were done, with Bonferroni or Dunnett *post hoc* tests conducted when appropriate. Because the data set for

session duration in the progressive ratio task was not normally distributed, the Log-rank non-parametric test was used to compare whether or not the independent variables significantly affected survival functions for session duration.

RESULTS

INCREASING EXCITABILITY OF DIRECT PATHWAY

First, I chronically increased excitability of the direct pathway by expressing the trans-dominant negative $K_{ir}2.1^{AAA}$ channel in dMSNs in the DMS. I used *Drd1*-Cre mice to selectively target the direct pathway. These animals were injected with the AAV2/1-Syn-DIO-Kir2.1AAA-IRES-mCherry virus, characterized in Chapter 2, or the control virus AAV2-EF1 α -DIO-mCherry into the DMS. The purpose of this experiment was to determine whether changes in chronic excitability of the direct pathway arising from the DMS might lead to specific changes in motivated behavior. After allowing the transgene to be expressed for several weeks, I tested these animals in a number of behavioral assays, the results of which are shown in Figure 14. This manipulation was carried out in two separate cohorts of mice, and most, but not all, behavior tests were conducted for both cohorts. In tests for which data from both cohorts were available, results were pooled to yield the plots presented in Figure 14. The number of subjects tested to generate each plot and statistics is reported.

In this first experiment, I found that *Drd1*-Cre mice expressing $K_{ir}2.1^{AAA}$ in dMSNs in the DMS did not show differences in locomotor activity in an open field compared to control littermates ($t_{(11)} = 1.337$, $p = 0.2082$; $n = 20$ mice per group) (Figure 14A). In addition, animals' preferences for laboratory chow and evaporated milk were also assayed, and no differences in

food consumption or preference between groups were detected for any of the food pairs tested ($F_{(1,18)} = 0.00004571$, $p = 0.9947$; $n = 10$ mice per group) (Figure 14B).

These animals were then trained to press a lever to earn a food reward. Increasing FI schedules were used during training to shape mice to press a lever at high rates to continue earning rewards. In each FI session, for each trial, a pre-determined time interval (4, 8, 12, 16, or 24 s) after the lever extension had to elapse before a lever press resulted in the presentation of a reward. As shown in Figure 14C, mice expressing Kir2.1^{AAA} in dMSNs in the DMS progressively increased their rate of responding with increasing FI schedules ($F_{(4,38)} = 247.0$, $p < 0.0001$; $n = 20$ mice per group). However, for each FI schedule, no difference in training performance was observed between mice expressing Kir2.1^{AAA} and those expressing a control gene in dMSNs in the DMS ($F_{(1,38)} = 0.08082$, $p = 0.7777$; $n = 20$ mice per group) (Figure 14C).

Once all animals were adequately trained, they were tested in a progressive ratio schedule of reinforcement, a test of motivation that measures how much effort an animal is willing to expend to obtain a food reward. I used a specific progressive ratio schedule in which the lever press requirement doubled with each successive reward and the session timed out if a mouse stopped responding for three minutes. Animals were tested in this schedule for multiple consecutive days, and the parameters used to compare performance between groups included the session duration, representing how long an animal continued to press a lever on average across all sessions, as well as total number of lever presses and lever press rate for each session. No significant differences were observed between mice expressing Kir2.1^{AAA} or a control gene in dMSNs in the DMS in the survival functions of their average session duration (Log-rank test: $\chi^2 = 1.907$, $p = 0.1763$; $n = 20$ mice per group), or in the number of lever press responses they made in each session ($F_{(1,38)} = 1.456$, $p = 0.2350$; $n = 20$ mice per group) (Figures 14D-E). Finally, in

all progressive ratio sessions, animals' press rates were not different between groups ($F_{(1,38)} = 0.0009894$, $p = 0.9751$; $n = 20$ mice per group) (Figure 14F).

Animals were also tested in a concurrent choice task, in which they were given the choice to press a lever to obtain a preferred food reward (evaporated milk) or to consume a less palatable food reward (laboratory chow) without expending any effort. In this assay, although I tested animals in different RR schedules, I only show the data from the highest RR schedule tested (RR 30). I found that chronically increasing excitability of dMSNs in the DMS did not affect how much animals were willing to press a lever to obtain a more palatable reward in an RR 30 schedule of reinforcement when given the option to freely consume a less palatable food ($F_{(1,18)} = 0.1271$, $p = 0.7256$; $n = 10$ mice per group) (Figures 14G). Both groups showed decreased operant responding when a freely available food was introduced (chow availability: $F_{(1,18)} = 70.44$, $p < 0.001$, group: $F_{(1,18)} = 0.4262$, $p = 0.5221$; $n = 10$ mice per group), demonstrating that animals in both groups could modulate their behavior based on the available choices (Figure 14G). In sessions in which laboratory chow was freely available, the amount of chow consumed by each mouse was measured, and no difference was observed in chow consumption between mice with more excitable dMSNs in the DMS and control animals ($F_{(1,18)} = 0.5920$, $p = 0.4516$; $n = 10$ mice per group) (Figure 14H).

I further tested whether mice with increased excitability of the direct pathway in the DMS showed any behavioral difference to controls in how well they could encode the value of the reward. Since all animals were trained to press a lever to obtain evaporated milk as a food reward, I tested whether decreasing the value of that reward by pre-feeding animals with evaporated milk would decrease their rate of operant responding in extinction trials. I found that,

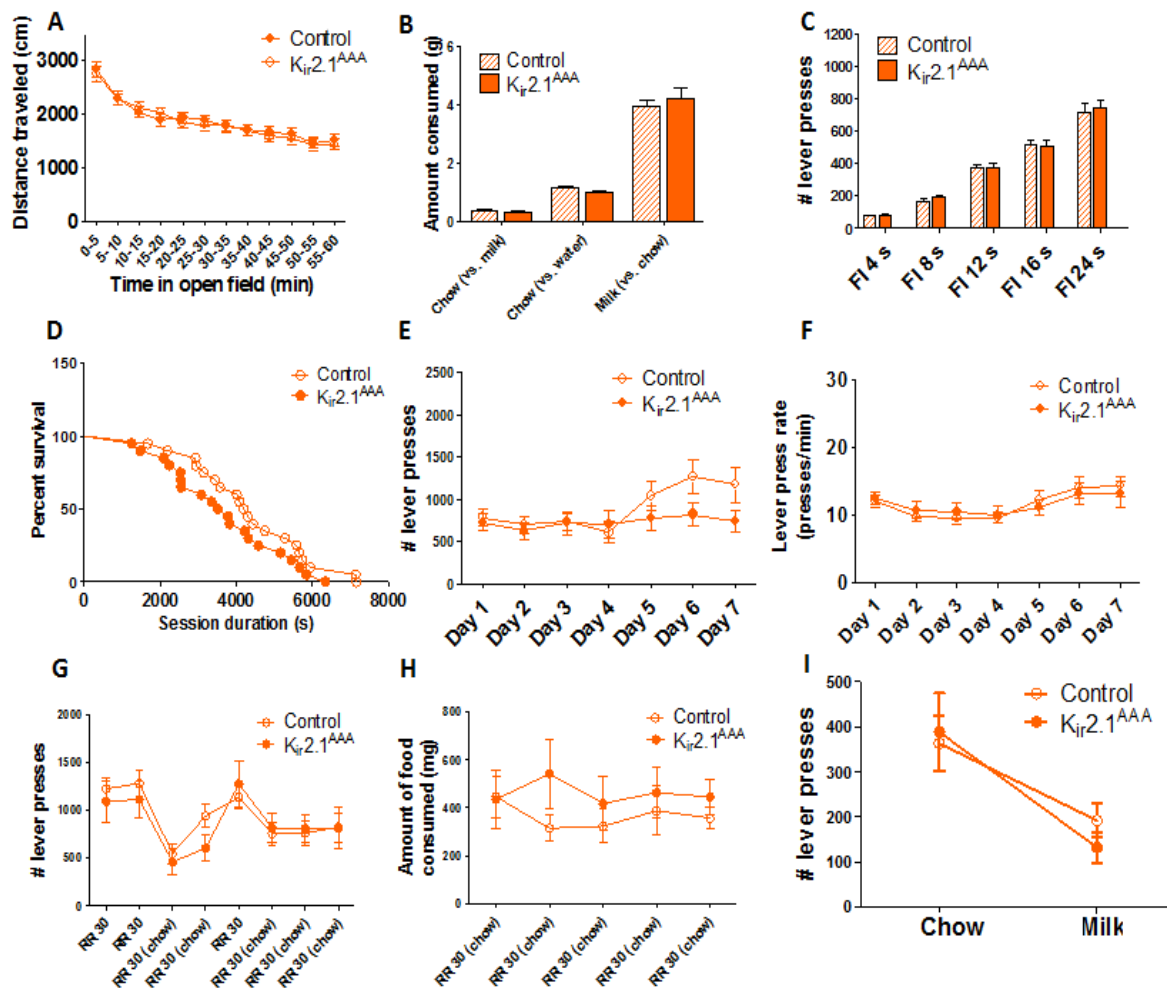


Figure 14: Effects of chronically increasing excitability of direct pathway in the DMS. **A.** Mice expressing $K_{ir2.1}^{AAA}$ in dMSNs in the DMS have similar baseline locomotor activity compared to controls, as measured by distance traveled in an open field for 1 h ($p = 0.2082$; $n = 20$ mice per group). **B.** No differences in food preference between groups were detected for any of the food pairs tested ($p = 0.9947$; $n = 10$ mice per group). **C.** All mice progressively increased their rate of responding with increasing FI schedules ($p = 0.7777$; $n = 20$ mice per group). **D-F.** No differences were observed between groups in the progressive ratio schedule of reinforcement, as measured by **(D)** the survival functions for average session duration ($p = 0.1763$; $n = 20$ mice per group), **(E)** number of responses in each session ($p = 0.2350$; $n = 20$ mice per group), and **(F)** rate of lever pressing ($p = 0.9751$; $n = 20$ mice per group). **G.** In the concurrent choice task, both groups showed decreased operant responding when a freely available food was introduced (chow availability; $p < 0.001$, group: $p = 0.5221$; $n = 10$ mice per group). **G-H.** There were also no performance differences between mice expressing $K_{ir2.1}^{AAA}$ or a control virus in the concurrent choice task, as measured by **(G)** the total number of responses in concurrent choice sessions with RR 30 schedule of reinforcement ($p = 0.7256$; $n = 10$ mice per group), and **(H)** amount of chow consumed by mice in each group during these concurrent choice sessions ($p = 0.4516$; $n = 10$ mice per group). **I.** In an outcome devaluation test, mice in both groups showed similar decreased rates of pressing after pre-feeding with evaporated milk compared to a control condition in which mice were pre-fed chow, a food that had never been associated with lever pressing (pre-fed food: $p = 0.0018$, group: $p = 0.7682$; $n = 10$ mice per group).

compared to a control condition in which mice were pre-fed chow, a food that had never been previously associated with lever pressing, mice in both groups showed similar decreased rates of pressing after pre-feeding with evaporated milk (pre-fed food: $F_{(1,17)} = 13.61$, $p = 0.0018$, group: $F_{(1,17)} = 0.08970$, $p = 0.7682$; $n = 10$ mice per group) (Figure 14I). This finding demonstrates that expressing Kir2.1^{AAA} in dMSNs in the DMS does not impair animals' sensitivity to outcome devaluation.

Given the negative results reported above, I attempted to determine whether it was possible to induce a behavioral phenotype in animals expressing Kir_{ir}2.1^{AAA} in the direct pathway in the DMS. Since acute amphetamine leads to extracellular levels of dopamine that are higher than physiological levels (Kuczenski and Segal, 1997), I predicted that increased dopamine activation of D1Rs in more excitable dMSNs could further potentiate the direct pathway's function to drive behavior. I therefore measured locomotion in freely behaving mice expressing Kir_{ir}2.1^{AAA} or a control gene in dMSNs in the DMS before and after acute systemic treatment with

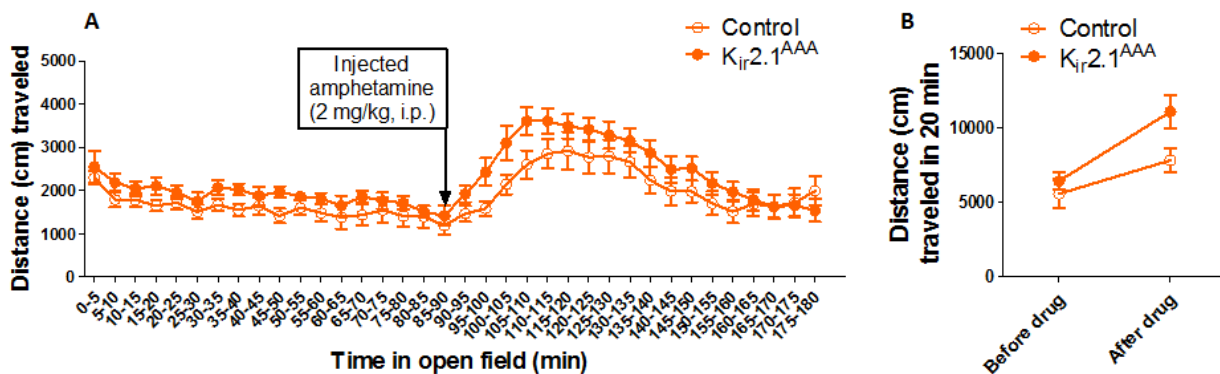


Figure 15. Chronically increasing excitability of dMSNs in the DMS potentiates locomotor response to acute amphetamine. **A.** Open field locomotor activity of mice expressing Kir_{ir}2.1^{AAA} or a control gene in dMSNs in the DMS 90 min before and 90 min after treatment with amphetamine (2 mg/kg). **B.** Comparing locomotor activity for both groups 20 min before and 20 min after treatment with amphetamine showed that mice in both groups increased locomotion in response to amphetamine ($p = 0.0006$), and mice expressing Kir_{ir}2.1^{AAA} had a potentiated response to the drug compared to controls ($p = 0.0437$). A total of 10 mice expressing Kir_{ir}2.1^{AAA} and 10 mice expressing the mCherry control gene were assayed for this analysis.

amphetamine. As expected, mice in both groups showed increased locomotion after acute treatment with amphetamine ($F_{(1,18)} = 17.33$, $p = 0.0006$; $n = 10$ mice per group) (Figure 15). And most importantly, mice expressing $K_{ir2.1}^{AAA}$ in dMSNs in the DMS exhibited a potentiated locomotor response to amphetamine treatment compared to control animals ($F_{(1,18)} = 4.705$, $p = 0.0437$; $n = 10$ mice per group) (Figure 15). Therefore, it is possible to induce a behavior read-out for chronically increasing excitability in a selective population of striatal MSNs using the AAV2/1-Syn-DIO-Kir2.1AAA-IRES-mCherry virus despite negative findings in behavioral measures of baseline locomotion and motivation for food.

I also conducted a similar experiment involving a similar series of behavioral assays in a separate cohort of *Drd1*-Cre mice, but this time expression of $K_{ir2.1}^{AAA}$ was targeted to dMSNs in the NA core instead of the DMS. The purpose of this experiment was to test whether chronically increased excitability of dMSNs in the NA core would affect incentive motivation in mice. The results for this experiment are presented in Figure 16 which includes data from one single cohort of mice tested in all behavioral assays.

Similar to what was observed when excitability was increased in the DMS, expressing $K_{ir2.1}^{AAA}$ in dMSNs in the NA core also did not change animal's baseline locomotor activity ($t_{(22)} = 0.1937$, $p = 0.8482$; $n = 9-10$ mice per group) or animal's food preferences ($F_{(1,16)} = 0.0008703$, $p = 0.9768$) (Figures 16A-B). Mice were then trained to press a lever to obtain a food reward and were trained in FI schedules with progressively longer intervals before testing in operant tasks of motivation. FI schedules with longer intervals led to higher number of lever press responses in both groups ($F_{(4,15)} = 140.5$, $p < 0.0001$; $n = 9$ mice per group) (Figure 16C). Although no differences were observed between groups when animals were tested in FI 4 s

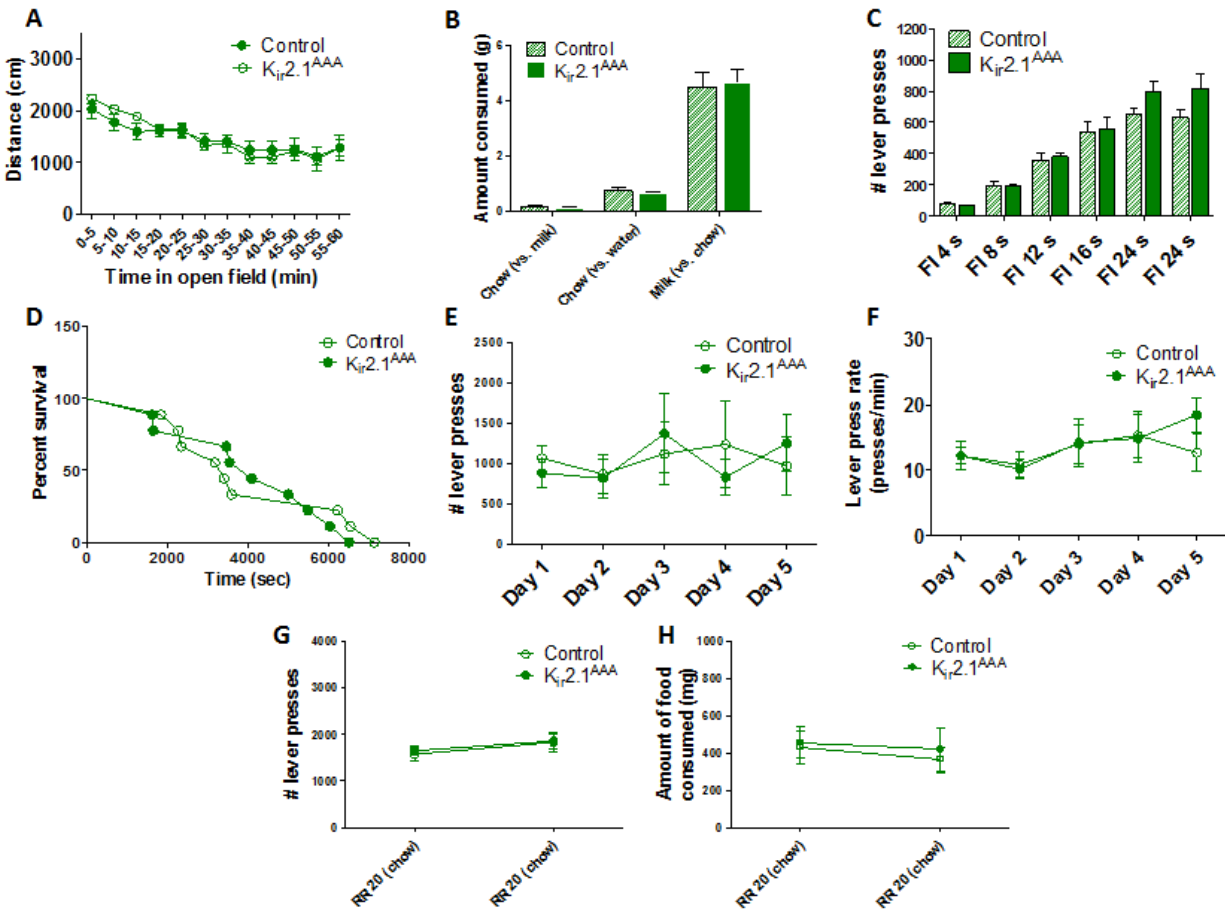


Figure 16: Effects of chronically increasing excitability of direct pathway in the NA core. **A.** Mice expressing $K_{ir}2.1^{AAA}$ in dMSNs in the NA core show similar baseline locomotor activity compared to controls, as measured by distance traveled in an open field for 1 h ($p = 0.8482$). **B.** No differences in food preference between groups were detected for any of the food pairs tested ($p < 0.0001$). **C.** No differences were observed between groups when animals were tested in FI 4 s through FI 16 s ($p = 0.8308$). At the longest FI interval, FI 24 s, mice with more excitable dMSNs in the NA core made significantly more lever presses in a session compared to the control group ($p = 0.0486$). **D-F.** No differences were observed between groups in the progressive ratio schedule of reinforcement, as measured by (**D**) the survival functions for average session duration ($p = 0.5982$), (**E**) number of responses in each session ($p = 0.9587$), and (**F**) rate of lever pressing ($p = 0.7580$). **G-H.** There were also no differences between performance in mice expressing $K_{ir}2.1^{AAA}$ or a control virus in the concurrent choice task, as measured by (**G**) the total number of responses in concurrent choice sessions with RR 20 schedule of reinforcement ($p = 0.8111$), and (**H**) the amount of chow consumed by mice in each group during these concurrent choice sessions ($p = 0.7535$). A total of 9 mice expressing $K_{ir}2.1^{AAA}$ and 9 mice expressing the mCherry control gene were assayed for this analysis.

through FI 16 s ($F_{(1,15)} = 0.04726$, $p = 0.8308$; 9 mice per group), at the longest intervals, FI 24 s, mice with more excitable dMSNs in the NA core made significantly more lever presses in a session compared to the control group ($F_{(1,15)} = 4.608$, $p = 0.0486$; $n = 9$ mice per group) (Figure 16C). However, when animals were tested in tasks of motivation, including the progressive ratio and concurrent choice tasks, no behavioral differences in performance were observed between groups (Figures 16D-H). In the progressive ratio task, the survival functions for session duration were not different between groups (Log-rank test: $\chi^2 = 0.2777$, $p = 0.5982$; $n = 9$ mice per group) (Figure 16D). Other parameters in this task, including total number of lever presses ($F_{(1,16)} = 0.002762$, $p = 0.9587$; $n = 9$ mice per group) and rate of responding ($F_{(1,16)} = 0.09826$, $p = 0.7580$; $n = 9$ mice per group) in each session were similarly not changed (Figures 16E-F). In the concurrent choice assay for this experiment, animals were given the choice to either press a lever to obtain a more palatable food reward at different RR schedules of reinforcement or to consume the freely available less palatable laboratory chow. Only data for the highest RR schedule tested (RR 20) is shown for this experiment. Mice expressing Kir2.1^{AAA} or a control gene in dMSNs in the NA core did not perform differently in this task, as measured by the total number of lever presses ($F_{(1,16)} = 0.05903$, $p = 0.8111$; $n = 9$ mice per group) and amount of chow consumed ($F_{(1,16)} = 0.1021$, $p = 0.7535$; $n = 9$ mice per group) in concurrent choice sessions (Figures 16G-H).

INCREASING EXCITABILITY OF INDIRECT PATHWAY

I also carried out a parallel set of experiments using *Drd2*-Cre mice to manipulate excitability in iMSNs selectively in the DMS or NA core. As in the set of experiments described above, I injected mice with the AAV2/1-Syn-DIO-Kir2.1AAA-IRES-mCherry viral vector or the

control virus AAV2-EF1 α -DIO-mCherry into either the DMS or NA core. Mice were tested in the same behavioral paradigms as those done for experiments targeting dMSNs in *Drd1*-Cre mice. In addition to testing how MSN excitability affects motivation, these experiments were also intended to determine whether increasing density of bridging collaterals could also affect motivation because in Chapter 2 I showed that injecting the AAV2/1-Syn-DIO-Kir2.1AAA-IRES-mCherry virus in the DMS of *Drd2*-Cre mice to increase excitability of iMSNs can induce growth of bridging collaterals (see Figure 9).

Chronically increasing excitability of the indirect pathway by expressing Kir2.1^{AAA} selectively in iMSNs in the DMS did not lead to behavior effects in most assays tested. There were no differences in baseline locomotor activity ($t_{(22)} = 0.5121$, $p = 0.6137$; $n = 9-10$ mice per group) or food preferences ($F_{(1,17)} = 0.07919$, $p = 0.7818$; $n = 9-10$ mice per group) between groups (Figures 17A-B). Moreover, when animals of both groups were trained to press a lever to obtain a food reward, they showed a similar progressive increase in lever pressing with increasing FI schedule intervals ($F_{(4,17)} = 95.49$, $p < 0.0001$; group: $F_{(1,17)} = 0.1091$, $p = 0.7452$; $n = 9-10$ mice per group) (Figure 17C). In the progressive ratio task, mice expressing either Kir2.1^{AAA} or a control gene in iMSNs in the DMS continued to respond for a similar amount of time (Log-rank test: $\chi^2 = 0.01734$, $p = 0.8952$; $n = 9-10$ mice per group) and made similar total number of lever presses ($F_{(1,17)} = 3.854$, $p = 0.0662$; $n = 9-10$ mice per group) (Figures 17D-E). However, the rate of lever pressing was significantly different between groups, with mice injected with the Kir2.1^{AAA} virus showing increased rates of responding compared to controls ($F_{(1,17)} = 10.45$, $p = 0.0049$; $n = 9-10$ mice per group) (Figure 17F). In the concurrent choice task, a trend towards increased total number of lever presses was observed when animals were tested

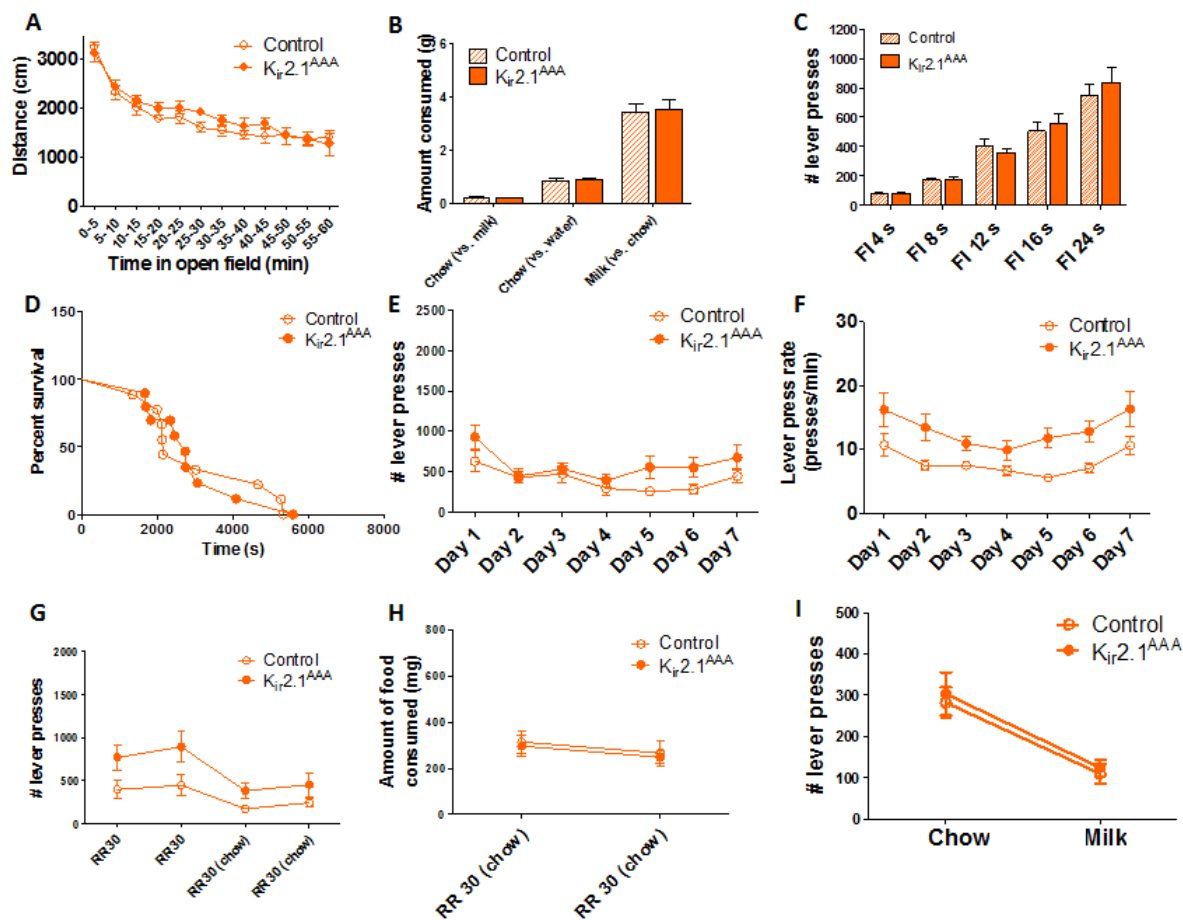


Figure 17: Effects of chronically increasing excitability of indirect pathway in the DMS. **A.** Mice expressing $K_{ir}2.1^{AAA}$ in iMSNs in the DMS show similar baseline locomotor activity compared to controls, as measured by distance traveled in an open field for 1 h ($p = 0.6137$). **B.** No differences in food preference between groups were detected for any of the food pairs tested ($p = 0.7818$). **C.** All mice progressively increased their rate of responding with increasing FI schedules ($p < 0.0001$; group: $p = 0.7452$). **D-E.** No differences were observed between groups for two parameters in the progressive ratio schedule of reinforcement, (**D**) the survival functions for average session duration ($p = 0.8952$) and (**E**) the number of responses in each session ($p = 0.0662$). **F.** The rate of lever pressing in the progressive ratio schedule was increased in mice expressing $K_{ir}2.1^{AAA}$ compared to controls ($p = 0.0049$). **G.** In RR 30 sessions without concurrent choice, a trend towards increased total number of lever presses for mice expressing $K_{ir}2.1^{AAA}$ compared to controls was observed ($p = 0.0546$). Both groups showed decreased operant responding when a freely available food was introduced (chow availability: $p < 0.0001$). **G-H.** There were also no differences between mice expressing $K_{ir}2.1^{AAA}$ or a control virus in the concurrent choice task, as measured by (**G**) the total number of responses in concurrent choice sessions with RR 30 schedule ($p = 0.1150$), and (**H**) the amount of chow consumed by mice in each group during these concurrent choice sessions ($p = 0.7592$). **I.** In an outcome devaluation test, mice in both groups showed similar decreased rates of pressing after pre-feeding with evaporated milk compared to a control condition in which mice were pre-fed chow, a food that had never been previously associated with lever pressing (pre-fed food: $p = 0.0003$, group: $p = 0.5916$). A total of 10 mice expressing $K_{ir}2.1^{AAA}$ and 9 mice expressing the mCherry control gene were assayed for this analysis.

in the RR 30 schedule of reinforcement at baseline ($F_{(1,17)} = 4.262$, $p = 0.0546$; $n = 9-10$ mice per group). When animals were given the choice to either press a lever to obtain evaporated milk or freely eat laboratory chow, they reduced their number of responses compared to baseline (chow availability: $F_{(1,17)} = 27.94$, $p < 0.0001$; $n = 9-10$ mice per group) (Figure 17G). However, on concurrent choice sessions, no differences were observed between groups in either total number of lever presses ($F_{(1,17)} = 2.759$, $p = 0.1150$; $n = 9-10$ mice per group) or amount of food consumed ($F_{(1,17)} = 0.09700$, $p = 0.7592$; $n = 9-10$ mice per group) (Figures 17G-H). In addition, animals in this cohort were subjected to an outcome devaluation test, and both groups were similarly sensitive to pre-feeding with evaporated milk (pre-fed food: $F_{(1,16)} = 20.90$, $p = 0.0003$, group: $F_{(1,16)} = 0.2997$, $p = 0.5916$), suggesting that chronically increasing excitability of the indirect pathway in the DMS does not affect how animals encode the value of a reward (Figure 17I).

Finally, I also injected the AAV2/1-Syn-DIO-Kir2.1AAA-IRES-mCherry virus into the NA core of *Drd2*-Cre mice in order to selectively increase excitability of the indirect pathway in that striatal region. Subsequent behavioral testing yielded the results presented in Figure 18. As can be seen in Figures 18A-B, baseline locomotor activity ($t_{(22)} = 0.1140$, $p = 0.9103$; $n = 8$ mice per group) and food preferences ($F_{(1,42)} = 0.005533$, $p = 0.9411$; $n = 8$ mice per group) were not changed between groups. Mice were also trained in operant tasks including FI schedules with progressively longer time intervals, and no differences between groups were observed for FI schedule with interval requirements between 4 and 16 s ($F_{(3,14)} = 0.1254$, $p = 0.7285$; $n = 8$ mice per group) (Figure 18C). However, in striking contrast to what was observed in *Drd1*-Cre mice (see Figure 16C), *Drd2*-Cre mice expressing $K_{ir2.1}^{AAA}$ in the NA core made significantly fewer

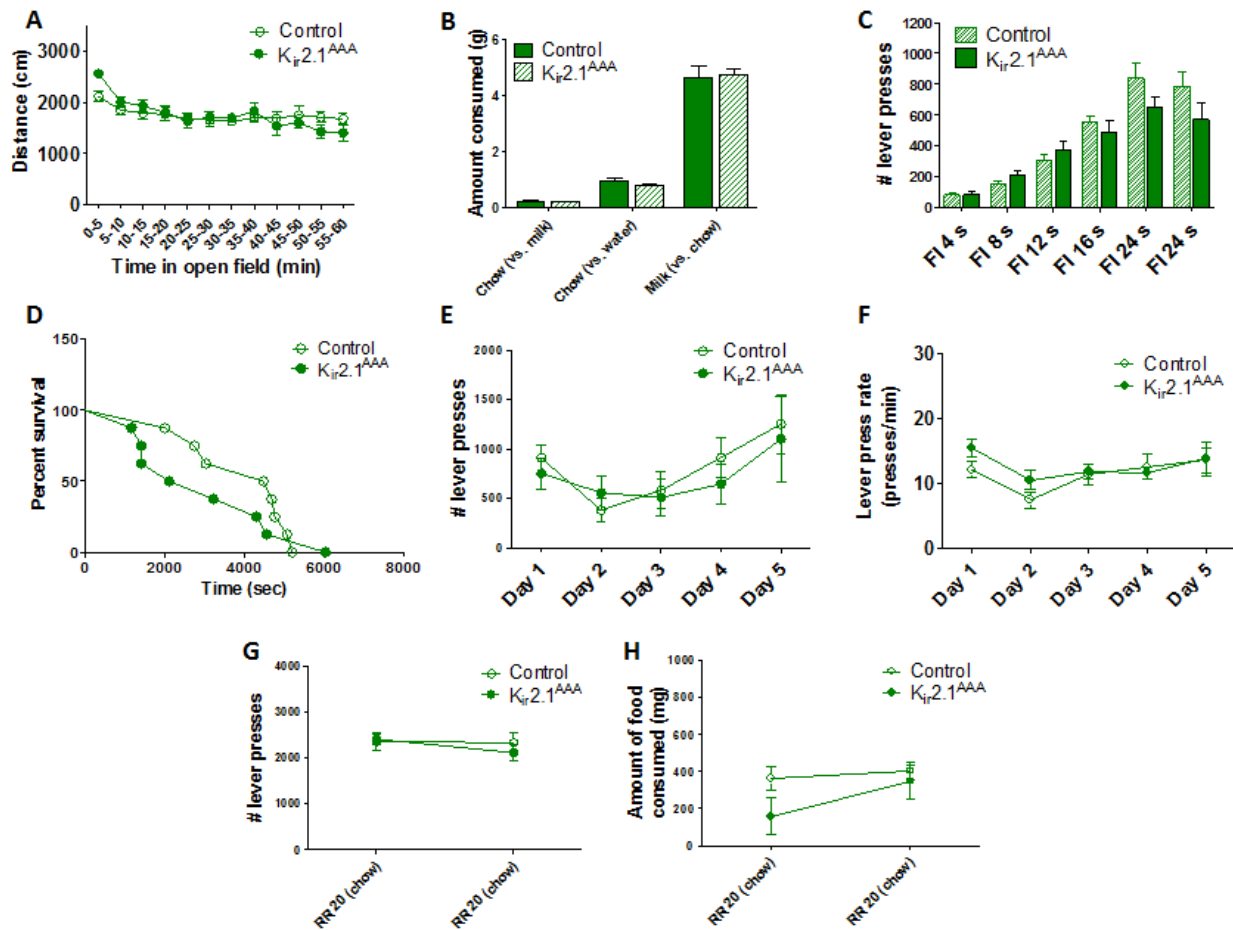


Figure 18: Effects of chronically increasing excitability of iMSNs in the NA core. **A.** Mice expressing $K_{ir}2.1^{AAA}$ in iMSNs in the NA core show similar baseline locomotor activity compared to controls, as measured by distance traveled in an open field for 1 h ($p = 0.9103$). **B.** No differences in food preference between groups were detected for any of the food pairs tested ($p = 0.9411$). **C.** No differences were observed between groups when animals were tested in FI 4 s through FI 16 s ($p = 0.7285$). At the longest interval, FI 24 s, mice with more excitable dMSNs in the NA core made significantly more lever presses in a session compared to the control group ($p = 0.0346$). **D-F.** No differences were observed between groups in the progressive ratio schedule of reinforcement, as measured by **(D)** the survival functions for average session duration ($p = 0.4762$), **(E)** number of responses in each session ($p = 0.6822$), and **(F)** rate of lever pressing ($p = 0.4833$). **G-H.** There were also no differences in performance between mice expressing $K_{ir}2.1^{AAA}$ or a control virus in the concurrent choice task, as measured by **(G)** the total number of responses in concurrent choice sessions with RR 20 schedule of reinforcement ($p = 0.7100$), and **(H)** the amount of chow consumed by mice in each group during concurrent choice tasks ($p = 0.1573$). A total of 8 mice expressing $K_{ir}2.1^{AAA}$ and 8 mice expressing the mCherry control gene were assayed for this analysis.

lever presses when compared to controls in the FI 24 s schedule ($F_{(1,14)} = 0.5480$, $p = 0.0346$; $n = 8$ mice per group) (Figure 18C). However, when animals were then tested in tasks of motivation, including the progressive ratio and the concurrent choice tasks, no differences in performance were observed between animals with chronically increased excitability of iMSNs in the NA core and controls (Figures 18D-H). The survival functions for average session duration were not statistically different between groups (Log-rank tests: $\chi^2 = 0.5076$, $p = 0.4762$; $n = 8$ mice per group) (Figure 18D). And the total number of lever presses ($F_{(1,14)} = 0.1748$, $p = 0.6822$; $n = 8$ mice per groups) and rate of responding ($F_{(1,14)} = 0.5185$, $p = 0.4833$; $n = 8$ mice per group) were also not different between groups expressing $K_{ir}2.1^{AAA}$ or a control gene in iMSNs in the NA core (Figures 18E-F). Finally, in the concurrent choice task, mice were given the option to either press a lever to obtain a more palatable reward (RR 20 schedule of reinforcement) or to consume a freely available less palatable reward. No differences were observed between groups in the number of lever presses made ($F_{(1,14)} = 0.1440$, $p = 0.7100$; $n = 8$ mice per group) or in the amount of food consumed ($F_{(1,14)} = 2.233$, $p = 0.1573$; $n = 8$ mice per group) in this task (Figures 18G-H).

For all experiments involving expression of Cre-dependent $K_{ir}2.1^{AAA}$ by injecting

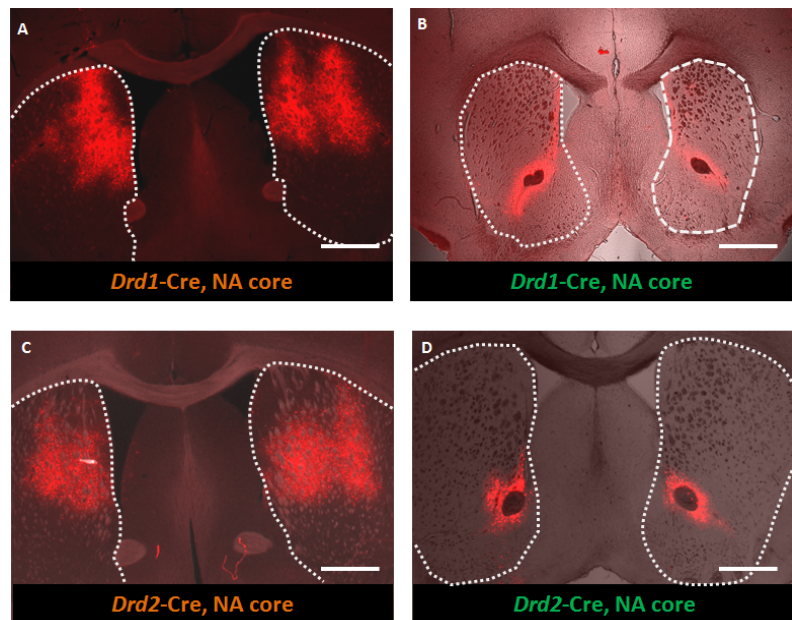


Figure 19: $K_{ir}2.1^{AAA}$ was selectively expressed in targeted regions. Sample micrographs of coronal sections from mice injected with the AAV2/1-Syn-DIO-Kir2.1AAA-IRES-mCherry virus used in each of the experiments in the current study. **A.** *Drd1*-Cre mice injected in the DMS. **B.** *Drd1*-Cre mice injected in the NA core. **C.** *Drd2*-Cre mice injected in the DMS. **D.** *Drd2*-Cre mice injected in the NA core. Scale bar: 1 mm.

the AAV2/1-Syn-DIO-Kir2.1AAA-IRES-mCherry virus in selective striatal sub-region of *Drd1*-Cre and *Drd2*-Cre mice, histological confirmation of virus expression was done for all subjects. As shown in Figure 19, the stereotaxic coordinates and virus injection protocol used in this study were appropriate to selectively transfect neurons in either the DMS or NA core.

DISCUSSION

In summary, I conducted a series of experiments in which I selectively increased excitability of the direct or indirect pathway in specific striatal sub-regions that have been implicated in goal-directed behavior, namely the DMS and NA core. I found that this manipulation did not lead to significant changes in different behavioral assays, such as locomotor activity in an open field and tasks of motivation, including the progressive ratio and concurrent choice tasks.

Even though I did not observe any clear effect on motivation after increasing excitability of striatal MSNs in a pathway-specific and region-specific manner, I did identify a few behavioral effects of this manipulation. One interesting finding was that among mice targeted in the NA core, expressing $K_{ir}2.1^{AAA}$ in dMSNs led to increased responding in an FI 24 s schedule, while expressing $K_{ir}2.1^{AAA}$ in iMSNs led to the exact opposite effect, with animals showing decreased responding in this same operant schedule. For this study, I decided to use FI schedules to train animals to press at high rates because this schedule has been previously used for the same purpose in other studies that investigated the effects of basal ganglia manipulations on incentive motivation (Drew et al., 2007, Trifilieff et al., 2013). However, it is known that mice can learn to time the interval and will scale their rate of responding to the FI schedule with repeated training on the same schedule (Taylor et al., 2007). In the current study, mice were not

subjected to the same FI schedule more than twice precisely to avoid this effect. Nevertheless, a specific effect in operant responding in the FI 24 s schedule, with no differences observed in all other behavioral assays in this study, suggest that excitability of dMSNs and iMSNs in the NA core may have a specific effect related to timing. Additional experiments with mice expressing $K_{ir2.1}^{AAA}$ selectively in dMSNs or iMSNs in the NA core could be done to test for a behavioral effect on a peak interval timing task (Taylor et al., 2007), potentially establishing a new link between NA function and timing in mice.

One possibility for the lack of effect of increasing MSN excitability on motivation is that protein expression or function of the $K_{ir2.1}^{AAA}$ channel was not efficient in dMSNs and iMSNs. The data presented in Chapter 2 showing an effect of chronic excitability on bridging collaterals goes against this possibility, as the same virus, AAV2/1-Syn-DIO-Kir2.1AAA-IRES-mCherry, was used in both studies. Moreover, I also demonstrated potentiated amphetamine-induced locomotion in animals expressing $K_{ir2.1}^{AAA}$ in dMSNs in the DMS, consistent with what would be expected with increased function of the direct pathway. In addition, electrophysiological recordings done in the Kellendonk laboratory in iMSNs from *Drd2*-Cre mice injected with the AAV2/1-Syn-DIO-Kir2.1AAA-IRES-mCherry virus in the NA have shown that resting membrane in these neurons have a mean of -74.62 mV (95% C.I.: -79.25 to -69.99 mV), a value statistically higher than the mean of -79.62 mV (95% C.I.: -80.70 to -78.53 mV) observed in iMSNs in the NA in animals injected with a control virus. Together, these data indicate that Cre-dependent expression of the $K_{ir2.1}^{AAA}$ channel using the AAV2/1-Syn-DIO-Kir2.1AAA-IRES-mCherry virus leads to a physiological effect on excitability of striatal MSNs that can induce a behavioral phenotype under specific pharmacological conditions. Nevertheless, as discussed in Chapter 2, a more comprehensive and direct demonstration that transfection of MSNs using this

Cre-dependent $K_{ir2.1}^{AAA}$ virus leads to a robust effect on neuronal excitability is still lacking. Despite this limitation, the negative results on motivation presented here suggest that chronically increasing excitability of dMSNs or iMSNs in a striatal sub-region-specific manner does not affect incentive motivation in mice.

When testing animals in tasks of motivation, I did observe a significant effect on rate of responding when I manipulated excitability of iMSNs in the DMS. Similar manipulation to dMSNs in the DMS did not lead to differences in rate of responding in any of the motivation assays. Some measurable parameters of goal-directed behavior that characterize motivation can be isolated and interpreted individually. These parameters include latency to initiate behavior, vigor of behavior, and duration of behavior. In this study, mice expressing $K_{ir2.1}^{AAA}$ in the DMS were not different from controls in their latency to initiate lever pressing (data not shown) or in the amount of time it took for them to “give up” lever-pressing behavior as the ratio requirement to obtain a reward increased. Lever press rate, which can be considered a measure of action vigor in the progressive ratio task, was specifically increased in mice with increased excitability of iMSNs in the DMS. These results can appear counterintuitive because the indirect pathway is traditionally thought to inhibit behavior initiation, and here I increased excitability of the indirect pathway. However, consistent with the known role of the DMS on performance vigor (Wang et al., 2013), it is plausible that disturbing excitability of the indirect pathway may interfere with the function of that pathway in inhibiting behaviors, rendering the influence of the direct pathway on vigor unrestrained by the indirect pathway and, consequently, stronger compared to controls. In support of this interpretation, in a separate cohort of *Drd2*-Cre mice injected with the AAV2/1-Syn-DIO-Kir2.1AAA-IRES-mCherry virus in the DMS, albeit in a smaller region of the DMS (data not shown), the same specific increase in press rate in the progressive ratio task

was observed. To further explore these findings, the role of iMSNs in the DMS on restricting the vigor of goal-directed actions should be studied using different strategies to manipulate function of the indirect pathway, ideally with better temporal control, including optogenetic and chemogenetic approaches.

As described in Chapter 2, increasing excitability of iMSNs in the DMS using the same genetic strategy used in the current study leads to growth of direct-pathway bridging collaterals into the GPe. My initial hypothesis was that increased collateral density may be responsible for the motivational deficit in D2R-OE_{dev} mice. This one-to-one relationship does not hold true, as increasing the density of bridging collaterals by increasing excitability of iMSNs in the DMS was not sufficient to affect motivation in mice. It can be concluded, therefore, that plasticity involving the bridging collaterals likely does not mediate the reversible deficit in motivation observed in D2R-OE_{dev} mice. Nevertheless, another strategy that could be used to confirm this conclusion would be to attempt to rescue the motivational deficit of D2R-OE_{dev} mice by overexpressing the wild-type K_{ir}2.1 protein in selective populations of striatal MSNs to decrease neuronal excitability. If the interpretation of the current data is correct, overexpression of the wild-type K_{ir}2.1 channel would also not be sufficient to rescue the motivational deficit of D2R-OE_{dev} mice. For technical reasons, I was not able to carry out this experiment. Instead, I attempted to perform a similar pathway-specific manipulation using a designer receptor exclusively-activated by a designed drug (DREADD), which provided additional temporal control of neuronal function and, as described in Chapter 4, led to further insight on how basal ganglia circuits regulate motivated behavior.

Another consideration for the data presented in this study is that, as I also showed in Chapter 2, behavioral training leads to plasticity involving the bridging collaterals, and the

density of these collaterals were never measured in either D2R-OE_{dev} mice or mice expressing Kir2.1^{AAA} in the striatum after testing on operant tasks of motivation. It is conceivable that, in this study, expressing Kir2.1^{AAA} in iMSNs in the DMS induced growth of bridging collaterals in mice but the daily operant training that preceded the actual behavioral assays for motivation may have led to retraction of collaterals, masking a potential effect of bridging collaterals on motivation.

The results of this study were largely negative, although some specific behavioral phenotypes were identified that can be further explored. One of the aims of the study was to determine the role of basal ganglia sub-circuits on motivation for natural rewards, but it may be possible that the manipulation was too mild to induce behavioral effects in the absence of higher levels of extracellular dopamine in the striatum. The observation that Kir2.1^{AAA} expression in dMSNs in the DMS potentiated animals' locomotor response to a psychostimulant supports this speculation. It might be possible that by producing a mild shift in the balance between the direct and indirect pathways, expression of Kir2.1^{AAA} in iMSNs might also lead to a behavioral effect on psychostimulant-induced locomotion. A reduced response to psychostimulant would be expected because Kir2.1^{AAA} expression in the indirect pathway would increase excitability of iMSNs, presumably counteracting the effect of dopamine to inhibit activity of iMSNs via D2Rs. Thus, to expand on some of the negative findings presented in this study, it would be interesting to test mice expressing Kir2.1^{AAA} in different striatal sub-circuits in similar behavioral assays after treatment with psychostimulants that increase extracellular levels of dopamine in the striatum, including amphetamine and cocaine. Moreover, it would also be informative to conduct the comprehensive set of manipulations and behavioral assays done in the current study using other strategies to selectively target function of striatal dMSNs and iMSNs. Some of such

selective strategies include the use of DREADDs and opsins, which can be selectively expressed in dMSNs and iMSNs and has been shown to affect behaviors regulated by the striatum (Kravitz et al., 2010, Ferguson et al., 2011, Kravitz et al., 2012). Other strategies that could be used to further study motivated behavior and have been previously shown to affect how dMSNs and iMSNs regulate behavior include inactivation of specific neuronal populations using neurotoxins (Durieux et al., 2009, Hikida et al., 2013) or selective deletion of DARPP32 in specific MSN populations (Bateup et al., 2010). Although these strategies have been used by researchers to probe specific aspects of basal ganglia function, comprehensive descriptions of how each of these strategies for disrupting basal ganglia function affect motivation when applied to specific striatal sub-circuits are still lacking.

CHAPTER 4

INDIRECT PATHWAY FUNCTION AND MOTIVATION

INTRODUCTION

The findings presented in Chapter 3 demonstrate that downregulation of $K_{ir}2.1$ function in MSNs is not sufficient to impair motivation in wild-type mice. Nevertheless, these findings do not discard the alternative that increased MSN excitability and activity may be necessary in D2R-OE_{dev} mice for their motivational deficit. I therefore attempted to rescue the motivational deficit of D2R-OE_{dev} mice by increasing function of the indirect pathway of the basal ganglia in these mice. For the current study, in addition to manipulating neuronal function chronically, as I did with $K_{ir}2.1^{AAA}$ expression in *Drd1*-Cre and *Drd2*-Cre animals in Chapter 2, I also manipulated indirect-pathway function acutely, with the aim to dissociate the acute effect on neuronal activity from the chronic plasticity effects that may alter the density of bridging collaterals. To address the question of whether the increase in excitability of iMSNs in D2R-OE_{dev} mice could explain the motivational deficit induced by striatal D2R upregulation, I used hM4D, a designer G_{ai} -coupled receptor exclusively-activated by the designer drug clozapine-*N*-oxide (CNO) to selectively decrease function of the indirect pathway in D2R-OE_{dev} and control mice. CNO can be used to activate hM4D receptors – and consequently activate intracellular G_{ai} signaling – both acutely and chronically to test if these manipulations in striatal iMSNs could be sufficient to rescue the motivational deficit of D2R-OE_{dev} mice.

For the acute manipulation, I first tested how activating G_{ai} -coupled signaling in the indirect pathway affected locomotion and motivation in D2R-OE_{dev} and control mice. I further tested animals expressing hM4D in striatal iMSNs in a novel behavioral assay, the progressive

hold-down task, that attempts to dissociate the directional from the activational components of motivation. I found that activating $G_{\alpha i}$ -signaling in iMSNs boosts motivation in both D2R-OE_{dev} and control mice by energizing behavior at the cost of goal-directed efficiency. Moreover, I also used the DREADD system to selectively activate $G_{\alpha i}$ signaling in iMSNs in either the DMS or NA core, and I found that both striatal sub-regions contribute to the acute effect on motivation of decreasing indirect-pathway function.

In order to further characterize the acute behavioral effects and understand how activating $G_{\alpha i}$ -coupled signaling in MSNs affects striatal circuit function, I probed activity of iMSNs expressing hM4D after CNO treatment both *in vitro* and *in vivo*. First I tested whether I could measure a change in intrinsic excitability in iMSNs expressing hM4D in the absence and presence of CNO using slice electrophysiology. In addition, I used *in vivo* calcium imaging in freely-behaving animals to probe how neurons at different nodes in the indirect pathway respond to activation of hM4D receptors in iMSNs. I tested whether activating $G_{\alpha i}$ signaling could lead to a change in somatic MSN activity. Then I also tested how neuronal activity in the GPe, which receives monosynaptic inhibition from the indirect pathway, was affected by activation of hM4D receptors in iMSNs. I found that activating $G_{\alpha i}$ -signaling does not lead to a significant change in somatic MSN activity. In contrast, neurons in the GPe, which receive monosynaptic inhibition from the indirect pathway, show increased activity when striatal hM4D receptors are activated. Consistent with these findings, I found that excitability of iMSNs was not affected by hM4D activation at the somatic level, and recent work from the Kellendonk laboratory and others has demonstrated that activation of hM4D receptors in iMSNs can inhibit GABAergic synaptic transmission to the pallidum (Bock et al., 2013). My observations, therefore, suggest that acutely

inhibiting indirect-pathway output to the pallidum arising from the DMS and NA core are potential therapeutic strategies for energizing behavior and thereby enhance motivation.

Previous work from the Kellendonk laboratory has shown that, similar to the effects of restoring MSN excitability in D2R-OE_{dev} mice by overexpressing wild-type Kir2.1 channels (Cazorla et al., 2014), expressing hM4D receptors non-conditionally in the DMS of D2R-OE_{dev} and treating these animals with CNO chronically is sufficient to retract bridging collaterals. To expand on these findings, I also investigated whether selectively decreasing iMSN function in D2R-OE_{dev} and control littermates chronically using the DREADD system could affect motivation in these animals. To this end, I treated mice expressing hM4D in iMSNs in the DMS and NA core chronically with CNO before testing for changes in locomotor activity and motivation. In an attempt to dissociate the acute effects of the drug on neuronal activity from the potential chronic effects of the drug on circuit rewiring, animals were tested both while on chronic CNO treatment and after allowing the drug to clear for 48 h. Having found that chronically activating hM4D receptors in iMSNs does not lead to a measurable effect on motivation, I conducted additional experiments to show that the lack of behavioral response to the chronic manipulation may be due to receptor desensitization or to short-term circuit-level compensation to a chronic decrease in iMSN function. These findings have important implications for drug therapies that target GPCRs in the striatum, and the behavioral desensitization effect described in this study should be considered in predicting how chronic pharmacologic manipulations of G_{ai} signaling in the striatum may affect behavior.

MATERIALS AND METHODS

Animals

All animal protocols used in the present study were approved by the Institutional Animal Care and Use Committees of Columbia University and New York State Psychiatric Institute. The generation of D2R-OE_{dev} mice has been described previously (Kellendonk et al., 2006). TetO-D2R mice have been backcrossed onto the C57BL/6J background and CaMKII α -tTA mice backcrossed onto the 129SveVTac background. To generate D2R-OE_{dev} mice, tetO-D2R/C57BL6 mice were crossed to CaMKII α -tTA/129SveVTac mice. Double transgenic mice express the transgenic D2R, and these animals were crossed to *Drd2*-Cre (ER44Gsat/Mmcd) mice, purchased from the Mutant Mice Resource & Research Centers, to obtain the transgenic D2R-OE/*Drd2*-Cre mice. For experiments that included D2R-OE_{dev} animals, controls were littermates of D2R-OE/*Drd2*-Cre mice that were positive for the Cre transgene but negative for the TetO or tTa transgenes. For experiments that did not include D2R-OE_{dev} mice, animals were *Drd2*-Cre backcrossed onto the C57BL/6J background. Both male and female adult mice at least 8-weeks old were used in this study. Mice were housed under a 12:12-hour light:dark cycle in a temperature-controlled environment, and all behavioral testing was done during the light cycle. Food and water were available *ad libitum* except for experiments that required restriction. Animals were food-deprived when being trained or tested in operant behavioral tasks. During such training or testing each animal was restricted to 1.8 g of food per day, provided immediately after each operant session. For chronic CNO treatment, mice had *ad libitum* access to CNO-treated water instead of regular drinking water. Animals were water-restricted for 16 h prior to experiments that involved acute oral CNO treatment.

Stereotaxic injections

For viral injection surgeries that did not involve lens implantation, including surgeries done for mice used for behavioral assays of motivation and for electrophysiology, mice were anesthetized with a mixture of ketamine and xylazine (100 mg/kg and 10 mg/kg) administered by intraperitoneal injection. Since viral injection surgeries that included lens implantation last longer than suitable for anesthesia with ketamine/xylazine, mice were anesthetized by inhalation with isoflurane (3.0% for induction, 1.0% for maintenance) mixed with oxygen (1 L/min) for such surgeries. For all surgeries, once anesthetized, animals were placed in a stereotaxic apparatus and body temperature was maintained at 37 °C with a heating pad. Surgical incisions to expose the cranium were made, and small cranial windows (<0.5 mm) were drilled at the appropriate sites. Virus was delivered at an average rate of 100 nL/min using glass pipettes (tip opening 10-15 μ m). All stereotaxic coordinates were measured relative to bregma. A total of 0.4-0.5 μ L volume was delivered into each site for all injections. For co-injection of two viruses in the case of AAV1-Syn-flexed-GCaMP6F and AAV5/hSyn-DIO-hM4D-mCherry delivered into the DMS for calcium imaging, equal volumes of each virus were mixed and loaded into the injection pipette. Unless otherwise indicated, two sites of injection were used for bilaterally targeting the DMS to allow diffusion of the virus to the entire region (site A: anterior-posterior (AP): +1.3 mm, medial-lateral (ML): \pm 1.4 mm, dorsal-ventral (DV): -3.3; site B: AP +0.9 mm, ML \pm 2.0 mm, DV -3.4 mm). The NA core was targeted bilaterally with one set of coordinates (AP: +1.7 mm, ML: \pm 1.2 mm, DV: 4.0 mm). For calcium imaging in the striatum, the DMS was targeted unilaterally using a single injection site (AP: +1.3 mm, ML: \pm 1.4 mm, DV: -3.3 mm). The GPe was targeted unilaterally for calcium imaging with virus injected in discrete pulses covering a 0.3-mm distance in the DV axis (AP: 0.0 mm, ML: +1.8 mm, DV: -3.9-4.1 mm).

For viral injections accompanied by lens implantation, a microlens composed of a pair of gradient refractive index lenses fused to a relay lens was used. A 2-mm cranial window was drilled over the intended implantation site, followed by removal of the dura and aspiration of portions around the edges of the craniotomy. Following unilateral injection of AAV1-Syn-GCaMP6F into the GPe or co-injection of AAV1-Syn-flexed-GCaMP6F and AAV5/hSyn-DIO-hM4D-mCherry into the DMS, as described above, the microlens was lowered into the same site used for viral injection with alternate retractions of 0.5 mm for every 1 mm ventral increment to allow penetrated tissue to properly settle around the lens. For implants into the DMS, microlenses measuring 0.6 mm in diameter and ~7.3mm in length were used, and for implants into the GPe, microlenses measuring 0.5 mm in diameter and ~8.4 mm in length were used (Inscopix). After implantation, the portion of the lens extending above the skull was fixed in place using dental cement and anchored by 3 screws attached to different plates on the skull. The lens was covered with a silicone elastomer to protect the imaging surface from external damage. The silicone elastomer was removed four weeks after surgery for attachment of a baseplate (Inscopix) to support the miniature microscope on each animal's head. For this procedure, mice were once again anesthetized with isoflurane. The silicone mold was removed, and the miniature microscope (Inscopix) with a baseplate attached and the 475-nm LED turned on was positioned above the implanted lens and lowered with a micromanipulator until fluorescence could be detected. Once the microscope was positioned for imaging in an adequate focal plane, the magnetic baseplate was cemented around the lens adjoined to the dental cement previously placed at the time of surgery. The microscope was subsequently detached and a magnetic cover plate (Inscopix) was secured onto the baseplate with a screw set to protect the lens until imaging.

Drug treatments

CNO was provided by the National Institutes of Health as part of the National Institutes of Mental Health Chemical Synthesis and Drug Supply Program. For behavioral experiments, CNO was always dissolved in sterile PBS on the same day it was used for treatment. For acute treatment, the drug was always prepared at 0.2 mg/mL and delivered at 2 mg/kg dose by intraperitoneal injections 30 minutes prior to a behavioral task, unless otherwise indicated. Saline injections for control condition consisted of 0.25 mL sterile PBS. For chronic treatment, CNO was dissolved in animals' regular drinking water at a concentration of 0.25 mg/mL. Animals treated with CNO chronically had this CNO solution as their only source of drinking water for at least two weeks, to which they had access *ad libitum*. Except where otherwise indicated, CNO solution in the drinking water was freshly-prepared on the day prior to start of chronic treatment, and freshly-prepared solution was replenished as needed approximately every 2-4 days for the duration of chronic treatment. Vehicle chronic treatment consisted of regular mouse drinking water. For acute oral CNO administration, animals were allowed to freely consume CNO solution in drinking water at 0.25 mg/mL for 1 h before behavioral testing. Crossover designs for drug treatment were used for testing in all behavioral assays, unless otherwise indicated, with animals receiving CNO or saline/vehicle on alternate days of testing counterbalancing for variables such as genotype, virally-targeted brain region, and sex. CNO solutions used for electrophysiology experiments were first dissolved at 1 mM or 100 μ M in artificial cerebrospinal fluid (ACSF, exact composition described in "*In vitro* electrophysiology" section) and stored at -20 °C until the day of recording, at which time an aliquot was thawed and diluted 1:100 in oxygenated ACSF to a final concentration of 10 μ M or 1 μ M.

Behavioral assays

Progressive ratio

Training and testing for the progressive ratio schedule of reinforcement were conducted similarly to the training and testing conducted for the study presented in Chapter 3, with a few differences detailed below. The first exception was that in the current study, mice were never subjected to FI schedules. Instead, in order to get animals pressing at high rates, they were trained in random interval (RI) schedules. In RI schedule training, the lever remained extended throughout the session but lever presses were not reinforced until after a random interval had elapsed. Between reinforcements, there was a variable ITI, defined by the RI schedule. All mice began on RI 3 s schedule, meaning that the first lever press occurring on average 3 s after start of a trial was reinforced. When a mouse earned at least 40 rewards in one session, the RI schedule was increased. The RI schedules used were 3 s, 10 s, 15 s, and 20 s. When all mice reached the criterion of 40 rewards in one session on the RI 20 s schedule, they began experimental testing on the progressive ratio schedule. Mice continued to be trained in RI 20 s sessions for 1-2 days in between each progressive ratio session in order to prevent lever pressing behavior from extinguishing with the low reinforcement rate characteristic of the progressive ratio schedule. Mice were subjected to 1-3 progressive ratio sessions for each condition, and measures for each condition were averaged.

Progressive hold-down

All mice tested in the progressive hold-down test were subjected to this task after being tested in the progressive ratio task. Specific training for the progressive hold-down test consisted of variable interval hold-down (VIH) schedules. Each session involved up to 40 trials and, at the beginning of each trial, the required hold duration was drawn randomly from a distribution with

a mean specified by the session. Each session ended when a mouse successfully completed 40 trials or when 1 h elapsed. This hold requirement remained in place until the subject was reinforced for completing the trial. During the first session, the distribution of required hold durations had a mean of 0.5 s (VIH 0.5 s). When all mice in the cohort earned 40 rewards in one session, they were moved to the subsequent VIH schedule, following the sequence VIH 0.5 s, 1 s, 2 s, 4 s, 6 s, 8 s, and 10 s. Animals only started being tested in the progressive hold-down test when all subjects in the cohort were able to complete all 40 trials in VIH 10 s. For the progressive ratio task, the first required hold duration was fixed at 3 s, and the requirement for subsequent hold durations was increased sequentially by a factor of 1.4. The sessions could last up to 2 h but ended early if the mouse did not press the lever for 10 minutes. The energizing component of motivation was assessed by the number of lever presses made and how long subjects continued to respond, while the goal-directed component was assessed by the number of rewards earned in a session and the proportion of rewarded presses. Mice were subjected to two progressive hold-down sessions for each condition, and measures for each condition were averaged.

Outcome devaluation

In this task, mice are tested to determine whether or not they are pressing the lever because they have formed a habit, or if they are still sensitive to the outcome. The reward is therefore devalued by allowing mice to have unlimited access to the reward for a specified time period prior to the trial. If mice are truly pressing the lever in order to obtain the reward, they should press the lever fewer times throughout the session if they have been exposed to the reward beforehand. Here, the valued reward was sweetened evaporated milk, and standard mouse chow served as the control. Mice were therefore pre-fed with the valued reward a non-

valued reward before testing. The mice were then placed in an operant chamber with a lever extended, but lever presses were not reinforced throughout the session. Because this non-reinforced task should extinguish pressing behavior, mice were trained in random ratio (RR) sessions for 2-3 days in between devaluation testing days in order to maintain high press rates. In an RR schedule there is a constant probability of reinforcement for each lever press. The specific schedule used, RR 20, required that the animal press the lever on average 20 times before receiving a reward.

On outcome devaluation testing days, mice were first pre-fed with either the valued reward (sweetened evaporated milk) for 30 min or laboratory chow – a control food which they had never been trained to associate as a reward for lever pressing – for 1 h. Mice were only given 30 min of access to the valued reward in order to prevent complete satiation with milk, which might have resulted in complete loss of motivation to obtain the reward during the session. All mice were single-housed during pre-feeding. After 1 h passed from the start of pre-feeding, mice were treated with either CNO or saline. Thirty minutes after the injection, mice were placed in an operant chamber with an extended lever for 15 minutes without ever receiving a reward. Testing occurred on four different days in a randomized design so that each mouse received each experimental manipulation once (pre-feeding with milk or chow and injected with either an acute CNO or saline injection). The number of lever presses made in each session was measured for assessment of outcome devaluation.

Open field

For experiments that did not involve calcium imaging, exploration and reactivity to an open field was assessed in acrylic activity chambers (42 cm long × 42 cm wide × 38 cm high) equipped with infrared photobeams for motion detection (Kinder Scientific). Mice were placed

in the open field, and activity was automatically recorded for a specified amount of time (90 or 120 min). The open field system was programmed to interrupt recording 20 or 30 min after the start, at which point mice were administered CNO or saline and placed back in the open field. Recording of locomotor activity resumed immediately after injections.

For calcium imaging experiments, cellular activity and locomotor activity were simultaneously measured while animals moved freely in an open field. Before each imaging session, the miniature microscope was connected to the magnetic baseplate attached to each animal's cranium and fixed in place by the baseplate screw set while the mouse was briefly anesthetized with isoflurane. Each animal was placed back into its home cage for 20 min to recover from anesthesia before drug injection or imaging. For imaging sessions, mice were placed in acrylic activity chambers (42 cm long × 42 cm wide × 38 cm high) less than 1 min before optical recording with the miniature microscope was initiated. The Ethovision XT system (Noldus) was used to trigger both start and end of recording sessions using a TTL pulse converter. This software was also used to track each animal's locomotor activity using a video camera placed over the open field area.

Histology and immunohistochemistry

For all histological analysis of brain tissue following behavioral experiments, mice were anesthetized with a mixture of ketamine and xylazine (100 mg/kg and 10mg/kg, respectively), delivered by intraperitoneal injection, and transcardially perfused, first with PBS and then with 4% paraformaldehyde (PFA). Following perfusion, brains were post-fixed in 4% PFA for 24 hours, and then transferred to PBS. Brains were then sliced into 50- μ m sagittal or coronal sections using a vibratome and every section was collected. Immunohistochemistry using fluorescence was performed on these free-floating sections by treating sections first with

blocking buffer (0.5% bovine serum albumin, 5% horse serum, 0.2% Triton X-100), followed by overnight incubation with one or more primary antibody and subsequently with the appropriate secondary antibody conjugated to a fluorophore. The primary antibodies used included rabbit anti-DsRed (1:250, Clontech, cat. 632496), mouse anti-RFP (1:1000, Abcam, cat. AB65856), rabbit anti-Cre (1:2000 (Kellendonk et al., 1999)), and goat anti-ChAT (1:100, Millipore, cat. AB144P). Sections were washed with 0.2% Triton X-100 in between primary and secondary antibody incubations and with 50 mM Tris-Cl pH 7.4 before mounting. Sections were mounted on glass slides and subsequently coverslipped for imaging with VectaShield containing DAPI (Vector Labs). For confirmation of spread of viral infection in targeted structures, images were acquired at 2.5x magnification using a Hamamatsu camera attached to a Carl Zeiss epifluorescence microscope. For analysis of co-expression of fluorescent and immune-labelled proteins, images were acquired at 20x or 40x using a Nikon Ti Eclipse inverted microscope for scanning confocal microscopy. Micrographs were processed using ImageJ software (National Institutes of Health).

***In vitro* electrophysiology**

Mice injected with AAV5/hSyn-DIO-hM4D-mCherry into the DMS, were sacrificed four weeks after surgery by rapid decapitation and brains were harvested into ice-cold, oxygenated ACSF containing 1.25 mM NaH₂PO₄, 2.5 KCl mM, 10 mM glucose, 26.2 mM NaHCO₃, 126 NaCl mM, 2 CaCl₂ mM and 2 MgCl₂ mM (pH 7.4, 300–310 mOsm). Coronal sections (300 μm thick) containing striatum were cut using a vibratome in ice-cold oxygenated ACSF and incubated at 32 °C for 30 min, followed by at least 30 min incubation at room temperature before recordings. Voltage- and current-clamp whole-cell recordings were performed using standard techniques (Cazorla et al., 2012). Electrode resistance was 3-6 MΩ when filled with internal

solution composed of 130 mM K⁺-gluconate, 5 mM NaCl, 10 mM HEPES, 0.5 mM EGTA, 2.0 mM Mg⁺-ATP, and 0.3 mM Na⁺-GTP (pH 7.3, 280 mOsm). Cells expressing the hM4D receptor in the striatum were identified by mCherry fluorescence under epifluorescence microscopy. Measures of excitability were obtained by injecting 500-ms currents ranging from -150 to 350 pA in 20 pA steps. The resting membrane potential was determined from this protocol as each patched cell's potential with 0 pA current. Rheobase was determined as the minimal injected current that resulted in an action potential. Spike frequency was determined from the initial pair of action potentials as previously described (Cazorla et al., 2012). For each cell patched, measures of excitability were obtained 5 min after the cell was patched first with ACSF in the bath and then 15 min after maintaining ACSF in the bath solution or exchanging the bath solution to 1 μ M CNO or 10 μ M CNO diluted in ACSF.

Data analysis and statistics

All data collected in the current study were processed with Excel (Microsoft) or with custom scripts and functions written with MATLAB (Mathworks). Statistical analyses were done with either one of the latter software or with Prism 5 (GraphPad). All statistical tests were 2-tailed and alpha level was set to 0.05.

For operant tests of motivation, the behavioral measures used for analysis included the total number of lever presses and reinforcers earned in a session for the progressive ratio and progressive hold-down tests. For outcome devaluation tests, total number of lever presses made in a session was the parameter analyzed. To compare normally-distributed parameters, such as number of lever presses and reinforcers earned, under different conditions, repeated measures analysis of variance (ANOVA) tests were used to test for statistical significance. The log-rank

Mantel-Cox test, a nonparametric statistical test, was used to compare whether or not the independent variables significantly affected session durations.

To analyze the effect of drug on locomotor activity in an open field, the sums of the total ambulatory distance from a time point 30 min after i.p. injection until the end of each session were obtained. These measures were tested for statistical significance using repeated measures ANOVA tests.

Calcium imaging recordings acquired at 15-20 Hz were processed using Mosaic (Inscopix). First, movies were spatially down-sampled using a spatial binning factor of 4 to reduce the large file size and decrease processing time. To correct for brain movement, all frames in movie sequences acquired from the same mouse and same focal plane were registered to one single frame. Multiple movie sequences registered to the same frame were then concatenated in time and a sub-region within the field of view in the concatenated movie was cropped in order to remove post-registration black borders. Using the mean z-projection image of the entire movie as reference (F_0) to normalize fluorescence signals to the average fluorescence of the entire frame, a movie representing percent-change-over-baseline ($\Delta F/F_0$) was generated. The $\Delta F/F_0$ movie was temporally binned by a factor of 4. Calcium transients from individual cells were isolated and identified with an automated cell-sorting algorithm that employs independent and principal component analyses of each $\Delta F/F_0$ movie. The independent components identified by the algorithms were visually inspected for spatial configuration and temporal properties of calcium traces and those that appeared like calcium transients from individual cell bodies were used for further analysis. These raw calcium traces for each cell measured as z-scores over the entire time recorded were separated into 12-s time bins for statistical analysis. For individual cell analysis, the sums of calcium activity in 12-s bins

measured from each 5-min recording session done after treatment with either saline or CNO – or after two treatments with saline – were compared using one-factor ANOVA tests. Cells that displayed significant increases or decreases in activity in between sessions were identified and the proportions of significantly changed and unchanged cells were used in a chi-squared test to determine whether these proportions were expected by chance. Additional analyses were done for data obtained from calcium imaging in the striatum after thresholding the raw traces to obtain estimates of individual calcium events. The sums of these events (either counting each event as a single unit or summing the z-scores for each event) were obtained in 12-s bins. Since the latter data sets were not normally distributed, individual cell analyses were performed using the non-parametric Wilcoxon rank sum test to identify cells that showed significantly decreased or increased calcium activity after treatment with either saline or CNO – or after two treatments with saline. Proportions of significantly changed and unchanged cells were compared using the chi-squared test as described above.

RESULTS

ACUTE BEHAVIORAL EFFECTS OF DECREASING INDIRECT-PATHWAY FUNCTION

The D2R-OE_{dev} mouse overexpress D2Rs selectively in striatal MSNs and exhibit a deficit in motivation (Kellendonk et al., 2006, Drew et al., 2007). Since chronic upregulation of striatal D2Rs leads to increased excitability of MSNs (Cazorla et al., 2012), I questioned whether an increase in iMSN function in D2R-OE_{dev} mice could explain the motivational deficit induced by developmental D2R upregulation in the striatum. I therefore expressed hM4D receptors in indirect-pathway MSNs of the DMS and NA core of *Drd2-Cre/D2R-OE_{dev}* mice and *Drd2-Cre*

control littermates. The hM4D protein is a genetically modified $G_{\alpha i}$ -coupled receptor that can no longer be activated by endogenous ligands, but instead can be activated by CNO (Armbruster et al., 2007). Activation of hM4D in the indirect pathway of the rat has been shown to decrease excitability of MSNs (Ferguson et al., 2011). Thus, I attempted to use this chemogenetic approach to study how activating $G_{\alpha i}$ signaling, and presumably decreasing excitability and function, of the indirect pathway acutely would affect motivation D2R-OE_{dev} and control mice.

To study the behavioral consequences of acutely activating $G_{\alpha i}$ signaling in the indirect pathway of D2R-OE_{dev} mice and control littermates, I selectively targeted iMSNs in the DMS and NA core, sub-regions of the striatum known to support motivated behavior (Corbit and Balleine, 2011, Hilario et al.,

2012, Burton et al., 2015). I injected *Drd2*-Cre mice with an AAV vector for Cre-dependent expression of the hM4D receptor. The virus was delivered bilaterally to target either the medial striatum, encompassing both DMS and NA core (Figure 20B), or each of these striatal sub-regions separately (Figures 20C-D). The hM4D protein expressed virally is fused to the

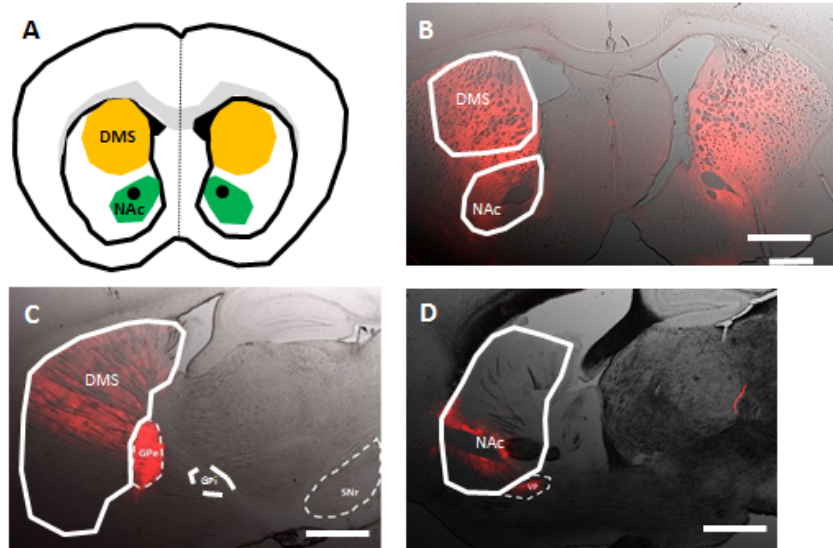


Figure 20: The $G_{\alpha i}$ -coupled designer receptor hM4D can be expressed selectively in specific striatal regions. **A.** Diagram of coronal section showing targeted injection sites in DMS and NA. **B.** Coronal section micrograph showing hM4D-mCherry expression in the DMS and NA core of *Drd2*-Cre mouse. Scale bar: 1 mm. **C.** Sagittal section micrograph showing hM4D-mCherry expression in the DMS, as well as immune-positive axon terminals present in the GPe and absent in the SNr. Scale bar: 1 mm. **E.** Sagittal section micrograph showing hM4D-mCherry expression in the NA core and axon terminals in the VP. Scale bar: 1 mm.

fluorophore mCherry, allowing for detection of the subcellular localization of the receptor by probing for mCherry. Expression of hM4D receptor in the injected sites was observed at the soma and dendrites of infected cells. In addition, hM4D expression was also observed in the neuropil and in regions where axons of iMSNs terminate: the GPe, in the case of animals injected in the DMS (Figure 20C), and the VP, in the case of animals injected in the NA core (Figure 20D). No fluorescence signal was observed in the output nuclei of the direct pathway, the SNr and GPi, in animals injected in the DMS (Figure 20C), evidencing that expression was restricted to iMSNs, as these neurons are known to only project to the GPe (Gerfen and Surmeier, 2011).

I also quantified the selectivity of this expression system by immunohistochemistry. Co-staining for hM4D and Cre revealed that 95% of hM4D-positive cells were also immune-positive for Cre, and the efficiency of transfection was also high, as 86% of Cre-positive cells within the constraints of the virally-infected region were immune-positive for hM4D (Figure 21A). Cholinergic interneurons that represent less than 2% of neurons in the striatum are also known to

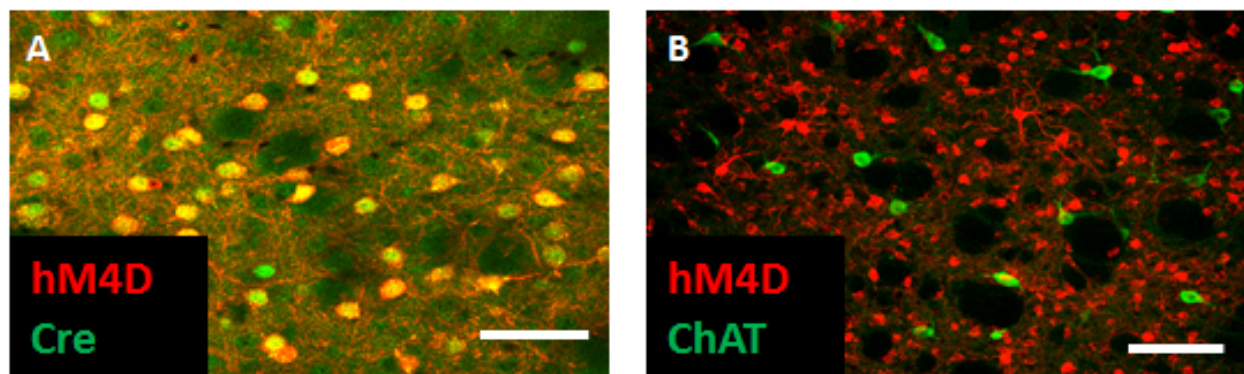


Figure 21: The $G_{\alpha i}$ -coupled designer receptor hM4D can be expressed selectively in iMSNs. A. Micrograph of immunostained striatal tissue from *Drd2*-Cre mouse expressing hM4D-mCherry (red) in neurons that also express Cre (green); 95% of mCherry-positive neurons are also Cre-positive and 86% of Cre-positive neurons in virally-targeted region are positive for hM4D-mCherry ($n = 175$ cells). Scale bar: 50 μm . **B.** Micrograph of striatal tissue from *Drd2*-Cre mouse immunostained for hM4D-mCherry (red) and the marker for cholinergic neurons, ChAT; 5% of ChAT-positive neurons express hM4D-mCherry in virally-targeted region ($n = 110$ cells). Scale bar: 100 μm .

express D2Rs (Dawson et al., 1990). I therefore quantified what proportion of these interneurons also expressed hM4D in our viral transfection system. I found that only 5% of neurons positive for choline acetyltransferase (ChAT), a marker for cholinergic interneurons, were also immunopositive for hM4D in the virally-infected region (Figure 21B), in agreement with previous results using this BAC transgene Cre mouse line (Kravitz et al., 2010). Hence, I demonstrated that I can selectively and efficiently express hM4D receptors in the striatal indirect pathway and that these receptors localize to both somatic and axonal regions of MSNs.

To test for the effect of hM4D receptor activation in the indirect pathway of mice chronically overexpressing striatal D2Rs, I trained *Drd2*-Cre/D2R-OE_{dev} mice and *Drd2*-Cre control littermates expressing Cre-dependent hM4D in the DMS and NA core to press a lever to earn a food reward. Once all animals were adequately trained, they were tested in a progressive ratio schedule of reinforcement, a test of motivation that measures how much effort an animal is willing to expend to obtain a reward. I used a specific progressive ratio schedule in which the lever press requirement doubled with each successive reward.

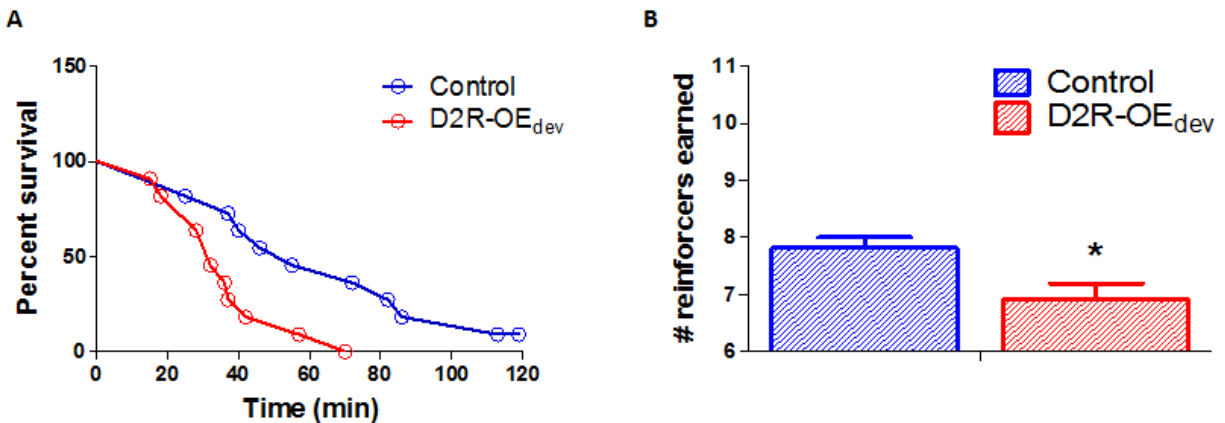


Figure 22: Motivational deficit of D2R-OE_{dev} mice can be reproduced in animals expressing hM4D in iMSNs. At baseline without any drug treatment, D2R-OE_{dev} expressing hM4D in iMSNs show impaired performance in the progressive ratio task of motivation compared to control animals, as measured by (A) the survival functions for session durations ($p = 0.0121$) and (B) the total number of reinforcers earned in a session ($p = 0.0140$). A total of 11 D2R-OE_{dev} mice and 11 control mice were assayed for this analysis.

I first tested whether I could measure the motivation deficit of D2R-OE_{dev} mice in our experimental system. I confirmed the previously reported impairment in performance of D2R-OE_{dev} mice in the progressive ratio task, as D2R-OE_{dev} stopped responding sooner than control littermates (Log-rank test: $\chi^2 = 4.235$, $p = 0.0121$, $n = 11$ mice) and earned fewer rewards ($t_{(20)} = 2.692$, $p = 0.0140$; $n = 11$ mice) (Figure 22) (Drew et al., 2007).

I then retested the animals after treatment with saline or CNO using a within-group

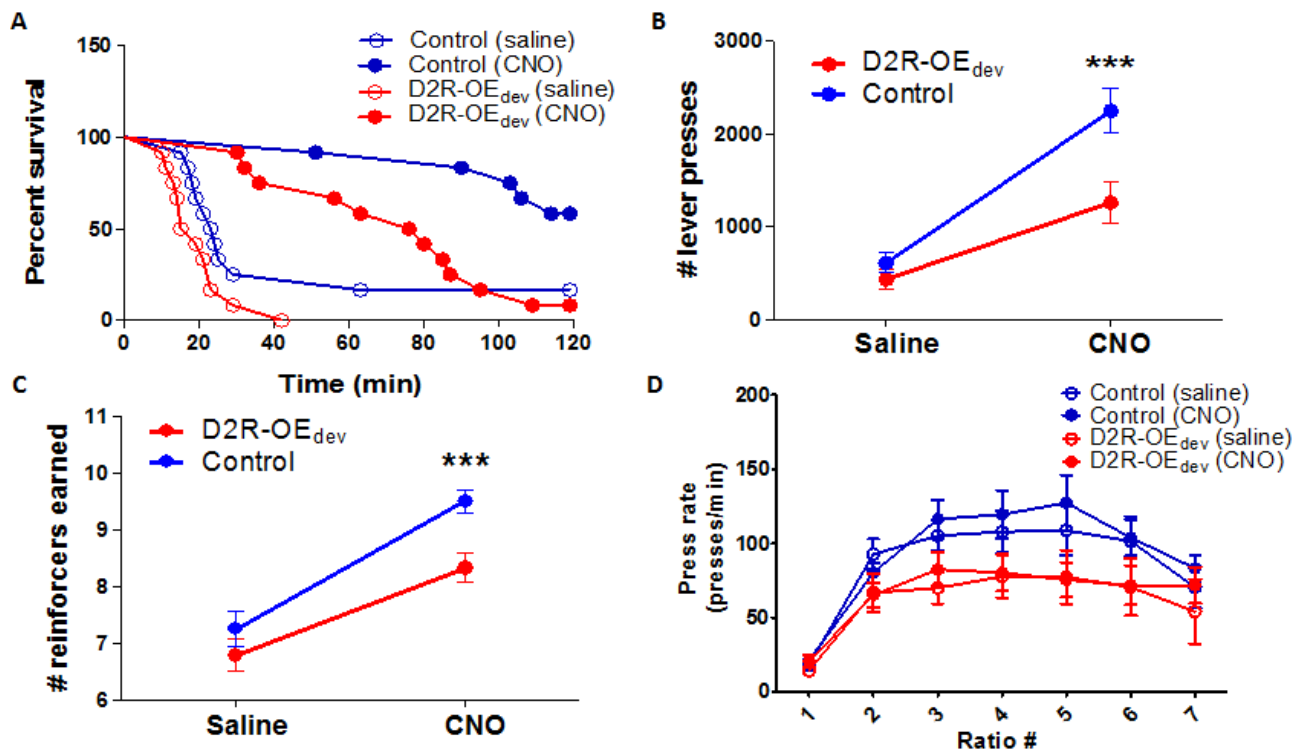


Figure 23: Decreasing function of indirect pathway increases motivation in D2R-OE_{dev} and control littermates. A-C. Both D2R-OE_{dev} and control mice expressing hM4D in iMSNs in the DMS and NA core show enhanced performance in the progressive ratio test of motivation after treatment with CNO compared to saline, as measured by (A) survival functions for session duration (D2R-OE_{dev}: $p < 0.0001$; control: $p = 0.0019$), (B) total number of lever presses made ($p < 0.001$), and (C) total number of reinforcers earned ($p < 0.001$). A-C. When comparing performance between genotypes after treatment with CNO in the progressive ratio test, (A) D2R-OE_{dev} continued to respond in the task for shorter times ($p < 0.0012$), (B) made fewer total lever presses ($p < 0.0101$, Bonferroni post hoc test: $p < 0.001$) and (C) earned fewer reinforcers ($p < 0.0119$, Bonferroni post hoc test, $p < 0.01$) per session compared to control littermates. Analysis of animals' press rate per ratio requirement show that subjects of either genotype did not exhibit a general increase in rate of pressing when treated with CNO compared to saline (D) ($p = 0.1446$). A total of 12 D2R-OE_{dev} mice and 12 control mice were assayed for this analysis.

design in which animals received treatment with saline or CNO on alternate days of testing. I found that D2R-OE_{dev} mice continued to respond by pressing a lever for significantly longer times after treatment with CNO compared to treatment with saline (Log-rank test: $\chi^2 = 19.56$, $p < 0.0001$, Log-rank test; $n = 12$ mice) (Figure 23A). Control littermates also responded to CNO treatment by continuing to press the lever for longer times compared to the saline control condition ($\chi^2 = 9.671$, $p = 0.0019$, Log-rank test; $n = 12$ mice) (Figure 23A). Both D2R-OE_{dev} and control animals showed increased total number of lever presses in sessions after CNO treatment compared to saline treatment ($F_{(1,22)} = 69.21$, $p < 0.001$; $n = 12$ mice per genotype) (Figure 23B). Consistent with these results, both D2R-OE_{dev} and control mice also earned more reinforcers after treatment with CNO compared with saline ($F_{(1,22)} = 65.49$, $p < 0.001$; $n = 12$ mice per genotype) (Figure 23C). Moreover, although mice in both groups showed enhanced performance in the progressive ratio task after CNO treatment, this enhancement cannot be attributed to a general increased rate of pressing because, for each ratio requirement, mice in both groups showed unaltered press rates after treatment with CNO when compared with saline ($F_{(1,44)} = 1.894$, $p = 0.1446$; $n = 12$ mice per genotype) (Figure 23D). However, while CNO robustly enhanced motivation in both groups, D2R-OE_{dev} still displayed decreased performance in the task compared to control littermates after acute treatment with the drug, as measured by how long animals continued to respond in the task ($\chi^2 = 10.49$, $p < 0.0012$, Log-rank test; $n = 12$ per genotype) (Figure 23A), the number of lever presses made ($F_{(1,22)} = 7.912$, $p < 0.0101$, Bonferroni *post hoc* test, $p < 0.001$, $n = 12$ per genotype) (Figure 23B), and the number of reinforcers earned ($F_{(1,22)} = 7.526$, $p < 0.0119$, Bonferroni *post hoc* test, $p < 0.01$, $n = 12$ per genotype) (Figure 23C).

The indirect pathway of the basal ganglia has been strongly linked to regulation of motor behaviors (Lenz and Lobo, 2013) and optogenetic activation of MSNs expressing D2Rs inhibit motor activity, (Kravitz et al., 2010). Thus, I hypothesized that acutely activating hM4D receptors in iMSNs in the DMS and NA core would also energize motor behavior. To test this hypothesis, I tracked locomotion of D2R-OE_{dev} and control littermates expressing hM4D in iMSNs before and after treatment with CNO or saline. I found that both D2R-OE_{dev} and control littermates showed increased ambulation after treatment with CNO ($F_{(1,22)} = 32.36$, $p < 0.0001$; 12 mice per genotype), which peaked approximately 30 min after drug injection and remained elevated for the remainder of the testing session (Figure 24). There were, however, no differences between D2R-OE_{dev} mice and control littermates in their locomotor response to CNO ($F_{(1,22)} = 1.388$, $p = 0.2513$; 12 mice per genotype) (Figure 24).

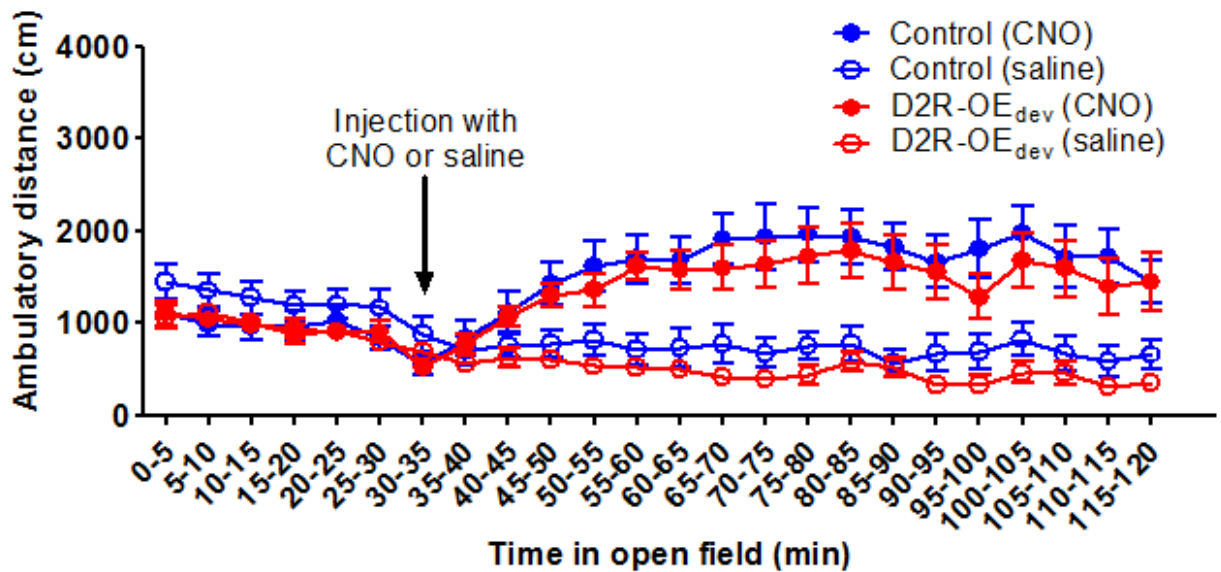


Figure 24: Decreasing function of indirect pathway increases locomotion in D2R-OE_{dev} and control littermates. Plot of locomotion in open field across time showed that both D2R-OE_{dev} and control mice increased ambulatory activity after treatment with CNO compared to saline ($p < 0.0001$). The increase in locomotion reached maximum level approximately 30 min after injection with CNO for mice of both genotypes. No difference was observed between D2R-OE_{dev} and control littermates in their response to CNO treatment ($p = 0.2513$). A total of 12 D2R-OE_{dev} mice and 12 control mice were assayed for this analysis.

Behaviorally, incentive motivation is thought to consist of at least two components. Both changes in directional action selection, the goal-directed component, and changes in arousal, the activational component, can lead to changes in motivation measured by behavioral tasks such as the progressive ratio schedule of reinforcement (Salamone and Correa, 2002, Bailey et al., 2015). Given that activating hM4D receptors in iMSNs leads to hyperactivity in the open field and enhanced performance in the progressive ratio task, I

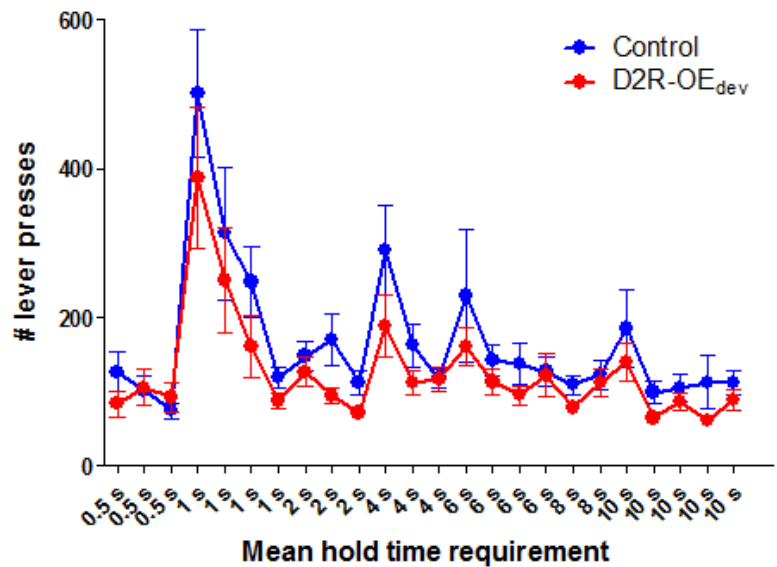


Figure 25: Both D2R-OE_{dev} mice and control littermates can learn to hold down a lever to obtain a food reward. Before testing in the progressive hold-down test, mice were trained to hold down a lever to obtain a food reward. Animals underwent daily VIH sessions in which the mean hold requirement increased progressively from 0.5 s to 10 s; each session ended when 40 trials were completed or when 1 h elapsed. On transitions to more difficult VIH schedules, mice tended to show decreased performance, requiring a greater number of lever presses to complete the trials, but efficiency improved with repeated training in the same schedule. Both D2R-OE_{dev} and control mice showed similar progression of efficiency throughout training, measured by the number of lever presses made during a session for different VIH schedules ($p = 0.1066$). Mice of both genotypes were able to complete all 40 trials in the VIH 10 s schedule before being tested in the progressive hold-down test. A total of 12 D2R-OE_{dev} mice and 12 control mice were assayed for this analysis.

questioned whether this manipulation differentially affects the directional and activational components of motivation. To this end, I tested these animals in the progressive hold-down task, which requires animals to hold-down a lever for progressively longer intervals of time to earn each subsequent reward (Bailey et al., 2015). During training, both D2R-OE_{dev} and control mice

showed similar learning curves ($F_{(1,21)} = 2.842$, $p = 0.1066$, $n = 12$ mice per genotype) and were able to successfully learn to hold-down a lever to obtain a food reward (Figure 25).

When tested on the progressive hold-down task after acute treatment with CNO or saline, both D2R-OE_{dev} mice and control littermates responded to acute treatment with CNO by continuing to engage in the task for longer times (Log-rank tests: control: $\chi^2 = 12.02$, $p = 0.005$; D2R-OE_{dev}: $\chi^2 = 21.23$, $p < 0.0001$, $n = 12$ mice per genotype) (Figure 26A). However, after acute treatment with CNO, mice of both genotypes also showed reduced efficiency at making longer presses, as confirmed by calculating the proportion of rewarded presses per hold requirement; this measure was decreased at hold requirements of 8.2 s and longer when mice were treated with CNO compared to saline ($F_{(1,21)} = 7.080$, $p = 0.0143$; $n = 12$ mice per genotype) (Figure 26B). Consistent with reduced efficiency, both D2R-OE_{dev} and control mice made more lever presses ($F_{(1,21)} = 44.82$, $p < 0.0001$; $n = 12$ mice per genotype) (Figure 26C) and earned fewer rewards after treatment with CNO ($F_{(1,21)} = 31.92$, $p < 0.0001$; $n = 12$ mice per genotype) (Figure 26D). Figure 26E shows representative histograms of press durations on different days of testing for one subject. While this mouse made progressively longer presses on saline treatment days, it made generally shorter presses and a greater number of presses on days when it was treated with CNO. These results demonstrate that activating G_{ai} signaling in iMSNs in the DMS and NA core leads to increased motivation by energizing behavioral performance at the cost of goal-directed efficiency.

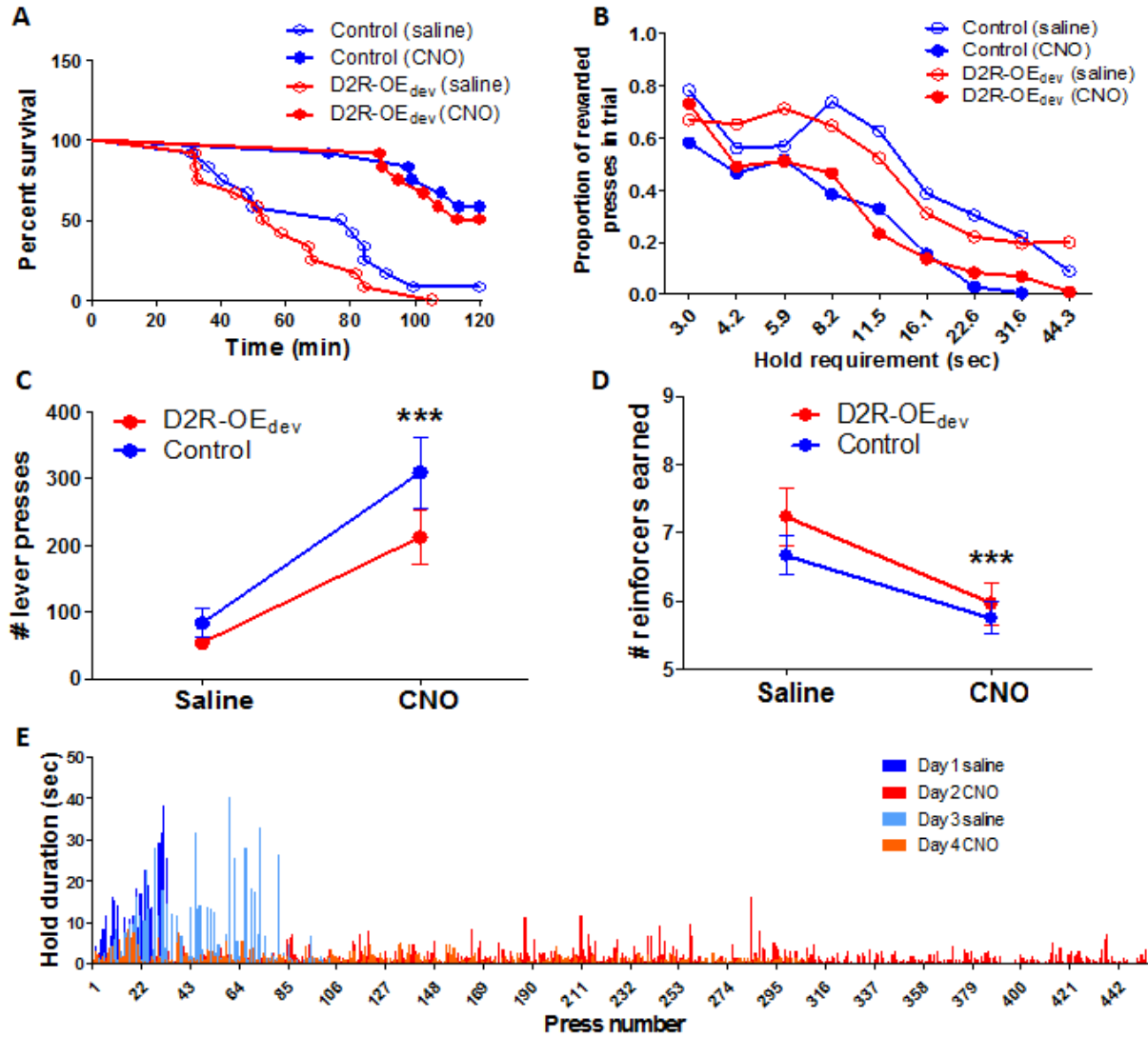


Figure 26: Decreasing function of indirect pathway energizes behavioral performance at the expense of goal-directed efficiency. **A-D.** D2R-OE_{dev} and control littermates expressing hM4D in iMSNs show decreased efficiency in the progressive hold-down test after treatment with CNO compared to saline. **A.** Mice of both genotypes continued to respond for longer times on CNO compared to saline, as measured by survival functions for session durations (control: $p = 0.005$; D2R-OE_{dev}: $p < 0.0001$). **B.** For each hold requirement, mice treated with CNO showed lower efficiency in responding compared to treatment with saline, as measured by the proportion of rewarded presses ($p = 0.0143$). **C-D.** Other behavioral parameters of the progressive hold-down task also demonstrate that both D2R-OE_{dev} and control mice expressing hM4D in iMSNs were less efficient after treatment with CNO: **(C)** mice on CNO made a greater number of lever presses ($p < 0.0001$) and **(D)** earned fewer reinforcers ($p < 0.0001$) in a session compared to performance after treatment with saline. **E.** Histograms of press durations on different days of testing for one representative subject: while this mouse made progressively longer presses on saline treatment days, it made generally shorter presses and a greater number of presses on days when it was treated with CNO. A total of 12 D2R-OE_{dev} mice and 12 control mice were assayed for this analysis.

In the results presented above, all manipulations targeted both the DMS and NA core, medial regions of the striatum that have been specifically shown to support incentive motivation in instrumental tasks of reinforcement (Corbit and Balleine, 2011, Hilario et al., 2012, Burton et al., 2015). I therefore sought to determine the contribution of each of these regions to the effects on motivation of acutely decreasing function of the indirect pathway. I injected the Cre-dependent hM4D virus in *Drd2*-Cre mice bilaterally in either the DMS or NA core and then trained and tested these animals in the progressive ratio task. I found that there was no difference in the response to CNO between mice expressing the hM4D receptor in the DMS or NA core. After treatment with CNO, both groups showed no significant differences in how long they

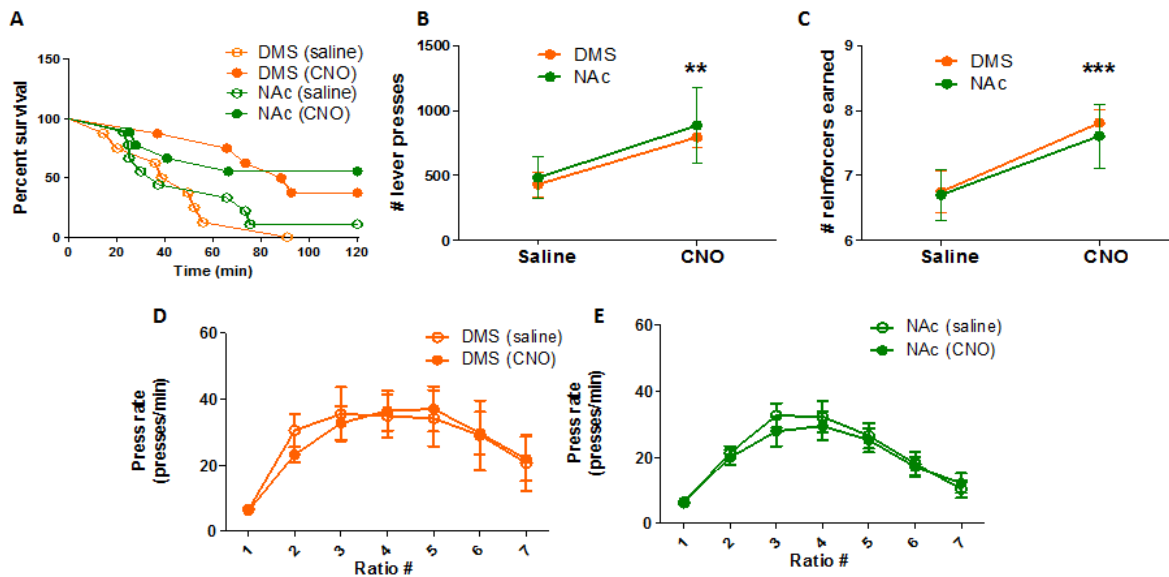


Figure 27: Inhibiting the indirect pathway in either DMS or NA core leads to enhanced motivation. A-C. Mice expressing hM4D in iMSNs selectively in the DMS or NA show enhanced performance in the progressive ratio task of motivation after treatment with CNO compared to saline, as measured by (A) survival functions for session duration (DMS and NA: $p = 0.0183$), (B) total number of lever presses made ($p = 0.0014$), and (C) total number of reinforcers earned ($p = 0.0003$) in a session. There were also no differences in the relative responses to CNO between animals expressing hM4D in iMSNs in the DMS and those expressing hM4D in the NA core, as measured by (A) survival functions for session duration ($p = 0.7547$), (B) total number of lever presses made ($p = 0.7723$), and (C) total number of reinforcers earned ($p = 0.8038$). D-E. Plot of animals' press rate per ratio requirement show that CNO treatment did not lead to increased rate of pressing in animals expressing hM4D in either (D) the DMS ($p = 0.9422$) or (E) the NA core ($p = 0.7126$). A total of 8 mice expressing hM4D in iMSNs in the DMS and 9 mice expressing hM4D in iMSNs in the NA core were used for this analysis.

continued to engage in the task (Log-rank test: $\chi^2 = 0.09760$, $p = 0.7547$, $n = 8-9$ mice per site) (Figure 27A), the total number of lever presses they made ($F_{(1,15)} = 0.08685$, $p = 0.7723$, $n = 8-9$ mice per site) (Figure 27B), or the total number reinforcers they earned ($F_{(1,15)} = 0.1355$, $p = 0.8038$; $n = 8-9$ mice per site) (Figure 27C). Moreover, as observed for mice expressing hM4D in both DMS and NA core, the response to CNO in mice expressing hM4D separately in each striatal sub-region cannot be attributed to higher rates of pressing: for each ratio requirement reached by all animals in the study, mice in each group showed similar rates of lever pressing after treatment with CNO or saline (DMS: $F_{(1,14)} = 0.005455$, $p = 0.9422$, $n = 8$ mice; NA core: $F_{(1,16)} = 0.1406$, $p = 0.7126$, $n = 9$ mice) (Figures 27D-E).

A comparison of the responses to CNO treatment across experiments, including *Drd2*-Cre animals expressing hM4D in both DMS and NA core or in each region separately are presented in Figure 28. It is clear that decreasing function of iMSNs in either region separately led to smaller effects than those of manipulation to both regions combined, as measured by parameters such as session duration ($F_{(2,25)} = 7.496$, $p = 0.0028$, Dunnett *post hoc* tests: DMS: $p <$

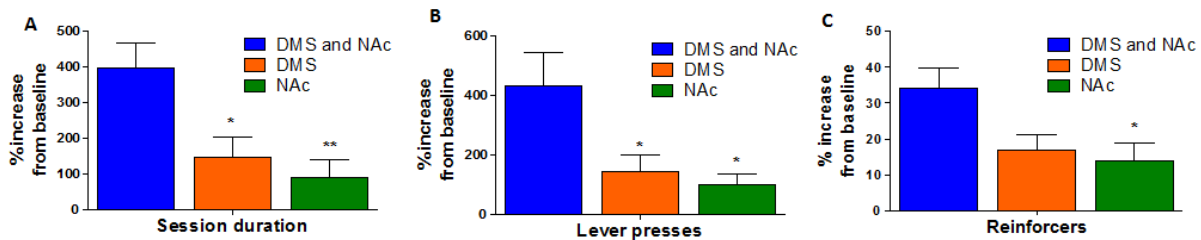


Figure 28: Inhibiting the indirect pathway in both DMS and NA core has larger effect on motivation than separate inhibition of either DMS or NA core. When comparing results across experiments (i.e. the effect of response to CNO when expressing hM4D in both the DMS and NA core compared to expressing hM4D in each of these sub-regions selectively), it can be seen that the response to CNO when hM4D was expressed in both NA and DMS was greater than when hM4D was expressed selective in either striatal sub-region, as measured by (A) session duration ($p = 0.0028$, Dunnett *post hoc* tests: DMS: $p < 0.05$, NA core: $p < 0.001$), (B) number of lever presses ($p = 0.0155$, Dunnett *post hoc* tests: DMS: $p < 0.05$, NA core: $p < 0.05$), and (C) number of reinforcers earned ($p = 0.0187$; Dunnett *post hoc* tests: NA core: $p < 0.05$).). A total of 11 mice expressing hM4D in iMSNs in both the DMS and NA core, 8 mice expressing hM4D in iMSNs only in the DMS, and 9 mice expressing hM4D in iMSNs only in the NA core were used for this analysis.

0.05, NA core: $p < 0.001$; $n = 8-11$ mice per site) (Figure 28A), lever presses ($F_{(2,25)} = 4.950$, $p = 0.0155$, Dunnett *post hoc* tests: DMS: $p < 0.05$, NA core: $p < 0.05$; $n = 8-11$ mice per site) (Figure 28B), and number of reinforcers earned ($F_{(2,25)} = 4.683$, $p = 0.0187$; Dunnett *post hoc* tests: NA core: $p < 0.05$; $n = 8-11$ mice per site) (Figure 28C).

I also investigated the contributions of the DMS and NA core to the locomotor effect of acutely decreasing function of the indirect pathway. As shown in Figure 29, I tracked locomotor

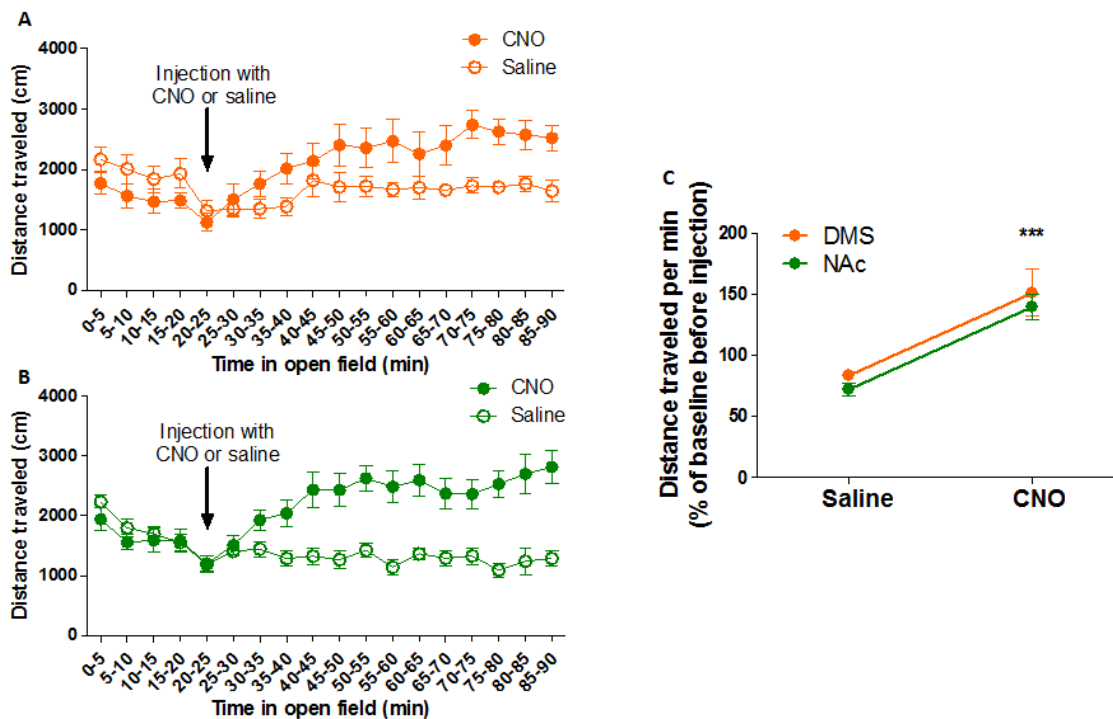


Figure 29: Mice expressing hM4D receptors in iMSNs in either DMS or NA core respond to acute CNO treatment with increased locomotion. A. Plot of locomotor activity in 5-min time bins of mice expressing hM4D in the DMS before and after receiving acute treatment with either saline or CNO. Animals displayed increased locomotion after treatment with CNO but not with saline ($p = 0.0141$). The effect peaked approximately 30 min after injection and persisted through the remainder of the testing session **B.** Plot of locomotor activity in 5-min time bins of mice expressing hM4D in the NA core before and after receiving acute treatment with either saline or CNO. Animals displayed increased locomotion after treatment with CNO but not with saline ($p = 0.0102$). The effect peaked approximately 30 min after injection and persisted through the remainder of the testing session. **C.** Mice expressing hM4D in iMSNs in either the DMS or NA core responded to acute CNO treatment with increased ambulatory activity compared to baseline before drug administration ($p = 0.0002$). There was no difference in the relative response to CNO between animals expressing hM4D in the DMS compared to those expressing hM4D in the NA core ($p = 0.6162$). A total of 8 mice expressing hM4D in iMSNs in the DMS and 9 mice expressing hM4D in iMSNs in the NA core were used for this analysis.

activity of *Drd2*-Cre mice expressing hM4D in either the DMS or NA core before and after treatment with CNO or saline. The kinetics of the effects CNO on locomotion with this sub-region-selective manipulation appeared to be similar to that observed in mice expressing the hM4D receptor in both striatal sub-regions (Figures 29A-B, compare to Figure 24). Moreover, I observed that animals in both groups displayed increased ambulatory activity after treatment with CNO ($F_{(1,15)} = 22.96$, $p = 0.0002$; $n = 8-9$ mice per site) (Figure 29C). There was no difference in the relative effects on CNO for mice expressing the hM4D receptor in the DMS compared to the NA core ($F_{(1,15)} = 0.6162$, $p = 0.6162$; $n = 8-9$ mice per site) (Figure 29C).

I then tested whether after activating G_{oi} signaling in the striatal indirect pathway mice are still sensitive to the value of a reward or whether this manipulation causes animals to become habit-driven. Since all animals expressing hM4D in the DMS or NA core were trained to press a lever to obtain evaporated milk as a food reward, I tested whether decreasing the value of the reward by pre-feeding animals with evaporated milk would

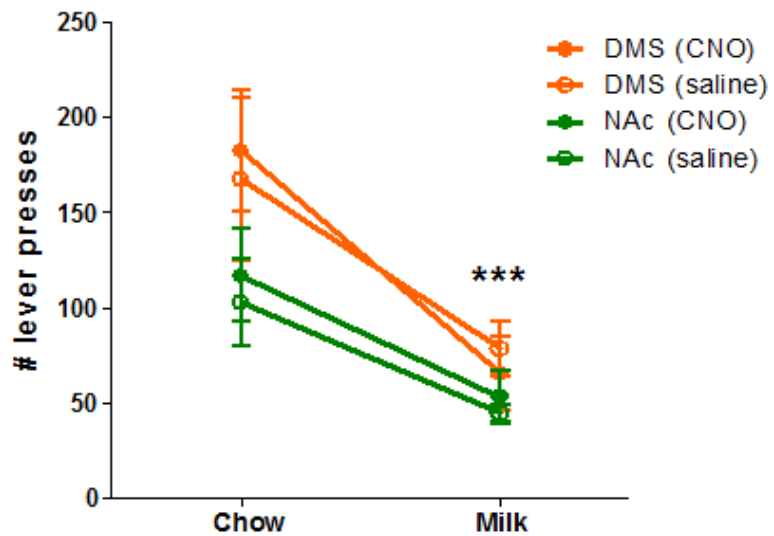


Figure 30: Activating hM4D receptors in iMSNs in the DMS or NA core does not affect sensitivity to reward value. In a test of outcome devaluation, compared to a control condition in which mice were pre-fed chow, a food that had never been previously associated with lever pressing, mice in all groups showed similar decreased rates of pressing after pre-feeding with evaporated milk and treatment with CNO or saline (pre-feeding: $p < 0.0001$; striatal sub-region: $p = 0.0790$). A total of 8 mice expressing hM4D in iMSNs in the DMS and 9 mice expressing hM4D in iMSNs in the NA core were used for this analysis.

decrease their rate of operant responding in extinction trials. Specifically, I was interested in determining if CNO treatment could affect the animals' ability to encode the value of the reward. I found that, compared to a control condition in which mice were pre-fed chow, a food that had never been previously associated with lever pressing, mice in all groups showed similar decreased lever pressing after pre-feeding with evaporated milk and treatment with CNO or saline (pre-feeding: $F_{(3,1)} = 23.95$, $p < 0.0001$; striatal sub-region: $F_{(3,1)} = 2.392$, $p = 0.0790$; $n = 8-9$ mice per site) (Figure 30). This finding suggests that activating $G_{\alpha i}$ signaling in iMSNs in the DMS or NA core does not affect how animals encode the value of the reward. It further suggests that these mice are still sensitive to changes in the value of the reward and do not become habit-driven after treatment with CNO.

ELECTROPHYSIOLOGICAL EFFECTS ON EXCITABILITY

We then investigated how acute hM4D activation affects neuronal function of the indirect pathway. $G_{\alpha i}$ -coupled GPCRs have been shown to activate a family of inwardly-rectifying potassium, the GIRK channels, to evoke inhibitory currents in many cells types (Luscher and Slesinger, 2010). In neurons with high levels of GIRK channels, such as the thalamus, it has been previously observed in the Kellendonk laboratory that the resting membrane potential of neurons expressing hM4D decreases by approximately 7 mV when 1 μ M CNO is applied to the bath (Parnaudeau et al., 2013). In the striatum, one study in rats found that bath application of CNO to acute slices similarly reduced resting membrane potential as well as the spike frequency of hM4D-positive iMSNs (Ferguson et al., 2011). To determine whether hM4D activation also affects iMSN excitability in the mouse, I patched iMSNs expressing the hM4D receptor in acute slices and measured intrinsic excitability properties of these neurons before and after applying CNO to the bath. I found no effect of 1 μ M or 10 μ M CNO on the current-voltage relationship (1

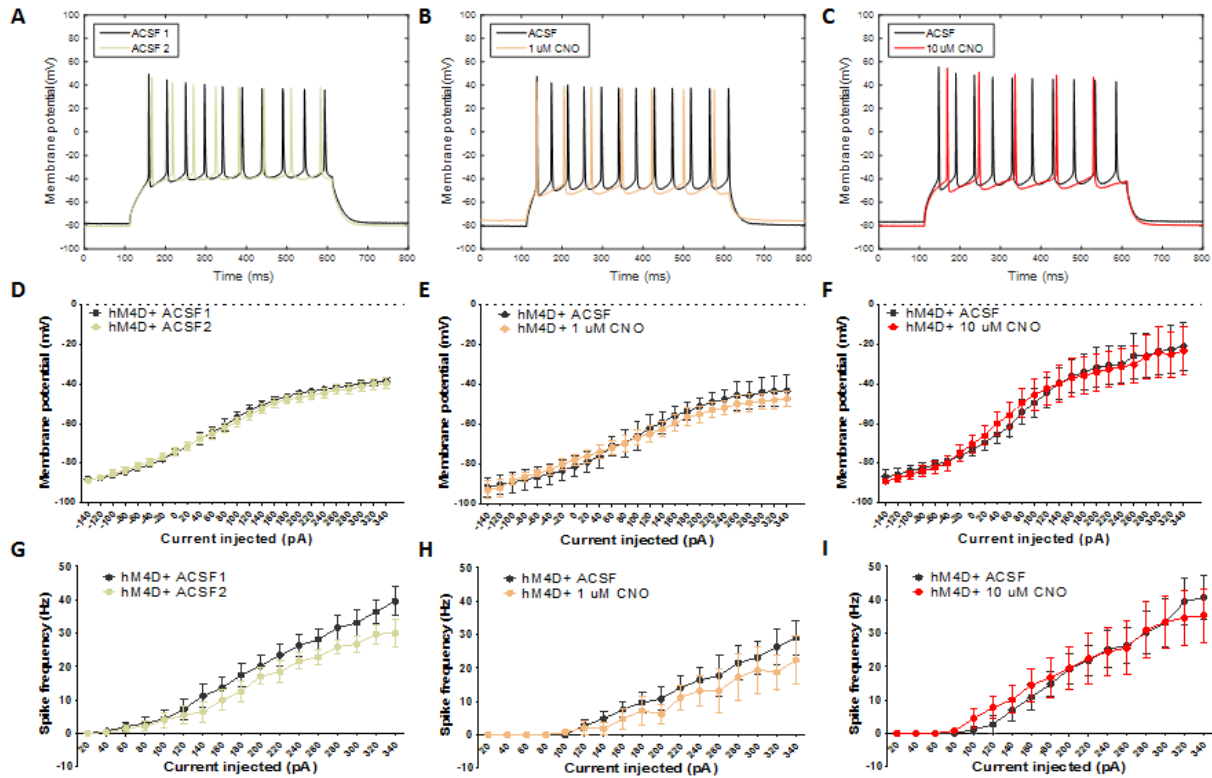


Figure 31: Membrane excitability properties at the soma of iMSNs expressing hM4D are not changed *in vitro* by treatment with CNO (part 1). A-C. Sample traces of voltage response of patched cells to injection of 280 pA current in regular ACSF and after incubation for 15 min with (A) regular ACSF, (B) 1 μ M CNO, or (C) 10 μ M CNO. D-F. Current-voltage curves of all cells patched in regular ACSF and after incubation for 15 min with (D) regular ACSF, (E) 1 μ M CNO, or (F) 10 μ M CNO. No differences were observed between curves obtained before and after incubation with (D) regular ACSF ($p = 0.7387$), (E) 1 μ M CNO ($p = 0.9258$), or (F) 10 μ M CNO ($p = 0.9669$). G-I. Input-output curves of all cells patched in regular ACSF and after incubation for 15 min with regular (G) ACSF, (H) 1 μ M CNO, or (I) 10 μ M CNO. No differences were observed between curves obtained before and after incubation with (G) regular ACSF ($p = 0.2981$), (H) 1 μ M CNO ($p = 0.5148$), or (I) 10 μ M CNO ($p = 0.9367$). A total of 25 hM4D-positive cells from 16 mice were patched (6-11 cells from 6-8 mice per drug condition) to calculate all statistics reported above.

μ M: $F_{(1,8)} = 0.0092$, $p = 0.9258$, $n = 6$ cells; 10 μ M: $F_{(1,14)} = 0.001789$, $p = 0.9669$, $n = 8$ cells), spike frequency (1 μ M: $F_{(1,10)} = 0.4561$, $p = 0.5148$, $n = 6$ cells; 10 μ M: $F_{(1,14)} = 0.006540$; $p = 0.9367$, $n = 8$ cells), resting membrane potential (1 μ M: $t_{(8)} = 0.5527$, $p = 0.5956$, $n = 6$ cells; 10 μ M: $t_{(12)} = 0.5307$, $p = 0.6053$, $n = 8$ cells), or rheobase (1 μ M: $t_{(5)} = 1.400$, $p = 0.2204$, $n = 6$ cells; 10 μ M: $t_{(7)} = 0.4213$, $p = 0.6852$, $n = 8$ cells) in the neurons recorded (Figures 31-32).

These findings suggest that G_{ai} signaling in iMSNs does not change intrinsic excitability

measured at the cellular soma. Instead, Bock et al. have used slice physiology to show that stimulation of iMSNs exposed to CNO leads to decreased amplitude of inhibitory post-synaptic currents in pallidal neurons (Bock et al., 2013), a finding that has been recently replicated in the Kellendonk laboratory.

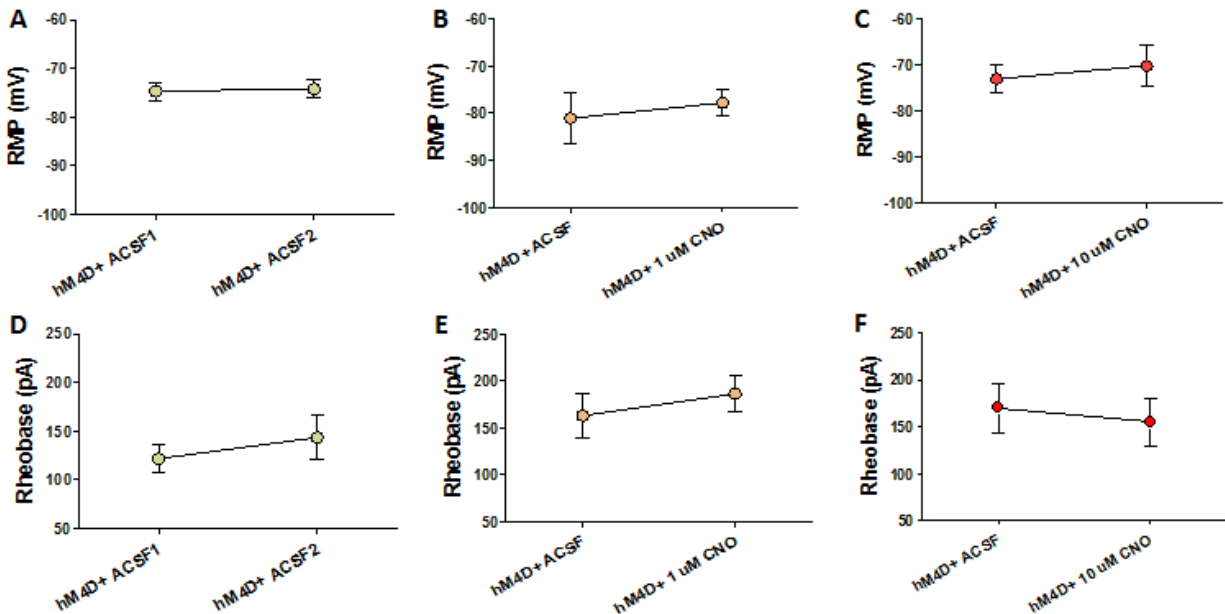


Figure 32: Membrane excitability properties at the soma of iMSNs expressing hM4D are not changed *in vitro* by treatment with CNO (part 2). A-C. Resting membrane potential for all cells patched in regular ACSF or after incubation for 15 min with (A) regular ACSF, (B) 1 μ M CNO, or (C) 10 μ M CNO. No differences were observed for the resting membrane potential of cells measured before and after incubation with (A) regular ACSF ($p = 0.7380$), (B) 1 μ M CNO ($p = 0.5956$), or (C) 10 μ M CNO ($p = 0.6053$). M-O. Rheobase calculated for all cells patched in regular ACSF or after incubation for 15 min with (D) regular ACSF, (E) 1 μ M CNO, or (F) 10 μ M CNO. No differences were observed between rheobase calculated before and after incubation with (D) regular ACSF ($p = 0.1038$), (E) 1 μ M CNO ($p = 0.2204$), or (F) 10 μ M CNO ($p = 0.6852$). A total of 25 hM4D-positive cells from 16 mice were patched (6-11 cells from 6-8 mice per drug condition) to calculate all statistics reported above.

SOMATIC EFFECTS ON NEURONAL ACTIVITY IN THE INTACT ORGANISM

I then used *in vivo* calcium imaging to probe how neurons at different nodes in the indirect pathway respond to activation of hM4D. I first co-expressed the hM4D receptor and the calcium sensor GCaMP6f in a small region of the DMS of *Drd2-Cre* mice. The selectivity of this manipulation is presented in Figure 33. Using immunohistochemistry, I confirmed that

GCaMP6f was only expressed in cells immune-positive for Cre, and 88% of Cre-positive cells in the region of viral infection expressed GCaMP6f (Figure 33B). Moreover, at the center of the virus injection site, 86% of cells positive for GCaMP6f were also immune-positive for hM4D (Figure 33C).

By implanting a microlens into the region expressing hM4D and GCaMP6f, I was able to

visualize and measure activity of iMSNs before and after activation of G_{ai} signaling with CNO. To compare activity across conditions, each experiment consisted of two sessions on two consecutive days in which each animal was allowed to behave freely while I imaged somatic activity of the same neurons after treatment with CNO on one day and treatment with saline on a different day (SAL/CNO; $n = 339$ cells from 4 animals). As a control, I also ran experiments in which I tested animals after treatment with saline on both days (SAL/SAL; $n = 231$ cells from 4 animals).

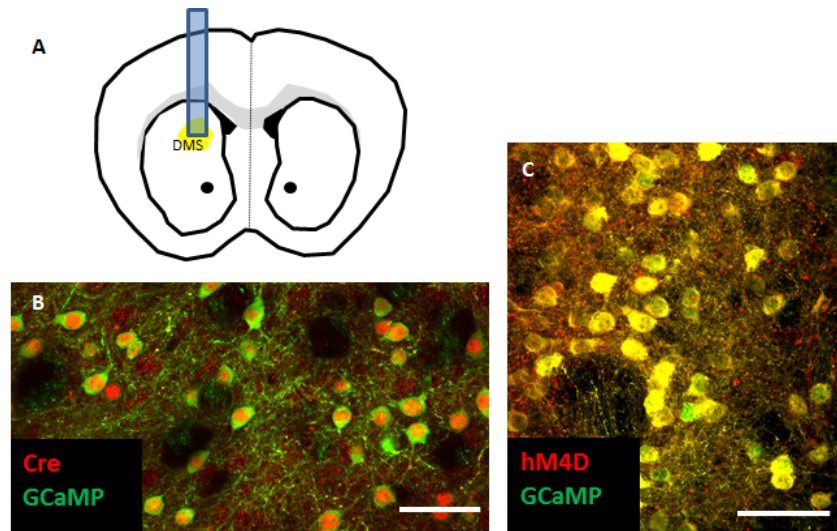


Figure 33: The G_{ai} -coupled designer receptor hM4D and the calcium sensor GCaMP can be co-expressed in iMSNs in the DMS. **A.** Diagram of coronal section showing region in the DMS virally targeted for in vivo calcium imaging of iMSNs expressing the hM4D receptor. A microlens was implanted over the same virally-targeted region in the DMS for imaging using a miniature microscope. **B.** Representative micrograph of brain section showing GCaMP6f fluorescence signal (green) and immunohistochemistry signal for Cre recombinase (green). GCaMP6f was only expressed in cells immune-positive for Cre, and 88% of Cre-positive cells in the region of viral infection expressed GCaMP6f ($n = 96$ cells). Scale bar: 50 μm . **C.** Representative micrograph of brain section showing co-localization of GCaMP6f (green) and hM4D (red) detected by immuno-staining for mCherry. At the center of virally-targeted site, 86% of cells positive for GCaMP6f were also immune-positive for hM4D ($n = 120$ cells). Scale bar: 50 μm .

One clear finding in these set of experiments was that activity in iMSNs is closely linked to locomotor activity, and positive significant correlations with similar slopes were observed between ambulatory distance and calcium activity for the same cells over discrete time intervals after treatment with CNO or saline (SAL: Pearson $r = 0.5001$, $p < 0.0001$, slope = 0.09681; CNO: Pearson $r = 0.2395$, $p = 0.0164$, slope = 0.04930; SAL vs. CNO: $F_{(1,196)} = 3.25681$, $p = 0.07266$) (Figure 34A). Figure 34B show an example heat map of calcium traces for one mouse with superimposed trace for locomotor activity. Traces for locomotor activity and total calcium activity for the entire population of neurons recorded during a 2-min interval illustrate the correlation between population-level iMSN activity and locomotion (Figure 34C). Heat maps and traces of locomotor activity and population calcium activity for SAL/CNO experiments in all mice are shown in Figure 35, and reveal that, although there is a clear relationship between population calcium activity and locomotion, distance traveled by the mouse cannot account for calcium activity at all time points during imaging. Nevertheless, I also found significant positive

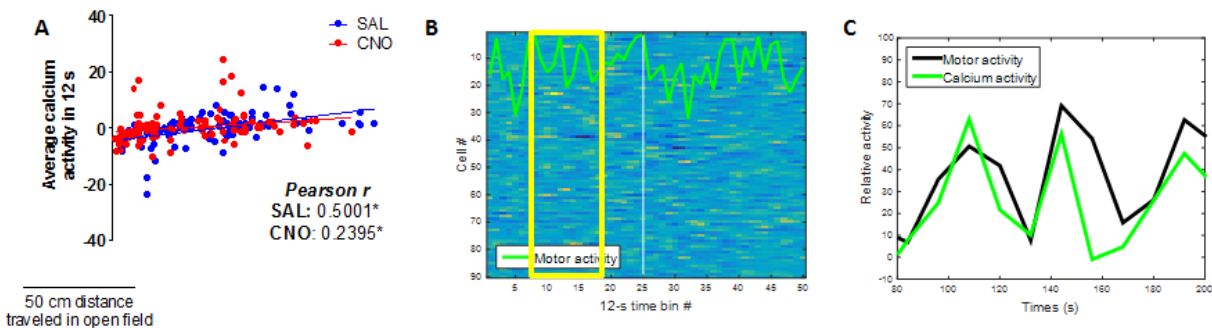


Figure 34: Somatic calcium activity of iMSNs in the DMS is correlated with motor activity in freely-behaving mice. **A.** Scatter plots and regression lines for calcium activity and locomotor activity in 12-s time bins of all mice tested after treatment with CNO or saline. Significant correlations were observed for data collected after treatment with CNO (Pearson $r = 0.2395$, $p = 0.0164$) or saline (Pearson $r = 0.2395$, $p = 0.0164$). **B.** Representative heat map of calcium traces from 90 cells binned in time for one mouse imaged after treatment with saline (time bins 1-25) or CNO (time bins 26-50). The animal's relative locomotor activity measured in the same time bins during the recording is also plotted. The yellow rectangle indicates the time interval in the recording used to generate the plot in C. **C.** Plot of relative locomotor activity and sum of calcium transients from 90 cells during the time interval indicated by the yellow rectangle in B, illustrating the relationship between these measures.

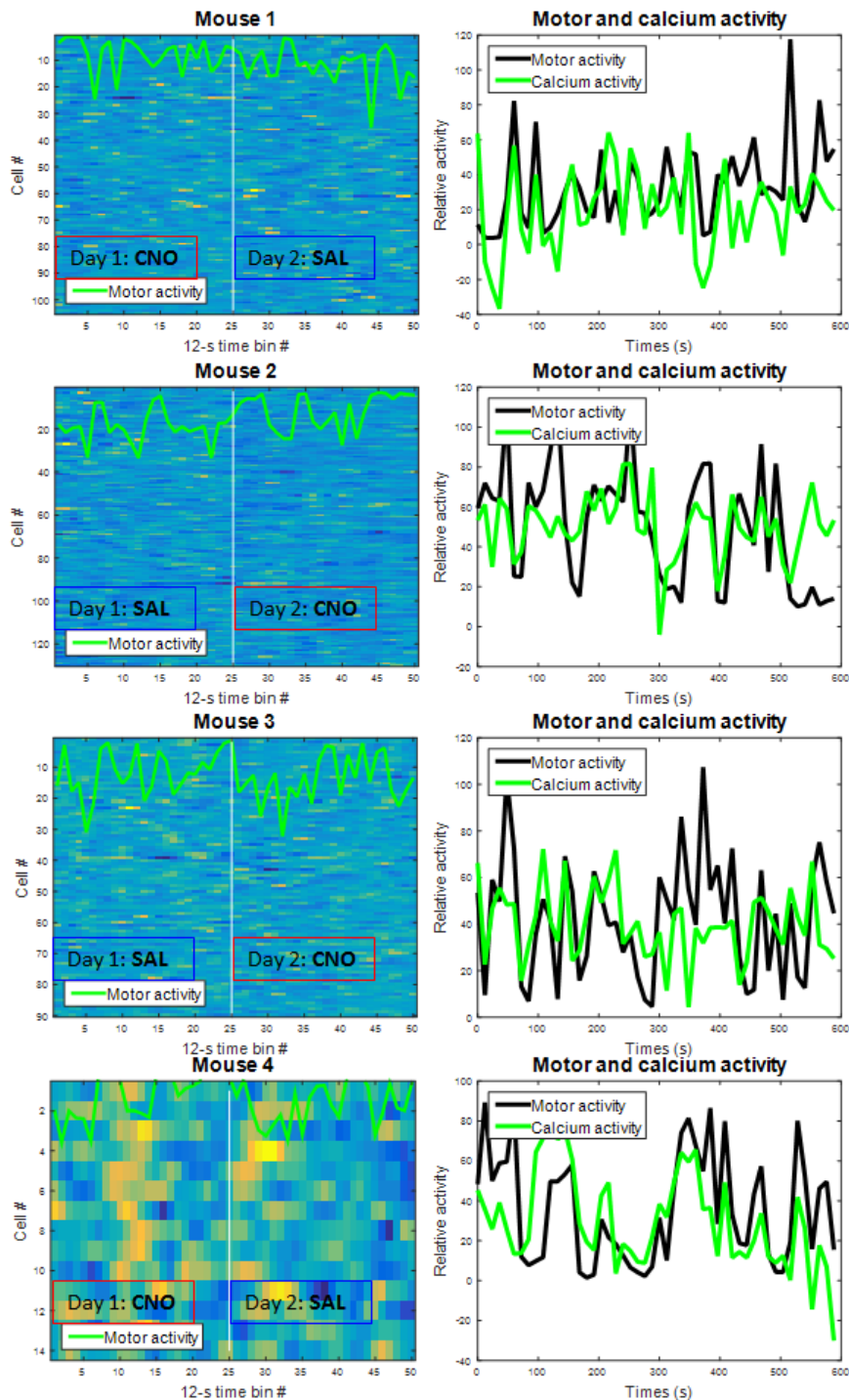


Figure 35: Heat maps and traces of motor activity and calcium activity for all SAL/CNO experiments imaging iMSNs in DMS. Left. Heat map of calcium traces from all cells imaged in SAL/CNO experiments for each mouse. Data is binned in time for each mouse imaged after treatment on day 1 (time bins 1-25) and after treatment on day 2 (time bins 26-50), with saline or CNO treatment as indicated. Each animal's relative locomotor activity measured in the same time bins during the recording is also plotted. **Right.** Plot of relative locomotor activity and sum of calcium transients from all cells imaged in SAL/CNO experiments for each mouse, illustrating the relationship between activity of the population of iMSNs imaged and the mouse's locomotor activity.

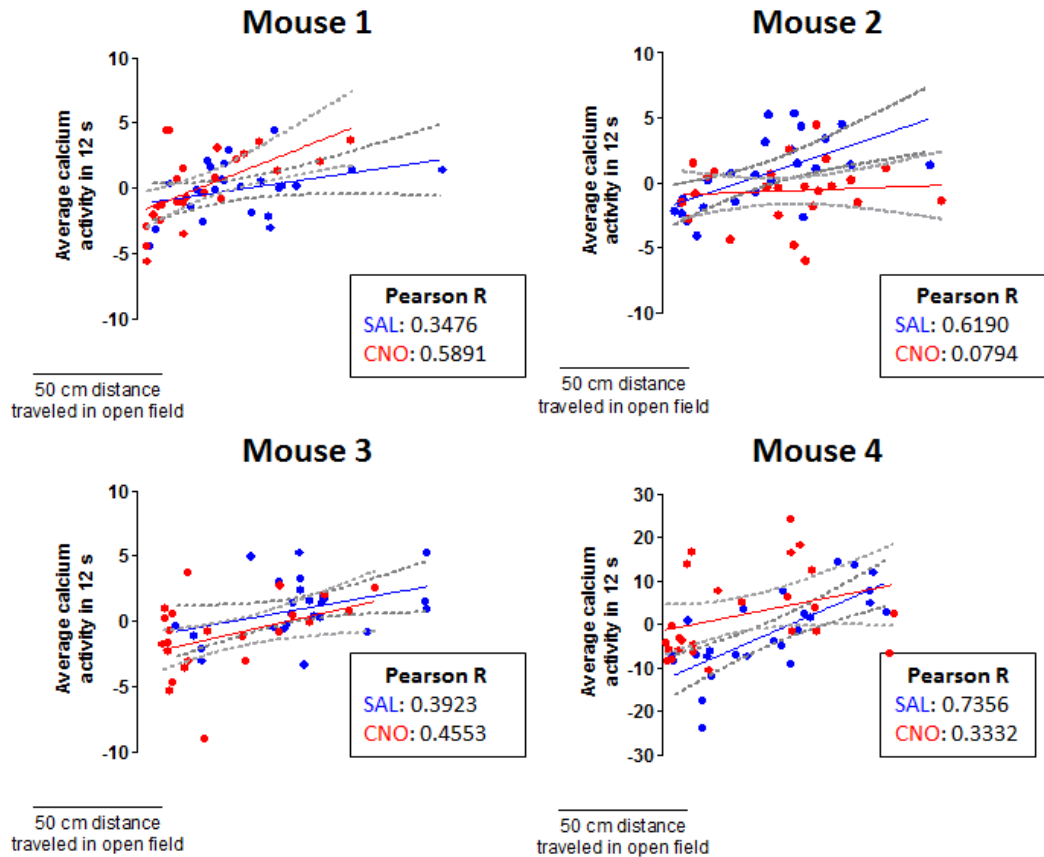


Figure 36: Correlation between iMSN calcium activity and motor activity was observed in all mice tested. Scatter plots and regression lines for calcium activity and locomotor activity in 12-s time bins for each mouse used for calcium imaging in the striatum tested after treatment with CNO or saline. Significant correlations or correlation trends between locomotion and calcium activity were observed for all mice (mouse 1, SAL: Pearson $r = 0.3476$, $p = 0.0887$, CNO: Pearson $r = 0.5891$, $p = 0.0019$; mouse 2, SAL: Pearson $r = 0.6190$, $p = 0.0010$, CNO: Pearson $r = 0.07936$, $p = 0.7061$; mouse 3, SAL: Pearson $r = 0.3923$, $p = 0.0524$, CNO: Pearson $r = 0.4553$, $p = 0.0222$; mouse 4, SAL: Pearson $r = 0.7356$, $p < 0.0001$, CNO: Pearson $r = 0.3332$, $p = 0.1036$).

correlations between calcium activity and locomotor activity for each individual recording session (Figures 36).

I then proceeded to analyze raw calcium traces to test for an effect of CNO compared to saline. Figure 37A shows sample calcium traces for ten neurons imaged in one SAL/CNO experiment, revealing that MSNs display characteristic long periods of little activity with

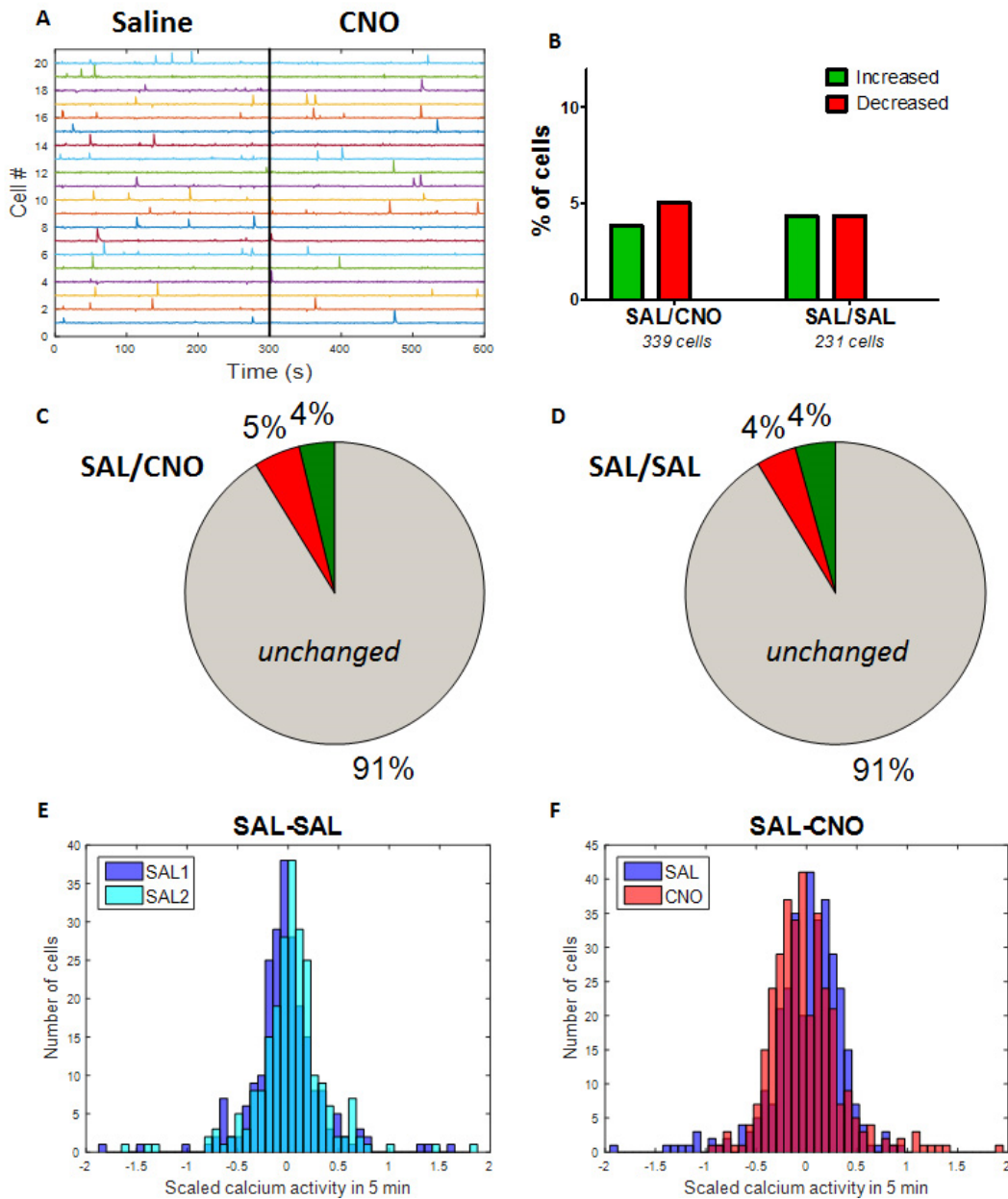


Figure 37: Activating hM4D receptors in iMSNs does not decrease MSN calcium activity at the somatic level. **A.** Representative calcium traces for twenty isolated indirect-pathway MSNs imaged in a freely-behaving mouse after treatment with saline or CNO. **B** Plot of percentage of cells that showed a significant decrease or increase in activity when comparing sessions after treatment with CNO to sessions after treatment with saline (SAL/CNO condition), and as a control, when comparing paired sessions done after treatment with saline (SAL/SAL condition). No difference was observed in the proportion of neurons that showed significant decrease or increase in activity across conditions ($p = 0.9741$). **C.** Pie chart showing percentage of neurons that significantly increase (3.83%), decrease (5.01%), or did not change (91.16%) activity in SAL/CNO experiments. **D.** Pie chart showing percentage of neurons that significantly increase (4.33%), decrease (4.33%), or did not change (91.33%) activity in SAL/SAL experiments. A total of 339 cells for the SAL/CNO condition and 231 cells for the SAL/SAL condition from 4 different animals were used to calculate all statistics reported above. **E-F.** Histograms of scaled calcium activity for all cells imaged in **(E)** SAL-SAL experiments, revealing no change in activity in the second session compared to the first session ($t_{(231)} = 1.134$, $p = 0.2579$, $n = 231$), and **(F)** SAL-CNO experiments, showing no effect of CNO treatment compared to saline treatment ($t_{(338)} = 0.4202$, $p = 0.6746$, $n = 339$).

occasional short-lived large events thought to represent transient burst activity. Calculation of the proportion of cells imaged that showed a significant change in activity with CNO treatment compared to saline treatment revealed that 5.01% of cells decreased activity, while 3.83% increased activity (Figure 37B). I performed similar comparisons for control experiments in which the same animals received injections of saline on two recording sessions, and I found that 4.33% of the cells recorded significantly decreased or increased activity across sessions (Figure 37B). For the SAL/CNO and SAL/SAL experiments, the percentage of cells that increased activity, decreased activity, or remained unchanged are shown in Figures 37C-D. Analysis of the proportion of cells showing decreased or increased activity across experiments revealed that there were no differences between these proportions in SAL/CNO and SAL/SAL experiments ($\chi^2 = 0.05247$, $p = 0.9741$) (Figure 37B-D). In addition, histograms for average activity of all iMSNs imaged in SAL-SAL and SAL-CNO experiments are shown in Figure 37E-F, confirming the lack of

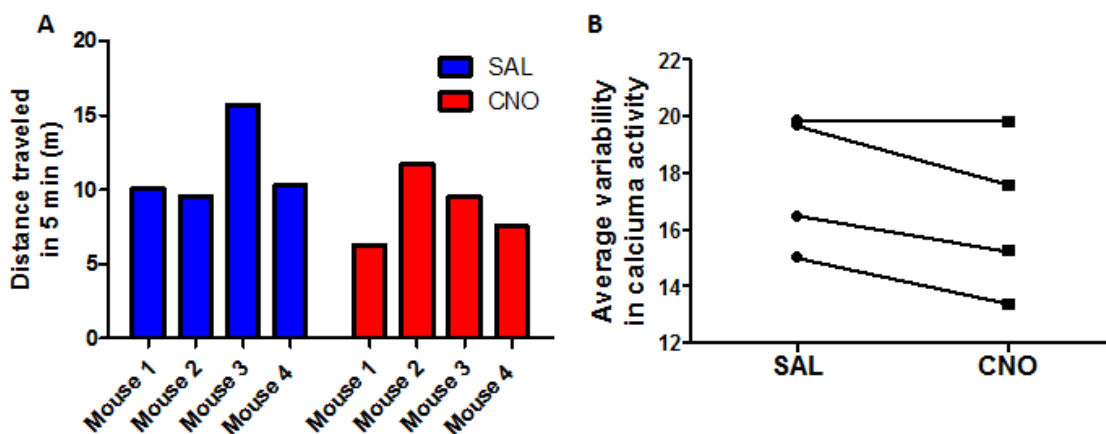


Figure 38: Locomotor activity and variability of calcium transients were not affected by CNO in mice co-expressing hM4D and GCaMP6f in iMSNs unilaterally in small region of DMS. A. Locomotor activity of all subjects were comparable during striatal calcium imaging sessions after treatment with saline or CNO, as measured by distance traveled in an open field during recording sessions for each mouse. There was no significant difference in locomotor activity across drug conditions ($p = 0.7685$). **B.** Average variability (standard deviations from the mean) of calcium activity for each mouse in 12-s bins, recorded after treatment with saline or CNO. There was no significant difference in the variability of calcium activity across drug conditions ($p = 0.0673$).

effect on cellular activity in response to CNO. Moreover, since calcium activity was strongly associated with locomotor activity, I verified that total locomotor activity was not different between sessions when animals were treated with saline or CNO ($F_{(1,3)} = 2.253$, $p = 0.7685$) (Figure 38A). The variability in calcium activity across cells for each mouse were also not different between recordings after treatment with saline or CNO ($t_{(3)} = 2.810$; $p = 0.0673$) (Figure 38B).

Additionally, I also tested for an effect of CNO on the proportion of cells that showed a significant decrease or increase in activity after normalizing the calcium activity to each animal's locomotor activity, and again, no differences were observed ($\chi^2 = 3.252$, $p = 0.1968$). Finally, I detected individual calcium events of recorded MSNs for all experiments and performed similar statistical analysis. Compared to analysis with the raw calcium traces, using the event data, I was able to detect similar correlations between calcium activity and behavior, and I did not identify an effect of CNO treatment on the activity of the cells recorded (Figure 39). Thus, in line with the observation that activation of $G_{\alpha i}$ signaling does not alter intrinsic excitability properties of striatal iMSNs measured at the cellular soma *in vitro*, measures of somatic neuronal activity of these cells were also not changed after a similar manipulation was performed *in vivo* in freely behaving animals.

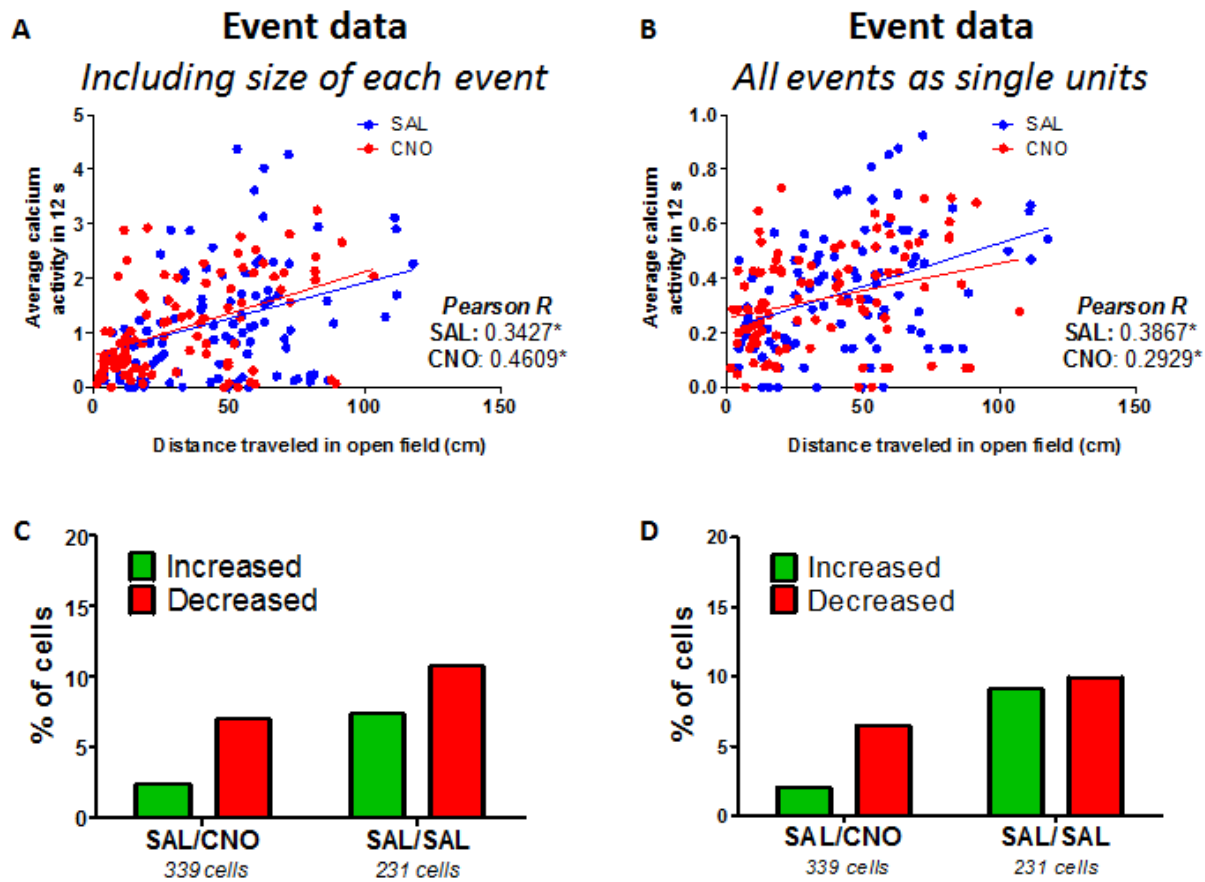


Figure 39: Analysis of event calcium imaging data yields similar findings as analysis of raw calcium transients. **A-B.** Scatter plots and regression lines for calcium activity and locomotor activity in 12-s time bins of all mice tested after treatment with CNO or saline (**A**) using single-event data set and weighing for size of calcium events or (**B**) using single-event data set considering each event as a single unit. Significant correlations with similar slopes were observed for data collected after treatment with CNO or saline using either type of analysis, weighing size of events (SAL: Pearson $r = 0.3427$, $p = 0.0005$ slope = 0.01326; CNO: Pearson $r = 0.4609$, $p < 0.0001$, slope = 0.01536; SAL vs. CNO: $p = 0.6579$) (**A**) and considering all events as single units (SAL: Pearson $r = 0.3867$, $p < 0.0001$, slope = 0.003165; CNO: Pearson $r = 0.2929$, $p = 0.0031$, slope = 0.002017; SAL vs. CNO: $p = 0.258$) (**B**). **C-D.** Plots of percentage of cells that showed a significant decrease or increase in activity when comparing sessions after treatment with CNO to sessions after treatment with saline; and, as a control, when comparing paired sessions done after treatment with saline. The data was analyzed using either (**C**) the single event data set and weighing for size of calcium events, or (**D**) using the single event data set considering each event as a single unit. No difference was observed in the proportion of neurons that showed significant decrease or increase in activity across conditions with either type of analysis, weighing size of events ($p = 0.6387$) (**C**) or considering all events as single units ($p = 0.5580$) (**D**). A total of 339 cells for the SAL/CNO condition and 231 cells for the SAL/SAL condition from 4 different animals were used to calculate all statistics reported above.

EFFECT ON NEURONAL ACTIVITY OF PALLIDAL NEURONS

Previous work has shown that activating hM4D receptors in iMSNs in the NA core *in vitro* inhibits inhibitory post-synaptic currents (IPSCs) amplitude in the ventral pallidum after optogenetic stimulation of the indirect pathway (Bock et al., 2013). I hypothesized that this manipulation in the DMS should also lead to a disinhibition of the GPe *in vivo*. To address this question, I injected a non-conditional GCaMP6f virus in the GPe and Cre-dependent hM4D virus in the DMS of *Drd2*-Cre mice and further implanted a microlens in the GPe (Figures 40A-CD). I then imaged activity of cells in the GPe in freely-behaving animals after two treatments with CNO or saline. Figure 40D shows sample calcium traces for ten neurons imaged in one SAL-CNO experiment, illustrating the activity of individual GPe neurons after treatment with saline and CNO. Similar analysis as that performed for neurons imaged in the DMS were performed for neurons imaged in the GPe. As a control, when animals were imaged in two sequential sessions after treatment with saline, only 2.40% of cells increased activity and 3.85% decreased activity (SAL-SAL, 211 cells from 3 animals) (Figure 40E). Most remarkably, however, I observed a significant increase in calcium activity in the GPe after treatment with CNO compared to saline, with 10.05% of cells imaged showing an increase in activity, while only 0.48% showed a decrease in activity (SAL/CNO, 209 cells from 3 animals) (Figure 40F). Analysis of these proportions demonstrated that the frequency of cells showing increased activity after CNO treatment was greater than expected by chance ($\chi^2 = 8.889$, $p = 0.0117$). In addition, histograms for average activity of all GPe cells imaged in SAL-SAL and SAL-CNO experiments are shown in Figure 41.

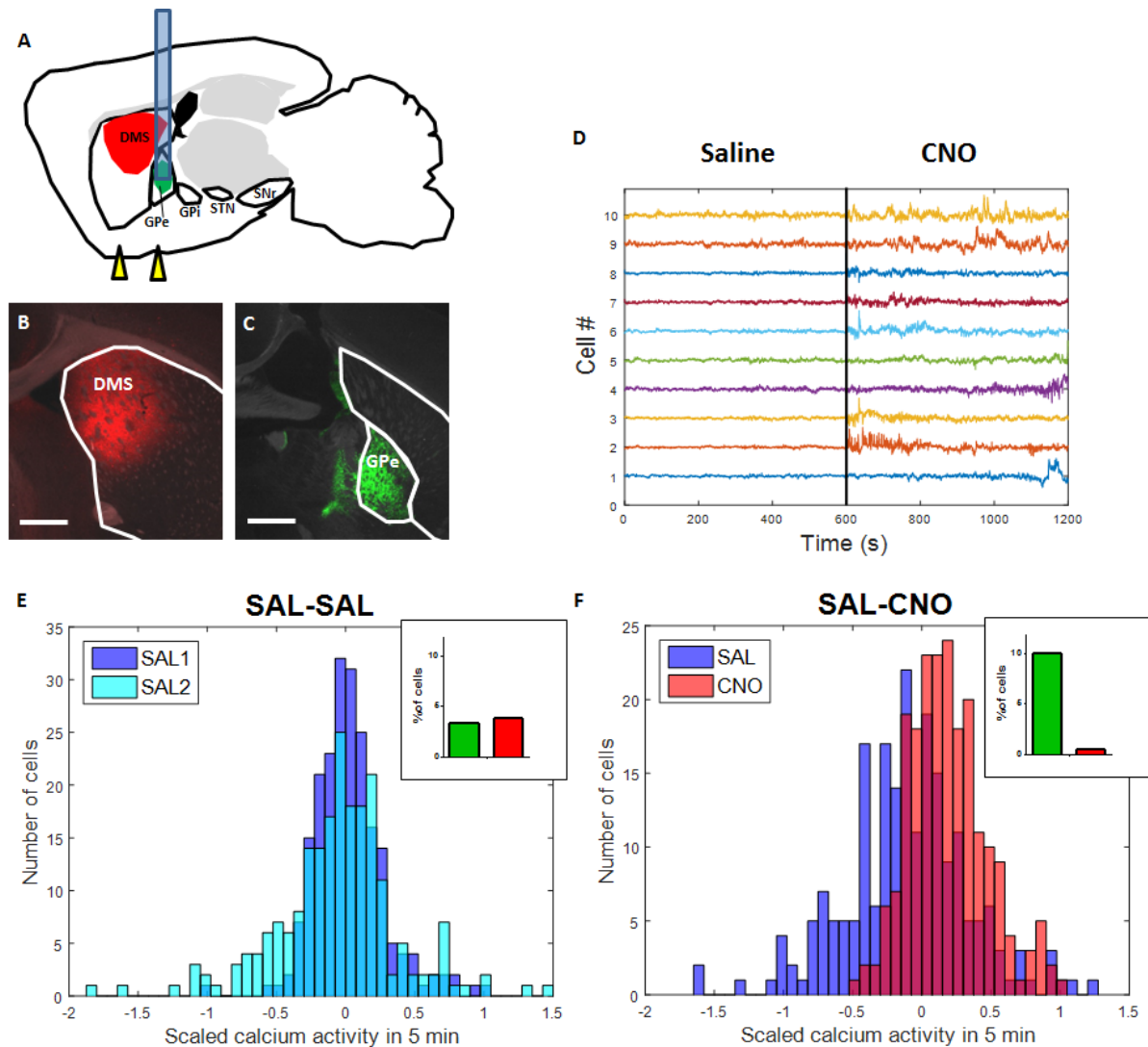


Figure 40: Activating hM4D receptors in striatal iMSNs leads to increased neuronal activity in GPe. **A.** Diagram of sagittal section showing region in the DMS and GPe virally targeted for *in vivo* calcium imaging of GPe cells expressing GCaMP6f and iMSNs in the DMS expressing hM4D. A microlens was implanted into the GPe for imaging using a miniature microscope. The yellow arrowheads indicate the approximate AP level of the sections in the micrographs shown in C and D. **B.** Micrograph of representative coronal section through dorsal striatum (at the level of most anterior yellow arrowhead in A) immunostained for mCherry showing region in DMS expressing hM4D. Scale bar: 1 μ m. **C.** Micrograph of representative coronal section posterior to section shown in C (most posterior yellow arrowhead in A) showing expression of GCaMP6f in GPe. Scale bar: 1 μ m. **D.** Representative calcium traces for ten isolated GPe neurons imaged in a freely-behaving mouse after treatment with saline or CNO. **E-F.** Histograms of scaled calcium activity for all cells imaged in (**E**) SAL-SAL experiments, revealing a small decrease in activity in the second session compared to the first session ($t_{(210)} = 2.308$, $p = 0.0220$, $n = 211$), and (**F**) SAL-CNO experiments, showing a robust increase in activity after CNO treatment compared to saline treatment ($t_{(208)} = 6.857$, $p < 0.0001$, $n = 209$). **Insets:** Plots of percentage of cells that showed a significant decrease or increase in activity when (**E, inset**) comparing control paired sessions done after treatment with saline (SAL-SAL condition, 3.37% significantly increased, 3.79% significantly decreased), and (**F, inset**) comparing sessions done after treatment with saline to sessions after treatment with CNO (SAL-CNO condition, 10.05% significantly increased, 0.48% significantly decreased). A significant increase in the proportion of cells that showed increased activity can be attributed to CNO treatment when comparing proportions across conditions ($p = 0.0117$). A total of 211 cells for the SAL-CNO condition and 209 cells for the SAL-SAL condition from 4 different animals were used to calculate all statistics reported above.

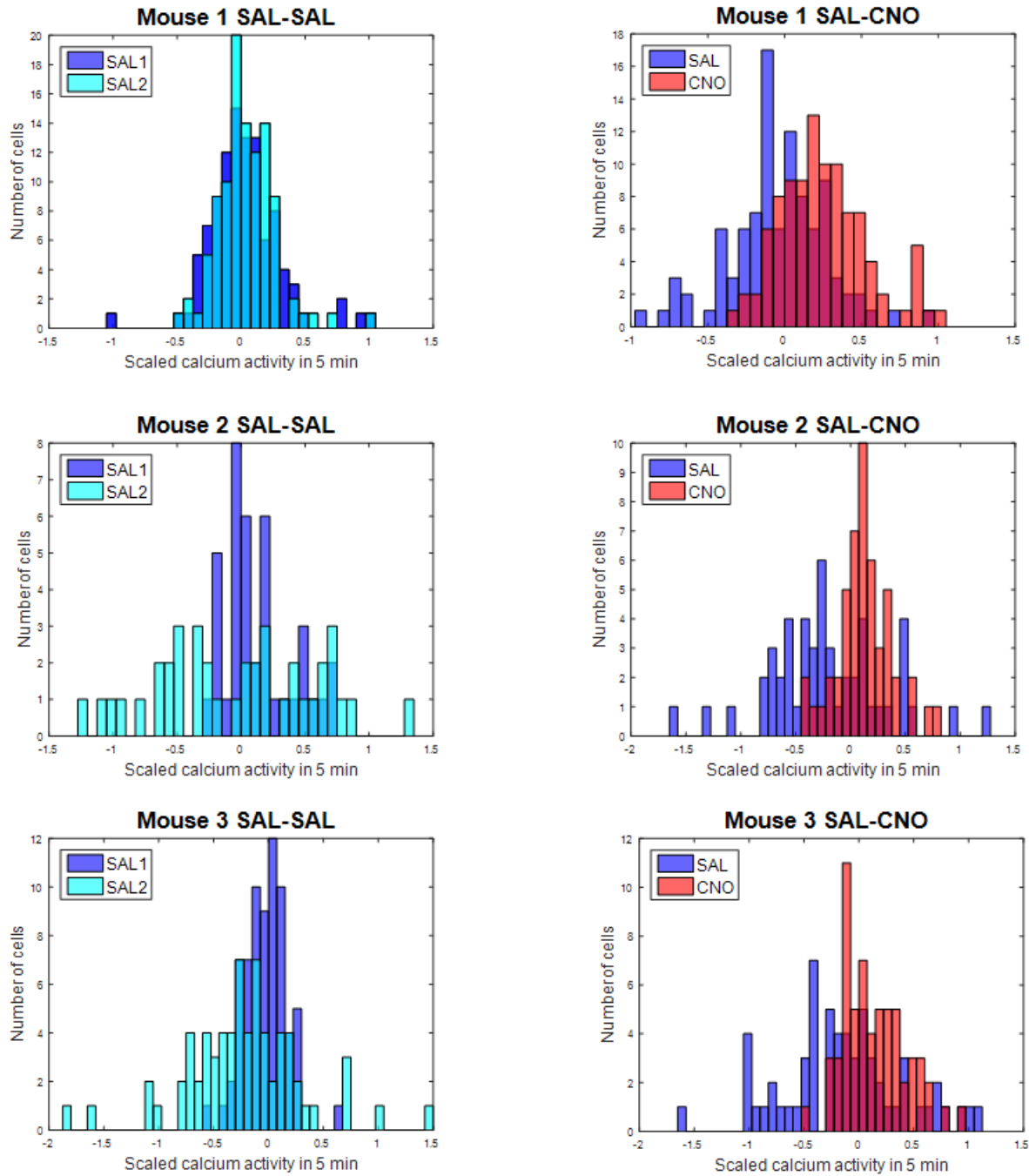


Figure 41: Increased GPe activity after treatment with CNO was observed in all mice imaged. Histograms of scaled calcium activity for all cells imaged for each mouse in (left) SAL-SAL experiments (mouse 1: $t_{(102)} = 0.2217$, $p = 0.8250$, $n = 103$ cells; mouse 2: $t_{(39)} = 1.329$, $p = 0.1917$, $n = 40$ cells; and mouse 3: $t_{(68)} = 2.577$, $p = 0.0121$, $n = 69$ cells) and (right) SAL-CNO experiments (mouse 1: $t_{(97)} = 4.803$, $p < 0.0001$, $n = 98$; mouse 2: $t_{(49)} = 3.755$, $p = 0.0005$, $n = 50$; and mouse 3: $t_{(60)} = 3.225$, $p = 0.0020$, $n = 61$).

Detailed statistical analysis comparing these histograms are reported for all cells pooled in Figure 40 and for each individual mouse in Figure 41, confirming a significant increase in GPe cell activity in response to CNO. Hence, while activating G_{oi} signaling in iMSNs did not elicit a robust change in the cells' intrinsic excitability or activity at the somatic level, the circuit-level effect of this manipulation could be readily observed *in vivo* as a disinhibition of neuronal activity in the GPe.

CHRONIC EFFECTS OF DECREASING INDIRECT PATHWAY FUNCTION

In addition to investigating the effect on acute activation of G_{oi} signaling in iMSNs in selective striatal sub-regions on motivated behavior, membrane excitability, and calcium activity, I also investigated the behavioral effects of chronically increasing indirect-pathway function by continuous activation of hM4D receptors in the iMSNs in the DMS and NA core. I found that, in *Drd2-Cre* mice expressing the hM4D receptor in both the DMS and NA core, motivated behavior was not affected by chronic treatment with CNO in the drinking water for two weeks. Chronic CNO treatment did not affect performance of D2R-OE_{dev} mice or control littermates in the progressive ratio schedule of reinforcement, as measured by comparing the survival functions of average session duration for each group (Log-rank test: control: $\chi^2 = 0.2393$, $p = 0.6247$, $n = 6$ mice per treatment; D2R-OE_{dev}: $\chi^2 = 3.690$, $p = 0.2969$, $n = 6$ mice per treatment) (Figure 42A), or the total number of lever presses for each group ($F_{(1,20)} = 1.671$, $p = 0.2108$, $n = 6$ mice per genotype and treatment) (Figure 42B). Moreover, 48 h after chronic treatment with CNO or vehicle ended, mice were again tested in the progressive ratio schedule. Once again, no differences in performance were detected that could be attributed to previous chronic drug treatment with CNO, as measured by survival functions of average session duration (Log-rank

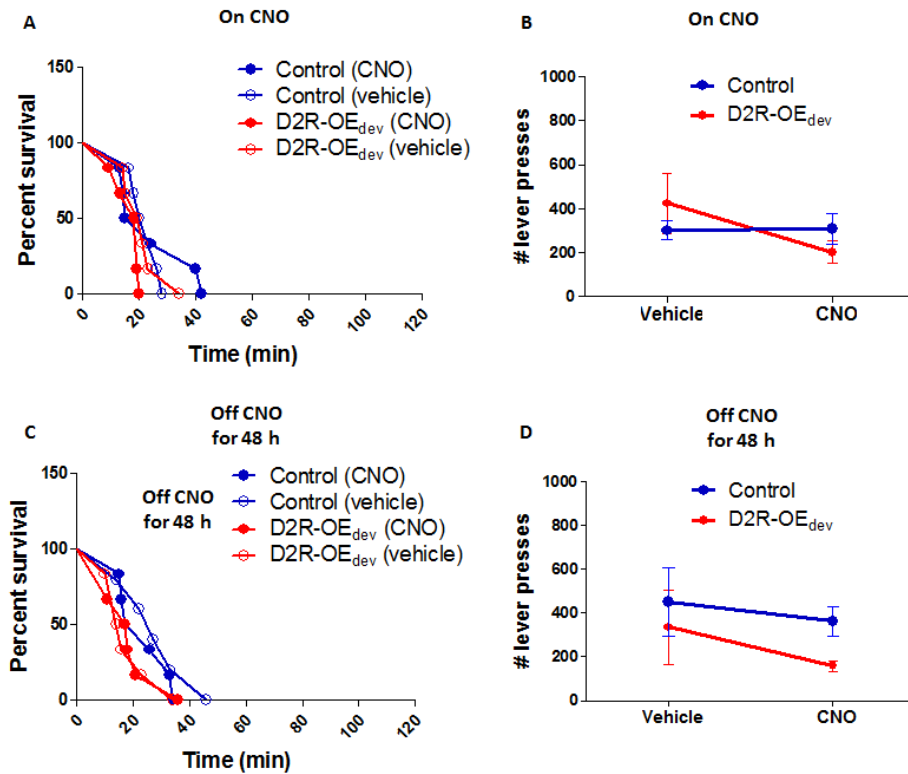


Figure 42: Chronically activating $G_{\alpha i}$ signaling in iMSNs in both the DMS and NA core does not affect motivation in D2R-OE_{dev} or control littermates. **A.** No differences were observed in the survival function for average session duration in the progressive ratio schedule for D2R-OE_{dev} and control mice being treated with CNO or vehicle for at least 2 weeks (control: $p = 0.6247$; D2R-OE_{dev}: $p = 0.2969$). **B.** The number of lever presses made in a progressive ratio session was also not changed in D2R-OE_{dev} and control mice being treated with CNO or vehicle for at least 2 weeks ($p = 0.2108$). **C.** No differences were observed in the survival function for average session duration for D2R-OE_{dev} and control mice tested in the progressive ratio schedule 48 h after ending chronic treatment with CNO or vehicle (control: $p = 0.5225$; D2R-OE_{dev}: $p = 0.5864$). **D.** The total number of lever presses was also not affected by drug treatment in D2R-OE_{dev} and control mice tested in the progressive ratio schedule 48 h after ending chronic treatment with CNO or vehicle ($p = 0.2719$). A total of 12 D2R-OE_{dev} mice expressing hM4D in iMSNs in the DMS and NA core (6 mice treated with chronic CNO and 6 mice treated with chronic vehicle) and 12 control mice expressing hM4D in iMSNs in the DMS and NA core (6 mice treated with chronic CNO and 6 mice treated with chronic vehicle) were used for this analysis. A crossover design was not used for this experiment; each subject was subjected to only one chronic treatment (CNO or vehicle).

test: control: $\chi^2 = 0.4089$, $p = 0.5225$, $n = 5$ mice per treatment; D2R-OE_{dev}: $\chi^2 = 1.933$, $p = 0.5864$, $n = 6$ mice per treatment) (Figure 42), and total number of lever presses ($F_{(1,19)} = 1.867$, $p = 0.2719$, $n = 5-6$ mice per genotype and treatment) (Figure 42D).

These negative results led to the question of whether chronic CNO treatment in the drinking water was effective in producing CNO levels in the brain that was sufficient to induce

any behavior effect in mice. Alternatively, CNO solution in the drinking water maintained at room temperature for several days may have been unstable and may have become ineffective throughout the two-week treatment period. To get at these questions, one month after conducting the last motivation assay in D2R-OE_{dev} and controls expressing hM4D in iMSNs in the DMS and NA core, I attempted to induce acute oral consumption of CNO by water-depriving animals for 16 h and subsequently allowing them to drink CNO-treated water for 1 h before assaying locomotion in an open field. Each animal was subjected to three total sessions, including control sessions, on different days, counterbalancing the order of sessions for genotype and treatment group. In one session animals were given untreated water before testing, in another session animals were given freshly-prepared CNO-treated water (fresh CNO) before testing, and in yet

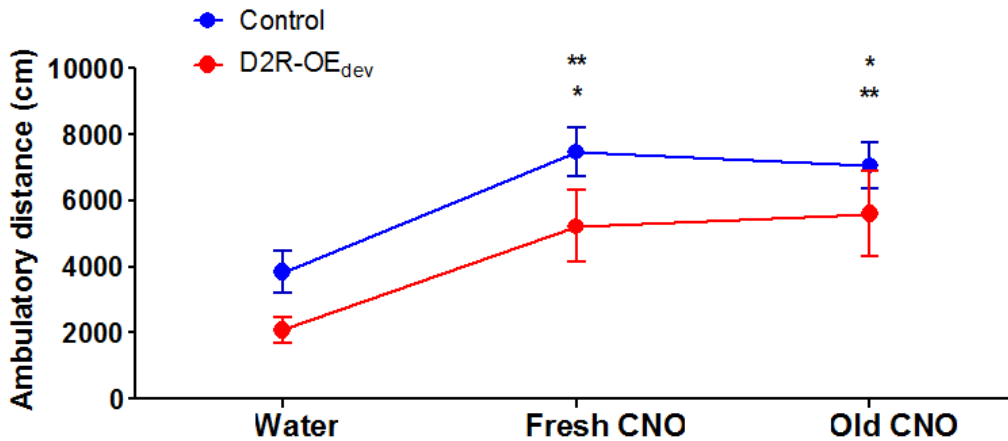


Figure 43: Oral consumption of CNO induces a behavior response in mice. Distance traveled in an open field for 1 h immediately after water-deprived D2R-OE_{dev} or control mice expressing hM4D in striatal iMSNs were allowed to freely consume water, freshly-prepared CNO, or a CNO solution prepared 1 month prior and stored at room temperature. This acute oral consumption of fresh CNO or old CNO led to comparable increases in locomotion in both D2R-OE_{dev} and control mice $p = 0.0001$; Bonferroni *post hoc* tests: water vs. fresh CNO: control: $p < 0.01$, D2R-OE_{dev}: $p < 0.05$; water vs. old CNO: control: $p < 0.05$, D2R-OE_{dev}: $p < 0.01$; fresh CNO vs. old CNO: control: $p > 0.05$, D2R-OE_{dev}: $p > 0.05$). A total of 12 D2R-OE_{dev} and 12 control mice expressing hM4D in iMSNs in the DMS and NA core were used for this analysis.

another session animals were given CNO-treated water that had been prepared one month prior and stored at room temperature (old CNO). CNO-treated water (fresh CNO and old CNO) contained CNO at the same concentration used for chronic treatment in the experiments described above. I found that, compared to the baseline condition in which animals were given plain water, acute oral consumption of fresh CNO or old CNO led to comparable increases in locomotion in both D2R-OE_{dev} and control mice ($F_{(2,22)} = 11.42$, $p = 0.0001$, $n = 12$ mice per group; Bonferroni *post hoc* tests: water vs. fresh CNO: Control: $p < 0.01$, D2R-OE_{dev}: $p < 0.05$; water vs. old CNO: Control: $p < 0.05$, D2R-OE_{dev}: $p < 0.01$; fresh CNO vs. old CNO: Control: $p > 0.05$, D2R-OE_{dev}: $p > 0.05$) (Figure 43). Thus, oral consumption of CNO can induce a behavior response in mice, and CNO solution appears to be stable at room temperature since a one-month old solution was just as effective as a fresh solution in inducing hyperlocomotion in mice expressing hM4D in striatal iMSNs.

To expand on these findings, I further investigated the lack of response on motivation of chronically decreasing function of iMSNs specifically in the DMS or the NA core. In addition, I also further tested whether or not mice are able to respond to an acute injection of CNO while being chronically administered CNO for two weeks. First, I found that similarly to mice expressing the hM4D receptor in iMSNs in both the DMS and NA core, mice expressing the receptor in iMSNs of either region separately did not respond to chronic treatment with CNO in the drinking water. While mice were on CNO, no difference in performance was observed in the progressive ratio task, as measured by the survival functions for average session duration (Log-rank test: DMS: $\chi^2 = 0.02327$, $p = 0.8788$, $n = 8$ mice; NA core: $\chi^2 = 0.02327$, $p = 0.8788$, $n = 9$ mice) (Figure 44A), and total number of lever presses ($F_{(1,15)} = 1.062$, $p = 0.3192$, $n = 8-9$ mice per site) (Figure 44B). Likewise, there was no effect of previous CNO treatment on performance

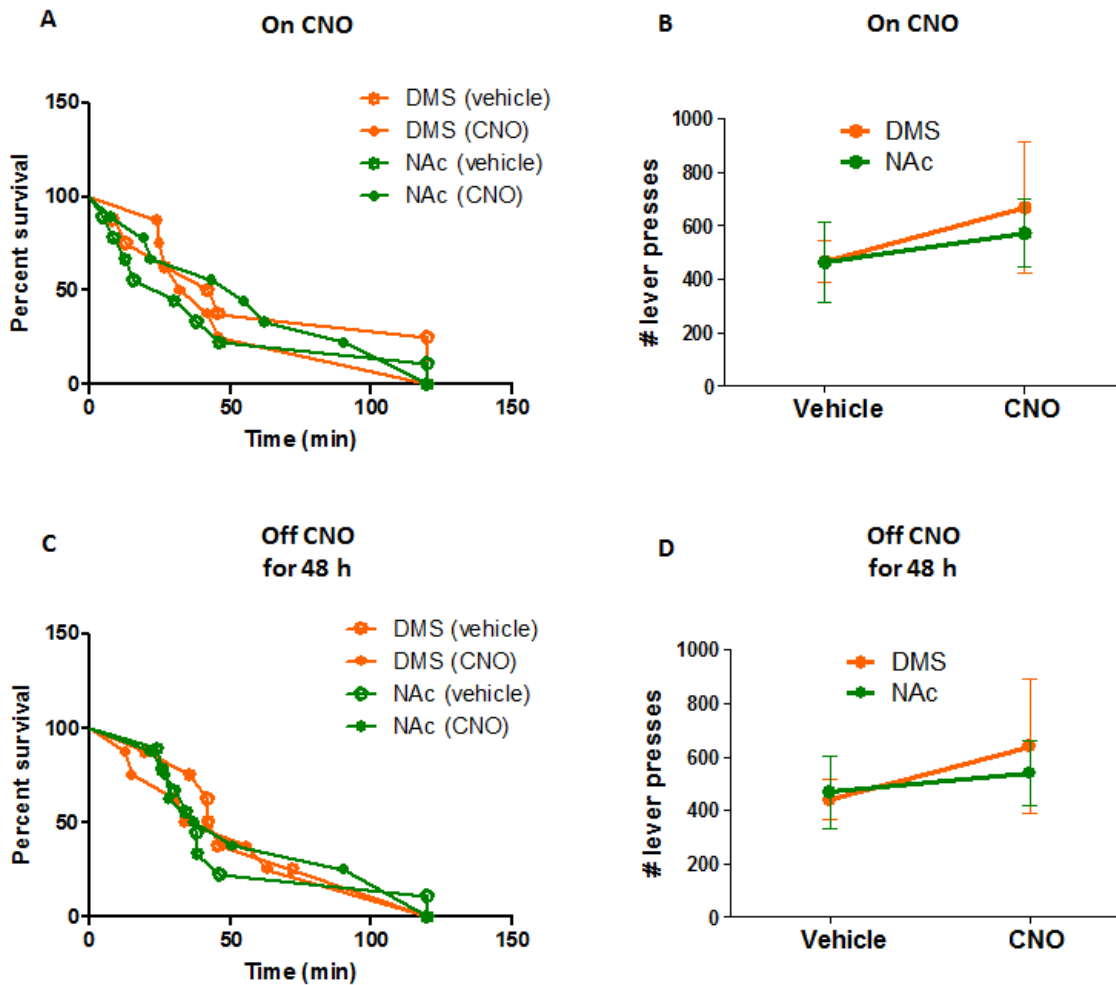


Figure 44: Chronically activating $G_{\alpha i}$ signaling in iMSNs in either the DMS or NA core does not affect motivation in mice. **A.** No differences were observed in the survival function for average session duration in the progressive ratio schedule for mice expressing hM4D in the DMS or NA core being treated with CNO or vehicle for at least 2 weeks (DMS: $p = 0.8788$; NA core: $p = 0.8788$). **B.** The number of lever presses made in a progressive ratio session was also not changed in mice expressing hM4D in the DMS or NA core being treated with CNO or vehicle for at least 2 weeks ($p = 0.3192$). **C.** No differences were observed in the survival function for average session for mice expressing hM4D in the DMS or NA core tested in the progressive ratio schedule 48 h after ending chronic treatment with CNO or vehicle (DMS: $p = 0.7496$; NA core: $p = 0.5934$). **D.** The total number of lever presses was also not affected by drug treatment in mice expressing hM4D in the DMS or NA core tested in the progressive ratio schedule 48 h after ending chronic treatment with CNO or vehicle ($p = 0.8347$). A total of 8 mice expressing hM4D in iMSNs in the DMS and 9 mice expressing hM4D in iMSNs in the NA core were used for this analysis.

in the progressive ratio task when animals were tested 48 h after ending chronic treatment. This lack of effect was determined from the survival functions for average session duration (Log-rank test: DMS: $\chi^2 = 0.1018$, $p = 0.7496$, $n = 8$ mice; NA core: $\chi^2 = 0.2851$, $p = 0.5934$, $n = 9$ mice)

(Figure 44C), and total number of lever presses ($F_{(1,15)} = 0.9435$, $p = 0.8347$, $n = 8-9$ mice per site) (Figure 44D).

The lack of response to chronic treatment with CNO in mice expressing hM4D in iMSNs in either the DMS or NA core was expected given that, in a different cohort, mice expressing hM4D in iMSNs in both DMS and NA core also did not respond to chronic CNO. In the cohort of mice targeted specifically in the DMS or NA core, I also tested whether animals on chronic CNO treatment for at least two weeks could exhibit a behavioral response to an acute intraperitoneal administration of CNO in tests of motivation and locomotion. In the progressive ratio schedule, I found that, while animals expressing hM4D in either DMS or NA core on chronic treatment with vehicle responded to acute CNO treatment with increased total number of lever presses ($F_{(1,15)} = 8.785$, $p = 0.0097$, $n = 8-9$ mice per site), animals on chronic treatment with CNO did not exhibit an acute response to the drug ($F_{(1,15)} = 1.108$, $p = 0.3092$, $n = 8-9$ mice per site) (Figure 45A). Session duration times of mice expressing hM4D in the DMS were compared with those of mice expressing hM4D in the NA core and there was no difference in performance between these groups while animals were on chronic vehicle and treated acutely with CNO (Log-rank test, $\chi^2 = 0.7529$, $p = 0.3855$, $n = 8-9$ mice per site). Likewise, there was no difference in performance between mice expressing hM4D in the DMS or NA core on chronic CNO after acute treatment with CNO (Log-rank test: $\chi^2 = 0.5967$, $p = 0.4512$, $n = 8-9$ mice per site). Therefore, the data were pooled for mice expressing hM4D in the DMS or NA core, and a significant difference was observed in average session duration when mice were being treated with chronic CNO and received an acute administration of CNO compared to when these mice

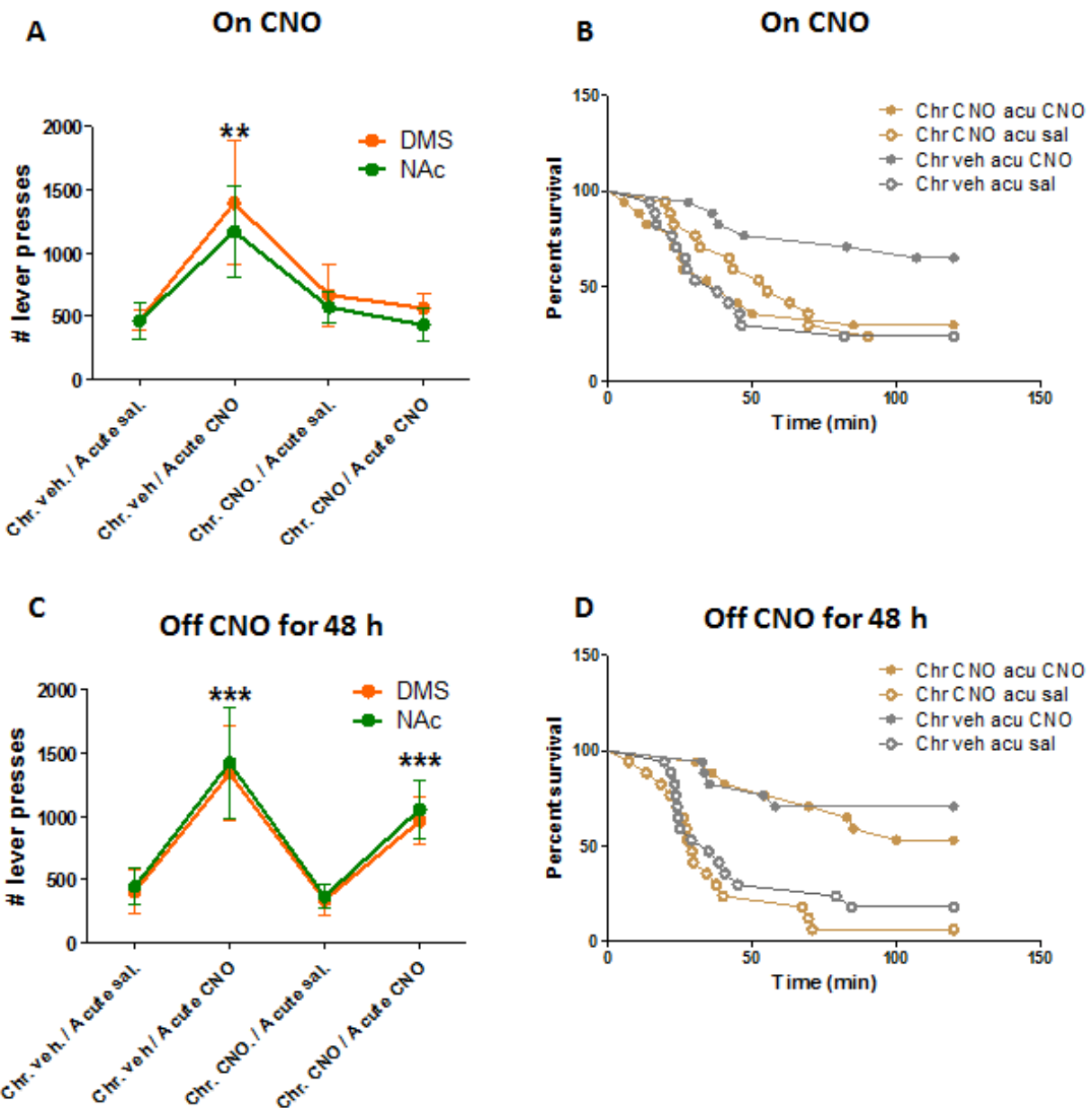


Figure 45: Mice expressing hM4D in iMSNs in either DMS or NA core being chronically treated with CNO no longer respond to acute CNO treatment, but response is recovered 48 h after ending chronic treatment. **A.** The number of lever presses made in a progressive ratio session was increased after acute CNO treatment in mice chronically treated with vehicle ($p = 0.0097$) but not in mice chronically treated with CNO ($p = 0.3092$). **B.** For session duration in the progressive ratio schedule, pooling data for mice expressing hM4D in the DMS and NA core revealed a significant difference in session duration when mice were being treated with chronic CNO and acutely administered CNO compared to when mice were being treated with chronic vehicle and acutely administered CNO ($p = 0.0143$). **C.** After discontinuing chronic treatment with CNO or saline, mice were re-tested 48 h later and all groups responded to acute CNO with increase total number of lever presses (previous chronic vehicle: $p = 0.0007$; previous chronic CNO: $p < 0.0001$). **D.** Discontinuing chronic treatment with CNO or vehicle was sufficient to re-elicite a response to acute CNO in mice measured by session duration (previous chronic vehicle: $p = 0.0039$; previous chronic CNO: $p = 0.0143$). A total of 8 mice expressing hM4D in iMSNs in the DMS and 9 mice expressing hM4D in iMSNs in the NA core were used for this analysis.

received chronic vehicle and were treated with an acute administration of CNO (Log-rank test: $\chi^2 = 6.000$, $p = 0.0143$, $n = 17$ mice) (Figure 45B). Thus, a response to acute CNO in the progressive ratio task could no longer be elicited when animals were being chronically treated with CNO for two weeks (Figures 45A-B).

I also tested whether or not mice are able to once again display a response to an acute injection of CNO after ending chronic CNO treatment. This experiment tested the hypothesis that hM4D receptors may become permanently desensitized after a long period of continued activation with CNO. Mice that had been treated with chronic CNO for two weeks were taken off chronic CNO treatment for 48 hours and were subsequently treated with an acute administration of CNO or saline to test whether or not they had recovered their sensitivity to this drug. After being taken off chronic treatment, mice expressing hM4D in either DMS or NA core and previously treated with either CNO or vehicle demonstrated a significant increase in lever presses in response to acute CNO (previous chronic vehicle: $F_{(1,15)} = 17.89$, $p = 0.0007$; previous chronic CNO: $F_{(1,15)} = 33.30$, $p < 0.0001$; $n = 8-9$ mice per site) (Figure 45C). No significant differences were observed between mice expressing hM4D receptors in the DMS or the NA core in average session duration when the performance of mice in both groups were compared 48 h after discontinuing treatment with chronic vehicle (Log-rank test: $\chi^2 = 0.3035$, $p = 0.5817$, $n = 8-9$ per site). Similarly, there were no differences for average session duration when performance in the two groups was compared 48 h after discontinuing treatment with chronic CNO (Log-rank test: $\chi^2 = 0.3035$, $p = 0.5817$, $n = 8-9$ per site). Thus, the data for average session duration after ending chronic treatment were pooled to show that discontinuing chronic treatment with CNO or vehicle was sufficient to re-elicite a response to acute CNO in mice (previous chronic vehicle: Log-rank test: $\chi^2 = 8.335$, $p = 0.0039$; previous chronic CNO: Log-rank test: $\chi^2 =$

6.000, $p = 0.0143$; $n = 17$ mice) (Figure 45D). Finally, I also tested mice expressing hM4D in iMSNs in the DMS and NA core for baseline locomotor activity in an open field in response to an acute intraperitoneal injection of CNO while they were on chronic treatment with CNO or vehicle in their drinking water for two weeks, as well as after discontinuing chronic treatment for 48 h. Remarkably, the results for tests of locomotor activity closely paralleled those obtained for measures of motivation. For analysis of locomotor data, the distance traveled per min as a percent of baseline before acute treatment was used for comparison between groups. While mice

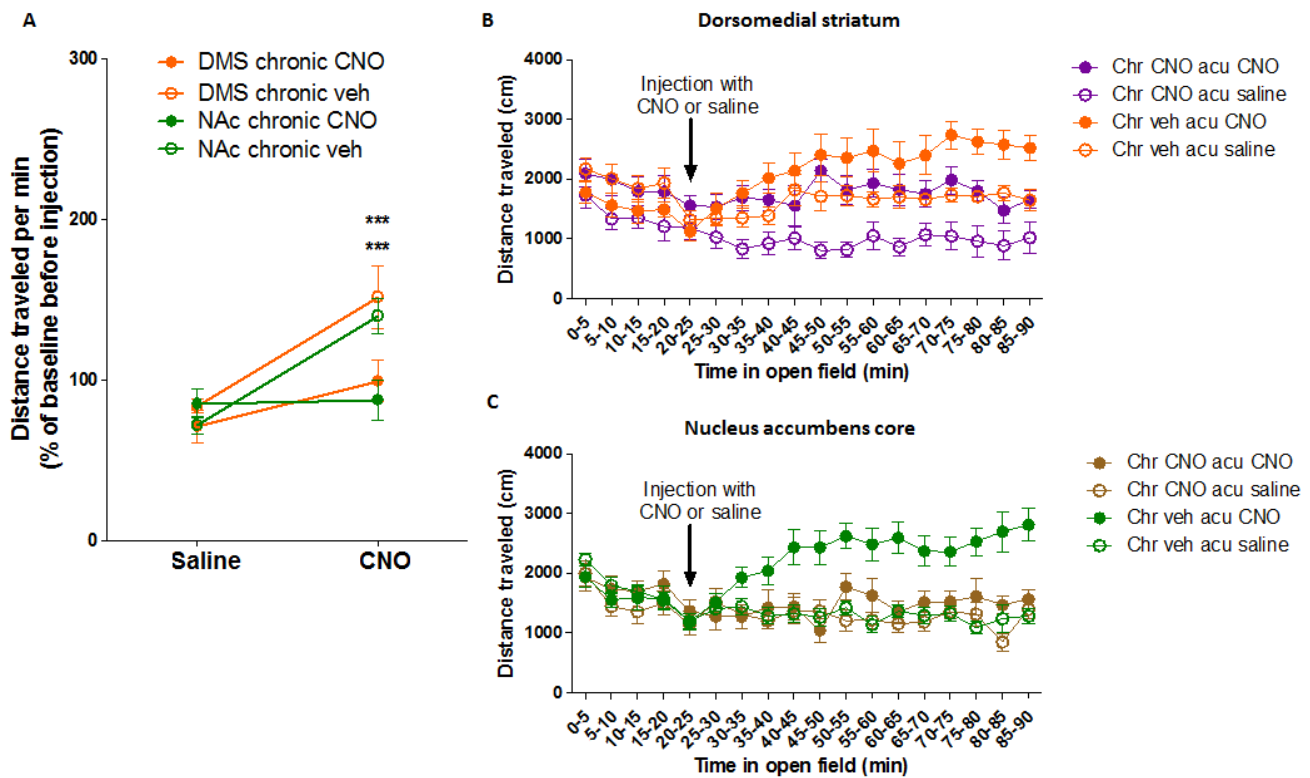


Figure 46: Mice expressing hM4D in iMSNs in either DMS or NA core being chronically treated with CNO do not display locomotor response to acute CNO treatment. **A.** While mice were still on chronic treatment, animals on chronic vehicle showed a locomotor response to an acute administration of CNO ($p < 0.0001$; Bonferroni *post hoc* tests, DMS: $p < 0.001$, NA: $p < 0.001$), and animals on chronic CNO did not respond to acute CNO ($p = 0.1873$; $n = 8-9$ mice per site). **B-C.** Plots of distance traveled in an open field by mice expressing hM4D in iMSNs in (**B**) the DMS or (**C**) the NA core on chronic treatment with CNO or vehicle for 2 weeks. Data is shown in 5-min bins 20 min before and 70 min after acute injection with CNO or saline. A total of 8 mice expressing hM4D in iMSNs in the DMS and 9 mice expressing hM4D in iMSNs in the NA core were used for this analysis.

were still on chronic treatment, animals expressing hM4D in iMSNs in either the DMS or the NA core on chronic vehicle showed a locomotor response to an acute administration of CNO ($F_{(1,15)} = 45.16$, $p < 0.0001$; Bonferroni *post hoc* tests, DMS: $p < 0.001$, NA: < 0.001 ; $n = 8-9$ mice per mice) (Figure 46). In contrast, animals on chronic CNO did display a locomotor response to an acute administration of CNO ($F_{(1,15)} = 1.909$, $p = 0.1873$; $n = 8-9$ mice per site) (Figure 46). Similar to what was observed for assays of motivation, after discontinuing chronic treatment for 48 h, an acute CNO administration was sufficient to re-elicited a locomotor response

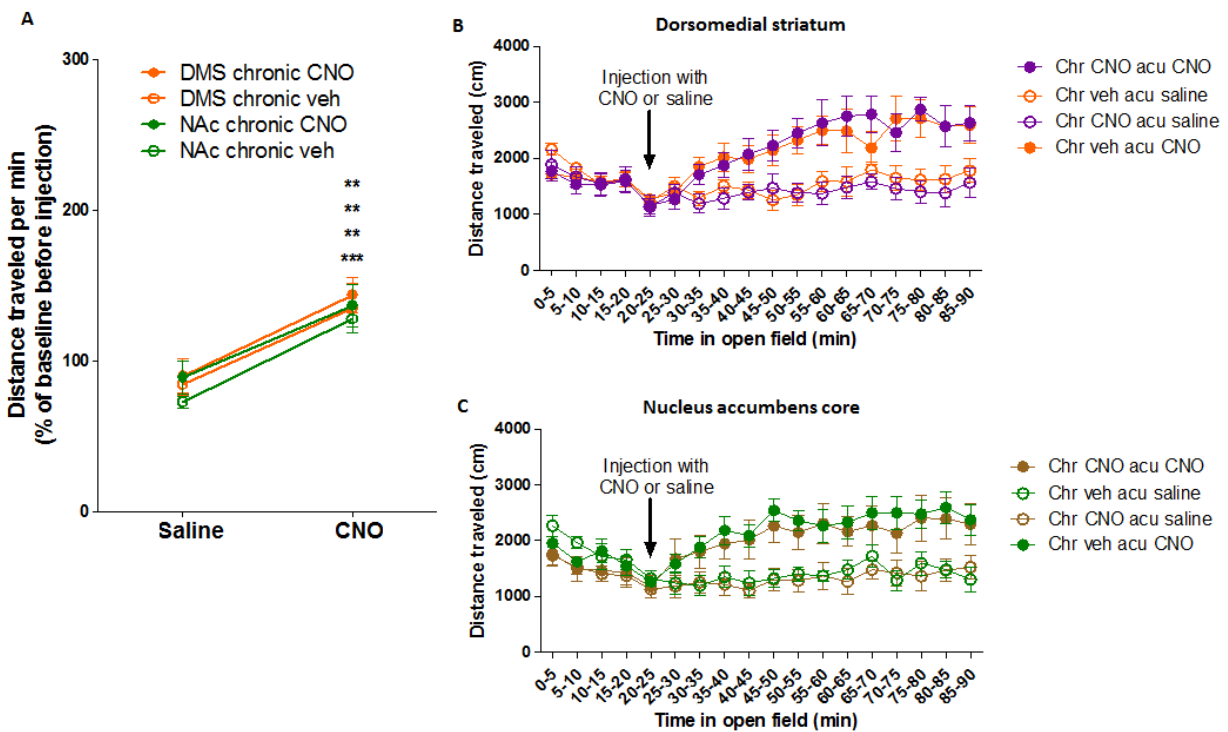


Figure 47: Mice expressing hM4D in iMSNs in either DMS or NA core recover locomotor response to acute CNO treatment after being taken off chronic CNO treatment for 48 h. **A.** After being taken off 2-week chronic treatment with CNO or vehicle, animals that had been on chronic vehicle showed a locomotor response to an acute administration of CNO ($p < 0.0001$; Bonferroni *post hoc* tests, DMS: $p < 0.01$, NA: < 0.001). A locomotor response was also elicited in animals that were previously treated with chronic CNO ($p = 0.0001$; Bonferroni *post hoc* tests, DMS: $p < 0.01$, NA: < 0.01). **B-C.** Plots of distance traveled in an open field by mice expressing hM4D in iMSNs in **(B)** the DMS or **(C)** the NA core 48 h after discontinuing chronic treatment with CNO or vehicle. Data is shown in 5-min bins 20 min before and 70 min after acute injection with CNO or saline. A total of 8 mice expressing hM4D in iMSNs in the DMS and 9 mice expressing hM4D in iMSNs in the NA core were used for this analysis.

in both groups. Mice previously treated with chronic vehicle responded to acute CNO as before ($F_{(1,15)} = 39.06$, $p < 0.0001$; Bonferroni *post hoc* tests, DMS: $p < 0.01$, NA: < 0.001) (Figure 47). And a locomotor response could also be elicited in animals that had been previously treated with chronic CNO ($F_{(1,15)} = 25.84$, $p = 0.0001$; Bonferroni *post hoc* tests, DMS: $p < 0.01$, NA: < 0.01) (Figure 47).

DISCUSSION

The original aim of this study was to determine whether the motivational deficit of D2R-OE_{dev} mice, induced by upregulation of D2Rs in the striatum, could be reversed by acutely activating G_{ai}-coupled signaling in the indirect pathway in these animals. I found that this manipulation increased motivation in D2R-OE_{dev} mice but also in control littermates. This effect was due to energized behavioral performance, which, however, came at the cost of goal-directed efficiency. Moreover, selective manipulation of iMSNs in either the DMS or NA core showed that both striatal regions contribute to this effect on motivation. Further investigation aimed at understanding how activating G_{ai}-coupled signaling affects striatal circuit function revealed that activating G_{ai} signaling did not lead to a significant change in somatic iMSN activity *in vivo* or to a change in neuronal excitability *in vitro*. In contrast, the GPe, which receives monosynaptic inhibition from the indirect pathway, showed disinhibited activity when G_{ai}-signaling was activated in striatal MSNs.

In testing my initial hypothesis that MSN excitability might underlie the motivational deficit of D2R-OE_{dev} mice, I found that decreasing function of the indirect pathway by acutely activating the hM4D receptor in striatal iMSNs boosts motivation in mice, as both D2R-OE_{dev} and control mice showed increased performance in the progressive ratio schedule of reinforcement after treatment with CNO. Since both genotypes improved performance, it is

unclear whether hM4D activation rescued the underlying neuronal mechanism that caused the motivational deficit of D2R-OE_{dev} mice or whether it enhanced motivation by an independent mechanism. Nevertheless, since I reversed the motivational deficit, I propose that inhibiting function of the indirect pathway by activating G_{ai} signaling in iMSNs may represent a more general strategy to ameliorate deficits in motivation.

Using the progressive hold-down task, I demonstrated that inhibiting function of the indirect pathway energizes behavior, which however came at the cost of goal-directed efficiency. In this task of motivation, maximal efficiency requires animals to suppress hyperactive behavior in order to successfully maintain a lever held down until a reward is obtained. Both D2R-OE_{dev} and control mice on CNO made more responses and continued to respond for longer times in the task, but they earned fewer rewards. These observations suggest that inhibition of the indirect pathway in the NA core and DMS enhances motivation by regulating the arousal and readiness to initiate behaviors rather than specifically affecting processes related to the optimal selection of specific behaviors, such as positively affecting the value of the reward. Ideally, a manipulation that enhances motivation would enhance performance in both the progressive ratio and progressive hold-down tasks so that the best results with regard to positive outcome would be achieved independently of external conditions (Bailey et al., 2015). Thus, therapeutic strategies aimed at manipulating the indirect pathway to treat abnormal motivation should take into consideration the risks of enhancing motivation while impairing goal-directed efficiency.

I also addressed the question of whether the DMS and NA core contributed differently to the enhancement in motivation observed in the progressive ratio task after inhibition of iMSNs. Previous studies have placed emphasis on the NA core as playing a key role in goal-directed behavior by regulating how animals allocate effort to achieve specific outcomes based on the

rewarding value of those outcomes (Nowend et al., 2001, Mai et al., 2012). However, the role the DMS in the performance of goal-directed actions based on action-outcome associations has also been clearly established (Yin et al., 2005, Shiflett et al., 2010, Hilario et al., 2012). The progressive ratio task is a task of goal-directed behavior that measures how much effort a subject is willing to expend to obtain a reward. Acutely decreasing function of the indirect pathway selectively in either the NA core or DMS led to similar increased performance in this task, without affecting outcome devaluation, suggesting that both striatal regions can regulate goal-directed behavior by modulating indirect-pathway output. Nevertheless, more refined behavioral assays of instrumental performance, such as tasks that measure sensitivity to response contingencies or effort/value relationships, after inhibiting the function of the indirect pathway in the DMS or NA core may potentially reveal specific dissociations between these two striatal sub-regions.

Using *in vitro* electrophysiology and *in vivo* calcium imaging, I found that hM4D activation in iMSNs disinhibits activity of downstream pallidal neurons without changes in somatic excitability or iMSN activity. Given the well-established effect of G_{ai} signaling on neuronal excitability via GIRK channels (Luscher and Slesinger, 2010), it was surprising that I did not observe changes in excitability in striatal MSNs expressing the hM4D receptor after CNO treatment. However, MSNs only express low levels of GIRK channels (Karschin et al., 1996). Consistent with low GIRK levels, D2R-dependent outward currents that are characteristic of GIRKs cannot be readily measured somatically in MSNs unless GIRK channels are artificially overexpressed (Marcott et al., 2014). Furthermore, slice physiology experiments using D2R agonists generally report little or no change in MSN resting membrane potential, and, instead, D2R activation alters membrane conductances thought to affect synaptic integration and lead to

decreased synaptic output (Hernandez-Lopez et al., 2000, Sun et al., 2000, Cepeda et al., 2001, Salgado et al., 2005, Perez et al., 2006, Gerfen and Surmeier, 2011, Tritsch and Sabatini, 2012). Of note, using the exact same methodology used in the present study, the Kellendonk laboratory previously showed that CNO reliably hyperpolarizes thalamic neurons expressing hM4D (Parnaudeau et al., 2013). In contrast to the excitability measurements reported in the current study, one study has shown an effect of hM4D receptor activation on excitability of iMSN; however, this study was performed in rats while I used mice (Ferguson et al., 2011).

In line with unaltered excitability, I found no effect of hM4D activation on calcium activity of iMSNs measured somatically in freely behaving mice. In all conditions tested, calcium activity of iMSNs in the DMS was correlated with the animal's locomotor activity. The experimental design I used controlled for a potential effect of this correlation on my ability to detect an effect of CNO on somatic calcium activity. I co-expressed hM4D and GCaMP6f unilaterally in a small region of the DMS in an effort to image the cells being manipulated without broadly affecting basal ganglia output and behavior. I was indeed able to image animals across sessions in which they displayed comparable levels of locomotor activity after treatment with CNO or saline. Moreover, in my analysis, I tested for the effect of CNO treatment on the correlation between activity of iMSNs and locomotion, and I also conducted statistical analysis after normalizing calcium activity to locomotor activity. In all cases, I found no effect of CNO treatment on somatic calcium activity of iMSNs expressing hM4D. A change in calcium activity in these neurons would be expected if hM4D activation led to increased firing of action potentials generated near the soma. However, intracellular changes in free calcium resulting from changes in spike activity and synaptic input can be compartmentalized in the neuron (Yasuda et al., 2004). Axons of iMSNs project out of the striatum to the adjacent pallidum, and changes in

firing activity specifically localized to these presynaptic terminals would not be detectable using our imaging system in the striatum.

In contrast to unaltered activity in the indirect pathway, I found that CNO enhanced activity in the GPe. This observation suggests that hM4D receptors in the presynaptic axon terminals of iMSNs may mediate the effect of CNO on pallidal activity. In support of this hypothesis, I found that (a) virally expressed hM4D was transported to the terminals and (b) electron microscopy has revealed that the $G_{i\alpha}$ heterotrimeric subunit can be found in axon terminals in the GPe, consistent with the distribution characteristic of projections from iMSNs (Aronin and DiFiglia, 1992). More importantly, previous work from the Kellendonk laboratory and others using slice physiology have shown that optogenetic stimulation of presynaptic terminals of iMSNs expressing hM4D leads to decreased light-evoked IPSCs in VP neurons in the presence of CNO compared to control conditions (Bock et al., 2013).

In dopaminergic neurons, the $K_v1.2$ and other voltage-gated potassium channels have been shown to mediate inhibition of axonal dopamine release in a G-protein dependent manner upon activation of D2Rs (Martel et al., 2011). RT-PCR analysis has shown that K_v1 family channels, including $K_v1.2$, are also expressed in striatal MSNs (Shen et al., 2004). Future work on the mechanism proposed here should probe for specific channels, including K_v1 family channels, which may mediate the presynaptic effect of activating $G_{\alpha i}$ signaling in iMSNs.

Previous work has also shown that MSNs can laterally inhibit activity of neighboring MSNs, and inhibition of iMSNs onto other iMSNs has been established in the striatum (Tunstall et al., 2002, Taverna et al., 2008, Tecuapetla et al., 2009, Kohnomi et al., 2012). By expressing hM4D in the indirect pathway, I therefore expected to observe decreased inhibition after CNO treatment not only of the GPe but also of neighboring iMSNs. As a consequence, some neurons

of the indirect pathway would be expected to show enhanced firing and activity upon treatment with CNO. I may not have observed the effect of lateral inhibition using *in vivo* calcium imaging because of biological or technical reasons. One biological reason could be that hM4D activation may have led to decreased activity at the soma that was compensated for by decreased lateral inhibition. If this were the case, I nevertheless would have expected that variability of calcium transients would increase after hM4D activation. Another reason could be that hM4D does not mediate local inhibition to other iMSNs. And a technical reason could be that calcium imaging did not capture all aspects of neuronal activity. Compared to other types of neurons, MSNs are hyperpolarized at rest and require excitatory inputs from cortex and thalamus to fire action potentials (Wilson and Kawaguchi, 1996). Consistent with this idea, I found that activity of MSNs measured at the soma was highly correlated with animals' engagement in voluntary actions, as has been previously described (Cui et al., 2013). However, the calcium imaging system I used to measure striatal activity may have predominantly measured burst activity, and sparser individual spikes were likely below detection threshold, as they were difficult to distinguish from signal noise in the recording conditions I used. In fact, when detecting individual calcium events as single units, I found that the average firing rate of iMSNs in freely behaving animals was about 0.03 Hz, while *in vivo* electrophysiology studies report firing rates closer to 1 Hz (Kim et al., 2014). Since I did not record activity of iMSNs using electrophysiology and calcium imaging in parallel, I cannot reliably infer how many action potentials a single calcium transient represents. As a result, I may have not have captured all activity in the striatal neurons imaged *in vivo*, potentially masking some of the more subtle effects of CNO treatment. In addition, since I co-expressed hM4D together with GCaMP6f using two viruses *in vivo*, calcium imaging may have been inefficient if areas were imaged that did not

have high co-localization of transfected proteins. Although histology revealed that the majority of the targeted region had high co-localization of GCaMP6f and hM4D, some regions in the periphery of the virally-targeted site were observed where transfection of each virus appeared to be segregated in striatal cells. Since I could not identify the cells that were imaged *in vivo* using *post hoc* histological methods, I cannot confirm that all striatal cells imaged in the current study expressed hM4D.

In addition to the acute manipulations, animals were also chronically treated with CNO in order to characterize what happens when function of iMSNs is continuously suppressed. The finding in the current study that the chronic manipulation had no effect on motivation or locomotion raised several alternative interpretations. Some of these alternatives could be ruled out in this study. For instance, I showed that acute oral consumption of CNO (as was done for chronic administration of this drug) can induce behavioral effects on locomotion, demonstrating that this route of administration is effective. However, given that the exact concentration of CNO in the blood or brain was not determined, it is difficult to compare the relative effectiveness of oral and intraperitoneal administration of CNO. I was also able to rule out the possibility that the CNO solution used in the drinking water is unstable for two weeks at room temperature. I showed that the acute effect of oral CNO was similar regardless of whether I used freshly prepared solution or a one-month old solution stored at room temperature.

One alternative explanation for the lack of behavioral response after chronic CNO treatment is that the mutated $G_{\alpha i}$ -protein coupled hM4D receptor could become desensitized during chronic CNO administration. To address this question, I administered an acute intraperitoneal injection of CNO or saline to mice expressing hM4D in iMSNs while they were chronically consuming CNO. The persistent lack of behavioral response to an acute CNO

injection supports the hypothesis that a compensatory mechanism takes place that fully occludes the effect on motivation and locomotion mediated by hM4D receptor activation. However, this observation is consistent with both desensitization at the receptor level and circuit-level re-wiring as a consequence of continuous activation of $G_{\alpha i}$ signaling.

In order to test whether or not hM4D receptors were permanently suppressed after chronic CNO administration, I re-tested mice in the progressive ratio task 48 hours after discontinuing chronic treatment with CNO. These mice once again received acute intraperitoneal injections of either CNO or saline, and the results indicate that the response to CNO was fully recovered within this timeframe. These findings suggest that hM4D receptors are not permanently altered after being chronically activated by CNO. However, these results do not exclude the possibility that circuit-level rewiring may still mediate this behavioral desensitization effect. The fast recovery of the response suggests that structural anatomical rewiring may not be required, but circuit-level synaptic plasticity is known to occur in shorter timescales (Caroni et al., 2014). One likely possibility given the known regulatory pathways of GPCR activity (Gainetdinov et al., 2004) is that the hM4D receptor becomes internalized after chronic stimulation. All of these possibilities, therefore, represent new research avenues for advancing the findings presented in this study on the chronic effects of activating $G_{\alpha i}$ signaling in iMSNs.

In conclusion, the present study shows that acute activation of $G_{\alpha i}$ signaling in indirect-pathway striatal neurons enhances motivation in mice, although at the cost of goal-directed efficiency. It further demonstrates that neurons in both the DMS and NA core mediate this effect, consistent with both striatal sub-regions playing a role in performance of motivated behavior. In addition, the observation that activation of $G_{\alpha i}$ signaling in the striatal indirect pathway leads to disinhibition of activity in the GPe without affecting intrinsic excitability of iMSNs suggests that

$G_{\alpha i}$ signaling may be specifically exerting its effects at presynaptic terminals. And finally, this study also characterizes a behavioral desensitization effect of continuous activation of $G_{\alpha i}$ -coupled receptors in striatal iMSNs. Future work investigating the proposed mechanisms of action for the effects reported here, including $G_{\alpha i}$ signaling in presynaptic terminals of iMSNs and desensitization after continuous activation, should provide insight on basal ganglia function and guide the development of new treatments for neuropsychiatric disorders caused by basal ganglia dysfunction, including those that involve changes in D2R activity and abnormal motivation.

CHAPTER 5

GENERAL DISCUSSION

SUMMARY AND IMPLICATIONS OF MAIN FINDINGS

The first study presented in this dissertation investigated the bridging collaterals and their relevance for basal ganglia function, including behavior and potentially neuropsychiatric disorders. First, I demonstrated that the bridging collaterals form synaptic contacts in the GPe. Then I generated a viral construct to study the neural and behavioral effects of chronically increasing excitability of dMSNs and iMSNs. Using this construct, I showed that chronically increasing excitability of the indirect pathway, but not the direct pathway, of the basal ganglia is sufficient to induce growth of bridging collaterals. Furthermore, I also showed that chronic pharmacologic blockade of D2Rs can rescue an abnormal behavioral phenotype associated with the bridging collaterals. I also showed that, in addition to genetic and pharmacologic interventions, changes in anatomical connectivity in the basal ganglia involving the bridging collaterals can also be induced by behavioral intervention, as motor training was sufficient to retract bridging collaterals and to rescue an abnormal behavioral phenotype associated with increased density of these collaterals.

In the second study presented in this dissertation, I used the viral construct I created as part of the first study to selectively increase excitability of the direct or indirect pathway in specific sub-regions of the basal ganglia. Even though these manipulations did not lead to clear effects on motivated behavior, the results of this study identified specific behavioral findings that contribute to the field of research on basal ganglia function and behavior.

Finally, in the third study of this dissertation, I conducted a series of experiments using a chemogenetic approach to alter the function of the indirect pathway both acutely and chronically, revealing a number of novel findings about basal ganglia function and cell signaling in MSNs. I found that acutely activating $G_{\alpha i}$ -coupled signaling in the indirect pathway increases motivation by energizing behavioral performance, which, however, comes at the cost of goal-directed efficiency. Furthermore, I also demonstrated both *in vitro* and *in vivo* that activating $G_{\alpha i}$ signaling does not lead to a significant change in somatic excitability or activity in MSNs. Instead, I show that the effect of activating a $G_{\alpha i}$ -coupled receptor in MSNs can be measured downstream as disinhibition of the GPe. In addition, I also provide compelling behavioral results showing that chronically decreasing function of the indirect pathway using a chemogenetic approach may not be effective in increasing motivation because it induces compensatory desensitization.

Even though these three studies had their own specific aims, I argue that the findings are not independent from each other. The main commonality between the studies is that all of them provide useful insight on how MSN excitability is related to neuronal activity and behavior. In Chapter 2, I learned that increasing excitability of MSNs can presumably induce compensatory changes in basal ganglia connectivity through a network effect. In Chapter 3, I found that using the same manipulation to change MSN excitability does not lead to robust behavioral effects on incentive motivation for natural rewards, but instead suggests a potential role for the NA core on timing and implicates the balance of direct and indirect pathway on action vigor. Finally, in Chapter 4, I attempted to affect neuronal excitability of iMSNs by activating $G_{\alpha i}$ signaling, but instead, I found that this manipulation produces a robust effect on motivated behavior but not by changing MSN excitability at the cell soma and likely via effects on presynaptic axon terminals.

First, although the bridging collaterals have been linked to excitability, my results do not establish an association between these collaterals and motivation in developmentally normal animals. However, it may still be possible that in models of disease states, such as the behavioral endophenotypes of schizophrenia modeled by overexpression of D2Rs in the striatum, basal ganglia connectivity may be abnormal. Thus, testing whether rescuing $K_{ir2.1}$ function in D2R- OE_{dev} , both globally in all types of MSNs and selectively in dMSNs and iMSNs, may be worthwhile to determine whether impaired motivation in an animal model of schizophrenia endophenotypes is linked to bridging collaterals. Second, the results from all three studies beg the question of whether activating G_{ai} signaling in iMSNs, which does not affect somatic excitability in these neurons can still affect the bridging collaterals. One experiment done in the Kellendonk laboratory showed that non-conditionally expressing the hM4D receptor in the DMS to decrease neuronal excitability with chronic CNO treatment is sufficient to retract bridging collaterals in D2R- OE_{dev} mice without affecting density of collaterals in control animals. It is not known, however, whether chronically activating hM4D receptors selectively in the iMSNs of D2R- OE_{dev} mice is also sufficient to retract bridging collaterals. Such experiment can be done, but they would require breeding animals with four mutant alleles, D2R- OE_{dev} mice ($CaMKIIa-tTa^+/TetO-D2R^+$) that are also positive for *Drd1*-GFP, and *Drd2*-Cre. If this experiment reveals that bridging collaterals of D2R- OE_{dev} mice can be retracted by chronically activating G_{ai} signaling in iMSNs in the DMS, it would suggest that collaterals were retracted in some of the experiments with chronic CNO treatment presented in Chapter 4. Since chronic CNO treatment in that study did not affect motivation in D2R- OE_{dev} mice, this potential finding would further dissociate the bridging collaterals from motivation. On the other hand, if bridging collaterals are not retracted by chronically activating G_{ai} signaling in the indirect pathway in the DMS of D2R-

OE_{dev} mice, then the implication would be that affecting neuronal function via G_{ai} signaling may be fundamentally different from affecting neuronal excitability by regulating K_{ir}2.1 function. In the case of G_{ai} signaling, it may be the case that globally targeting dMSNs and iMSNs, and not only iMSNs, in the striatum may be required to induce connectivity changes via the bridging collaterals. These potential results would still leave open the alternative that the bridging collaterals may be involved in the motivation deficit of D2R-OE_{dev} mice. Thus, although the studies I conducted for this dissertation answer many questions about MSN excitability and motivation in an animal model of negative symptoms of schizophrenia, some questions remain open and should be further investigated.

Another common ground among the studies, and especially between the studies presented in Chapters 2 and 4, is the relevance of the findings for therapies for neuropsychiatric disorders. Both pharmacological and behavior therapies for many psychiatric disorders require patients to either take a drug continuously, with effects being optimal after weeks of treatment, or, likewise, engage in behavior or talk therapy for weeks to months to achieve beneficial outcomes. In Chapter 2, I show that behavioral training for three weeks can induce changes in connectivity in the basal ganglia, leading to the same anatomical changes that may underlie the mechanism via which chronic haloperidol treatment exerts its beneficial effects in schizophrenia (Cazorla et al., 2014). This finding opens a broad avenue for research on the mechanisms of behavioral therapy for schizophrenia, particularly for psychosis which cannot be modelled in rodents but is relieved by haloperidol and other D2R antagonists. In support of this proposal, recent studies have shown that cognitive behavioral therapy can be effective in treating psychosis in schizophrenia (Leff et al., 2013, Mehl et al., 2015). Moreover, in Chapter 4 I show that long-term, continuous pharmacological activation of a G_{ai}-coupled receptor induces desensitization to the beneficial

effects of the drug on motivated behavior. These findings should be taken into consideration when developing therapies for neuropsychiatric disorders since treatments traditionally require continuous use of drugs. These results may even help explain why drugs that target GPCRs, including antipsychotic mediations for schizophrenia, may not affect motivation when taken chronically by patients. Moreover, also relevant for therapy, in Chapter 4 I found that pharmacologically targeting $G_{\alpha i}$ signaling in the indirect pathway of the basal ganglia can be effective acutely to boost motivation, but this effect comes at the cost of goal-directed efficiency. The dissociability between the directional and activational components of motivation can, therefore, be determined experimentally and should be considered when designing strategies for treating disorders of abnormal motivation. Hence, some of the findings presented across different studies in this dissertation have important implications for development of therapies for neuropsychiatric disorders.

Finally, the findings in Chapters 2 and 4 report two new types of plasticity in the basal ganglia that should be further explored by neuroscientists. One form of plasticity involves growth and retraction of the bridging collaterals that can be induced by neurophysiological and pharmacological manipulations directed at the indirect pathway of the basal ganglia. This form of plasticity has been linked to behavior in D2R-OE_{dev} mice both in the artificial setting in which activity in the direct pathway is driven with optogenetics and in the more natural setting in which animals undergo motor learning. Both of these links are, however, largely correlational. The second form of plasticity involves the behavioral desensitization effect induced by chronic activation of a $G_{\alpha i}$ -coupled receptor expressed in iMSNs. It is not immediately clear whether these two forms of plasticity are related. As discussed above, it would be important to determine whether chronically activating hM4D in the indirect pathway can affect the density of bridging

collaterals. Moreover, although I characterize many aspects of the behavioral desensitization induced by chronic activation of $G_{\alpha i}$ signaling in iMSNs, including the findings that it occurs in both the DMS and NA core and can be reversed within 48 h of discontinuing drug treatment, the mechanism for this phenomenon remains unknown. The data I report in Chapter 4 is consistent with either a cell autonomous effect, such as receptor internalization, or with a fast network effect involving compensatory circuit changes, possibly similar to that described for the bridging collaterals, but that occur at a much faster timescale. Thus, to expand on the findings involving plasticity presented in different studies in this dissertation, it would be interesting to test whether a causal link between bridging collaterals and behavior can be established and to further investigate the biochemical, physiological, and anatomical mechanisms that may underlie behavioral desensitization to chronic activation of $G_{\alpha i}$ signaling in MSNs.

FUTURE DIRECTIONS

In this final section, I will explicitly lay out some of the broader research avenues I have opened with the findings presented in this dissertation. These future directions pertain to a number of sub-fields of neuroscience and to efforts to understand how basal ganglia circuits (a) regulate normal behavior, (b) can be disrupted in neuropsychiatric disorders, (c) can undergo plasticity with learning, and (d) can compensate to perturbations during both development and adulthood. In addition, my findings also open avenues for more mechanistic studies of G protein function in MSNs.

In Chapter 2, I contributed to previous work done in the Kellendonk laboratory to show that plasticity involving the bridging collaterals is not regulated in a cell autonomous manner, but instead is mediated by a network mechanism. In light of these findings and knowledge about the

anatomy and connectivity in the basal ganglia, it is plausible that activity-dependent induction and retraction of the bridging collaterals may be controlled by regulated secretion of factors that guide, repel, or induce axonal growth. For instance, it is possible to conceive a scenario where increased activity of iMSNs targeting the GPe leads to secretion of an axon guidance molecule by cells in the GPe that selectively induces growth or releases inhibition for growth of dMSN axon collaterals into the GPe. Some studies have described activity-dependent synaptic plasticity mechanisms that regulate basal ganglia connectivity in development (Ding et al., 2012, Kozorovitskiy et al., 2012), but much less is known about similar phenomena in adulthood. Thus, strategies for screening axon guidance molecules for their effect on inducing growth or retraction of bridging collaterals should be developed in order to characterize the biochemical mechanisms that may underlie some of the behavioral findings I presented in this dissertation.

In light of the many parallels I drew between the bridging collaterals and schizophrenia, another potential continuation of my findings would be to determine whether structural elements homologous to the bridging collaterals exist in humans and are associated with neuropsychiatric disease states. Brain imaging techniques may not have the resolution to image axon collaterals or activity related to function of these collaterals. But collaborations with neuropathologists who may have access to postmortem tissue of patients who suffered from schizophrenia can be promising. It has been shown, for example, that D2R-OE_{dev} mice have decreased protein expression of the K_{ir}2.1 channel (Cazorla et al., 2012). Decreased K_{ir}2.1 protein expression may also be detectable in striatal tissue from patients with schizophrenia and would provide a clear translational link between bridging collaterals and schizophrenia. Thus, approaches to study the associations between the findings presented here on bridging collaterals and symptoms in patients with schizophrenia could be fruitful and would require interdisciplinary collaborations.

In addition to this translational potential, further work on the bridging collaterals can also aim to optimize methods to selectively target the collaterals. If selective methods are developed to decrease and increase function of the bridging collaterals, it would be possible to determine causal relationships between their function and specific behaviors. So far, the evidence linking the bridging collaterals to behavior is correlational, and it may be possible that the collaterals themselves do not directly regulate behavior. Identifying an axon guidance molecule that can drive or inhibit collateral growth, as discussed above, could be useful in this approach. Moreover, as alluded to in Chapter 2, genetic tools could also be used for this purpose, but they present some challenges because both passing fibers that target basal ganglia output nuclei and bridging collaterals of the direct pathway are present in the GPe and the current optogenetic and chemo genetic tools currently available do not allow for targeting one of these types of axons selectively. Efforts to overcome such challenges, therefore, should be employed to establish causal links for some of the correlational findings presented in this dissertation.

Another logical next step to expand on my findings related to G_{ai} -coupled signaling in MSNs is to characterize the compensatory mechanisms that mediate behavioral desensitization to chronic activation of hM4D receptors in iMSNs. Given that GPCRs are known to become internalized with repeated activation in many cell types (Doherty and McMahon, 2009), one strategy to test if internalization underlies desensitization to repeated activation of hM4D would be to perform electron microscopy imaging on immune-labeled hM4D receptors in animals expressing hM4D in iMSNs after chronic treatment with CNO.

Finally, the findings presented in Chapter 4 are consistent with the expression of hM4D receptor in presynaptic axon terminals driving the effect of CNO on motivation and GPe disinhibition. As discussed in that chapter, the effect of G_{ai} signaling on motivation may be

mediated both through iMSN collateral disinhibition of dMSNs and/or through iMSN disinhibition of the GPe. The tools used in the current study do not allow for selectively studying these presynaptic terminal-specific effects. Recently, a chemogenetic tool has been developed to selectively express DREADDs in presynaptic terminals (Stachniak et al., 2014). These new tools could be used to activate only presynaptic $G_{i\alpha}$ signaling in iMSNs in experiments designed to answer whether this mechanism can account for the effects presented in Chapter 4. It would also be interesting to investigate how activating hM4D receptors in iMSNs might affect lateral inhibition via iMSN-to-dMSN synapses using *in vivo* calcium imaging. Given that the vast majority of neurons in the striatum are either dMSNs or iMSNs, expressing D1Rs or D2Rs, respectively, using *Drd2*-Cre animals and co-injecting two viruses that lead to hM4D expression in Cre-positive neurons and GCaMP6f expression in Cre-negative neurons would provide a system in which hM4D is expressed in iMSNs and GCaMP6f is expressed in dMSNs, allowing activity of the direct pathway to be imaged while decreasing function of the indirect pathway with CNO treatment. Researchers have been able to successfully generate such “Cre-off” viral constructs that can be used together with the more traditional “Cre-on” constructs in the striatum to concomitantly express different genes in dMSNs and iMSNs (Saunders et al., 2012). If the hypothesis that hM4D acts on presynaptic sites to decrease axon terminal excitability or decrease neurotransmitter release is true, I would expect that, similar to the disinhibition of GPe activity reported in this study, CNO treatment in mice expressing hM4D in iMSNs would also lead to disinhibition of dMSNs in the striatum. Thus, developing new genetic tools for selectively targeting and imaging neuronal activity would be useful to advance my research and the field’s understanding of how basal ganglia output can be regulated.

Overall, therefore, the original research I present in this dissertation demonstrates that changes in connectivity in the basal ganglia can be induced by activity-dependent processes including behavioral training. I also show that selectively increasing excitability of specific pathways in the basal ganglia does not affect motivation for natural rewards. I further demonstrate that activating $G_{\alpha i}$ signaling in iMSNs does not affect excitability at the cell soma but leads to disinhibition of the GPe presumably by activating presynaptic axon terminals. And finally, I show that activating $G_{\alpha i}$ signaling acutely in the striatal indirect pathway can enhance motivation at the cost of goal directed efficiency and the same manipulation done chronically induces behavioral desensitization. I hope that these findings can contribute to neuroscience by providing a more complete understanding of how basal ganglia circuitry control motivated behavior and to neuropsychiatry by providing insight that can help guide therapeutic strategies for disorders of abnormal motivation.

REFERENCES

- Abi-Dargham A, Rodenhiser J, Printz D, Zea-Ponce Y, Gil R, Kegeles LS, Weiss R, Cooper TB, Mann JJ, Van Heertum RL, Gorman JM, Laruelle M (2000) Increased baseline occupancy of D2 receptors by dopamine in schizophrenia. *Proc Natl Acad Sci U S A* 97:8104-8109.
- Adamantidis AR, Tsai HC, Boutrel B, Zhang F, Stuber GD, Budygin EA, Tourino C, Bonci A, Deisseroth K, de Lecea L (2011) Optogenetic interrogation of dopaminergic modulation of the multiple phases of reward-seeking behavior. *J Neurosci* 31:10829-10835.
- Ade KK, Wan Y, Chen M, Gloss B, Calakos N (2011) An Improved BAC Transgenic Fluorescent Reporter Line for Sensitive and Specific Identification of Striatonigral Medium Spiny Neurons. *Front Syst Neurosci* 5:32.
- Aebischer P, Schultz W (1984) The activity of pars compacta neurons of the monkey substantia nigra is depressed by apomorphine. *Neuroscience letters* 50:25-29.
- Ahmari SE (2015) Using Mice to Model Obsessive Compulsive Disorder: From Genes to Circuits. *Neuroscience*.
- Ahmari SE, Spellman T, Douglass NL, Kheirbek MA, Simpson HB, Deisseroth K, Gordon JA, Hen R (2013) Repeated cortico-striatal stimulation generates persistent OCD-like behavior. *Science* 340:1234-1239.
- Albin RL, Young AB, Penney JB (1989) The functional anatomy of basal ganglia disorders. *Trends in neurosciences* 12:366-375.
- Alexander GE, DeLong MR, Strick PL (1986) Parallel organization of functionally segregated circuits linking basal ganglia and cortex. *Annu Rev Neurosci* 9:357-381.
- Alheid GF, Heimer L (1988) New perspectives in basal forebrain organization of special relevance for neuropsychiatric disorders: the striatopallidal, amygdaloid, and corticopetal components of substantia innominata. *Neuroscience* 27:1-39.
- Aosaki T, Tsubokawa H, Ishida A, Watanabe K, Graybiel AM, Kimura M (1994) Responses of tonically active neurons in the primate's striatum undergo systematic changes during behavioral sensorimotor conditioning. *J Neurosci* 14:3969-3984.
- Armbruster BN, Li X, Pausch MH, Herlitze S, Roth BL (2007) Evolving the lock to fit the key to create a family of G protein-coupled receptors potentially activated by an inert ligand. *Proc Natl Acad Sci U S A* 104:5163-5168.
- Aronin N, DiFiglia M (1992) The subcellular localization of the G-protein Gi alpha in the basal ganglia reveals its potential role in both signal transduction and vesicle trafficking. *The Journal of neuroscience : the official journal of the Society for Neuroscience* 12:3435-3444.

- Bach ME, Simpson EH, Kahn L, Marshall JJ, Kandel ER, Kellendonk C (2008) Transient and selective overexpression of D2 receptors in the striatum causes persistent deficits in conditional associative learning. *Proc Natl Acad Sci U S A* 105:16027-16032.
- Bailey MR, Jensen G, Taylor K, Meziar C, Williamson C, Silver R, Simpson EH, Balsam PD (2015) A novel strategy for dissecting goal-directed action and arousal components of motivated behavior with a progressive hold-down task. *Behavioral neuroscience* 129:269-280.
- Baldo BA, Sadeghian K, Basso AM, Kelley AE (2002) Effects of selective dopamine D1 or D2 receptor blockade within nucleus accumbens subregions on ingestive behavior and associated motor activity. *Behav Brain Res* 137:165-177.
- Bassareo V, Di Chiara G (1999) Differential responsiveness of dopamine transmission to food-stimuli in nucleus accumbens shell/core compartments. *Neuroscience* 89:637-641.
- Bateup HS, Santini E, Shen W, Birnbaum S, Valjent E, Surmeier DJ, Fisone G, Nestler EJ, Greengard P (2010) Distinct subclasses of medium spiny neurons differentially regulate striatal motor behaviors. *Proc Natl Acad Sci U S A* 107:14845-14850.
- Bateup HS, Svenningsson P, Kuroiwa M, Gong S, Nishi A, Heintz N, Greengard P (2008) Cell type-specific regulation of DARPP-32 phosphorylation by psychostimulant and antipsychotic drugs. *Nat Neurosci* 11:932-939.
- Baumeister AA, Francis JL (2002) Historical development of the dopamine hypothesis of schizophrenia. *J Hist Neurosci* 11:265-277.
- Beom S, Cheong D, Torres G, Caron MG, Kim KM (2004) Comparative studies of molecular mechanisms of dopamine D2 and D3 receptors for the activation of extracellular signal-regulated kinase. *J Biol Chem* 279:28304-28314.
- Berendse HW, Groenewegen HJ (1990) Organization of the thalamostriatal projections in the rat, with special emphasis on the ventral striatum. *J Comp Neurol* 299:187-228.
- Bernard V, Levey AI, Bloch B (1999) Regulation of the subcellular distribution of m4 muscarinic acetylcholine receptors in striatal neurons in vivo by the cholinergic environment: evidence for regulation of cell surface receptors by endogenous and exogenous stimulation. *J Neurosci* 19:10237-10249.
- Berridge KC, Robinson TE (1998) What is the role of dopamine in reward: hedonic impact, reward learning, or incentive salience? *Brain Research Reviews* 28:309-369.
- Bertran-Gonzalez J, Bosch C, Maroteaux M, Matamalas M, Herve D, Valjent E, Girault JA (2008) Opposing patterns of signaling activation in dopamine D1 and D2 receptor-expressing striatal neurons in response to cocaine and haloperidol. *J Neurosci* 28:5671-5685.

- Blesa J, Przedborski S (2014) Parkinson's disease: animal models and dopaminergic cell vulnerability. *Front Neuroanat* 8:155.
- Blum D, Torch S, Lambeng N, Nissou M, Benabid AL, Sadoul R, Verna JM (2001) Molecular pathways involved in the neurotoxicity of 6-OHDA, dopamine and MPTP: contribution to the apoptotic theory in Parkinson's disease. *Progress in neurobiology* 65:135-172.
- Bock R, Shin JH, Kaplan AR, Dobi A, Markey E, Kramer PF, Gremel CM, Christensen CH, Adrover MF, Alvarez VA (2013) Strengthening the accumbal indirect pathway promotes resilience to compulsive cocaine use. *Nat Neurosci* 16:632-638.
- Bodor AL, Giber K, Rovo Z, Ulbert I, Acsady L (2008) Structural correlates of efficient GABAergic transmission in the basal ganglia-thalamus pathway. *J Neurosci* 28:3090-3102.
- Bradshaw CM, Killeen PR (2012) A theory of behaviour on progressive ratio schedules, with applications in behavioural pharmacology. *Psychopharmacology (Berl)* 222:549-564.
- Brog JS, Salyapongse A, Deutch AY, Zahm DS (1993) The patterns of afferent innervation of the core and shell in the "accumbens" part of the rat ventral striatum: immunohistochemical detection of retrogradely transported fluoro-gold. *J Comp Neurol* 338:255-278.
- Burguiere E, Monteiro P, Feng G, Graybiel AM (2013) Optogenetic stimulation of lateral orbitofronto-striatal pathway suppresses compulsive behaviors. *Science* 340:1243-1246.
- Burrone J, O'Byrne M, Murthy VN (2002) Multiple forms of synaptic plasticity triggered by selective suppression of activity in individual neurons. *Nature* 420:414-418.
- Burton AC, Nakamura K, Roesch MR (2015) From ventral-medial to dorsal-lateral striatum: neural correlates of reward-guided decision-making. *Neurobiology of learning and memory* 117:51-59.
- Cachope R, Mateo Y, Mathur BN, Irving J, Wang HL, Morales M, Lovinger DM, Cheer JF (2012) Selective activation of cholinergic interneurons enhances accumbal phasic dopamine release: setting the tone for reward processing. *Cell Rep* 2:33-41.
- Calabresi P, Centonze D, Gubellini P, Pisani A, Bernardi G (2000) Acetylcholine-mediated modulation of striatal function. *Trends Neurosci* 23:120-126.
- Calzavara R, Maily P, Haber SN (2007) Relationship between the corticostriatal terminals from areas 9 and 46, and those from area 8A, dorsal and rostral premotor cortex and area 24c: an anatomical substrate for cognition to action. *Eur J Neurosci* 26:2005-2024.
- Caroni P, Chowdhury A, Lahr M (2014) Synapse rearrangements upon learning: from divergent-sparse connectivity to dedicated sub-circuits. *Trends in Neurosciences* 37:604-614.

- Carter AG, Sabatini BL (2004) State-dependent calcium signaling in dendritic spines of striatal medium spiny neurons. *Neuron* 44:483-493.
- Carter AG, Soler-Llavina GJ, Sabatini BL (2007) Timing and location of synaptic inputs determine modes of subthreshold integration in striatal medium spiny neurons. *J Neurosci* 27:8967-8977.
- Castro DC, Berridge KC (2014) Opioid hedonic hotspot in nucleus accumbens shell: mu, delta, and kappa maps for enhancement of sweetness "liking" and "wanting". *The Journal of neuroscience : the official journal of the Society for Neuroscience* 34:4239-4250.
- Catalano SM, Shatz CJ (1998) Activity-dependent cortical target selection by thalamic axons. *Science* 281:559-562.
- Cazorla M, de Carvalho FD, Chohan MO, Shegda M, Chuhma N, Rayport S, Ahmari SE, Moore H, Kellendonk C (2014) Dopamine D2 receptors regulate the anatomical and functional balance of basal ganglia circuitry. *Neuron* 81:153-164.
- Cazorla M, Shegda M, Ramesh B, Harrison NL, Kellendonk C (2012) Striatal D2 receptors regulate dendritic morphology of medium spiny neurons via Kir2 channels. *The Journal of neuroscience : the official journal of the Society for Neuroscience* 32:2398-2409.
- Cepeda C, Andre VM, Yamazaki I, Wu N, Kleiman-Weiner M, Levine MS (2008) Differential electrophysiological properties of dopamine D1 and D2 receptor-containing striatal medium-sized spiny neurons. *Eur J Neurosci* 27:671-682.
- Cepeda C, Hurst RS, Altemus KL, Flores-Hernandez J, Calvert CR, Jokel ES, Grandy DK, Low MJ, Rubinstein M, Ariano MA, Levine MS (2001) Facilitated glutamatergic transmission in the striatum of D2 dopamine receptor-deficient mice. *J Neurophysiol* 85:659-670.
- Chaudhury D, Walsh JJ, Friedman AK, Juarez B, Ku SM, Koo JW, Ferguson D, Tsai HC, Pomeranz L, Christoffel DJ, Nectow AR, Ekstrand M, Domingos A, Mazei-Robison MS, Mouzon E, Lobo MK, Neve RL, Friedman JM, Russo SJ, Deisseroth K, Nestler EJ, Han MH (2013) Rapid regulation of depression-related behaviours by control of midbrain dopamine neurons. *Nature* 493:532-+.
- Chen J, Rusnak M, Luedtke RR, Sidhu A (2004) D1 dopamine receptor mediates dopamine-induced cytotoxicity via the ERK signal cascade. *J Biol Chem* 279:39317-39330.
- Corbett D, Wise RA (1980) Intracranial self-stimulation in relation to the ascending dopaminergic systems of the midbrain: a moveable electrode mapping study. *Brain Res* 185:1-15.
- Corbit LH, Balleine BW (2011) The general and outcome-specific forms of Pavlovian-instrumental transfer are differentially mediated by the nucleus accumbens core and shell. *The Journal of neuroscience : the official journal of the Society for Neuroscience* 31:11786-11794.

- Corbit LH, Muir JL, Balleine BW (2001) The role of the nucleus accumbens in instrumental conditioning: Evidence of a functional dissociation between accumbens core and shell. *The Journal of neuroscience : the official journal of the Society for Neuroscience* 21:3251-3260.
- Costa RM, Cohen D, Nicoletis MA (2004) Differential corticostriatal plasticity during fast and slow motor skill learning in mice. *Curr Biol* 14:1124-1134.
- Creese I, Burt DR, Snyder SH (1976) Dopamine receptor binding predicts clinical and pharmacological potencies of antischizophrenic drugs. *Science* 192:481-483.
- Cui G, Jun SB, Jin X, Pham MD, Vogel SS, Lovinger DM, Costa RM (2013) Concurrent activation of striatal direct and indirect pathways during action initiation. *Nature* 494:238-242.
- Cumming P (2011) Absolute abundances and affinity states of dopamine receptors in mammalian brain: A review. *Synapse* 65:892-909.
- Czubayko U, Plenz D (2002) Fast synaptic transmission between striatal spiny projection neurons. *Proc Natl Acad Sci U S A* 99:15764-15769.
- Dal Toso R, Sommer B, Ewert M, Herb A, Pritchett DB, Bach A, Shivers BD, Seeburg PH (1989) The dopamine D2 receptor: two molecular forms generated by alternative splicing. *EMBO J* 8:4025-4034.
- Damsma G, Pfaus JG, Wenkstern D, Phillips AG, Fibiger HC (1992) Sexual behavior increases dopamine transmission in the nucleus accumbens and striatum of male rats: comparison with novelty and locomotion. *Behav Neurosci* 106:181-191.
- Dawson VL, Dawson TM, Wamsley JK (1990) Muscarinic and dopaminergic receptor subtypes on striatal cholinergic interneurons. *Brain research bulletin* 25:903-912.
- Day M, Wokosin D, Plotkin JL, Tian X, Surmeier DJ (2008) Differential excitability and modulation of striatal medium spiny neuron dendrites. *J Neurosci* 28:11603-11614.
- De Marco Garcia NV, Karayannis T, Fishell G (2011) Neuronal activity is required for the development of specific cortical interneuron subtypes. *Nature* 472:351-355.
- De Mei C, Ramos M, Iitaka C, Borrelli E (2009) Getting specialized: presynaptic and postsynaptic dopamine D2 receptors. *Curr Opin Pharmacol* 9:53-58.
- de Wit SJ, Alonso P, Schwenen L, Mataix-Cols D, Lochner C, Menchon JM, Stein DJ, Fouche JP, Soriano-Mas C, Sato JR, Hoexter MQ, Denys D, Nakamae T, Nishida S, Kwon JS, Jang JH, Busatto GF, Cardoner N, Cath DC, Fukui K, Jung WH, Kim SN, Miguel EC, Narumoto J, Phillips ML, Pujol J, Remijnse PL, Sakai Y, Shin NY, Yamada K, Veltman DJ, van den Heuvel OA (2014) Multicenter voxel-based morphometry mega-analysis of structural brain scans in obsessive-compulsive disorder. *Am J Psychiatry* 171:340-349.

- Di Chiara G, Imperato A (1988) Drugs abused by humans preferentially increase synaptic dopamine concentrations in the mesolimbic system of freely moving rats. *Proc Natl Acad Sci U S A* 85:5274-5278.
- Ding JB, Oh WJ, Sabatini BL, Gu C (2012) Semaphorin 3E-Plexin-D1 signaling controls pathway-specific synapse formation in the striatum. *Nat Neurosci* 15:215-223.
- Doherty GJ, McMahon HT (2009) Mechanisms of endocytosis. *Annu Rev Biochem* 78:857-902.
- Doig NM, Moss J, Bolam JP (2010) Cortical and thalamic innervation of direct and indirect pathway medium-sized spiny neurons in mouse striatum. *J Neurosci* 30:14610-14618.
- Drew MR, Simpson EH, Kellendonk C, Herzberg WG, Lipatova O, Fairhurst S, Kandel ER, Malapani C, Balsam PD (2007) Transient overexpression of striatal D2 receptors impairs operant motivation and interval timing. *The Journal of neuroscience : the official journal of the Society for Neuroscience* 27:7731-7739.
- Durieux PF, Bearzatto B, Guiducci S, Buch T, Waisman A, Zoli M, Schiffmann SN, de Kerchove d'Exaerde A (2009) D2R striatopallidal neurons inhibit both locomotor and drug reward processes. *Nat Neurosci* 12:393-395.
- Eilam D, Talangbayan H, Canaran G, Szechtman H (1992) Dopaminergic control of locomotion, mouthing, snout contact, and grooming: opposing roles of D1 and D2 receptors. *Psychopharmacology (Berl)* 106:447-454.
- Erro ME, Lanciego JL, Arribas J, Gimenez-Amaya JM (2001) Striatal input from the ventrobasal complex of the rat thalamus. *Histochem Cell Biol* 115:447-454.
- Esslinger C, Englisch S, Inta D, Rausch F, Schirmbeck F, Mier D, Kirsch P, Meyer-Lindenberg A, Zink M (2012) Ventral striatal activation during attribution of stimulus saliency and reward anticipation is correlated in unmedicated first episode schizophrenia patients. *Schizophr Res* 140:114-121.
- Ettinger U, Corr PJ, Mofidi A, Williams SC, Kumari V (2013) Dopaminergic basis of the psychosis-prone personality investigated with functional magnetic resonance imaging of procedural learning. *Front Hum Neurosci* 7:130.
- Fallon JH, Moore RY (1978) Catecholamine innervation of the basal forebrain. IV. Topography of the dopamine projection to the basal forebrain and neostriatum. *J Comp Neurol* 180:545-580.
- Fenton WS, McGlashan TH (1991) Natural history of schizophrenia subtypes. II. Positive and negative symptoms and long-term course. *Arch Gen Psychiatry* 48:978-986.
- Ferguson SM, Eskenazi D, Ishikawa M, Wanat MJ, Phillips PE, Dong Y, Roth BL, Neumaier JF (2011) Transient neuronal inhibition reveals opposing roles of indirect and direct pathways in sensitization. *Nat Neurosci* 14:22-24.

- Fervaha G, Foussias G, Agid O, Remington G (2013) Amotivation and functional outcomes in early schizophrenia. *Psychiatry Res* 210:665-668.
- Fiorentini C, Gardoni F, Spano P, Di Luca M, Missale C (2003) Regulation of dopamine D1 receptor trafficking and desensitization by oligomerization with glutamate N-methyl-D-aspartate receptors. *J Biol Chem* 278:20196-20202.
- Fiorino DF, Coury A, Phillips AG (1997) Dynamic changes in nucleus accumbens dopamine efflux during the Coolidge effect in male rats. *J Neurosci* 17:4849-4855.
- Floran B, Floran L, Sierra A, Aceves J (1997) D2 receptor-mediated inhibition of GABA release by endogenous dopamine in the rat globus pallidus. *Neuroscience letters* 237:1-4.
- Ford CP (2014) The role of D2-autoreceptors in regulating dopamine neuron activity and transmission. *Neuroscience* 282C:13-22.
- Fujiyama F, Sohn J, Nakano T, Furuta T, Nakamura KC, Matsuda W, Kaneko T (2011) Exclusive and common targets of neostriatofugal projections of rat striosome neurons: a single neuron-tracing study using a viral vector. *The European journal of neuroscience* 33:668-677.
- Gainetdinov RR, Caron MG (2001) Genetics of childhood disorders: XXIV. ADHD, part 8: hyperdopaminergic mice as an animal model of ADHD. *J Am Acad Child Adolesc Psychiatry* 40:380-382.
- Gainetdinov RR, Premont RT, Bohn LM, Lefkowitz RJ, Caron MG (2004) Desensitization of G protein-coupled receptors and neuronal functions. *Annu Rev Neurosci* 27:107-144.
- Galarraga E, Hernandez-Lopez S, Reyes A, Barral J, Bargas J (1997) Dopamine facilitates striatal EPSPs through an L-type Ca²⁺ conductance. *Neuroreport* 8:2183-2186.
- Galarraga E, Hernandez-Lopez S, Reyes A, Miranda I, Bermudez-Rattoni F, Vilchis C, Bargas J (1999) Cholinergic modulation of neostriatal output: a functional antagonism between different types of muscarinic receptors. *J Neurosci* 19:3629-3638.
- Gard DE, Fisher M, Garrett C, Genevsky A, Vinogradov S (2009) Motivation and its relationship to neurocognition, social cognition, and functional outcome in schizophrenia. *Schizophr Res* 115:74-81.
- Gerfen CR (1984) The neostriatal mosaic: compartmentalization of corticostriatal input and striatonigral output systems. *Nature* 311:461-464.
- Gerfen CR (1992) The neostriatal mosaic: multiple levels of compartmental organization. *Trends Neurosci* 15:133-139.
- Gerfen CR, Baimbridge KG, Miller JJ (1985) The neostriatal mosaic: compartmental distribution of calcium-binding protein and parvalbumin in the basal ganglia of the rat and monkey. *Proc Natl Acad Sci U S A* 82:8780-8784.

- Gerfen CR, Herkenham M, Thibault J (1987) The neostriatal mosaic: II. Patch- and matrix-directed mesostriatal dopaminergic and non-dopaminergic systems. *J Neurosci* 7:3915-3934.
- Gerfen CR, Surmeier DJ (2011) Modulation of striatal projection systems by dopamine. *Annual review of neuroscience* 34:441-466.
- Gerfen CR, Young WS, 3rd (1988) Distribution of striatonigral and striatopallidal peptidergic neurons in both patch and matrix compartments: an in situ hybridization histochemistry and fluorescent retrograde tracing study. *Brain Res* 460:161-167.
- Gertler TS, Chan CS, Surmeier DJ (2008) Dichotomous anatomical properties of adult striatal medium spiny neurons. *J Neurosci* 28:10814-10824.
- Ghahremani MH, Forget C, Albert PR (2000) Distinct roles for Galpha(i)2 and Gbetagamma in signaling to DNA synthesis and Galpha(i)3 in cellular transformation by dopamine D2S receptor activation in BALB/c 3T3 cells. *Mol Cell Biol* 20:1497-1506.
- Ghods-Sharifi S, Floresco SB (2010) Differential effects on effort discounting induced by inactivations of the nucleus accumbens core or shell. *Behavioral neuroscience* 124:179-191.
- Gholizadeh S, Tharmalingam S, Macaldaz ME, Hampson DR (2013) Transduction of the central nervous system after intracerebroventricular injection of adeno-associated viral vectors in neonatal and juvenile mice. *Hum Gene Ther Methods* 24:205-213.
- Gold JM, Strauss GP, Waltz JA, Robinson BM, Brown JK, Frank MJ (2013) Negative symptoms of schizophrenia are associated with abnormal effort-cost computations. *Biol Psychiatry* 74:130-136.
- Gong S, Zheng C, Doughty ML, Losos K, Didkovsky N, Schambra UB, Nowak NJ, Joyner A, Leblanc G, Hatten ME, Heintz N (2003) A gene expression atlas of the central nervous system based on bacterial artificial chromosomes. *Nature* 425:917-925.
- Goto Y, Grace AA (2005) Dopaminergic modulation of limbic and cortical drive of nucleus accumbens in goal-directed behavior. *Nat Neurosci* 8:805-812.
- Grace AA, Floresco SB, Goto Y, Lodge DJ (2007) Regulation of firing of dopaminergic neurons and control of goal-directed behaviors. *Trends Neurosci* 30:220-227.
- Graybiel AM, Ragsdale CW, Jr. (1978) Histochemically distinct compartments in the striatum of human, monkeys, and cat demonstrated by acetylthiocholinesterase staining. *Proc Natl Acad Sci U S A* 75:5723-5726.
- Graybiel AM, Ragsdale CW, Jr., Yoneoka ES, Elde RP (1981) An immunohistochemical study of enkephalins and other neuropeptides in the striatum of the cat with evidence that the opiate peptides are arranged to form mosaic patterns in register with the striosomal compartments visible by acetylcholinesterase staining. *Neuroscience* 6:377-397.

- Green MF, Kern RS, Braff DL, Mintz J (2000) Neurocognitive deficits and functional outcome in schizophrenia: are we measuring the "right stuff"? *Schizophr Bull* 26:119-136.
- Greengard P (2001) The neurobiology of slow synaptic transmission. *Science* 294:1024-1030.
- Greengard P, Allen PB, Nairn AC (1999) Beyond the dopamine receptor: the DARPP-32/protein phosphatase-1 cascade. *Neuron* 23:435-447.
- Haber SN, Calzavara R (2009) The cortico-basal ganglia integrative network: the role of the thalamus. *Brain Res Bull* 78:69-74.
- Haber SN, Kim KS, Maily P, Calzavara R (2006) Reward-related cortical inputs define a large striatal region in primates that interface with associative cortical connections, providing a substrate for incentive-based learning. *J Neurosci* 26:8368-8376.
- Hall J, Parkinson JA, Connor TM, Dickinson A, Everitt BJ (2001) Involvement of the central nucleus of the amygdala and nucleus accumbens core in mediating Pavlovian influences on instrumental behaviour. *Eur J Neurosci* 13:1984-1992.
- Hartman KN, Pal SK, Burrone J, Murthy VN (2006) Activity-dependent regulation of inhibitory synaptic transmission in hippocampal neurons. *Nat Neurosci* 9:642-649.
- Haynes WI, Haber SN (2013) The organization of prefrontal-subthalamic inputs in primates provides an anatomical substrate for both functional specificity and integration: implications for Basal Ganglia models and deep brain stimulation. *J Neurosci* 33:4804-4814.
- Heimer L, Alheid GF, de Olmos JS, Groenewegen HJ, Haber SN, Harlan RE, Zahm DS (1997) The accumbens: beyond the core-shell dichotomy. *J Neuropsychiatry Clin Neurosci* 9:354-381.
- Heimer L, Zahm DS, Churchill L, Kalivas PW, Wohltmann C (1991) Specificity in the projection patterns of accumbal core and shell in the rat. *Neuroscience* 41:89-125.
- Heiser P, Friedel S, Dempfle A, Konrad K, Smidt J, Grabarkiewicz J, Herpertz-Dahlmann B, Remschmidt H, Hebebrand J (2004) Molecular genetic aspects of attention-deficit/hyperactivity disorder. *Neuroscience and biobehavioral reviews* 28:625-641.
- Hemmings HC, Jr., Greengard P, Tung HY, Cohen P (1984) DARPP-32, a dopamine-regulated neuronal phosphoprotein, is a potent inhibitor of protein phosphatase-1. *Nature* 310:503-505.
- Herkenham M, Pert CB (1981) Mosaic distribution of opiate receptors, parafascicular projections and acetylcholinesterase in rat striatum. *Nature* 291:415-418.
- Hernandez-Lopez S, Bargas J, Surmeier DJ, Reyes A, Galarraga E (1997) D1 receptor activation enhances evoked discharge in neostriatal medium spiny neurons by modulating an L-type Ca²⁺ conductance. *J Neurosci* 17:3334-3342.

- Hernandez-Lopez S, Tkatch T, Perez-Garci E, Galarraga E, Bargas J, Hamm H, Surmeier DJ (2000) D2 dopamine receptors in striatal medium spiny neurons reduce L-type Ca²⁺ currents and excitability via a novel PLC[β]₁-IP₃-calcineurin-signaling cascade. *The Journal of neuroscience : the official journal of the Society for Neuroscience* 20:8987-8995.
- Hess EJ, Bracha HS, Kleinman JE, Creese I (1987) Dopamine receptor subtype imbalance in schizophrenia. *Life Sci* 40:1487-1497.
- Hikida T, Yawata S, Yamaguchi T, Danjo T, Sasaoka T, Wang Y, Nakanishi S (2013) Pathway-specific modulation of nucleus accumbens in reward and aversive behavior via selective transmitter receptors. *Proc Natl Acad Sci U S A* 110:342-347.
- Hilario M, Holloway T, Jin X, Costa RM (2012) Different dorsal striatum circuits mediate action discrimination and action generalization. *The European journal of neuroscience* 35:1105-1114.
- Howes OD, Kambitz J, Kim E, Stahl D, Slifstein M, Abi-Dargham A, Kapur S (2012) The nature of dopamine dysfunction in schizophrenia and what this means for treatment. *Arch Gen Psychiatry* 69:776-786.
- Howes OD, Montgomery AJ, Asselin MC, Murray RM, Valli I, Tabraham P, Bramon-Bosch E, Valmaggia L, Johns L, Broome M, McGuire PK, Grasby PM (2009) Elevated striatal dopamine function linked to prodromal signs of schizophrenia. *Arch Gen Psychiatry* 66:13-20.
- Hsu KS, Yang CH, Huang CC (1997) Carbachol induces inward current in rat neostriatal neurons through a G-protein-coupled mechanism. *Neuroscience letters* 224:79-82.
- Hsu KS, Yang CH, Huang CC, Gean PW (1996) Carbachol induces inward current in neostriatal neurons through M1-like muscarinic receptors. *Neuroscience* 73:751-760.
- Hua JY, Smear MC, Baier H, Smith SJ (2005) Regulation of axon growth in vivo by activity-based competition. *Nature* 434:1022-1026.
- Ikemoto S (2010) Brain reward circuitry beyond the mesolimbic dopamine system: a neurobiological theory. *Neuroscience and biobehavioral reviews* 35:129-150.
- Ikemoto S, Yang C, Tan A (2015) Basal ganglia circuit loops, dopamine and motivation: A review and enquiry. *Behavioural brain research* 290:17-31.
- Ilango A, Kesner AJ, Broker CJ, Wang DV, Ikemoto S (2014a) Phasic excitation of ventral tegmental dopamine neurons potentiates the initiation of conditioned approach behavior: parametric and reinforcement-schedule analyses. *Front Behav Neurosci* 8:155.
- Ilango A, Kesner AJ, Keller KL, Stuber GD, Bonci A, Ikemoto S (2014b) Similar roles of substantia nigra and ventral tegmental dopamine neurons in reward and aversion. *J Neurosci* 34:817-822.

- Jaber M, Jones S, Giros B, Caron MG (1997) The dopamine transporter: a crucial component regulating dopamine transmission. *Mov Disord* 12:629-633.
- Jin X, Tecuapetla F, Costa RM (2014a) Basal ganglia subcircuits distinctively encode the parsing and concatenation of action sequences. *Nature Neuroscience* 17:423-430.
- Jin X, Tecuapetla F, Costa RM (2014b) Basal ganglia subcircuits distinctively encode the parsing and concatenation of action sequences. *Nat Neurosci* 17:423-430.
- Joyce JN, Lexow N, Bird E, Winokur A (1988) Organization of dopamine D1 and D2 receptors in human striatum: receptor autoradiographic studies in Huntington's disease and schizophrenia. *Synapse* 2:546-557.
- Kaneda K, Isa K, Yanagawa Y, Isa T (2008) Nigral inhibition of GABAergic neurons in mouse superior colliculus. *J Neurosci* 28:11071-11078.
- Karschin C, Dissmann E, Stuhmer W, Karschin A (1996) IRK(1-3) and GIRK(1-4) inwardly rectifying K⁺ channel mRNAs are differentially expressed in the adult rat brain. *The Journal of neuroscience : the official journal of the Society for Neuroscience* 16:3559-3570.
- Kawaguchi Y, Wilson CJ, Emson PC (1989) Intracellular recording of identified neostriatal patch and matrix spiny cells in a slice preparation preserving cortical inputs. *Journal of neurophysiology* 62:1052-1068.
- Kawaguchi Y, Wilson CJ, Emson PC (1990) Projection subtypes of rat neostriatal matrix cells revealed by intracellular injection of biocytin. *J Neurosci* 10:3421-3438.
- Kegeles LS, Abi-Dargham A, Frankle WG, Gil R, Cooper TB, Slifstein M, Hwang DR, Huang Y, Haber SN, Laruelle M (2010) Increased synaptic dopamine function in associative regions of the striatum in schizophrenia. *Arch Gen Psychiatry* 67:231-239.
- Kellendonk C, Simpson EH, Polan HJ, Malleret G, Vronskaya S, Winiger V, Moore H, Kandel ER (2006) Transient and selective overexpression of dopamine D2 receptors in the striatum causes persistent abnormalities in prefrontal cortex functioning. *Neuron* 49:603-615.
- Kellendonk C, Tronche F, Casanova E, Anlag K, Opherk C, Schutz G (1999) Inducible site-specific recombination in the brain. *J Mol Biol* 285:175-182.
- Kemp JM, Powell TP (1971) The structure of the caudate nucleus of the cat: light and electron microscopy. *Philos Trans R Soc Lond B Biol Sci* 262:383-401.
- Kim N, Barter JW, Sukharnikova T, Yin HH (2014) Striatal firing rate reflects head movement velocity. *The European journal of neuroscience* 40:3481-3490.
- Kimura M, Rajkowski J, Evarts E (1984) Tonicly discharging putamen neurons exhibit set-dependent responses. *Proc Natl Acad Sci U S A* 81:4998-5001.

- Kisilevsky AE, Mulligan SJ, Altier C, Iftinca MC, Varela D, Tai C, Chen L, Hameed S, Hamid J, Macvicar BA, Zamponi GW (2008) D1 receptors physically interact with N-type calcium channels to regulate channel distribution and dendritic calcium entry. *Neuron* 58:557-570.
- Kisilevsky AE, Zamponi GW (2008) D2 dopamine receptors interact directly with N-type calcium channels and regulate channel surface expression levels. *Channels (Austin)* 2:269-277.
- Kita H, Kitai ST (1987) Efferent projections of the subthalamic nucleus in the rat: light and electron microscopic analysis with the PHA-L method. *J Comp Neurol* 260:435-452.
- Kitai ST, Surmeier DJ (1993) Cholinergic and dopaminergic modulation of potassium conductances in neostriatal neurons. *Adv Neurol* 60:40-52.
- Kohnomi S, Koshikawa N, Kobayashi M (2012) D(2)-like dopamine receptors differentially regulate unitary IPSCs depending on presynaptic GABAergic neuron subtypes in rat nucleus accumbens shell. *J Neurophysiol* 107:692-703.
- Koob GF, Riley SJ, Smith SC, Robbins TW (1978) Effects of 6-Hydroxydopamine Lesions of Nucleus Accumbens Septi and Olfactory Tubercle on Feeding, Locomotor-Activity, and Amphetamine Anorexia in Rat. *Journal of Comparative and Physiological Psychology* 92:917-927.
- Koos T, Tepper JM (1999) Inhibitory control of neostriatal projection neurons by GABAergic interneurons. *Nat Neurosci* 2:467-472.
- Kozorovitskiy Y, Saunders A, Johnson CA, Lowell BB, Sabatini BL (2012) Recurrent network activity drives striatal synaptogenesis. *Nature* 485:646-650.
- Kravitz AV, Freeze BS, Parker PR, Kay K, Thwin MT, Deisseroth K, Kreitzer AC (2010) Regulation of parkinsonian motor behaviours by optogenetic control of basal ganglia circuitry. *Nature* 466:622-626.
- Kravitz AV, Tye LD, Kreitzer AC (2012) Distinct roles for direct and indirect pathway striatal neurons in reinforcement. *Nat Neurosci* 15:816-818.
- Kreitzer AC, Malenka RC (2007) Endocannabinoid-mediated rescue of striatal LTD and motor deficits in Parkinson's disease models. *Nature* 445:643-647.
- Kuczenski R, Segal DS (1997) Effects of methylphenidate on extracellular dopamine, serotonin, and norepinephrine: comparison with amphetamine. *J Neurochem* 68:2032-2037.
- Kugler S, Kilic E, Bahr M (2003) Human synapsin 1 gene promoter confers highly neuron-specific long-term transgene expression from an adenoviral vector in the adult rat brain depending on the transduced area. *Gene Ther* 10:337-347.

- Kupchik YM, Brown RM, Heinsbroek JA, Lobo MK, Schwartz DJ, Kalivas PW (2015) Coding the direct/indirect pathways by D1 and D2 receptors is not valid for accumbens projections. *Nat Neurosci* 18:1230-1232.
- Kuzhikandathil EV, Yu W, Oxford GS (1998) Human dopamine D3 and D2L receptors couple to inward rectifier potassium channels in mammalian cell lines. *Mol Cell Neurosci* 12:390-402.
- Larisch R, Sitte W, Antke C, Nikolaus S, Franz M, Tress W, Muller HW (2006) Striatal dopamine transporter density in drug naive patients with attention-deficit/hyperactivity disorder. *Nucl Med Commun* 27:267-270.
- Laruelle M (1998) Imaging dopamine transmission in schizophrenia. A review and meta-analysis. *The quarterly journal of nuclear medicine : official publication of the Italian Association of Nuclear Medicine* 42:211-221.
- Lavine N, Ethier N, Oak JN, Pei L, Liu F, Trieu P, Rebois RV, Bouvier M, Hebert TE, Van Tol HH (2002) G protein-coupled receptors form stable complexes with inwardly rectifying potassium channels and adenylyl cyclase. *J Biol Chem* 277:46010-46019.
- Lee FJ, Xue S, Pei L, Vukusic B, Chery N, Wang Y, Wang YT, Niznik HB, Yu XM, Liu F (2002) Dual regulation of NMDA receptor functions by direct protein-protein interactions with the dopamine D1 receptor. *Cell* 111:219-230.
- Leff J, Williams G, Huckvale MA, Arbuthnot M, Leff AP (2013) Computer-assisted therapy for medication-resistant auditory hallucinations: proof-of-concept study. *Br J Psychiatry* 202:428-433.
- Lenz JD, Lobo MK (2013) Optogenetic insights into striatal function and behavior. *Behavioural brain research* 255:44-54.
- Levesque M, Parent A (2005) The striatofugal fiber system in primates: a reevaluation of its organization based on single-axon tracing studies. *Proc Natl Acad Sci U S A* 102:11888-11893.
- Levey AI, Hersch SM, Rye DB, Sunahara RK, Niznik HB, Kitt CA, Price DL, Maggio R, Brann MR, Ciliax BJ (1993) Localization of D1 and D2 dopamine receptors in brain with subtype-specific antibodies. *Proc Natl Acad Sci U S A* 90:8861-8865.
- Lex A, Hauber W (2008) Dopamine D1 and D2 receptors in the nucleus accumbens core and shell mediate Pavlovian-instrumental transfer. *Learn Mem* 15:483-491.
- Liu XY, Chu XP, Mao LM, Wang M, Lan HX, Li MH, Zhang GC, Parelkar NK, Fibuch EE, Haines M, Neve KA, Liu F, Xiong ZG, Wang JQ (2006) Modulation of D2R-NR2B interactions in response to cocaine. *Neuron* 52:897-909.
- Lobo MK, Covington HE, 3rd, Chaudhury D, Friedman AK, Sun H, Damez-Werno D, Dietz DM, Zaman S, Koo JW, Kennedy PJ, Mouzon E, Mogri M, Neve RL, Deisseroth K, Han

- MH, Nestler EJ (2010) Cell type-specific loss of BDNF signaling mimics optogenetic control of cocaine reward. *Science* 330:385-390.
- Lobo MK, Nestler EJ (2011) The striatal balancing act in drug addiction: distinct roles of direct and indirect pathway medium spiny neurons. *Front Neuroanat* 5:41.
- Lu XY, Ghasemzadeh MB, Kalivas PW (1998) Expression of D1 receptor, D2 receptor, substance P and enkephalin messenger RNAs in the neurons projecting from the nucleus accumbens. *Neuroscience* 82:767-780.
- Luo R, Janssen MJ, Partridge JG, Vicini S (2013) Direct and GABA-mediated indirect effects of nicotinic ACh receptor agonists on striatal neurones. *J Physiol* 591:203-217.
- Luscher C, Malenka RC (2011) Drug-evoked synaptic plasticity in addiction: from molecular changes to circuit remodeling. *Neuron* 69:650-663.
- Luscher C, Slesinger PA (2010) Emerging roles for G protein-gated inwardly rectifying potassium (GIRK) channels in health and disease. *Nature reviews Neuroscience* 11:301-315.
- Lyness WH, Friedle NM, Moore KE (1979) Destruction of dopaminergic nerve terminals in nucleus accumbens: effect on d-amphetamine self-administration. *Pharmacol Biochem Behav* 11:553-556.
- Mai B, Sommer S, Hauber W (2012) Motivational states influence effort-based decision making in rats: the role of dopamine in the nucleus accumbens. *Cognitive, affective & behavioral neuroscience* 12:74-84.
- Maldonado R, Robledo P, Chover AJ, Caine SB, Koob GF (1993) D1 dopamine receptors in the nucleus accumbens modulate cocaine self-administration in the rat. *Pharmacol Biochem Behav* 45:239-242.
- Mamad O, Delaville C, Benjelloun W, Benazzouz A (2015) Dopaminergic control of the globus pallidus through activation of D2 receptors and its impact on the electrical activity of subthalamic nucleus and substantia nigra reticulata neurons. *PLoS One* 10:e0119152.
- Marcott PF, Mamaligas AA, Ford CP (2014) Phasic dopamine release drives rapid activation of striatal D2-receptors. *Neuron* 84:164-176.
- Martel P, Leo D, Fulton S, Berard M, Trudeau LE (2011) Role of Kv1 potassium channels in regulating dopamine release and presynaptic D2 receptor function. *PLoS One* 6:e20402.
- Marzella PL, Copolov D (1997) [³H]nemonapride binding in human caudate and putamen. *Brain Res Bull* 44:167-170.
- Matamales M, Bertran-Gonzalez J, Salomon L, Degos B, Deniau JM, Valjent E, Herve D, Girault JA (2009) Striatal medium-sized spiny neurons: identification by nuclear staining and study of neuronal subpopulations in BAC transgenic mice. *PLoS One* 4:e4770.

- Max JE, Fox PT, Lancaster JL, Kochunov P, Mathews K, Manes FF, Robertson BA, Arndt S, Robin DA, Lansing AE (2002) Putamen lesions and the development of attention-deficit/hyperactivity symptomatology. *J Am Acad Child Adolesc Psychiatry* 41:563-571.
- McCown TJ, Xiao X, Li J, Breese GR, Samulski RJ (1996) Differential and persistent expression patterns of CNS gene transfer by an adeno-associated virus (AAV) vector. *Brain Res* 713:99-107.
- McCullough LD, Salamone JD (1992) Involvement of nucleus accumbens dopamine in the motor activity induced by periodic food presentation: a microdialysis and behavioral study. *Brain Res* 592:29-36.
- McFarland NR, Haber SN (2002) Thalamic relay nuclei of the basal ganglia form both reciprocal and nonreciprocal cortical connections, linking multiple frontal cortical areas. *J Neurosci* 22:8117-8132.
- McGregor A, Roberts DC (1993) Dopaminergic antagonism within the nucleus accumbens or the amygdala produces differential effects on intravenous cocaine self-administration under fixed and progressive ratio schedules of reinforcement. *Brain Res* 624:245-252.
- Mehl S, Werner D, Lincoln TM (2015) Does Cognitive Behavior Therapy for psychosis (CBTp) show a sustainable effect on delusions? A meta-analysis. *Front Psychol* 6:1450.
- Meredith GE, Agolia R, Arts MP, Groenewegen HJ, Zahm DS (1992) Morphological differences between projection neurons of the core and shell in the nucleus accumbens of the rat. *Neuroscience* 50:149-162.
- Missale C, Nash SR, Robinson SW, Jaber M, Caron MG (1998) Dopamine receptors: from structure to function. *Physiol Rev* 78:189-225.
- Mita T, Hanada S, Nishino N, Kuno T, Nakai H, Yamadori T, Mizoi Y, Tanaka C (1986) Decreased serotonin S2 and increased dopamine D2 receptors in chronic schizophrenics. *Biol Psychiatry* 21:1407-1414.
- Montmayeur JP, Bausero P, Amlaiky N, Maroteaux L, Hen R, Borrelli E (1991) Differential expression of the mouse D2 dopamine receptor isoforms. *FEBS Lett* 278:239-243.
- Moriizumi T, Hattori T (1992) Separate neuronal populations of the rat globus pallidus projecting to the subthalamic nucleus, auditory cortex and pedunclopontine tegmental area. *Neuroscience* 46:701-710.
- Moriwaki A, Wang JB, Svingos A, van Bockstaele E, Cheng P, Pickel V, Uhl GR (1996) c. *Neurochemical research* 21:1315-1331.
- Morris SJ, Van H, II, Daigle M, Robillard L, Sajedi N, Albert PR (2007) Differential desensitization of dopamine D2 receptor isoforms by protein kinase C: the importance of receptor phosphorylation and pseudosubstrate sites. *Eur J Pharmacol* 577:44-53.

- Moss J, Bolam JP (2008) A dopaminergic axon lattice in the striatum and its relationship with cortical and thalamic terminals. *J Neurosci* 28:11221-11230.
- Nakano K, Kayahara T, Tsutsumi T, Ushiro H (2000) Neural circuits and functional organization of the striatum. *J Neurol* 247 Suppl 5:V1-15.
- Nestler EJ (2013) Cellular basis of memory for addiction. *Dialogues Clin Neurosci* 15:431-443.
- Nicola SM (2010) The flexible approach hypothesis: unification of effort and cue-responding hypotheses for the role of nucleus accumbens dopamine in the activation of reward-seeking behavior. *J Neurosci* 30:16585-16600.
- Nielsen MO, Rostrup E, Wulff S, Bak N, Lublin H, Kapur S, Glenthøj B (2012) Alterations of the brain reward system in antipsychotic naive schizophrenia patients. *Biol Psychiatry* 71:898-905.
- Nishi A, Snyder GL, Greengard P (1997) Bidirectional regulation of DARPP-32 phosphorylation by dopamine. *J Neurosci* 17:8147-8155.
- Nowend KL, Arizzi M, Carlson BB, Salamone JD (2001) D1 or D2 antagonism in nucleus accumbens core or dorsomedial shell suppresses lever pressing for food but leads to compensatory increases in chow consumption. *Pharmacology, biochemistry, and behavior* 69:373-382.
- Pan WX, Mao T, Dudman JT (2010) Inputs to the dorsal striatum of the mouse reflect the parallel circuit architecture of the forebrain. *Front Neuroanat* 4:147.
- Panlilio LV, Thorndike EB, Schindler CW (2007) Blocking of conditioning to a cocaine-paired stimulus: testing the hypothesis that cocaine perpetually produces a signal of larger-than-expected reward. *Pharmacol Biochem Behav* 86:774-777.
- Parkinson JA, Dalley JW, Cardinal RN, Bamford A, Fehnert B, Lachenal G, Rudarakanchana N, Halkerston KM, Robbins TW, Everitt BJ (2002) Nucleus accumbens dopamine depletion impairs both acquisition and performance of appetitive Pavlovian approach behaviour: implications for mesoaccumbens dopamine function. *Behav Brain Res* 137:149-163.
- Parnaudeau S, O'Neill PK, Bolkan SS, Ward RD, Abbas AI, Roth BL, Balsam PD, Gordon JA, Kellendonk C (2013) Inhibition of mediodorsal thalamus disrupts thalamofrontal connectivity and cognition. *Neuron* 77:1151-1162.
- Pascoli V, Besnard A, Herve D, Pages C, Heck N, Girault JA, Caboche J, Vanhoutte P (2011) Cyclic adenosine monophosphate-independent tyrosine phosphorylation of NR2B mediates cocaine-induced extracellular signal-regulated kinase activation. *Biol Psychiatry* 69:218-227.
- Paterna JC, Moccetti T, Mura A, Feldon J, Bueler H (2000) Influence of promoter and WHV post-transcriptional regulatory element on AAV-mediated transgene expression in the rat brain. *Gene Ther* 7:1304-1311.

- Pecina S, Berridge KC (2005) Hedonic hot spot in nucleus accumbens shell: where do mu-opioids cause increased hedonic impact of sweetness? *The Journal of neuroscience : the official journal of the Society for Neuroscience* 25:11777-11786.
- Pedersen KF, Larsen JP, Alves G, Aarsland D (2009) Prevalence and clinical correlates of apathy in Parkinson's disease: a community-based study. *Parkinsonism & related disorders* 15:295-299.
- Percheron G, Fenelon G, Leroux-Hugon V, Feve A (1994) [History of the basal ganglia system. Slow development of a major cerebral system]. *Rev Neurol (Paris)* 150:543-554.
- Perez MF, White FJ, Hu XT (2006) Dopamine D(2) receptor modulation of K(+) channel activity regulates excitability of nucleus accumbens neurons at different membrane potentials. *J Neurophysiol* 96:2217-2228.
- Pozzi L, Hakansson K, Usiello A, Borgkvist A, Lindskog M, Greengard P, Fisone G (2003) Opposite regulation by typical and atypical anti-psychotics of ERK1/2, CREB and Elk-1 phosphorylation in mouse dorsal striatum. *J Neurochem* 86:451-459.
- Preisig-Muller R, Schlichthorl G, Goerge T, Heinen S, Bruggemann A, Rajan S, Derst C, Veh RW, Daut J (2002) Heteromerization of Kir2.x potassium channels contributes to the phenotype of Andersen's syndrome. *Proc Natl Acad Sci U S A* 99:7774-7779.
- Ranaldi R, Pocock D, Zereik R, Wise RA (1999) Dopamine fluctuations in the nucleus accumbens during maintenance, extinction, and reinstatement of intravenous D-amphetamine self-administration. *J Neurosci* 19:4102-4109.
- Redish AD (2004) Addiction as a computational process gone awry. *Science* 306:1944-1947.
- Reiner A, Albin RL, Anderson KD, D'Amato CJ, Penney JB, Young AB (1988) Differential loss of striatal projection neurons in Huntington disease. *Proc Natl Acad Sci U S A* 85:5733-5737.
- Ritter S, Stein L (1974) Self-stimulation in the mesencephalic trajectory of the ventral noradrenergic bundle. *Brain Res* 81:145-157.
- Roberts DC, Koob GF, Klonoff P, Fibiger HC (1980) Extinction and recovery of cocaine self-administration following 6-hydroxydopamine lesions of the nucleus accumbens. *Pharmacol Biochem Behav* 12:781-787.
- Rodman AM, Milad MR, Deckersbach T, Im J, Chou T, Dougherty DD (2012) Neuroimaging contributions to novel surgical treatments for intractable obsessive-compulsive disorder. *Expert Rev Neurother* 12:219-227.
- Romanelli P, Esposito V, Schaal DW, Heit G (2005) Somatotopy in the basal ganglia: experimental and clinical evidence for segregated sensorimotor channels. *Brain Res Brain Res Rev* 48:112-128.

- Rossi MA, Sukharnikova T, Hayrapetyan VY, Yang L, Yin HH (2013) Operant self-stimulation of dopamine neurons in the substantia nigra. *PLoS One* 8:e65799.
- Routtenberg A, Malsbury C (1969) Brainstem pathways of reward. *J Comp Physiol Psychol* 68:22-30.
- Salamone JD, Correa M (2002) Motivational views of reinforcement: implications for understanding the behavioral functions of nucleus accumbens dopamine. *Behavioural brain research* 137:3-25.
- Salamone JD, Correa M (2012) The mysterious motivational functions of mesolimbic dopamine. *Neuron* 76:470-485.
- Salamone JD, Correa M, Mingote S, Weber SM (2003) Nucleus accumbens dopamine and the regulation of effort in food-seeking behavior: implications for studies of natural motivation, psychiatry, and drug abuse. *J Pharmacol Exp Ther* 305:1-8.
- Salamone JD, Cousins MS, Bucher S (1994) Anhedonia or anergia? Effects of haloperidol and nucleus accumbens dopamine depletion on instrumental response selection in a T-maze cost/benefit procedure. *Behav Brain Res* 65:221-229.
- Salamone JD, Mahan K, Rogers S (1993) Ventrolateral striatal dopamine depletions impair feeding and food handling in rats. *Pharmacol Biochem Behav* 44:605-610.
- Salgado H, Tecuapetla F, Perez-Rosello T, Perez-Burgos A, Perez-Garci E, Galarraga E, Bargas J (2005) A reconfiguration of CaV2 Ca²⁺ channel current and its dopaminergic D2 modulation in developing neostriatal neurons. *J Neurophysiol* 94:3771-3787.
- Saunders A, Johnson CA, Sabatini BL (2012) Novel recombinant adeno-associated viruses for Cre activated and inactivated transgene expression in neurons. *Front Neural Circuits* 6:47.
- Schultz W (1986) Responses of midbrain dopamine neurons to behavioral trigger stimuli in the monkey. *Journal of neurophysiology* 56:1439-1461.
- Schultz W (1998) Predictive reward signal of dopamine neurons. *Journal of neurophysiology* 80:1-27.
- Seeman P, Lee T, Chau-Wong M, Wong K (1976) Antipsychotic drug doses and neuroleptic/dopamine receptors. *Nature* 261:717-719.
- Sesack SR, Aoki C, Pickel VM (1994) Ultrastructural localization of D2 receptor-like immunoreactivity in midbrain dopamine neurons and their striatal targets. *J Neurosci* 14:88-106.
- Shafritz KM, Marchione KE, Gore JC, Shaywitz SE, Shaywitz BA (2004) The effects of methylphenidate on neural systems of attention in attention deficit hyperactivity disorder. *Am J Psychiatry* 161:1990-1997.

- Shen W, Hernandez-Lopez S, Tkatch T, Held JE, Surmeier DJ (2004) Kv1.2-containing K⁺ channels regulate subthreshold excitability of striatal medium spiny neurons. *J Neurophysiol* 91:1337-1349.
- Shiflett MW, Brown RA, Balleine BW (2010) Acquisition and performance of goal-directed instrumental actions depends on ERK signaling in distinct regions of dorsal striatum in rats. *The Journal of neuroscience : the official journal of the Society for Neuroscience* 30:2951-2959.
- Shink E, Sidibe M, Smith Y (1997) Efferent connections of the internal globus pallidus in the squirrel monkey: II. Topography and synaptic organization of pallidal efferents to the pedunculopontine nucleus. *J Comp Neurol* 382:348-363.
- Shuen JA, Chen M, Gloss B, Calakos N (2008) *Drd1a*-tdTomato BAC transgenic mice for simultaneous visualization of medium spiny neurons in the direct and indirect pathways of the basal ganglia. *J Neurosci* 28:2681-2685.
- Simpson EH, Kellendonk C, Kandel E (2010) A possible role for the striatum in the pathogenesis of the cognitive symptoms of schizophrenia. *Neuron* 65:585-596.
- Simpson EH, Kellendonk C, Ward RD, Richards V, Lipatova O, Fairhurst S, Kandel ER, Balsam PD (2011) Pharmacologic rescue of motivational deficit in an animal model of the negative symptoms of schizophrenia. *Biol Psychiatry* 69:928-935.
- Simpson EH, Waltz JA, Kellendonk C, Balsam PD (2012) Schizophrenia in translation: dissecting motivation in schizophrenia and rodents. *Schizophr Bull* 38:1111-1117.
- Spektor BS, Miller DW, Hollingsworth ZR, Kaneko YA, Solano SM, Johnson JM, Penney JB, Jr., Young AB, Luthi-Carter R (2002) Differential D1 and D2 receptor-mediated effects on immediate early gene induction in a transgenic mouse model of Huntington's disease. *Brain Res Mol Brain Res* 102:118-128.
- Stachniak TJ, Ghosh A, Sternson SM (2014) Chemogenetic synaptic silencing of neural circuits localizes a hypothalamus-->midbrain pathway for feeding behavior. *Neuron* 82:797-808.
- Staines WA, Fibiger HC (1984) Collateral projections of neurons of the rat globus pallidus to the striatum and substantia nigra. *Exp Brain Res* 56:217-220.
- Starke K, Gothert M, Kilbinger H (1989) Modulation of neurotransmitter release by presynaptic autoreceptors. *Physiol Rev* 69:864-989.
- Steinberg EE, Boivin JR, Saunders BT, Witten IB, Deisseroth K, Janak PH (2014) Positive reinforcement mediated by midbrain dopamine neurons requires D1 and D2 receptor activation in the nucleus accumbens. *PLoS One* 9:e94771.
- Sullivan RM, Brake WG (2003) What the rodent prefrontal cortex can teach us about attention-deficit/hyperactivity disorder: the critical role of early developmental events on prefrontal function. *Behav Brain Res* 146:43-55.

- Sun XD, Lee EW, Wong EH, Lee KS (2000) ATP-sensitive potassium channels in freshly dissociated adult rat striatal neurons: activation by metabolic inhibitors and the dopaminergic receptor agonist quinpirole. *Pflugers Arch* 440:530-547.
- Surmeier DJ, Bargas J, Hemmings HC, Jr., Nairn AC, Greengard P (1995) Modulation of calcium currents by a D1 dopaminergic protein kinase/phosphatase cascade in rat neostriatal neurons. *Neuron* 14:385-397.
- Surmeier DJ, Carrillo-Reid L, Bargas J (2011) Dopaminergic modulation of striatal neurons, circuits, and assemblies. *Neuroscience* 198:3-18.
- Surmeier DJ, Mercer JN, Chan CS (2005) Autonomous pacemakers in the basal ganglia: who needs excitatory synapses anyway? *Curr Opin Neurobiol* 15:312-318.
- Surmeier DJ, Song WJ, Yan Z (1996) Coordinated expression of dopamine receptors in neostriatal medium spiny neurons. *J Neurosci* 16:6579-6591.
- Tai LH, Lee AM, Benavidez N, Bonci A, Wilbrecht L (2012) Transient stimulation of distinct subpopulations of striatal neurons mimics changes in action value. *Nat Neurosci* 15:1281-1289.
- Taverna S, Ilijic E, Surmeier DJ (2008) Recurrent collateral connections of striatal medium spiny neurons are disrupted in models of Parkinson's disease. *J Neurosci* 28:5504-5512.
- Taylor KM, Horvitz JC, Balsam PD (2007) Amphetamine affects the start of responding in the peak interval timing task. *Behav Processes* 74:168-175.
- Tecuapetla F, Koos T, Tepper JM, Kabbani N, Yeckel MF (2009) Differential dopaminergic modulation of neostriatal synaptic connections of striatopallidal axon collaterals. *The Journal of neuroscience : the official journal of the Society for Neuroscience* 29:8977-8990.
- Tepper JM, Tecuapetla F, Koos T, Ibanez-Sandoval O (2010) Heterogeneity and diversity of striatal GABAergic interneurons. *Front Neuroanat* 4:150.
- Thobois S, Ardouin C, Lhomme E, Klinger H, Lagrange C, Xie J, Fraix V, Coelho Braga MC, Hassani R, Kistner A, Juphard A, Seigneuret E, Chabardes S, Mertens P, Polo G, Reilhac A, Costes N, LeBars D, Savasta M, Tremblay L, Quesada JL, Bosson JL, Benabid AL, Broussolle E, Pollak P, Krack P (2010) Non-motor dopamine withdrawal syndrome after surgery for Parkinson's disease: predictors and underlying mesolimbic denervation. *Brain : a journal of neurology* 133:1111-1127.
- Threlfell S, Lalic T, Platt NJ, Jennings KA, Deisseroth K, Cragg SJ (2012) Striatal dopamine release is triggered by synchronized activity in cholinergic interneurons. *Neuron* 75:58-64.

- Trifilieff P, Feng B, Urizar E, Winiger V, Ward RD, Taylor KM, Martinez D, Moore H, Balsam PD, Simpson EH, Javitch JA (2013) Increasing dopamine D2 receptor expression in the adult nucleus accumbens enhances motivation. *Mol Psychiatry* 18:1025-1033.
- Tripathi A, Prensa L, Mengual E (2013) Axonal branching patterns of ventral pallidal neurons in the rat. *Brain Struct Funct* 218:1133-1157.
- Tritsch NX, Sabatini BL (2012) Dopaminergic modulation of synaptic transmission in cortex and striatum. *Neuron* 76:33-50.
- Tsai HC, Zhang F, Adamantidis A, Stuber GD, Bonci A, de Lecea L, Deisseroth K (2009) Phasic firing in dopaminergic neurons is sufficient for behavioral conditioning. *Science* 324:1080-1084.
- Tunstall MJ, Oorschot DE, Kean A, Wickens JR (2002) Inhibitory interactions between spiny projection neurons in the rat striatum. *J Neurophysiol* 88:1263-1269.
- Ungerstedt U (1968) 6-Hydroxy-dopamine induced degeneration of central monoamine neurons. *Eur J Pharmacol* 5:107-110.
- Ungerstedt U (1971) Stereotaxic mapping of the monoamine pathways in the rat brain. *Acta Physiol Scand Suppl* 367:1-48.
- Usiello A, Baik JH, Rouge-Pont F, Picetti R, Dierich A, LeMeur M, Piazza PV, Borrelli E (2000) Distinct functions of the two isoforms of dopamine D2 receptors. *Nature* 408:199-203.
- Vaidya CJ, Austin G, Kirkorian G, Ridlehuber HW, Desmond JE, Glover GH, Gabrieli JD (1998) Selective effects of methylphenidate in attention deficit hyperactivity disorder: a functional magnetic resonance study. *Proc Natl Acad Sci U S A* 95:14494-14499.
- Valjent E, Bertran-Gonzalez J, Herve D, Fisone G, Girault JA (2009) Looking BAC at striatal signaling: cell-specific analysis in new transgenic mice. *Trends Neurosci* 32:538-547.
- Valjent E, Corvol JC, Pages C, Besson MJ, Maldonado R, Caboche J (2000) Involvement of the extracellular signal-regulated kinase cascade for cocaine-rewarding properties. *J Neurosci* 20:8701-8709.
- Valjent E, Corvol JC, Trzaskos JM, Girault JA, Herve D (2006) Role of the ERK pathway in psychostimulant-induced locomotor sensitization. *BMC Neurosci* 7:20.
- Valjent E, Pascoli V, Svenningsson P, Paul S, Enslen H, Corvol JC, Stipanovich A, Caboche J, Lombroso PJ, Nairn AC, Greengard P, Herve D, Girault JA (2005) Regulation of a protein phosphatase cascade allows convergent dopamine and glutamate signals to activate ERK in the striatum. *Proc Natl Acad Sci U S A* 102:491-496.

- Van der Werf YD, Witter MP, Groenewegen HJ (2002) The intralaminar and midline nuclei of the thalamus. Anatomical and functional evidence for participation in processes of arousal and awareness. *Brain Res Brain Res Rev* 39:107-140.
- van Huijstee AN, Mansvelder HD (2014) Glutamatergic synaptic plasticity in the mesocorticolimbic system in addiction. *Front Cell Neurosci* 8:466.
- Vercelli A, Marini G, Tredici G (2003) Anatomical organization of the telencephalic connections of the parafascicular nucleus in adult and developing rats. *Eur J Neurosci* 18:275-289.
- Vilchis C, Bargas J, Ayala GX, Galvan E, Galarraga E (2000) Ca²⁺ channels that activate Ca²⁺-dependent K⁺ currents in neostriatal neurons. *Neuroscience* 95:745-752.
- Wang AY, Miura K, Uchida N (2013) The dorsomedial striatum encodes net expected return, critical for energizing performance vigor. *Nat Neurosci* 16:639-647.
- Wang C, Buck DC, Yang R, Macey TA, Neve KA (2005) Dopamine D2 receptor stimulation of mitogen-activated protein kinases mediated by cell type-dependent transactivation of receptor tyrosine kinases. *J Neurochem* 93:899-909.
- Wang H, Pickel VM (2002) Dopamine D2 receptors are present in prefrontal cortical afferents and their targets in patches of the rat caudate-putamen nucleus. *J Comp Neurol* 442:392-404.
- Ward RD, Kellendonk C, Simpson EH, Lipatova O, Drew MR, Fairhurst S, Kandel ER, Balsam PD (2009) Impaired timing precision produced by striatal D2 receptor overexpression is mediated by cognitive and motivational deficits. *Behav Neurosci* 123:720-730.
- Wei W, Li L, Yu G, Ding S, Li C, Zhou FM (2013) Supersensitive presynaptic dopamine D2 receptor inhibition of the striatopallidal projection in nigrostriatal dopamine-deficient mice. *Journal of neurophysiology* 110:2203-2216.
- Willis T (1664) *Cerebri anatome: cui accessit nervorum descriptio et usus*. London: Londini : typis Ja. Flesher, impensis Jo. Martyn & Ja. Allestry apud insigne Campanae in Coemeterio D. Pauli.
- Wilson CJ (1993) The generation of natural firing patterns in neostriatal neurons. *Prog Brain Res* 99:277-297.
- Wilson CJ, Kawaguchi Y (1996) The origins of two-state spontaneous membrane potential fluctuations of neostriatal spiny neurons. *The Journal of neuroscience : the official journal of the Society for Neuroscience* 16:2397-2410.
- Wise RA, Newton P, Leeb K, Burnette B, Pocock D, Justice JB, Jr. (1995) Fluctuations in nucleus accumbens dopamine concentration during intravenous cocaine self-administration in rats. *Psychopharmacology (Berl)* 120:10-20.

- Wolf DH, Satterthwaite TD, Kantrowitz JJ, Katchmar N, Vandekar L, Elliott MA, Ruparel K (2014) Amotivation in schizophrenia: integrated assessment with behavioral, clinical, and imaging measures. *Schizophr Bull* 40:1328-1337.
- Worbe Y, Baup N, Grabli D, Chaigneau M, Mounayar S, McCairn K, Feger J, Tremblay L (2009) Behavioral and movement disorders induced by local inhibitory dysfunction in primate striatum. *Cereb Cortex* 19:1844-1856.
- Wu Y, Richard S, Parent A (2000) The organization of the striatal output system: a single-cell juxtacellular labeling study in the rat. *Neurosci Res* 38:49-62.
- Yan Z, Song WJ, Surmeier J (1997) D2 dopamine receptors reduce N-type Ca²⁺ currents in rat neostriatal cholinergic interneurons through a membrane-delimited, protein-kinase-C-insensitive pathway. *Journal of neurophysiology* 77:1003-1015.
- Yasuda R, Nimchinsky EA, Scheuss V, Pologruto TA, Oertner TG, Sabatini BL, Svoboda K (2004) Imaging calcium concentration dynamics in small neuronal compartments. *Sci STKE* 2004:pl5.
- Yasukawa T, Kita T, Xue Y, Kita H (2004) Rat intralaminar thalamic nuclei projections to the globus pallidus: a biotinylated dextran amine anterograde tracing study. *J Comp Neurol* 471:153-167.
- Yin HH, Knowlton BJ, Balleine BW (2004) Lesions of dorsolateral striatum preserve outcome expectancy but disrupt habit formation in instrumental learning. *The European journal of neuroscience* 19:181-189.
- Yin HH, Ostlund SB, Knowlton BJ, Balleine BW (2005) The role of the dorsomedial striatum in instrumental conditioning. *The European journal of neuroscience* 22:513-523.
- Yung KK, Bolam JP, Smith AD, Hersch SM, Ciliax BJ, Levey AI (1995) Immunocytochemical localization of D1 and D2 dopamine receptors in the basal ganglia of the rat: light and electron microscopy. *Neuroscience* 65:709-730.